The University Of Sheffield.

Screening and development of natural compounds as tools to improve IgG production and quality in recombinant CHO cell cultures

By

L. Toronjo-Urquiza

A thesis submitted in partial fulfilment of the requirements for the degree of

Doctor of Philosophy

The University of Sheffield

Faculty of Engineering

Department of Chemical and Biological Engineering

Screening and development of natural compounds as tools to improve IgG production and quality in recombinant CHO cell cultures

By
Luis Toronjo-Urquiza

A thesis submitted in partial fulfilment of the requirements for the degree of

Doctor of Philosophy

The University of Sheffield

Faculty of Engineering

Department of Chemical and Biological Engineering

December 2018

Declaration

I, Luis Toronjo-Urquiza, declare that unless stated otherwise in the text, I am the sole author of this thesis and the results presented within are the result of my own efforts and achievements. I confirm that this work has not been submitted for any other degrees.

Abstract

The clonal producer cell lines are inherently variable and hardly predictable, despite the various advances in the field of biopharmaceutical production. These features are inherent to the process and are difficult to control. The number of strategies available to salvage a batch culture with undesired behaviour is limited, and this causes uncertainty in the production process.

During the present study, chemicals which had favourable traits and were previously described in unrelated fields of literature, were selected and screened, in order to identify possible improvements in the final and specific productivity. Of those selected, catechins and resveratrol were further investigated in order to check their effect on the cell cycle, to optimize their addition in scale-up cultures and to check their effect on the quality of the monoclonal antibody.

Resveratrol and the compounds from the catechin group, were able to increase the specific productivity by approximately 2.5 and 2-fold respectively. This was achieved by cytostaticity. Studies of resveratrol and catechins on cell cycle, showed that these chemicals stopped the cell cycle in the S and G2/M phase. This was probably due to their effect on topoisomerases. Furthermore, when added at late stages of the culture during the optimization experiments, resveratrol and catechin improved the final titre by 1.37- and 1.43-fold increase respectively, without causing any negative effects. Finally, the quality assessment of the monoclonal antibody did not show any changes in aggregation or fragmentation. Resveratrol and catechin caused a decrease of the acidic species by 6.75 ± 3.91% and 3.58 ± 0.28 respectively. The mass spectrometry analysis showed that the treated samples were less likely to suffer reduction in the variable region, indicating that these chemicals could preserve the antigen recognition site.

The present study suggests that resveratrol and catechin are promising additives that could improve the recombinant monoclonal antibody production and preserve the product from undesired degradation and modifications with potential improvements of the shelf-life and potency.

To my grandmother, my sister and my parents

Acknowledgements

Sincerest thanks to my supervisors Professor Robert J Falconer and Professor David C James for giving me the opportunity to learn in their laboratory and for guiding and supporting me through my Ph.D. I would also like to thank my industrial supervisor Dr Tobor Nagy for his invaluable advice and input into the project.

The completion of this thesis would not have been possible without the help of my colleagues and co-workers to whom I would like to express my gratitude. Finally, I would like to thank the Biological Sciences Research Council and FUJIFILM Diosynth Biotechnologies UK for supporting my academic research as well as the Department of Chemical and Biological Engineering for facilitating me with work opportunities to accomplish the completion of this project.

Table of contents

Table of figures

Table of tables

Table of acronyms and abbreviations

4-PBA	Sodium 4-phenylbutyrate
AmLs	Ammonia loss
ATCC	American type culture collection
Avg	Average
BHK	Baby hamster kidney
BL2-A	Blue laser fluorescence area
BL2-H	Blue laser fluorescence height
BSA	Bovine serum albumin
Btn	Betaine
Calc	Calculation
CAPE	Caffeic acid phenethyl ester
Cat	Catechin
CD20	B-lymphocyte antigen CD20
Cff	Caffeine
CHO	Chinese hamster ovary
CHO-S	Chinese hamster ovary in suspension
CSI	Cloner imager select
Ctyl	Carboxy-methylation
CEX	Cation exchange chromatography
DHFR	Dihydrofolate reductase
Diff	Difference
Dmdt	Deamidation
DMSO	Dimethyl sulfoxide
DNA	Deoxyribonucleic acid
EC	Epicatechin
ECACC	European collection of cell culture
ECG	Epicatechin gallate
EGCG	Epigallocatechin gallate
EMS	Ethyl methane sulfonate
ER	Endoplasmic reticulum
ERAD	Endoplasmic reticulum associated degradation
ESI	Electrospray ionisation
Fc	Fragment crystallisable
FDA	US food and drug administration
FDBK	Fujifilm Diosynth Biotechnologies UK
FSC-A	Forward scatter area
GCG	Gallocatechin gallate
GCG	Gallocatechin
GI_{50}	50% growth inhibition
HC	Heavy chain
HEK	Human embryonic kidney

HPLC	High performance liquid chromatography
IFPMA	International federation of pharmaceutical manufacturers & associations
IgG	Immunoglobulin G
LC	Liquid chromatography/Light chain
LC-MS/MS	Liquid chromatography mass spectrometry mass spectrometry
LC_{50}	50% Lethal concentration
LFQ	Label free quantification
Ltl	Luteolin
mAb	Monoclonal antibody
Met	Methionine amino acid
MS	Mass spectrometry
OxiM	Oxidation
PBS	Phosphate-buffered saline
Pcd	Piceid
q_p	Specific recombinant protein production
Redc	Reduction
RNA	Ribonucleic acid
rProt	Recombinant proteins
Rsv	Resveratrol
SD	Standard deviation
SDS-PAGE	Sodium dodecyl sulphate-polyacrylamide gel electrophoresis
SEC	Size exclusion chromatography
SSC-A	Side scatter area
Tcp	Tocopherol
TrOx	Tri-oxidation
UPR	Unfolded protein response
VCD	Viable cell density
VCD_0	Viable cell density at time zero
VCD_f	Final viable cell density
Δλ	Wavelength
μ	Specific growth rate

Chapter 1

Literature screening of chemicals

1.1 Biopharmaceutical industry

The development and production of drug molecules take place in the biopharmaceutical sector of the pharmaceutical industry. These drugs need to be produced in living systems due to their complexity. The traditional chemical engineering approach used to develop these drugs, known as biomanufacturing or bioproduction, is limited, due to technological and economic reasons.

During the last decades, this sector has increased drastically and continues to grow. The economic investment from companies has been substantial. According to the Research and Development investment scheme of 2013, almost 100 billion euros were spent in 2013, making it the top investment in their list (IFPMA, 2014).

The need for new biopharmaceuticals is fundamental, in order to improve the treatments for many diseases. However, their development is complex, long and expensive. The first stage of the process involves drug discovery; in this phase, the proof of concept is elaborated and tested. Then, safety and clinical efficiency are addressed in preclinical studies with animals. After that, clinical trials are implemented in humans and finally, the regulatory agency approves the biomanufacturing production. The average time to commercialise a drug molecule is approximately 15 years (IFPMA, 2012)(Figure 1).

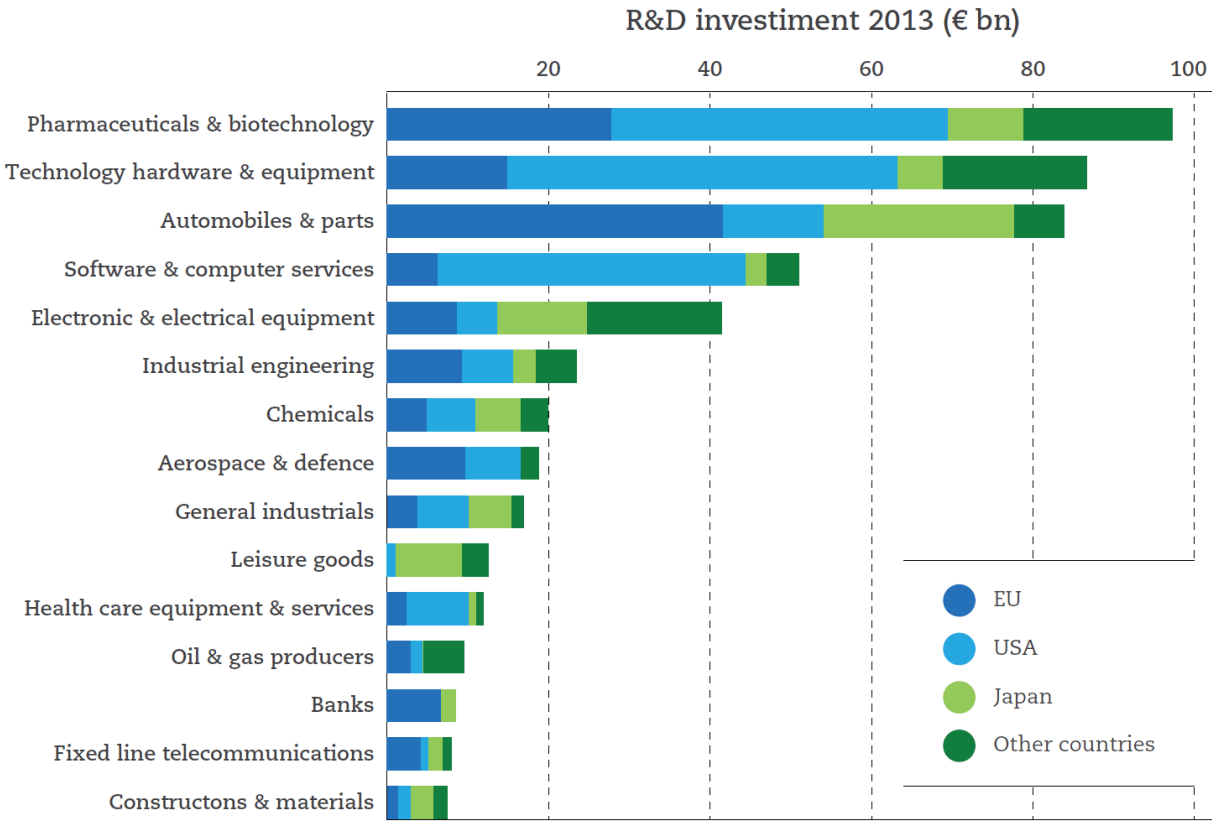

Figure 1 The investment in industry sectors in 2013
Modified from (IFPMA, 2014).

Successful products are incredibly expensive, as they need to counterbalance not only the economical income needed for the successful drug production, but also to recover the investment on other candidates that are not successful.

The first mass-produced biopharmaceutical drug, penicillin, was developed by Pfizer. It was directly obtained from the organism *Penicillium chrysogenum* (Ginsberg, 2008), which is a natural producer of penicillin. Decades later, biotechnological research led to DNA manipulation and its insertion into organisms, opening the possibility of using cells as production factories for non-native (recombinant) proteins.

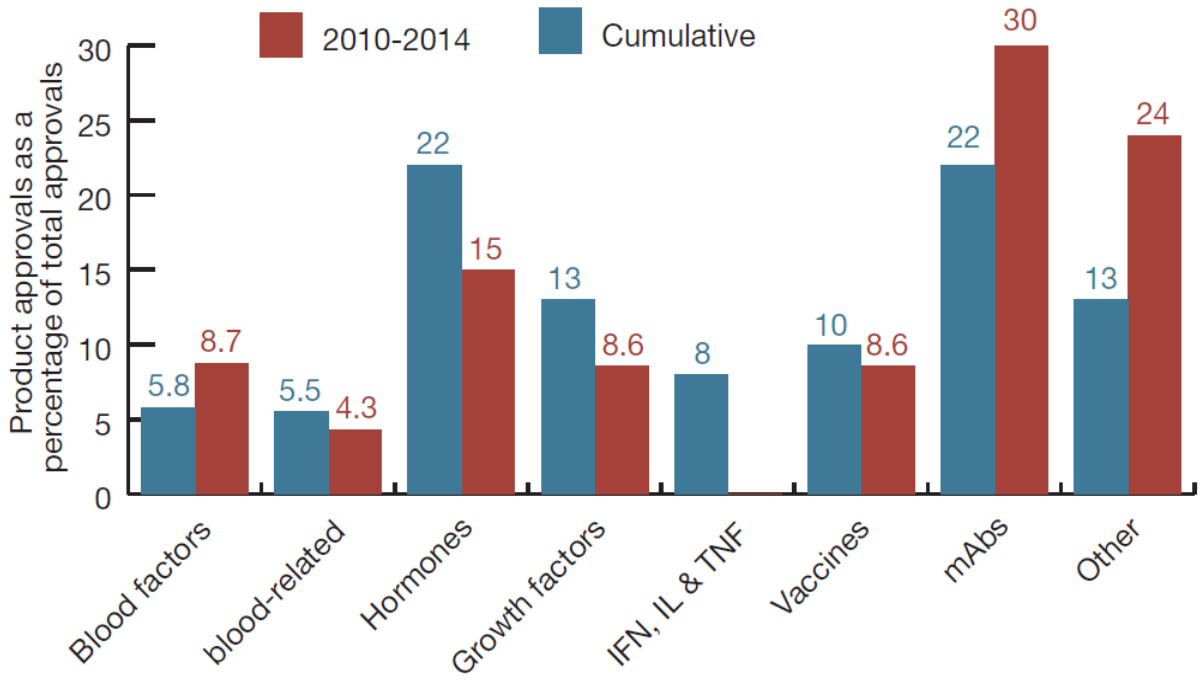

Figure 2 Approved products in the biopharmaceutical industry
Expressed as a percentage of total approvals. The red bars represent the period from 2010-2014, while the blue bars are the cumulative figures for the period 1982–2014. Image from (Walsh 2014)

Nowadays, the biopharmaceutical industry produces molecules of nucleic and amino acidic nature. The most characteristic representatives are proteins, and more specifically monoclonal antibodies (mAbs) and their derivatives (Walsh, 2014) (Figure 2).

1.1.1 Production system requirements

In order to have a production system that is suitable for biopharmaceutical purposes, cell lines need to hold specific characteristics that would allow them to perform efficiently at certain standards. Some of these requirements are:

Suspension culture: cell lines need to be able to grow in suspension. This is fundamental in order to maximize and standardize the production in reactors. Unicellular organisms are easy to adapt to suspension. On the other hand, mammalian cells are difficult to adapt due to their original conformation in tissues and their sensitivity to share stress because of their big dimensions and membrane thickness.

Cell growth: cell lines need to have a short doubling time, as this will shorten all the stages of the process. As an example, *Escherichia coli* has a doubling time of over half an hour (Prasad, Khadatare and Roy, 2011), while the Chinese hamster ovary (CHO) cell, one of the fastest mammalian organisms, doubles its population between 1 and 2 times a day, depending on the cell line (Percell Biologyca AB, 2000).

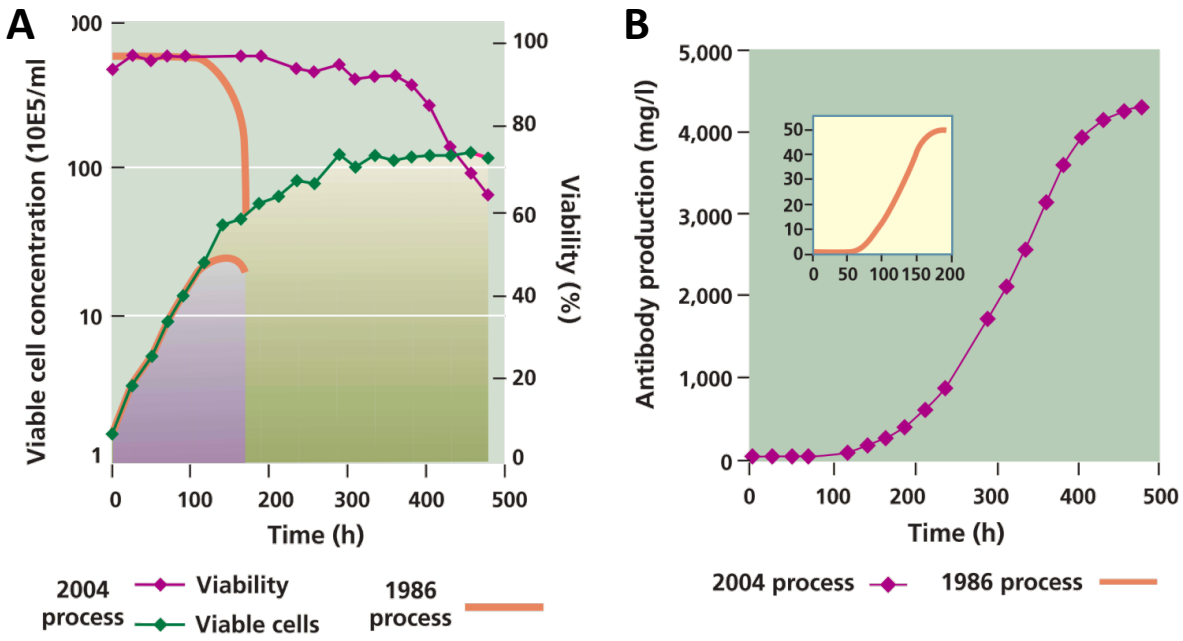

Figure 3 Comparison of different parameters of CHO culture in 1986 and 2004.
(A) Cell concentration (green-2004; orange bottom-1986) and viability (purple-2004; orange top-1986) of the cultures along time (hours). (B) Antibody production (purple-2004; orange small chart–1986) along time (hours). Image from (Wurm, 2004)

Final cell concentration is the maximum concentration to which producer cells can be cultured; it is considered a fundamental factor in order to obtain high recombinant protein titres, as these two parameters are often proportional. Cells can be stressed when cultured in high concentrations, limiting the production phase in fermenters. As an example, in 1986, the CHO final cell concentration was maintained over 1 million and cell viability preserved up to 180 hours. Following that time, cell viability and concentration were successfully engineered, with data from 2004 showing that a 100-fold increase in the antibody production (Wurm, 2004)(Figure 3).

Stable transfectants: cell lines transfected with a vector need to be stable, which means that the integration of the foreign DNA has to be inside the genome of the targeted system. When a subpopulation of the cell culture is not stable and no longer produces the desired protein, it gathers an energetic advantage, growing faster than the producer population. Therefore, the stability of transfectants is fundamental, as instability could lead to an overtake of these producers causing an economic loss. To avoid this phenomenon, selective chemicals are kept in the culture during the process.

Transient transfectants: in this case, the migration of DNA occurs within the cell without necessarily integrating into the genome. This is a fast, simple and efficient process to produce recombinant proteins and is mainly used for clinical trials.

Safety: producer cells have the potential to be infected by a disease or act as vectors of it. Consequently, it is important to identify and assess the level of jeopardy associated with this organism in order to meet regulatory agency standards for biopharmaceutical production.

1.1.2 Main host systems for recombinant production

There are different organisms used for biomanufacturing such as the prokaryote *Escherichia coli.* This was first used to generate recombinant insulin and currently, it is used to produce hormones and other biologics (Baeshen *et al.*, 2015). Another example is yeast *Pichia pastoris,* which, since its approval in 2009, has been mainly used to produce transmembrane proteins (Gonçalves *et al.*, 2013) (Walsh, 2010). These microorganisms are industrially attractive because their manufacture is cheap, it can be fastly implemented and is able to achieve high yields. At the same time, these systems have limitations due to their lower degree of complexity when maturing polypeptides.

Proteins that require an elaborated process of folding, assembling and posttranslational modifications are fabricated in mammalian cells.

Human cell lines such as human embryonic kidney cells (HEK), human retina derived cell line (PER C6) and human cells derived from amniocytes (CAP-T) are mildly used for industrial processes. Their ability to grow in suspension up to high concentrations under free serum conditions (Garnier *et al.*, 1994; Jones *et al.*, 2003) and to generate human posttranslational modifications, make them a promising future production platform (Fliedl, Grillari and Grillari-Voglauer, 2014). However, their drawback is their potential to carry human diseases, a fact that compromises safety. Recently, in 2014, HEK293 was approved for recombinant protein production of blood factors (Walsh, 2014).

Murine cells, on the other hand, are able to resemble many features of human posttranslational modifications (Walsh and Jefferis, 2006) and have a low risk of hosting

human diseases, making them the main organisms used in biomanufacturing at present. Some employed cell lines are: mouse myeloma NS0, baby hamster kidney cells (BHK) and Chinese hamster ovary cells (CHO). CHO cells are the most common mammalian expression system for large-scale commercial production of therapeutic proteins (Jayapal *et al.*, 2007).

1.2 Chinese hamster ovary (CHO) cells

Although many cell lines have been proved suitable for the production of recombinant proteins, the CHO cell line is the most common platform system used (Walsh, 2014). It is used in 66% of the total recombinant protein production and in 60% of the clinical trials (Wurm, 2013). In 2014, the FDA approved 11 new biopharmaceuticals, 8 of which were produced in CHO cells (Food and Drug Administration, 2015). The predominance of this murine cell line is due to different characteristics that make it more suitable for biomanufacturing.

To begin with, these cells have been proved safe, as their risk to host main human pathogens is low (Wiebe *et al.*, 1989). Secondly, their growth characteristics are suitable, as they grow fast in suspension and serum-free media, supporting high share stress conditions. Furthermore, they are able to fold, assemble and modify proteins at high titres, in a similar fashion to human cells (De Jesus and Wurm, 2011). Also, biotechnological tools that can genetically engineer CHO cells, are available. Finally, this cell line was the first mammalian cell line approved by the regulatory agencies for recombinant protein production, thus it now has a long, robust record of regulatory acceptance (J. Zhu, 2012).

1.2.1 History and cell lines

Chinese hamster ovary cells were isolated from a mammalian rodent (*Cricetulus griseus*) located at dry ecosystems such as the Gobi Desert in central Asia. This hamster was introduced as a model organism for laboratory experimentation in 1919, but it was not until 1957, that an ovary cell was isolated and used to start a cell line (CHO-ori) (Puck, Cieciura and Robinson, 1958).

Since then (1957-1970), this cell line was widely distributed among different laboratories. This was due to their fast growth rate, their low number of chromosomes and their big size and the fact that the cells can be easily mutated. The original cell line was used in monoculture studies with different purposes such as the study of gene function by the induction of spontaneous mutations. This situation created divergence across laboratory cell lines at a very fast pace and at the same time new desired features of culture behaviour were selected.

Puck and Kao studied and cultured CHO-ori for more than ten years and created a new cell line called “CHO-K1” with a considerably lower amount of DNA. This cell line became very popular and intensively distributed along many research laboratories. Afterwards, the CHO-DXB11 was originated by Urlaub and Chasin in 1980 (Urlaub and Chasin, 1980). This cell line is Dihydrofolate reductase (*DHFR)* negative, with one *DHFR* locus deleted and a missense mutation existing on the second one. This cell line became the first one to be used for the production of recombinant proteins in 1983.

Fintoff in 1976, characterized the CHO-Pro3^{-} cell line as unable to produce proline (Flintoff, Davidson and Siminovitch, 1976). After exposing it to ethyl methane sulfonate (EMS), one of

the *DHFR* copies was deleted (CHO-MTX^{RIII}) and further experimentation under gamma radiation by Urlaub and Chasin, caused a deletion of the second locus in 1983, giving birth to one of the most used cell lines, CHO-DG44 (Urlaub *et al.*, 1983).

Another CHO-ori cell line was sent to Tobey's lab and a variant was created after several years of study. In 1973, Thompson isolated a suspension-adapted culture from Tobey's variant, known as suspension CHO line (CHO-S) (Thompson and Baker, 1973). However, the lack of a gene amplification system was a major drawback for its later development into industry. Instead, lines like CHO-DG44 or CHO-DXB11 with amplification systems available, were preferred as producing lines and then adapted individually to suspension.

Along the years, different cell lines have been stored in different cell banks such as the American Type Culture Collection (ATCC) or the European Collection of Cell Culture (ECACC).

This has been done in order to cryopreserve original cell lines from evolutionary changes and to distribute them for research purposes.

Currently, there are three main streams used for research and product development, the stream CHO-K1, which uses a GS amplification system and the DG44 and CHO-DXB-11 lines, which have a DHFR amplification system (Lewis et al., 2013). When cells are transfected, a cell population with different numbers of exogenous DNA copies is created. The ones having more copies, are those with the potential for higher recombinant protein production. Therefore, during the first years of mammalian biotechnology, the focus was to develop systems that could select better producers (amplification systems) (Figure 4).

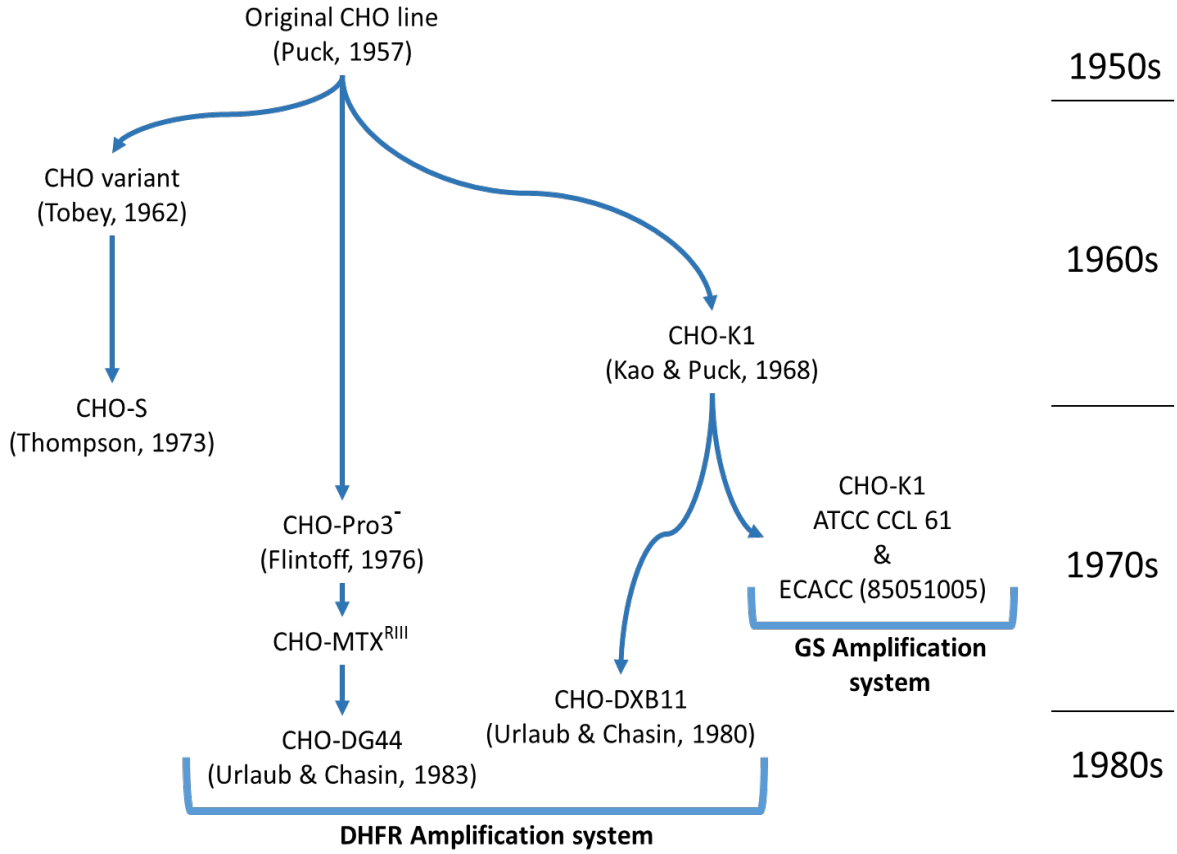

Figure 4 Chronologic diagram of the different CHO cell lines
Showing the main isolated CHO cell lines and their amplification systems

1.2.2 Genomic variability

During the last 50 years, CHO cells have been cultured and distributed creating high genome variation. In nature, hamsters possess eleven pairs of chromosomes. In cell cultures, this number can vary between cell lines and within the same population, due to the lack of constraints that a cell from the organism would have. Chromosomal structure and integrity

are also very unstable. As a result, over the years, chromosomes have changed drastically and at least one from each couple has been heavily affected (Figure 5).

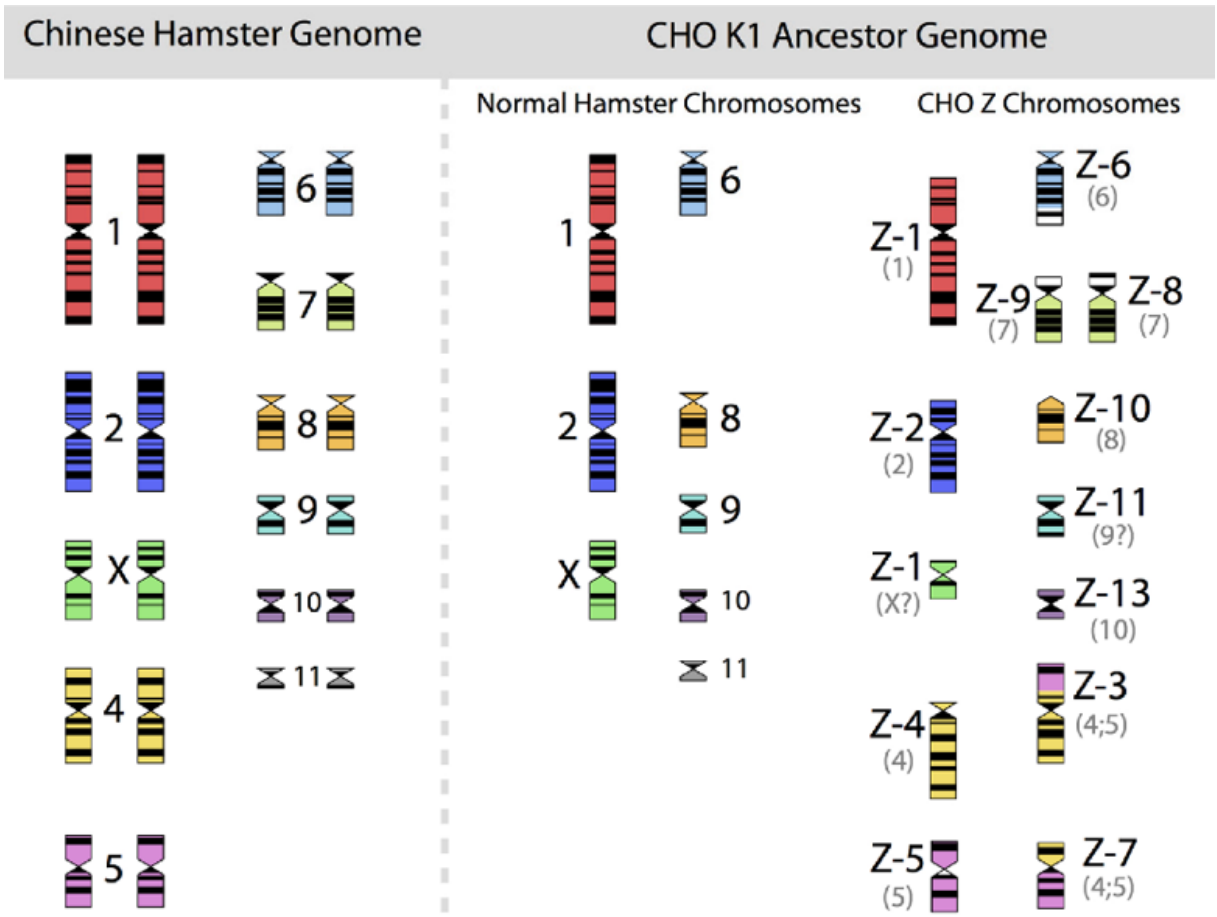

Figure 5 Chromosome structure and integrity
The figure shows a normal Chinese hamster genome (left) and a CHO-K1 cell line, which has eight normal chromosomes and thirteen considerably modified (right). Image from (Wurm, 2013) and adapted from (Wurm and Hacker, 2011).

In 2011, the first CHO cell genome was published (CHO-K1) (Xu *et al.*, 2011) and in 2013 the genome differences between the main cell culture lines (CHO-S, DG44, and CHO-K1) were studied (Lewis *et al.*, 2013). The comparison is limited as there is no CHO-ori genome to be

compared with. Therefore, until an outside CHO cell line that does not share the same history as the current culture lines is found, the amount of information is restricted. Finally, in 2015 the genome of the cell line CHO-DXBB11 was sequenced (Kaas *et al.*, 2015).

1.3 Production of recombinant proteins and challenges

CHO cells are widely used to make recombinant proteins. Many of these proteins are successfully produced at high titres, but this was not always the case. During the first days of recombinant CHO production, cultures were limited in the amount of heterologous protein that they could output.

The first strategies trying to overcome the low production, were focused on the expression phase. The aim was to increase and stabilize the gene expression through the increase of DNA intake, the use of a new vector system and the improvement in culture techniques and media development (Almo and Love, 2014).

Nowadays, the bottleneck is related to the maturation process (Le Fourn *et al.*, 2014). This could be due to the lack of common evolutionary history between the folding mechanism and the recombinant protein. This is also extenuated due to a constant culture pressure towards maximum production. As a result, recombinant proteins can be misfolded, poorly transported or undesirably targeted by molecular chaperones. This results in their retention and promotes aggregation. This in result causes agglomeration inside the cell, leading to ER stress, unfolded protein response (UPR) triggering and ends in apoptosis. These phenomena are not predetermined by genetic features (Sato *et al.*, 2004), leading to the unpredictable variability between batches (Pilbrough, Munro and Gray, 2009).

Although monoclonal antibodies have been produced for decades and improvement of the production pathway has been achieved, some limitations inherent to the process still remain. The production rate of the chains is not proportional, eventually accumulating the exceeding one and causing difficulties for the producer cell (Schlatter *et al.*, 2005; Ho *et al.*, 2013; Reinhart *et al.*, 2014).

1.3.1 Protein folding and stability

The protein function is linked to their 3D-structure (final conformation). The process of an amino acid chain or "primary structure", to reach its final folded or native state is very complex. The main principle of protein folding is that the information needed for the correct folding lies within its amino acid sequence. This principle, called *thermodynamic hypothesis*, states that under a specific set of conditions, the final structure of the folding protein (native state) is the one which causes the lowest Gibbs free energy of the system (Anfinsen, 1973).

This principle is true for most small globular proteins, which have a more direct process and can be easily studied in isolation to an atomic level, with techniques such as Nuclear Magnetic Resonance. Complex proteins, such as the ones produced in recombinant mammalian cells, are formed by multiple domains and are post-translationally modified. This affects the folding process, making it unpredictable. Cell-free studies cannot reproduce the folding process along the ER, and cell studies are only able to analyse slow or big changes in this process. Techniques for assessing protein conformation in intact cells are currently being developed to overcome these technical limitations (Sakakibara *et al.*, 2009).

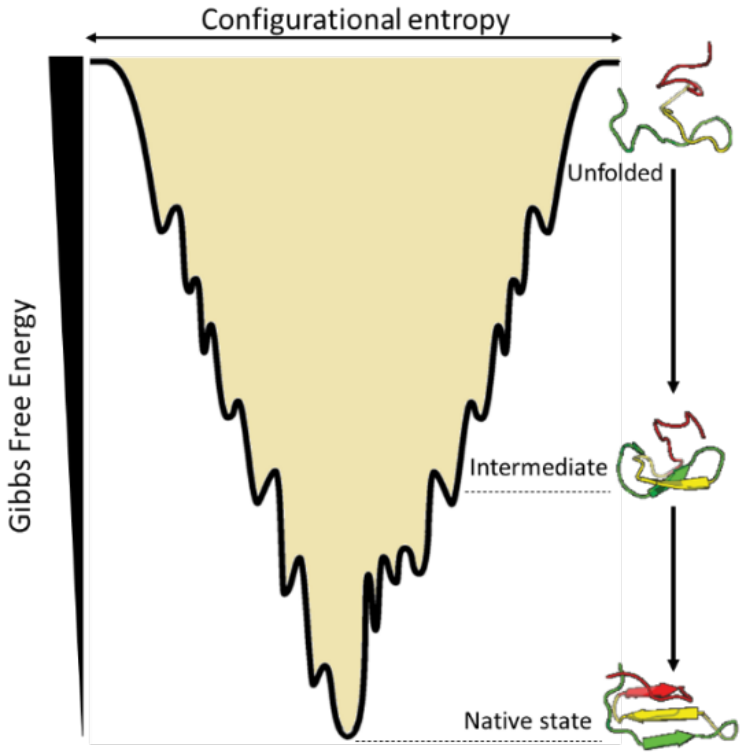

Figure 6 Diagram of the funnel protein folding
The vertical axis represents the Gibbs free energy of the system and how it decreases along the folding process until it reaches its native conformation. The width of the well represents the conformational entropy of the system giving a visual appreciation of the free movement of the chain and how it is restricted as it folded. Figure modified from (Mendoza-Espinosa *et al.*, 2009)

Independently of the protein type, the amino acid sequence resulting from years of evolution is based on the robustness of the folding process which is a broad concept influenced by many parameters (Onuchic and Wolynes, 2004). The funnelling theory supports the principle of robustness; it states that random alterations do not affect the capacity of the protein to fold. Generally, proteins tend to achieve their functional form by energetic drive; this process can be interpreted as a funnel of energy where polypeptides tend to approach their native state while energy is lost along the process (Figure 6).

Amino acid chains do not arrange themselves in structures, such as domains; that could be a conflict when considering the assembling process. Instead, successful proteins tend to have folding events that are cooperative and supportive. Thus, mild mutations could make proteins shift between different paths of the same route If the folding route is truncated, in the case of severe mutations, then another route can undertake the folding process, as long as the final structure stability is not compromised (Onuchic and Wolynes, 2004).

When the final protein conformation is compromised, proteins tend to expose hydrophobic residues to the media as their concentration increases, interacting with each other and giving form to aggregates (Dobson, 2003). This is sometimes the result of a domain swapping effect (Liu *et al.*, 2001). The nucleation phase, where proteins start to aggregate, is a slow stage, where the system's Gibbs free energy increases. Aggregation, on the other hand, becomes faster along the growth phase, because of a free energy decrease in the system. The length and transition between the stages are specific for each process (Eisele *et al.*, 2015).

Recombinant mammalian proteins are in most cases mAbs, which are large multidomain complexes with many post-translational modifications; their high production by cell factories (CHO cells) at the ER, often causes aggregation problems, making the industrial process less effective. The most studied case of aggregation nowadays is amyloid β peptides, intensively researched because of its relation to Alzheimer's and Huntington's disease (Eisele *et al.*, 2015); in this case the aggregation event is well understood and transferring knowledge to recombinant protein studies could be useful (Hartl and Hayer-Hartl, 2009).

1.3.2 Protein maturation and molecular chaperones

The process by which an amino acid chain achieves a fully functional protein structure is known as the maturation process. This mechanism can vary depending on the organism type or the final destination of the polypeptide. In eukaryotic cells, proteins with cytosolic function are directly produced in the cytoplasm, while proteins that need to be secreted or located in the membrane are produced and processed along the ER and Golgi; this is the case with mammalian recombinant proteins (Braakman and Bulleid, 2011).

During the maturation process, the protein is folded and additional modifications are implemented to form a fully functional polypeptide. These changes are known as post-translational modifications. Some examples are enzymatic changes or covalent adjustments which add specific features to proteins, such as recognition, half-life increase or quality control amongst others. One of the most important post-translational modification features is glycosylation, which can affect protein stability and track the protein folding process (Wang, Groenendyk and Michalak, 2015). This modification is fundamental in most recombinant proteins.

Protein maturation also involves molecular chaperones. These enzymes interact with newly synthesized proteins through their hydrophobic exposed areas. They then prevent aggregation and they assist the proteins to undergo through the correct folding pathways, although they do not assemble them. Their action also makes them capable of checking different points in transportation, by differentiating between properly and improperly folded polypeptides. This pool of proteins is also responsible for regulating the level of Ca^{2+} (Hayashi and Su, 2007), a signaling molecule that affects the ER function (Sambrook, 1990).

In the case of correctly folded proteins, the interaction with molecular chaperones along the maturation process is transient; they are then quickly released to continue with the next stages until they reach their final destination. On the contrary, misfolded proteins have a longer interaction with the enzymes and that prevents them from being transported into the Golgi system (Schuler *et al.*, 2010; Hartl, Bracher and Hayer-Hartl, 2011). If the proteins cannot be recovered, the chaperones will guide them to a translocon in the ER membrane, that will export them into the cytoplasm, where they will be targeted by proteasomes. This mechanism is known as the endoplasmic reticulum associated degradation path (ERAD) (Buchberger, Bukau and Sommer, 2010).

When the level of misfolded proteins is high, the degradation system cannot cope with it. As a result, accumulation and aggregation are induced at the endoplasmic reticulum, causing ER stress and triggering the UPR.

1.3.3 Unfolded protein response (UPR)

The endoplasmic reticulum is highly regulated as it supports and possesses many cell functions that are fundamental for cell survivability. This organelle processes secreted proteins, and when folding problems occur, a complex signal pathway is activated to resolve the issue or terminate the cell, called the UPR (Bertolotti *et al.*, 2000).

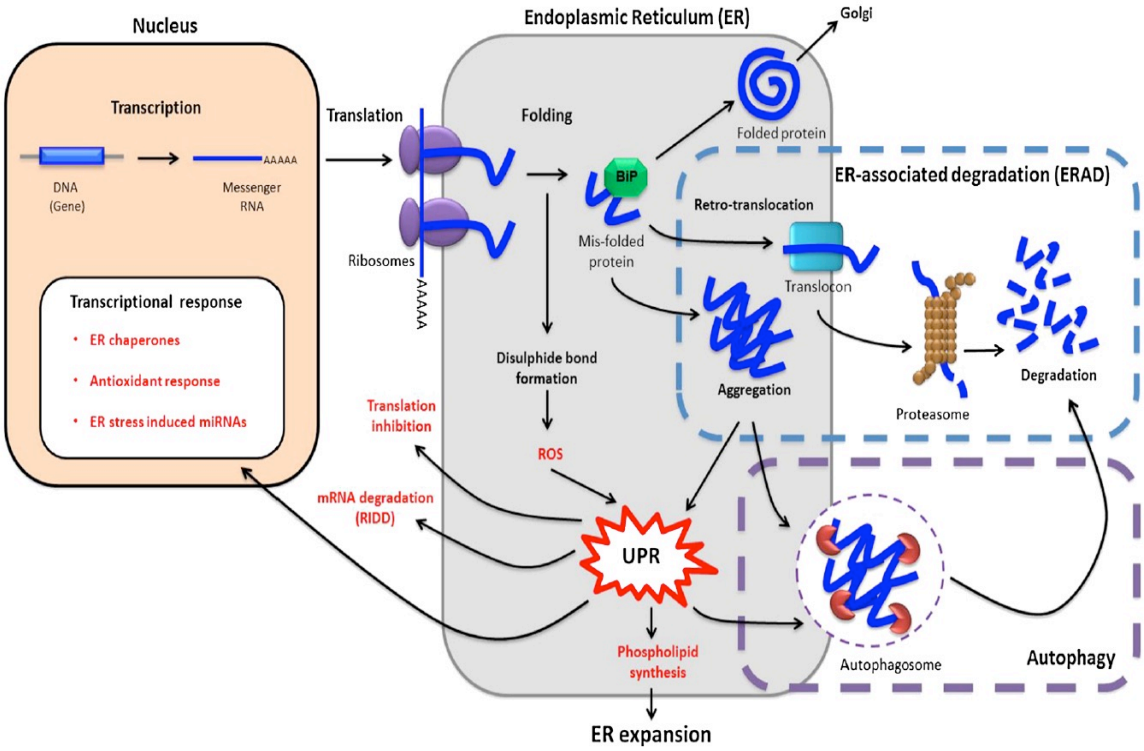

Figure 7 Unfolded protein response (UPR)
The mechanism is triggered by misfolding events. It can inhibit the translation and regulation at the transcriptional level to improve ER folding and restore homeostasis. The UPR also promotes the membrane expansion through phospholipid synthesis and degradation pathways (ERAD and Autophagy). Furthermore, UPR can be activated by reactive oxygen species (ROS) formed during the protein folding process. Image from (Hussain, Maldonado-Agurto and Dickson, 2014).

The UPR is normally activated to recover and preserve the integrity and functionality of the ER. In order to do so, the UPR works through a cascade of signalling pathways that cause different outcomes.

Some pathways are able to inhibit the translation and promote mRNA degradation, while others act at the transcriptional level, by affecting molecular chaperones and by regulating the expression of secretory proteins. Another route works through the expansion of the ER

through lipid synthesis. This route aims to make more room and facilitate the formation of autophagosomes, which can then isolate protein aggregates, in order to degrade them (Figure 7).

If the combination of responses fails to balance the ER homeostasis and functionality, the UPR takes a terminal path triggering apoptosis. Under some circumstances, when protein production is intense in the ER, considerable amounts of reactive oxygen species (ROS) are produced, which could activate the UPR apoptotic pathway directly (Eletto *et al.*, 2014).

Although a lot is understood about each path involved in the UPR system, there is still a lack of knowledge around the set process behaviour, making predictions uncertain (Hussain, Maldonado-Agurto and Dickson, 2014).

1.4 Optimization of recombinant protein production

The biopharmaceutical industry has been trying to reduce costs associated with the production of recombinant proteins. Different approaches have been tested in order to achieve improvements in recombinant protein production. These strategies include the use of better expression systems, enhancement of media composition and implementation of favourable culture conditions. The final scope is to extend the lifespan of the culture (Sunley and Butler, 2010) or reach higher cell densities (Sheikholeslami, Jolicoeur and Henry, 2013; Kishishita *et al.*, 2015) which would lead into an increase of the therapeutic protein produced.

Other strategies relay in the control of non-desirable metabolite production such as lactate or ammonia or the control of media depletion such as glucose (Lao and Toth, 1997; Tsao *et*

al., 2005; Freund and Croughan, 2018; Noh, Shin and Lee, 2018; Pereira *et al.*, 2018). One of the most reliable ways to accomplish this, is through the induction of cytostatic culture conditions.

1.4.1 Cytostatic culture conditions

Cell culture characteristics that could help the protein production, involve a delay of the cell growth and an increase of specific protein production during key moments, while maintaining viability. Cellular metabolic features result in a shift towards reducing nutrient consumption, low toxic compound formations and reactive oxygen species. This is done by increasing the protein half-life, by reducing the degradation pathways and by delaying their progress through the cell cycle and apoptosis. A combination of these features often accomplishes an increase in q_p (Avello *et al.*, 2017).

The addition of cytostatic components that are able to decrease the cell growth rate is one of the main strategies to achieve these conditions. The method by which cell growth is stopped in order to increase protein production, is likely to do with triggering secondary metabolism in the cells as differences in regulatory pathways between a cell fully growing and the one that is arrested is considerable (Pereira, Kildegaard and Andersen, 2018).

Growing cells are mainly committed to biomass production destined to increase their size and divide. Stationary cells are likely to be more prone to product synthesis. These cells do not need to spend the energy and molecules to grow and divide; they use the resources available for recombinant protein synthesis (Vergara *et al.*, 2014; Pereira, Kildegaard and Andersen, 2018). This principle is the base of many methods that help protein production, such as low-

temperature shifts, hyperosmolarity and chemical additives. The mechanism by which the different strategies accomplish the improvement of specific protein production is by cell cycle arrest (Sunley and Butler, 2010).

All these methods accomplish final titre increase through what is described as a cell culture biphasic strategy. The culture is initially kept under optimal conditions for cell growth, with the aim to accomplish fast cell concentration and biomass accumulation. The second stage focuses on implementing conditions to achieve the highest specific protein production while maintaining good quality (Kaisermayer *et al.*, 2016).

1.4.1.1 Role of the cell cycle phase in static cultures

Many parameters are of importance when maximising heterologous protein expression, such as media composition, gas diffusion, cell culture stage, cell size (Lloyd *et al.*, 1999, 2000). The effect of the cell cycle phase arrest is another variable studied. There is a correlation between the number of cells in G_1 and the increase of recombinant protein expression (Hendrick *et al.*, 1999; Dutton, Scharer and Moo-Young, 2006). The possible mechanism behind this is the fact that G_1 cells tend to be larger in size and have a more active metabolism (Carvalhal, Marcelino and Carrondo, 2003; Bi, Shuttleworth and Al-Rubeai, 2004). The proportion of G_1 cells can therefore be used as a marker of the improvement of production.

1.4.1.2 Strategies to improve recombinant protein production

Previous studies have used mild hypothermia, hyperosmotic pressure and the addition of small molecules with no direct nutritional value to improve the cell specific productivity (q_p).

These strategies have also been used to reduce problems in the production phase such as aggregation (Johari *et al.*, 2015a).

1.4.1.2.1 Temperature shift

Temperature is a variable that impacts both the cell growth rate and the protein expression rate. By modulating temperature conditions, we can initially favour cell growth to then allow shifting into conditions that increase protein synthesis. This optimises fed-batch cultures. Mild hypothermia (reduced temperature) has been used to slow down cellular growth while allowing protein synthesis to continue, improving q_p values (Chen, Wu and Liu, 2004; Trummer *et al.*, 2006; Kou *et al.*, 2011; Gomez *et al.*, 2012). Temperature reduction can also reduce protein aggregation in a cell culture reactor (Johari *et al.*, 2015a).

1.4.1.2.2 Osmotic pressure

Another method for modulating cell growth rates is by altering the osmotic pressure of the media. The negative effects caused by the hyperosmotic pressure conditions can be counteracted by the addition of the osmolyte glycine betaine. This can achieve slower cellular growth and, in some circumstances, can improve the q_p value (Ryu *et al.*, 2000; Tae Kyung *et al.*, 2000; Kim and Lee, 2002). It was believed that the presence of low concentrations of glycine betaine does not interfere with cell growth or protein synthesis and that its effect was just targeted on helping the cell to cope with the described conditions. However, more recent work has found glycine betaine to be capable of reducing aggregation (Mortazavi *et al.*, 2018).

1.4.1.2.3 Chemical additives

The addition of low-molecular weight molecules with no nutritional value is another strategy to improve recombinant protein production. These chemicals have the potential to improve product yields by either modulating cell growth, stabilising the product or reducing chemical modification. Butyric acid, valeric acid, valproic acid, 4-phenylbutyric acid and zinc have been used in recombinant CHO cell culture media (Yam *et al.*, 2007; Jiang and Sharfstein, 2008; Yang, Lu and Nguyen, 2014; Coronel *et al.*, 2016; Avello *et al.*, 2017; Paul *et al.*, 2018; Prabhu, Gadre and Gadgil, 2018). Valeric acid (pentanoic acid) produced higher product titres and increased q_p for an unnamed recombinant protein in CHO cells (Liu, Chu and Hwang, 2001; Coronel *et al.*, 2016). Valproic acid (2-propylpentanoic acid) addition to cell culture media has also been reported to improve antibody expression (Yang, Lu and Nguyen, 2014; Paul *et al.*, 2018). 4-phenylbutyrate has also been used to minimise aggregation in proteins expressed in CHO cells (Yam *et al.*, 2007).

The number of chemical additives developed and the understanding of their mechanism is limited. These chemicals are often very specific and can rarely be used across different cell lines or recombinant molecules reliably. With all this, the identification of further potential additives is desirable in order to increase the flexibility of engineering options during production processes.

1.5 Recombinant monoclonal antibodies

Monoclonal antibodies are the main proteins produced by recombinant CHO cells. These are highly complex proteins formed by four polypeptide chains, whose maturation process involves assembling while folding.

1.5.1 Heterogeneity of monoclonal antibodies

The improvement in the quantity of the heterologous protein produced is one of the main aims when trying to optimise the biopharmaceutical production process. However, the quantity produced should be constrained by the quality of the product (Hadavand, Valadkhani and Zarbakhsh, 2011).

The main factors that affect the quality are the monoclonal cell line, the process conditions and the culture media. The cell production process is affected by the surrounding environment creating different metabolic profiles in different conditions; this leads to a product with variable attributes. Therefore, media composition and culture conditions are fundamental in defining the quality of the product (Torkashvand and Vaziri, 2017).

Monoclonal antibodies are intrinsically heterogeneous. The variants can be classified to those having a negative impact on the quality of the product (product-related impurities) and to those that do not have any negative effect on the efficiency of the biologic or its safety (product-related substances). As many product-related molecules as possible are supposed to be removed during the production process in order to optimise the procedure. Nevertheless, there has to be a compromise between product purity, process complexity and

expenditure, leading to only partial purification. Subsequently, the initial heterogeneity of the product previous to processing, is the key to the final product quality (Liu *et al.*, 2016).

The heterogeneity of the recombinant monoclonal antibody, is a result of post-translational modifications and degradation reactions. These changes cause differences in molecular weight, charge, etc. Most of these modifications occur between the cell culture stage and the purification step with protein A columns. Modifications can occur due to enzymatic or non-enzymatic reactions inside or outside the cell (Liu *et al.*, 2008)

It is commonly assumed that antibodies are inherently variable in charge and that this profile is a representation of the modification state of the product. As a result, charge-based analytical techniques are commonly used to assess the quality and heterogeneity of the product. Compromised functionality is also linked to the structure of the compound. Understanding the integrity and behaviour of the drug produced is essential when identifying the quality of the heterologous protein. As a result, techniques that are able to assess the folding and assembling quality, as well as the product's behaviour when interacting within itself (eg. whether it causes aggregating patterns), are fundamental to ensure safety (Fekete *et al.*, 2013).

1.5.2 Monoclonal antibody modifications

The heterogeneity of the product, although sometimes intrinsic to the process, is often the result of specific modifications taking place. It is fundamental to understand the modifications that are causing these changes, as this could indicate the source of the change or the implications in the structure and functionality of the biopharmaceutical.

1.5.2.1 Disulphide bonds

The disulphide bond is a fundamental modification of the cysteine residues in order to form and maintain the structure of the monoclonal antibody. Although these modifications are highly consistent (Zhang and Czupryn, 2002), changes in the pattern of the disulphide bonds can be observed. Incomplete disulphide bonds are sometimes present in the culture, thus leaving behind two very reactive sulfhydryl groups which lead to free thiols (Lacy, Baker and Brigham-burke, 2008). The lack of a disulphide bond can be a result of either incomplete formation or posterior reduction of the already existing bond. In either case, this causes decreased stability to the monoclonal antibody and leads to an increase in aggregation (Huh *et al.*, 2013). These modifications are mainly found in the variable domains. The sulfhydryl group is not charged under neutral conditions and does not affect the charge heterogeneity. However, the lack of disulphide bonds could cause structural disturbances that could lead to changes in charge or size (Buren *et al.*, 2009).

1.5.2.2 Glycosylation

Glycosylation is a post-translation modification of the primary structure of the peptide and one of the most important ones in the cells. Glycosylation is an enzymatic reaction where monosaccharides are added, cleaved and modified as the antibody matures. Heterogeneity of the glycan structure is common and it is mainly a result of the synthesis and processing inside the cell. Studies with late culture conditions have shown that glycoside activity can also occur outside the cell (Gramer and Goochee, 1993; Gramer *et al.*, 1995). The glycosylation profile is influenced by many factors such as the cell line, the nutrient levels, the age of the culture and the accumulation of metabolic products. These different parameters can interfere

with the enzymatic activity of the glycosylation process or they can shift the availability of the nucleotide sugar precursor. One feature of the glycosylation pattern that can affect the quality of the product considerably, is the sialic acid addition, which triggers the human immune response. Sialic acid possesses a negative charge and can shift the isoelectric point of the molecule; CHO cell lines tend to have low quantities of this molecule (Maeda *et al.*, 2012). Another feature that can affect the quality is the high content of mannose, which is related to low immune system recruitment (Kanda *et al.*, 2006) and a shorter half-life (Goetze *et al.*, 2011; Alessandri *et al.*, 2012).

1.5.2.3 Peptide ends modifications

The N-terminal glutamine present in the heavy and light chains of the monoclonal antibody, is converted to pyroglutamate. This cyclisation is mainly a result of fermentation and is more prevalent in extended cultures. However, cyclisation can also occur as a result of purification steps (Dick *et al.*, 2007). A loss of the N-terminal primary amine can occur; this process would lead to a drop of the isoelectric point. Nevertheless, this modification does not seem to cause any change in potency (Lyubarskaya *et al.*, 2006).

The lysine can also be removed from the C-terminal of the heavy chain thus reducing the positive charge and causing an increase of the isoelectric point. Both modifications can appear fully or partially in IgG molecules, creating a diversity which can affect the charge heterogeneity considerably (Dick *et al.*, 2008). It has been shown that modifications such as lysine clipping to those regions do not cause structural changes (Tang *et al.*, 2013). However, a recent study showed that the removal or presence of complete terminal lysine residues,

lowers the complement-dependent cytotoxicity (CDC) response, by inhibiting the formation of hexametric rings (van den Bremer *et al.*, 2015).

1.5.2.4 Deamidation

Deamidation is a common non-enzymatic process which occurs mainly in asparagine residues in monoclonal antibodies (Wright and Urry, 2008). This modification is linked to ageing degradation pathways and it causes important shifts of the charge heterogeneity profile (Ponniah *et al.*, 2017). Long periods of culture, high temperature or high pH can increase the levels of deamidation (Pace *et al.*, 2013). This modification can occur at any given time, from the maturation of the antibody inside the cell to its storage. Deamidation causes the asparagine to be modified into aspartic acid, thus adding a negative charge and increasing the number of acidic species (L. Huang *et al.*, 2005).

1.5.2.5 Oxidation

Oxidation of methionine is one of the major degradation pathways in protein pharmaceuticals. Oxidation occurs in many amino acids, making the side chain more polar and increasing the isoelectric point of the recombinant protein. Although methionine is the most susceptible amino acid for this modification, other residues such as tryptophan, histidine and proline can go through this modification at a lower rate. Cysteine is also a plausible site, but due to the fact that these residues are often forming disulphide bonds, the chance of oxidation is limited. When oxidation occurs in methionine residues located in the conserved Fc region, this results to a loss of the neonatal Fc receptor binding and a decrease of the complement-dependent cytotoxicity (CDC) activity (Mo *et al.*, 2016).

1.5.3 Rituximab

Rituximab was the first monoclonal antibody approved for treating cancer in patients with leukaemia, in 1997. It was further approved for use in autoimmune related diseases. This chimeric Immunoglobulin G (IgG), is a subtype 1 and has the capacity to target the B lymphocyte surface receptor CD-20. The global sales for Rituximab were 7.78 billion dollars during the 2017 fiscal year and 29.1 billion dollars over the period 2014-2017. Due to its success and the fact that the patent would expire in 2018, a second wave of 6 drugs derived from Rituximab has been approved in 2017 (Walsh 2018).

1.5.3.1 Structure

Rituximab is an IgG type 1, which is the most abundant form in serum. This type of IgG is characterized by four peptide chains; two heavy chains and two light chains.

The light chain is composed of 213 amino acids and has two domains formed by interchain-disulphide bonds. The first domain is the variable light chain region (V_L), with a disulphide bond between amino acids 23 and 87. The second domain is a constant region of the light chain (C_L) and has a disulphide bond between 133 and 193.

The heavy chain is formed by 451 amino acids and is composed of 4 main domains. The first domain is the variable region of the heavy chain (V_H), formed by a disulphide bond between amino acid 22 and 96. The other three domains are the constant regions C_{H1}, C_{H2} and C_{H3} with sulphide bonds between 148-204, 265-325 and 371-429 respectively. The hinge is a region of 16 amino acids (220 to 235), located between C_{H1} and C_{H2}; this is where all the disulphide

bonds between the different peptide chains exist. Each heavy chain links to the light chain at residues Cys^{220} and Cys^{213} respectively. Cysteines in positions 230 and 233 form two sulphide bonds between the two heavy chains (Figure 8).

The structure also suffers post-translational modifications along the maturation and secretion processes. One of the main modifications is the addition of a glycan chain at Asn^{301}, in both C_{H2} of the heavy chains. This modification is fundamental to determine the structure of the fragment crystallisable (Fc) region, composed of the two C_{H3}-C_{H2} domains. Furthermore, the N-terminal glutamines of the peptides are cyclised to pyroglutamic-acid for both heavy and light chains. On the other end, C-terminal lysines from the heavy chain are often cut.

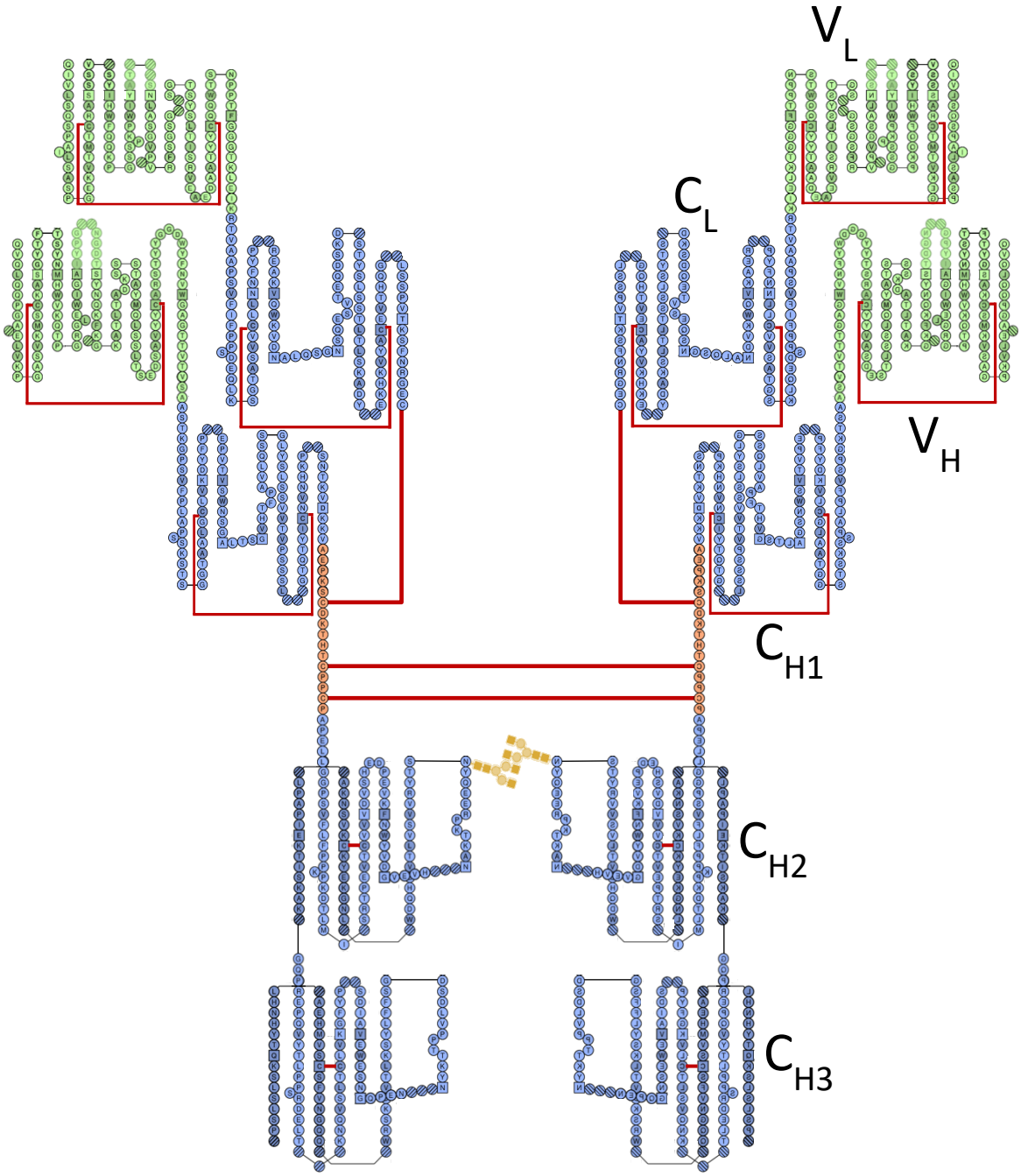

Figure 8 Rituximab structure
Rituximab as a "collier de perles" format with variable regions in green for the light (V_L) and heavy (V_H) chains and constant regions in blue for the light (C_L) and heavy (C_{H1}, C_{H2} and C_{H3}) chains. The hinge region is represented in orange. The disulphide bonds are represented as red lines between the cysteine residues. Glycosylation of the C_{H2} region is represented as a yellow sequence.

1.6 Database search and chemical selection

Web of science was the search engine used in this study in order to identify potential chemicals to test. The search terms used were: endoplasmic reticulum stress, unfolded protein response, protein aggregation, maturation, folding, stability.

Most of the information during the search was coming from biomedical studies. In order to assess this phenomenon, a study of different areas of research like biotechnology and microbiology and biochemistry and molecular biology was performed.

As expected, areas like biochemistry and molecular biology were found to be quite overlapping with biotechnology and microbiology (Table 1).

Table 1 Overlap (%) of biotechnology with other different areas of research

	Hits	Life Scn & BM	BC & MB	Cell Bio	Pharma	Scn Tch
ER stress	1327	17.6	74.2	50.0	42.6	15.5
UPR	779	13.2	78.4	70.5	34.3	18.0
Port. Maturation	7973	9.2	74.0	54.8	32.7	20.9
Prot. Aggregation	6476	6.0	62.4	24.2	46.9	24.7
Prot. Folding	34889	10.9	84.5	29.2	28.8	25.9
Prot. Stability	38942	6.3	63.2	13.6	35.8	22.2

Unfolded protein response (UPR), protein (Prot.), lifescience and biomedicine (LScn & BM), biochemistry and molecular biology (BC & MB), Cell biology (Cell Bio), Pharmacology pharmacy (Pharma), Science technology and other topics (Scn Tch)

On the other hand, life sciences and biomedicine were found to have a very small overlap. The number of hits from this area was equal or in most cases higher to the one from biotechnology and microbiology. This indicates that both fields of research are quite independent of each other, although they have the same degree of interest for the topics selected.

The reason that many of the hits came from biomedical studies, was the fact that events like aggregation are involved in human diseases. The most studied case of aggregation, is the one of amyloid β peptides, intensively researched because of their relation to Alzheimer's or Huntington's disease (Eisele *et al.*, 2015). In these cases, the aggregation event is well understood, therefore, transferring this utility to the recombinant proteins studies could be useful (Hartl and Hayer-Hartl, 2009).

As a result of this literature study, the selection process was focused on molecules with some, if not all characteristics (seen below) which could be beneficial for media culture addition in order to improve recombinant protein production. All the selected chemicals were heavily studied in other fields of research.

- The natural origin of the chemical and its presence in the diet. This would facilitate toxicological studies and it would positively affect their acceptance in the biopharmaceutical production process
- Ability to be easily produced, obtained and store. This would avoid shortage during process runs and find standard batches that will reduce variation of the chemical to a minimum.
- Previously described in the literature, with mechanistic understanding behaviour on their positive traits
    - Antioxidant
    - Antiaggregating
    - Anti-inflammatory or antiapoptotic
    - Cytostatic
    - Chaperone activity
- Affordable price

One family of chemicals that has received extensive research due to potential benefits to human health are the phenolic compounds, but research in their use as potential additives in cell culture media is limited (Hossler *et al.*, 2015; Tian, 2016; Chung *et al.*, 2019). Phenolic compounds are common in nature and play a range of roles, especially in vascular plants where they have been associated with antimicrobial activity, UV protection, antioxidant activity, antiaggregation and allelopathy (Jovanovic *et al.*, 1994; Pietta, 2000; Thorpe *et al.*, 2009). In some cases, plant-derived phenolic compounds have been credited with a diverse range of benefits for animal cells. Polyphenols have had diverse medical attributes allocated to them, including the treatment and prevention of cancer and cardiovascular disease. They have also been suggested to be antiulcer, antithrombotic, anti-inflammatory, antiallergenic, anticoagulant, immune modulating, antimicrobial, vasodilatory, and analgesic (Ozdal, Capanoglu and Altay, 2013). These group of chemicals heavily researched in the biomedical field possess traits that could be beneficial for recombinant protein production in CHO cell host systems.

A final group of fifteen molecules was selected, many of them were part of the phenol family, while others were previously researched in the biopharmaceutical industry. The next section of this thesis describes in more detail the structure and the characteristics of these molecules.

1.7 Chemical candidates

1.7.1 Sodium 4-phenylbutyrate (4-PBA)

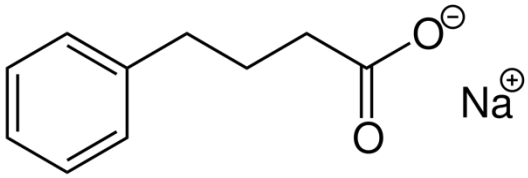

Figure 9 The chemical structure of sodium 4-phenylbutyrate

This is an aromatic fatty acid that has been extensively studied in the last two decades due to its potential chaperone activity as a hydrophobic soluble compound (Figure 9). Furthermore, cell-free studies demonstrated its capability to prevent aggregation (Kubota *et al.*, 2006).

Research on this component is mainly focused in the area of misfolding and ER-stress-related diseases (Kubota *et al.*, 2006; Kuryatov, Mukherjee and Lindstrom, 2013; Cho *et al.*, 2014). Although no specific mechanism of action is described, it was reported that sodium 4-phenylbutyrate is able to protect human cells from DNA damage and to reduce the ER stress (Lenin *et al.*, 2012) and the UPR (De Almeida *et al.*, 2007). Research done in CHO cells did not show any increase in the specific recombinant protein production(Roth *et al.*, 2012) nor any inhibition of aggregates (Hwang *et al.*, 2011).

1.7.2 Caffeine

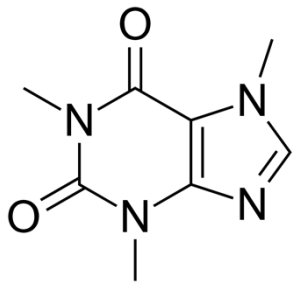

Figure 10 The chemical structure of caffeine

Caffeine is a chemical compound composed by trimethyl xanthine and is produced in plants (Figure 10). This chemical is found in foods such as coffee and tea. The compound is highly studied as it is a stimulant of the central nervous

system. This chemical was found to act by reducing ER stress (Hosoi *et al.*, 2014) and protective properties (Painter, 1980).

1.7.3 Caffeic acid phenethyl ester (CAPE)

CAPE is a molecule found in propolis, which is made by bees. It is used extensively in traditional medicine in Asia. This molecule is a phenethyl alcohol ester of caffeic acid and is highly bioactive. This compound was found to be protective against ER stress by some authors (Armagan *et al.*, 2008; Kavakli *et al.*, 2010). However, other recent studies show that this compound is highly toxic to the cell, causing apoptosis due to its pernicious effect over the mitochondrial dysregulation, through ER stress pathways (Jin *et al.*, 2008; Ozturk *et al.*, 2012). Cell resistance has been proven to be acquired (El-Khattouti *et al.*, 2015). Furthermore, CAPE is able to prevent the aggregation of platelets. This is due to the inhibition of platelet activation, by mobilisation of the calcium ion (Hsiao *et al.*, 2007).

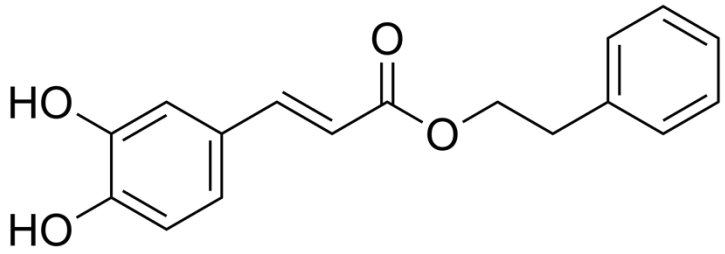

Figure 11 The chemical structure of caffeic acid phenethyl ester

Therefore, this compound has been heavily researched in food industry and medicine. However, the characteristics of the chemical are in principle undesirable for the production of recombinant proteins. There are no studies published on the effect of this chemical on recombinant producer cell lines and it was included in the present study.

1.7.4 Curcumin

This is a diarylheptanoid, grouped in the turmeric compounds (Figure 12). It has low solubility in water and it is used as a colouring agent in food industry (Yan, Geusz and Jamasbi, 2012).

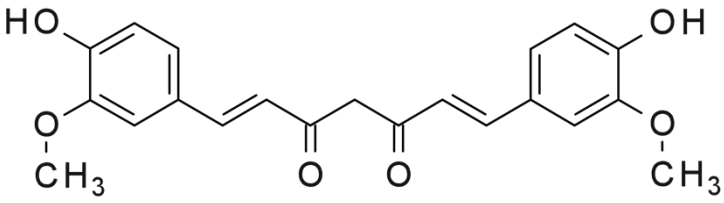

Figure 12 The chemical structure of curcumin

Curcumin folding activity was studied in a cell-free system and it was found that it can inhibit the nucleation of amyloid β aggregates. However, it was not able to inhibit or reverse the expansion phase (Borana *et al.*, 2014). Other studies showed destabilizing effects in the fibril formation of amyloid β aggregates, caused by this compound (Ono *et al.*, 2004). A study using different curcumin analogues, showed that the chaperone activity was different amongst them, highlighting how small changes in the chemical structure could lead to considerable changes in the chaperone behaviour (Endo *et al.*, 2014).

In vitro cell study experimentations, showed that this molecule has the capability to rescue the maturation of a mutated protein unable to properly fold which seemed to be linked to a drop in calcium levels at the ER (Robben *et al.*, 2006). Finally, studies done in CHO cells to assess whether the molecule would enhance the protein production titre, did not show any positive effects. On the other hand, there was a tendency to increase productivity when used in combination with glycine betaine (Roth *et al.*, 2012).

1.7.5 Catechin compounds

These are a group of antioxidants that belong to the flavan-3-ols (flavanols)(Figure 13). They are naturally produced from plants by secondary metabolism. They can be found in tea and wine as well as other food products derived from plants. In general, this group of chemicals seemed to have properties that would be of interest to this study.

Epigallocatechin gallate (EGCG) is the most studied compound of this group, as it is the most predominant in green tea. Medical research showed that this compound is able to help against aggregation problems (Ehrnhoefer *et al.*, 2008; Bieschke *et al.*, 2010; Bleiholder *et al.*, 2013). Furthermore, it can reduce the levels of ER stress, protein oxidation and apoptosis (Ferreira, Saraiva and Almeida, 2012).

Unlike other chemical components from the same group, the catechin chaperone activity has not been thoroughly studied. Medical studies showed that this molecule was able to protect cells against amyloid β peptides aggregation (Conte, Pellegrini and Tagliazucchi, 2003) and against ER stress (Lee, Kim and Heo, 2011), although this is probably connected to a mechanism not involving its antioxidant potential (Auger et al., 2005).

Epicatechin is an epimer of catechin and has not been extensively studied. Bastianetto published data indicating that this chemical did not prevent induced amyloid β aggregates in cell cultures. Furthermore, the combination of EGCG, ECG and Gallic acid inhibited apoptosis mediated by the accumulation of Aβ-aggregation (Bastianetto *et al.*, 2006).

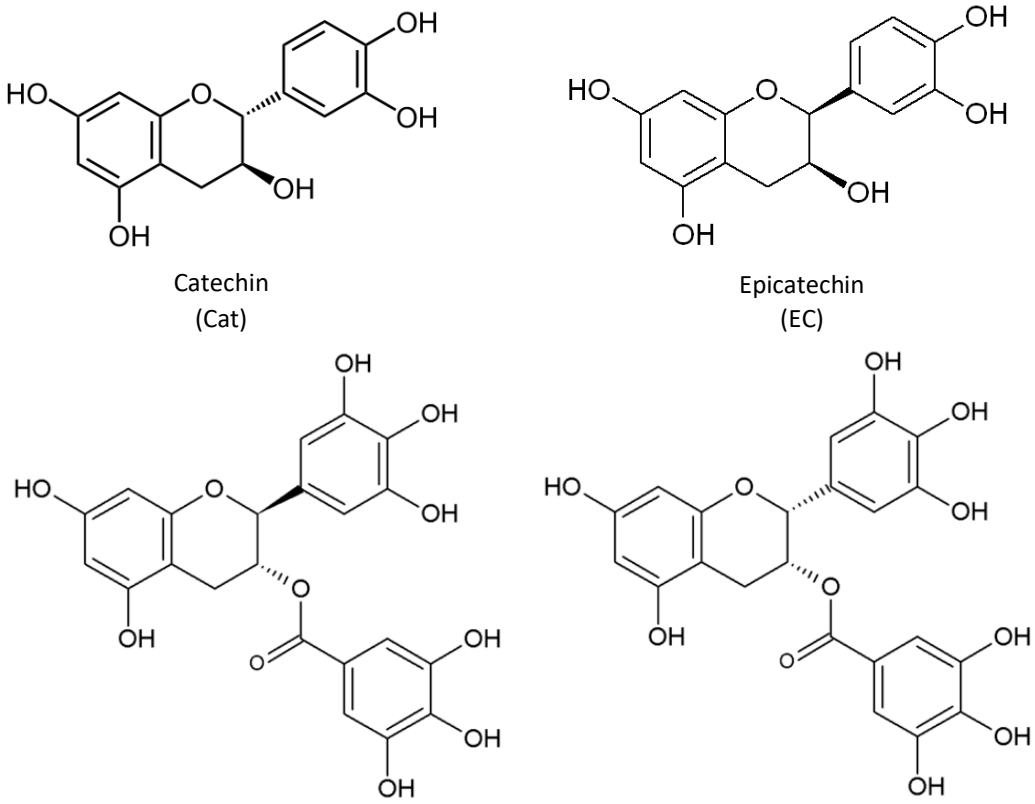

Figure 13 The chemical structure of catechins

1.7.6 Glycine betaine

Betaine (glycine betaine) is a natural amino acid derivate, produced by plants which use it as an osmolyte (Figure 14). It is abundant in foods like wheat, quinoa or spinach. Due to its osmo-protective properties, this chemical has already

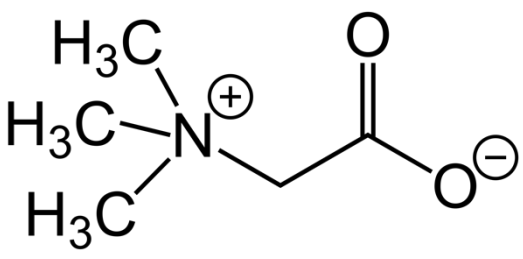

Figure 14 *The* chemical structure of betaine

been applied to biopharmaceutical industry under hyperosmotic pressure conditions, leading to an improvement of the specific protein production (DeZengotita *et al.*, 2002) and cell growth (Ahn *et al.*, 1999). This effect has been shown to vary, depending on the cell line (Tae Kyung *et al.*, 2000). The increase in production is mainly due to the elongation of the cell viability culture (Yoon and Ahn, 2007). This compound although heavily researched within recombinant IgG production process was studied as a positive control.

1.7.7 Kaempferol

This is a flavanol (Figure 15) found in plants and it can prevent amyloid β aggregates by inhibiting nucleation in cell-free studies (Nisha *et al.*, 2014) (Borana *et al.*, 2014).

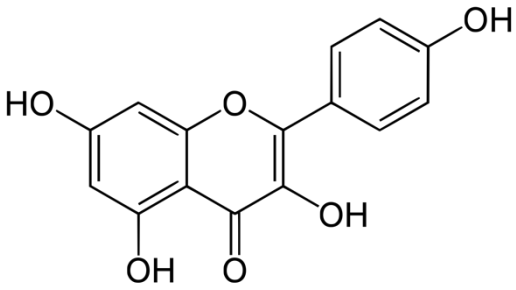

Figure 15 The chemical structure of kaempferol

The mechanism of action on the aggregation of proteins by kaempferol is not clear. Some studies indicate that the mechanism of action does not seem to be related to its antioxidant activity (Roth, Schaffner and Hertel, 1999). On the other hand, it is not clear whether its performance is due to a direct interaction with the protein, an indirect effect by interacting with estrogen receptors (Kim *et al.*, 2010) or a combination of both.

1.7.8 Luteolin

Luteolin or luteolol, is a naturally occurring chemical produced by plants. This type of polyphenol (Figure 16) is found in fresh vegetables such as green peppers or celery. As with most polyphenols, luteolin has been proven to be a very bioactive compound, able to interact with cells at different parts of the regulatory pathway, such as dopamine activation (J. J. Zhang *et al.*, 2010). Furthermore, this compound has been found to help against cell cellular stress (J. J. Zhang *et al.*, 2010) and more specifically induced mitochondrial stress (Murugesan and Manju, 2013). Luteolin was initially found capable of inducing ER stress and triggering apoptosis (Choi *et al.*, 2011; Park *et al.*, 2013). However, recent experimentations contradict this idea (Tai *et al.*, 2015; Wu *et al.*, 2015). Finally, this molecule is able to interact with molecules at the molecular level and prevent aggregation (Lee *et al.*, 2010; Churches *et al.*, 2014).

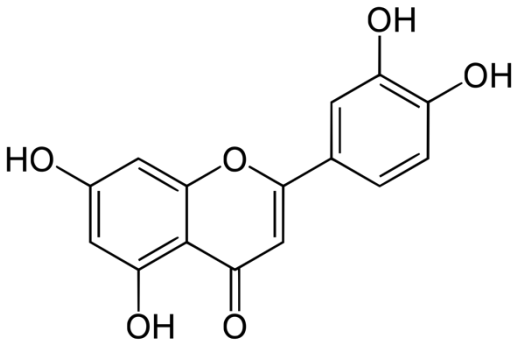

Figure 16 The chemical structure of luteolin

1.7.9 Piceid

Piceid or polydatin, is a stilbenoid glucoside produced by plants and found in great quantities in the skin of grapes. It is a derivate of resveratrol and is substituted with a glucosyl residue at position 3 (Figure 17). Recent studies show that this

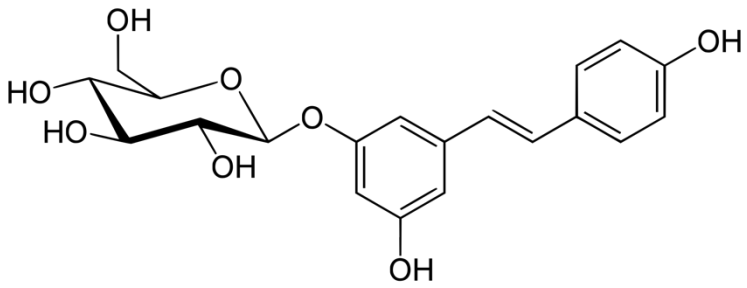

Figure 17 The chemical structure of piceid

compound is able to increase stress resistance, by creating a mitochondrial response in cells (Robb and Stuart, 2014). Furthermore, it seems that this chemical is a strong antioxidant, a characteristic that does not seem to relate to the release of a resveratrol molecule (Storniolo *et al.*, 2014). This is especially true when affecting lipids (Fabris *et al.*, 2008). Piceid is probably less studied due to its lower bioactivity when compared to resveratrol; this seems to be a result of the compound being more difficult to be assimilated by cells (Su *et al.*, 2013).

1.7.10 Resveratrol

It is a natural phenol from the group of the phenylpropanoids (Figure 18). Less toxic aggregates were formed during cell-free system studies using this molecule. However, the molecule could not shift or reverse more noxious conformations already aggregated (Ladiwala et al., 2010). Cell assays displayed two different behaviours depending on the molecule's concentration; concentrations above 50µM were toxic and arrested cell growth. Concentrations below 50 µM, prevented amyelation (Conte, Pellegrini and Tagliazucchi, 2003). Resveratrol' s mechanism of action, seems to be linked to an enhancement in the degradation path through the proteasome (Marambaud, Zhao and Davies, 2005), and it is proven not to be related to its antioxidant activity (Auger *et al.*, 2005).

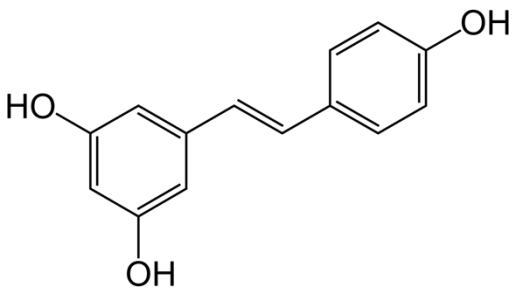

Figure 18 The chemical structure of resveratrol

1.7.11 Tocopherols

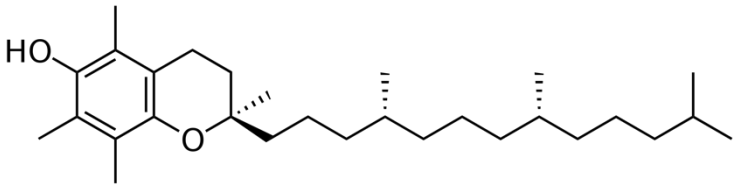

Figure 19 The chemical structure of alpha-tocopherol

Tocopherols are a group of organic, soluble, lipid compounds, that can be found in vegetable oils and fats. They are formed of four main types; alfa, beta, delta and gamma. All of them are compounds of vitamin E. They consist of a 2H-1-benzopyran-6-ol nucleus with a long hydrocarbon chain of 13 carbons, decorated with isoprenoid units; this gives these molecules antioxidant properties (Figure 19). Research in CHO cells found that the alpha and beta forms can alter the gene expression, by inhibiting the protein kinase C (Fazzio, Marilley and Azzi, 1997). Furthermore, tocopherol was found to be helpful against induced oxidative stress (Li *et al.*, 2008).

1.8 Aims of the study

The process and variability of recombinant protein production in CHO cell lines are still not fully understood. Clonal producer cell lines are inherently variable and difficult to predict. This is due to the fact that the process is related to many different features such as epigenetic traits, culture conditions and cell growth behaviour. These features cannot be fully controlled during the manufacturing production process. Nevertheless, control over the process is fundamental as it affects the quantity and quality of the biopharmaceutical. Uncontrolled batch cultures can pose problems such as aggregation, misfolding, degradation of the product leading to ER-stress, UPR response and apoptosis. This uncertainty in the production process can lead to economic losses and a potential shortage of needed drugs in the market.

A biphasic culture is one of the most common strategies to help the production and to control behaviour in the cell culture batch. The general mechanism involves stopping the cell growth in the final phase through cytostatic conditions. Strategies used include temperature shift, osmotic pressure and addition of low-molecular weight molecules. The development of chemical additives for recombinant protein production improvement in running CHO cells batch cultures is limited. Moreover, their use is very specific, with low transferability of the effect to other cell lines or recombinant products.

A number of studies on the use of natural chemical molecules is included in the biomedical research literature. These studies report the effect of these chemicals on mammalian cell cultures and describe their mechanism. Many parameters such as antiaggregation, antitumor and chaperone activity, associated with molecules studied in medical research, could be transferable to biopharmaceutical production processes in CHO cells. Therefore, one of the first steps of this study, was to select natural chemical compounds studied in biomedical literature. The selection would be based on traits that could favour recombinant protein production in CHO cells. Only chemicals not yet developed for biopharmaceutical process as chemical additives at the time of this study would be selected.

The overall aim of the project was to study and develop new chemicals as additives in order to improve protein production for recombinant IgG produced in CHO cells.

The objectives of this project were to:

- Identify the concentrations at which selected chemicals are capable of increasing q_p without jeopardising the viability of the culture

- Study the effects of successful treatment over time with screened chemical candidates on cell culture growth, cell morphology and cell cycle phase arrest
- Determine whether chemical treatments found to have an increase in q_p during screening, have the same effect in scale-up cultures and whether they cause an increase in the final titre production through optimization of feeding strategies
- Determine whether the increase in the final titre of IgG by the chemical additives has an effect on the quality of the product

The results of this dissertation are divided into four chapters.

- Chapter 3 focuses on developing a reliable method in order to assess the effect of chemical candidates on cell culture growth and specific productivity
- Chapter 4 studies the effect over time on cell culture conditions and cell cycle phase arrest
- Chapter 5 optimises feeding strategies of the chemical additives in scale-up cultures to assess the increase of the final recombinant IgG titre
- Chapter 6 examines the effect of the optimised feeding conditions on the quality of the product

Chapter 7 summarizes all the results and compares the findings to the available literature, suggesting areas of further work.

Chapter 2

Materials and methods

2.1 Cell culture

2.1.1 Maintenance of CHO cells

The cell line used in the experimentation was an IgG recombinant CHO-DG44 producer cell line, kindly provided by Fujifilm Diosynth Biotechnologies UK (FDBK). This cell line was maintained for the entirety of the project. The recombinant protein produced was a monoclonal antibody (mAb) called Rituximab; this targets a B-cell lymphocyte membrane protein called CD20. Cells were grown in 125 mL Erlenmeyer flacks, with 30 mL of culture media in a shaking incubator at 130 rpm and a 5% CO_2 modified atmosphere. The culture media used to grow the cells was an already prepared CD Opti-CHO™ (Life technologies ™) with L-Gln added to 8 mM and Hygromycin b to 100 µg/mL. Subcultures were done every 3-4 days alternatively, with an initial seeding density of 0.2 x 10^6 viable cells/mL.

2.1.2 Generation of CHO cell cultures in well plates

96-well and 24-well plates were set up with an initial volume of 200 µL and 1000µL respectively at a concentration of 0.2 x 10^6 viable cells/mL. Plates were incubated for 3 days in a static humidified incubator.

2.1.3 Generation of CHO cell cultures in Erlenmeyer flask

Cells were seeded to an initial concentration of 0.2 x 10^6 viable cells/mL, from a previous exponential phase culture. An initial volume of 33 mL of culture was seeded to a 125mL

Erlenmeyer culti-flask (Corning, Tewksbury, MA, US). The cultures were run under shaking humid conditions as specified in section 2.1.1 for a period of 10 days.

2.1.4 Detection of cell density, viability, diameter and circularity

A volume of 500 µL of each sample was used to measure the density, viability and morphology of the cell with a trypan blue exclusion method carried out by a Vi-cell™ XR (Beckman-Coulter, Brea, CA, USA). For 96-well plates, 150 µL from each sample was collected, mixed with Phosphate-buffered saline (PBS) buffer up to 500 µL previous to taking the measurement.

2.1.4.1 Measurement of LC_{50} and GI_{50}

Data from the Vi-cell was used to further calculate the lethal concentration at 50% LC_{50}. To do so, the number of alive and dead cells for each sample were analyzed by an R function developed by Pacheco and Revelo in 2013; this was based on Probit statistical test. Furthermore, the growth inhibition at 50% (GI_{50}) was calculated by analyzing the viable concentration and the viable cells' data coming from the Vi-cell reading. The R program tool requires the data to be positive integers. The two variables were determined as follows:

- Cell growth: number of cells that duplicated over this period of incubation
- Cell inhibition: cells that were not able to grow with respect to the control

"Cell growth" was calculated as the net VCD of the sample (subtracting the VCD at time 0) divided by the average of the Net VCD of the control samples, and multiplied by the number of viable cells in the sample (**Error! Reference source not found.**).

$$Cell\ Growth = \frac{VCD_f - VCD_0}{Avg(VCD_c - VCD_0)} \times\ Total\ Cells$$

Equation 1

"Cells inhibition" was calculated as the difference between the total cells of the sample and the previously calculated cells grew (**Error! Reference source not found.**).

$$Cell\ Inhibition = Total\ Cells - Cell\ Growth$$

Equation 2

When using the average to compare values at the end and beginning of the concentration range may lead to negative values of cells for cell growth or inhibition. The code used in these calculations is unable to process negative values, as it lays information as cells alive and dead. As a result of this, the negative values were corrected as specified in the following equations for cell growth (**Error! Reference source not found.**) and cell inhibition (**Error! Reference source not found.**).

$$Corrected\ Cell\ Growth = \frac{\left(\left(\left|\frac{Positive\ value}{Negative\ value}\right|\right) \times\ Positive\ value\right) + Cell\ Growth}{\left(\left|\frac{Positive\ value}{Negative\ value}\right|\right)}$$

Equation 3

$$Corrected\ Cell\ Inhibition = \frac{\left(\left(\left|\frac{Positive\ value}{Negative\ value}\right|\right) \times\ Positive\ value\right) + Cell\ Inhibition}{\left(\left|\frac{Positive\ value}{Negative\ value}\right|\right)}$$

Equation 4

Finally, the data was entered into the R coding system previously used for LC_{50} (Appendix 1).

This method is only used as a way to indicate toxicity and cytostaticity and does not pretend to generate accurate values. Complete and more define curves would have to be investigated and this was not the present work.

2.1.5 Direct protein quantification

Samples were centrifuged for 10 minutes at 400 g. Then, 200 µL of the supernatant is transferred (for 96-well plates, 100 µL of supernatant from each well was collected and mixed with 100 µL of PBS buffer) into a solid black 96-well plate (Greiner-bio-one, Kremsmünster, Austria). Finally, the plate was put in storage overnight at -80°C, and later used to analyze protein concentration with an Octet® QK^e (Pall FortéBio, Fremont, California, USA).

For specific protein production (q_p) traked over 10 day cultures, $q_p$was determined by dividing the total protein produced after ten days incubation by the integral of the VCD curve over the same duration (Renard *et al.*, 1988).

$$q_p(pg/cell \cdot day) = \frac{Final\ Recombinant\ titter\ Concentration(\mu g/mL)}{\int_0^{10} VCD(10^6\ viable\ cells/mL)}$$

2.1.6 Chemicals

The chemicals tested to validate the screening methods were selected based on previous studies (Table 1).

All the chemicals, due to their hydrophobic character, were dissolved into Dimethyl sulfoxide (DMSO) to its highest possible concentration and put into storage at -80ºC. Then, different dilutions from the stock concentration were pipetted into DMSO, in order to study their impact on the Cho cell cultures and their capacity to produce recombinant protein.

2.2 Flow cytometry

2.2.1 Propidium iodide staining protocol

This protocol is an optimized version adapted from Krishan (1975), the process of optimization s described below (section 4.2.1)

First, cells were collected from 24-well plate cultures and transferred into a 1.5 mL Eppendorf to be centrifuged at 300 g for 5 minutes. The pellet was then discarded. CHO cells are very robust and can endure high centrifugation speeds. This centrifugal force was selected based on empirical data from previous work done with this cell type in the laboratory. More extreme centrifugation at 400 g, had the same results in terms of pellet formation and cells were able to maintain integrity. These conditions can be adapted when cells are more difficult to collect

in the early stages, but if not needed it is better to use 300g as a conservative measurement to preserve the cell's integrity until fixation. Later, the cell pellet was resuspended gently into 30 µL of ice-cold PBS buffer. This step was performed in order to avoid clumps of cells and facilitate the fixation of cells that would follow. If the pellet was to be very abundant at this step, then 60 µL of PBS buffer could be used instead of the 30 µL one. However, this would also mean that the amount of ethanol in the subsequent steps should be doubled.

Next, cells were fixated with ice cold ethanol at 70% which was added drop by drop to the cell suspension, while vortexing the Eppendorf at medium intensity. Vortexing allows for the fast dissolution of the ethanol in the media. It also allows the ethanol to act on the cells homogenously, thus avoiding the formation of clumps and aggregates. Fixation was allowed for 30 minutes at 4^{o}C but this was flexible ranging from 20 minutes to overnight. Following fixation, cells were centrifugated at 400 g for 5 minutes followed by removal of the ethanol supernatant. At this stage centrifugation should not be a problem; cells come out from the solution easily and form a very compact pellet. In order to avoid future PBS passages without compromising the removal of ethanol, the maximum amount of supernatant possible, has to be removed at this stage. As ethanol is removed, the pellet would be exposed and rapidly dried due to the fast evaporation of the ethanol remaining in the pellet. That is why, the immediate subsequent addition of PBS buffer to the pellet in order to avoid the formation of aggregates and lumps, is crucial.

The pellet was then resuspended gently in 1 mL. Cells were left to rehydrate for at least 15 minutes. The volume of the PBS buffer wash needed to be maximized in order to counteract the lack of future washes and reduce the amount of ethanol left in the vial. Then, cells were centrifuged at 400 g for 5 minutes. At this stage cells tended to rehydrate and lose density, thus forming very fussy pellets. Therefore, this could result in considerable cell loss. For that

reason, it is recommended to use high speed when centrifuging in order to obtain the best pellet possible. Next, a supernatant removal and addition of 30 µL of RNAase (100µg/mL) and 200 µL of propidium iodide (50 µg/mL) were performed. Finally the sample was left to incubate for 5 to 10 minutes.

2.2.2 Flow cytometry and data analysis

Samples were analyzed with an Attune™ NxT Flow Cytometer & autosampler (Thermo Fisher scientific), The acquisition volume for each well was 200 µL the device was set to a high sensitivity with a flow speed of 100 µL per minute and 50.000 events per well.

Finally, the data collected was analyzed with FlowJo™ v10 (San Carlos, California, USA). In order to obtain reliable histograms, the information coming out of the flow cytometer needed to be gated. First, the cells were graphed in forward Scatter vs side scatter FCS-A vs SSC-A (Figure 20A). This graph shows the distribution of the cell population; it distinguishes different cell types and is used in this instance to identify that there is no more than one cell type in the sample. Secondly, the cell population is graphed by the height of the intensity vs the area (Figure 20B), this is in order to discriminate signals associated with two cells passing at the same time (doublets) they are characterized by having the same high but an increased area. As a result, only signals inside the diagonal between blue laser fluorescence area (BL2-A) and blue laser fluorescence height (BL2-H) are gaited for further reading. Finally, singlets are then studied by gating the area vs the width (Figure 20C), this graph shows two hot spots that indicate the G_1/G_0 and the G_2/M phases linked by the S phase in between. This graph allows for further discrimination of duplicates and aggregates as well as debris. For the gating draw

a square in this area, then this gating is saved to be used for all the samples. All histograms were displayed as the number of cells vs the width of the signal (Figure 20D). The assignment of the cell cycle phases was done automatically by the FlowJo software. The graphs were displayed in number of cells vs the height of the signal.

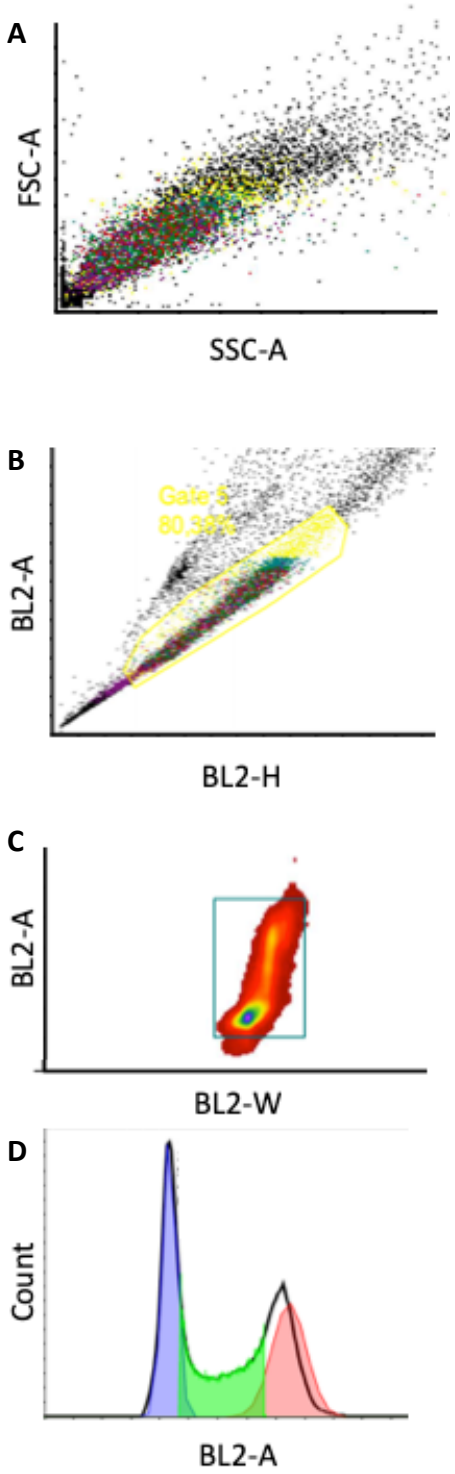

Figure 20 Gating workflow of flow cytometry data
(A) forward scatter area (FSC-A) by side scatter area (SSC-A) graph to visualize the cell types of the sample. (B) distribution of signal events graphing area (BL2-A) versus height (BL2-H) to identify singlets by a gate (yellow delimited area). (C) distribution of area (BL2-A) over width (BL2-H) with a density plot to identify and gate cells in the cell cycle. (D) Histogram of the distribution of cells (Count) by the area (BL2-A) of the signal. CHO cell culture cells were fixed and stained with propidium iodide. BL2 is the scattering signal of the second channel of blue light.

2.3 Antibody purification

2.3.1 ÄKTA

To analyze the characteristics of the recombinant protein of interest, the media was processed in order to isolate the product through affinity chromatography. The cell culture was centrifuged at 800g for 10 minutes. The supernatant was filtered with a hydrophilic PVDF membrane with a 0.22 µm pore size (Starlab, Milton Keynes, UK) and mixed up to 50 mL with a binding buffer for adaptation. 20 mM of sodium phosphate and 0.15 M of NaCl, (pH 7.2) were used as binding and equilibration buffers respectively. The flow rate was set at 5 mL/min for 100 mL, after injecting the sample during the binding phase. The elution of the IgG was obtained by a sudden swap of the buffer to 0.1 M of citric acid (pH 3). The elution phase was prolonged for 50 mL to ensure the detachment of the IgG. The peak sample was collected manually. After the citric acid wash, the column was equilibrated again for 25 mL, previous to the next sample run. Purification was carried with an ÄKTA^{TM} pure (GE Healthcare) with the use of a 1x5mL HiTrap^{TM} MabSelect Sure^{TM} protein A column (GE Healthcare) and then stored at -80^{o}C until further analysis.

Note: resveratrol was found to have a specific binding affinity for the protein A column, even stronger than that one of the IgG. Most of the resveratrol was eluted after washing with sodium hydroxide.

2.3.2 SDS-PAGE

To further corroborate the purity of the product after the ÄKTA purification step and the behaviour of the column, the first and last samples run for purification each set were run in an SDS-PAGE gel. One µL of control samples were diluted with 4 µL of eluent buffer from the purification step and mixed with 5 µL of Laemmli buffer while 5 µL of the treatment at 500 µM resveratrol was mixed directly with 5 µM of Laemmli buffer. The mixture was incubated for five minutes at 95ºC.

SDS gel electrophoresis was performed under reducing conditions with 1.0 M Tris-HCl buffer (pH 6.8) for the stacking gel (4% acrylamide) and 1.5 M Tris-HCl buffer (pH 8.8) for the separating gel (10% acrylamide). Migration was performed at 120V for one hour. The gel was stained with Page Blue Protein Staining Solution, left shaking overnight (8 hours) and then it was distained with 4 washes of milliQ water every 2 hours for 8 hours. The molecular weight ladder was P7706S (Appendix 3).

2.4 High-performance liquid chromatography (HPLC)

2.4.1 Size exclusion chromatography (SEC)

The Thermo UltiMate 3000 Rapid Separation HPLC System (Thermo Fisher Scientific, Waltham, MA, United States) was used to study how the addition of resveratrol and catechin to a recombinant CHO culture media, affects the final aggregation or fragmentation of the recombinant antibody produced. A MabPac SEC-1 4x300 mm column with 10 µm particles (Thermo Fisher Scientific) was used in an isocratic regime with a buffer of 20mM MES+0.3M

NaCl at a pH of 6.1. Samples were run for cycles of 30 minutes each at 0.2 mL/min at 25°C. In order to eliminate the noise of the chromatogram, only peaks above 0.1% were considered significant.

The identification and relative quantification of the peaks was performed automatically by Chromeleon software. Bovine serum albumin (BSA) was used to condition the column. Furthermore, BSA was used along the process of chromatography, to ensure that there would not be any changes in the behaviour of the experiment over time. Finally, the BSA conditioned spectrum was used to create a correlation curve between the time of elution and the molecular weight.

2.4.2 Cation exchange chromatography (CEX)

The samples were first treated with carboxypeptidase-B from porcine pancreas (Merk, Kenilworth, NJ , United States) at a temperature of 37°C for a period of two hours with an enzyme to protein ratio of 1:25, as previously described (Flores-Ortiz *et al.*, 2014). The Thermo UltiMate 3000 Rapid Separation HPLC System (Thermo Fisher Scientific, Waltham, MA, United States) was used to perform high-performance liquid chromatography to discriminate different recombinant IgG species based on their charge. A MAbPac SCX-10 4x250 mm (Thermo Fisher Scientific) column with 10 μm diameter particles was used under a 1 mL/min flow regime, at a temperature of 50°C. A gradient system, ranging from 15% to 36.4% of buffer B (20 mM + 300mM NaCl at pH 5.6) in buffer A (20 mM + 60mM NaCl at pH 5.6) was used for 25 minutes, followed by two minutes of cleaning with buffer C (20 mM + 1M NaCl at pH 5.6) and 15 minutes of reconditioning at 15% buffer B in buffer A.

After the chromatograms were run, the files were exported in CDF format from the Chromeleon software and they were processed and analyzed by R software. First, the chromatograms were delimited between sample injection and cleaning, as those parts contain no relevant information related to the study. Then the files were compiled and colour-coded by treatment type (Figure 21A). To further process the data, the spectra were aligned by their maximum peak (Figure 21B). Antibody ion-exchange chromatograms were characterized with a high peak, when fully cleaved from C-terminal lysine; the peak corresponded to the mean charge variation of the molecule. This peak was used as a landmark in the chromatogram profile, in order to align all the different chromatograms. The shift between the spectra observed in this data could be a result of small changes in the pH when preparing the buffers. The alignment process causes the spectra to shift and some data could be missing at one end or another. As a result, the next step in formatting the data, was to crop both sides of the spectrum, in order to remove these regions without relevant parts (Figure 21C). Furthermore, the baseline spectrum was assessed with a linear model and then corrected (Figure 21D). The data were then corrected for negative values (Figure 21E). This was done because negative values could create problems during normalization, as they are subtracted from the final area under the curve. Each spectrum was corrected by adjusting the most negative value to zero. The data was normalized (Figure 21F), the extension of the mean peak was stated and the regions were defined. Finally, the acidic species, the mean variant and basic species of the IgG were measured. Results were evaluated for statistical significance by one-way ANOVA, p-values were considered significant bellow 0.05. Further information of the process is displayed in Appendix 4.

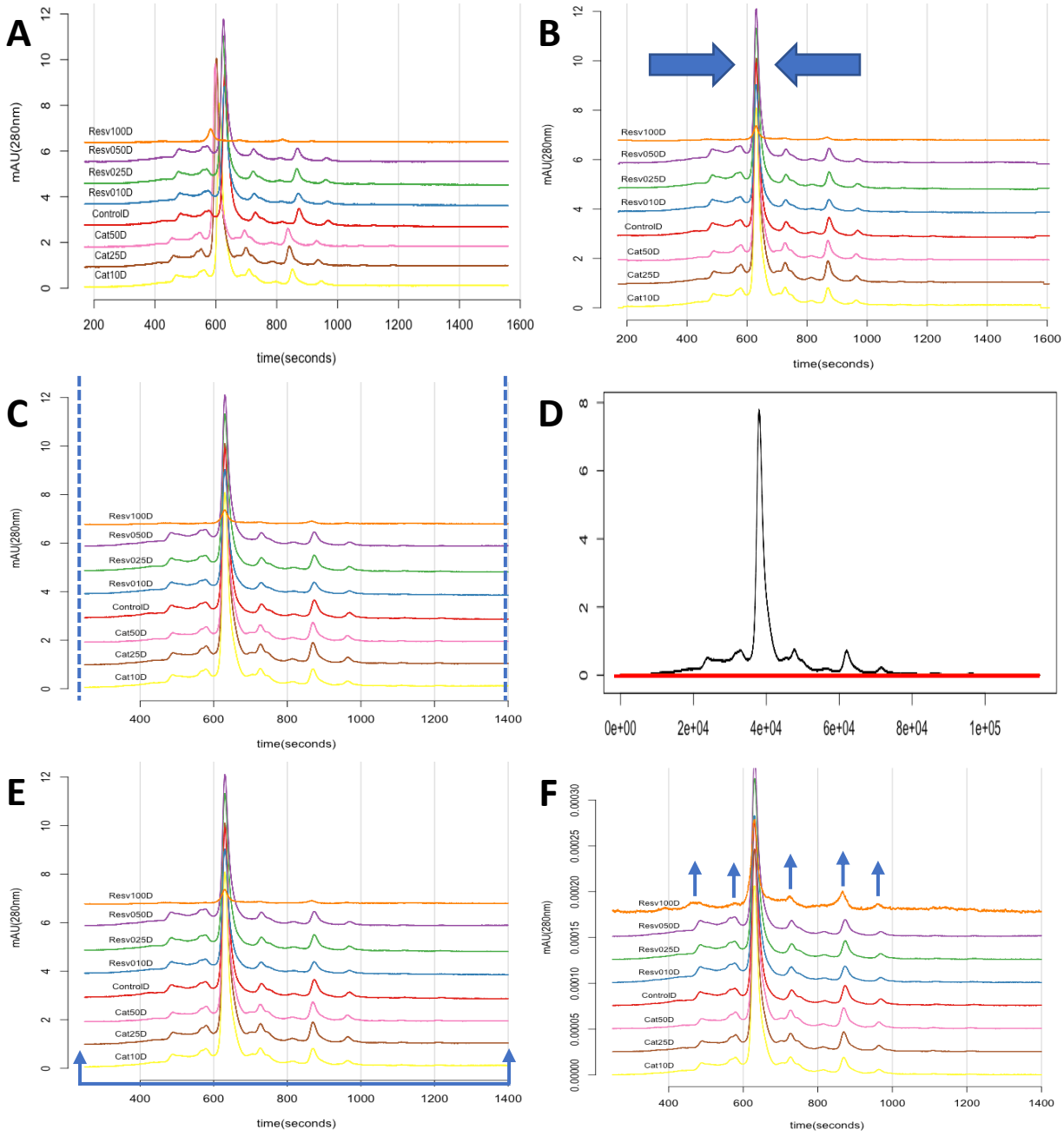

Figure 21 Data analysis of the ion-exchange chromatography spectra with the R software
(A) Compilation of the data by the program and assignment of the treatment groups (colours). (B) Alignment of the data by the maximum peak intensity. (C) Cropping excess of the chromatogram from both sides to standardize the distance in chromatographic time to the maximum intensity peak. (D) Baseline correction for each individual chromatogram with a linear model. (E) Correction of negative values. (F) Normalization of the area under the curve.

2.5 Mass spectrometry

2.5.1 IgG digestion

In order to study the modifications of the recombinant IgG, previously purified samples were used to measure the concentration of IgG after purification, using Nanodrop™ 2000c (Thermo Fisher Scientifics). 40 μg were retrieved in a final volume of 200 μL by addition of pH 7.5 denaturation buffer (7.5M GdnHCl and 0.25 M Tris). Reduction was performed by the addition of 1 μL of TCEP at 50 mM and incubation for 10 minutes at 70°C. After cooling the samples in ice for 5 minutes, 2 μL of 0.5 M IAA were added and the samples were left in the dark for 30 min at room temperature, in order to achieve carboxy-methylation. Finally, 100 mM ammonium-bicarbonate (AB) was added to a final volume of 500 μL. IgG samples were buffer-exchanged into a pH 7.5 digestion buffer (100 mM AB) using a NAP-5 column (GE Healthcare, Piscata-way, NJ, USA).

Lyophilized trypsin was dissolved in 100 mM AB to a final concentration of 0.1 μg/μL and added to the samples in a 1:25 ratio. Digestion was performed in an oven at 37°C in a period of 30 minutes. The reaction was then stopped by lowering the pH to 3.0, by adding 5.5 μL of 100% formic acid. Samples that were not used immediately, were stored at -20°C. The protocol was adapted from (Ren *et al.*, 2009).

2.5.2 Liquid chromatography tandem mass spectrometry (LC-MS/MS)

Samples were run through a Dionex Ultimate 3000 uHPLC with a PepMap™ RSLC C18 2 µm 100 Å 50 µm x 15 cm coupled to an Orbitrap Elite MS (Thermo Fisher Scientific, Waltham, MA, United States) with an EASY-Spray™ Ion Source.

A volume of 18 µL of each digested IgG sample was used for LC-MS/MS analysis. Peptides were separated in a Dionex Ultimate 3000 uHPLC (Thermo Fisher Scientific, Waltham, MA, United States) with an Acclaim™ PepMap™ 100 C18 trap column (3 µm particle size, 75 µm x 150 mm) and an EASY-Spray™ C18 column (2 µm particle size, 50 µm x 150 mm) using a 35 min method at 0.25 µL/min with 0.1% formic acid in water (mobile phase A) and 0.1% formic acid in 80% acetonitrile (mobile phase B) as follows: 0-3 min, hold at 3% B; 3-21 min, from 3% B to 40% B; 21-21.1 min, from 40% B to 90% B; 21.1-26 min, hold at 90% B; 26-26.1 min, from 90% B to 3% B; 26.1-35 min, re-equilibrate at 3% B. MS analysis was performed on a LTQ Orbitrap Elite (Thermo Scientific) hybrid ion trap-orbitrap mass spectrometer equipped with an EASY-SprayTM Ion Source. MS survey scans in positive ion mode were acquired in the FT-orbitrap analyzer using an m/z window from 375 to 1600, a resolution of 60,000, and an automatic gain control target setting of 1×10^6. The 20 most intense precursor ions were selected for the acquisition of MS/MS spectra in the ion trap (Normal Scan Rate) using collision-induced dissociation (CID) with normalized collision energy of 35%, activation time of 10 ms, isolation width of 2 Th, and automatic gain control target value of 1×10^3. The charge states 1+ were excluded from precursor selection. Monoisotopic precursor selection was activated. Dynamic exclusion for precursor ions was applied for 45 s after 1 fragmentation count and a repeat duration of 30 s.

2.5.3 Data processing

Processed raw data files were then used for dependent peptide search. This was performed with the MaxQuant (v 1.6.2.6) software (Max Planck Institute for Biochemistry, Munich, Germany), and then the data was processed with an R software code previously published (Acosta-martin *et al.*, 2016). The data for mass shift differences from each sample were gathered together into a single file. The treatment files were then compared versus the control individually. Firstly, the mass shift spectrum was broken into discrete pockets (0.05 Da); the number of mass shift events in each pocket was compared between the control and the treated sample. Then a Z-score was calculated to identify outliers (>3.5) within the comparison test (Figure 22A) (Appendix 6). Unusual mass shift differences were characterized as significant differences and were plot in a histogram to visually assess the reliability of the mass shift difference (Appendix 7). Peaks that were high and had a consistent shape (Figure 22B) were taken forward to identify the modification. Histograms that did not show reliable peaks were discarded (Figure 22C). This process for the light and the heavy chain were done independently.

Modifications that were predominant and those of interest for the functionality of the IgG (Table 2), were studied with a direct modification search using the label-free quantification method in the MaxQuant (v 1.6.2.6) software (Max Planck Institute for Biochemistry, Munich, Germany).

Table 2 Mass spectrometry searched modifications

Modification	Composition	Monomeric peak
Oxidation	O	15.994915
Trioxidation	O (3)	47.984744
Acetylation	H(2) C(2) O	42.010565
Reduction	O (-1)	-15.994915
Deamidation	H(-1) N(-1) O	0.984016
Carbamidomethylation	H(3) C(2) N O	57.021464
Hydroxykynurenine	C(-1) O(2)	19.989829
Kynurenine	C(-1) O	3.994915
loss of ammonia	H(-3) N(-1)	-17.026549
Pyroglutamate	H(-2) O	13.979265
Gln->Ala	H(-3) C(-2) N(-1) O(-1)	-57.021464
Asn->Gly	H(-3) C(-2) N(-1) O(-1)	-57.021464

The obtained files were then processed by a code (Appendix 8) in the R software and the files were integrated into one data set. Modifications were only considered significant if they appeared consistently (in 3 out 4 replicates) for every treatment. Finally, they were compared based on their ratio of modified peptides per non-modified ones.

Obtained peptide files were also used to study the sequence coverage of the analysis, with the use of the R software. Files with all the peptides combined, were loaded to the software, and accumulative intensity was calculated for each amino acid under specific treatment conditions by applying R coding (Appendix 5), to then be displayed as a heatmap.

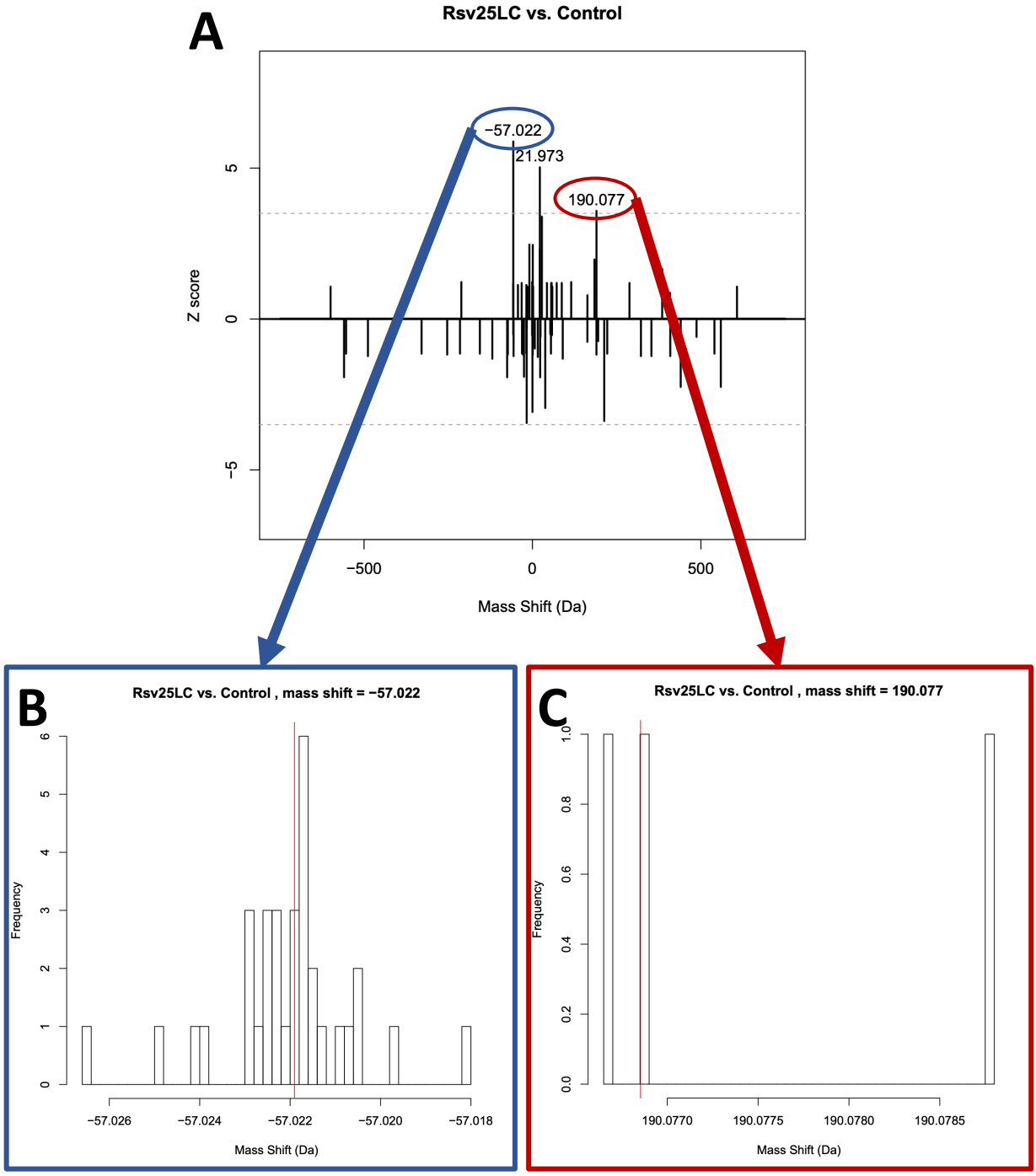

Figure 22 Identification process of the mass shift differences between sample treatments
Graphical representation of the selection of mass shift differences between the control and the 25 µM-treatment with resveratrol for the light chain (LC) of rituximab by a non-specific search for modifications. (A) The spectrum of molecular weight studied and the differences between the samples are graphed as z-scores; the molecular weight of significantly different signals is displayed. (B & C) histograms of the frequency of differences for the specific section of the molecular weight spectrum.

2.6 Statistical methods

Experimental results were expressed as mean ± 1 standard deviation (SD). Standard deviation was selected over standard error of the mean in order to emphasis the deviation of the replicates in the sample (Altman and Bland, 2005). Relevant differnces between means was addressed thorugh statistical test. The t-tests analysis or ANOVA were run with $\alpha = 0.05$.

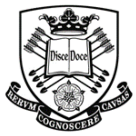
Disce Doce
Rerum Cognoscere Causas

Chapter 3

Initial toxicological and recombinant production screening

3.1 Initial remarks

The development of chemical additives for improving the recombinant protein production in running CHO cells batch cultures is limited. Their use is very specific with low transferability

of the effect on other cell lines or recombinant products. This chapter focuses on the development of a robust screening process to assess naturally occurring low-molecular weight molecules in a broad range of concentrations, in order to study their effect on cell growth and viability as well as recombinant IgG expression levels.

In order to assess the different chemicals identified as potential tools for recombinant IgG production in previous literature (Chapter 1), the feasibility of a 96-well plate-system was studied and compared to a 24-well plate-platform. Further, the chemical candidates were screened to identify possible candidates for future stages of research.

3.2 96-well plates

96-well plate cultures were set-up according to section 2.1.2 and eight wells were treated for each chemical concentration (Table 3). From each treatment, four wells were used to measure cell concentration and viability as specified in section 2.1.4. The remaining four wells of each column were used to measure protein production following section 2.1.5.

Table 3 The study range of the chemicals screened

Chemicals	Acronym	Study Range (µM)				
4-phenylbutyric acid	4-PBA	500	10^3	$2{\cdot}10^3$	$4{\cdot}10^3$	$8{\cdot}10^3$
Caffeine	Cff	13	31	63	94	125
Caffeic acid phenethyl ester	CAPE	2	10	20	30	40
Curcumin	Cur	5	10	20	40	80
Catechin hydrate	Cat	10	25	50	75	100
Epicatechin	EC	1	5	10	15	20
Epicatechin gallate	ECG	10	25	50	75	100
Epigallocatechin gallate	EGCG	5	25	50	75	100
Gallocatechin gallate	GCG	5	25	50	75	100
Glycine Bettaine	Bet	10	25	50	75	100
Kaempferol	Kmp	10	50	100	150	200
Luteolin	Ltl	2	5	10	15	20
Piceid	Pcd	10	25	50	75	100
Resveratrol	Resv	10	25	50	75	100
Tocopherol	Tcp	35	175	350	525	700

To screen through a high number of components in a fast and reliable way it is fundamental to scale down the process in order to make it more affordable. To do so, well plates were used as the main platforms to grow cells in different conditions. 96-well plates were used (Greiner-bio-one, Kremsmünster, Austria).

The use of shallow 96-well plates constrained conditions of the experiment to static conditions and the use of small volumes; therefore, the behaviour of the cell growth was first studied.

3.2.1.1 Vi-cell vs CSI cell density measurement

The Vi-cell is the gold standard system to study cell concentration and viability in cell cultures. This device can directly study the culture growth and viability under the presence of the chemical candidates. However, this instrument is not adapted to perform analysis in 96-well plate platforms. This would entail transferring each sample to a tube and then be analyzed, making it a long and very expensive process.

As an alternative, and to facilitate a high throughput system of screening, the Cloner Imager Select (CSI) was used. The CSI is a device able to measure cell growth in a 96-well plate format by assessing the confluence of each well after focusing and capturing images from bellow. This method allows fast scanning of the entire plate. It also preserves the samples, allowing multiple analyses over time and making it possible to track the growth. Due to the advantages that CSI brings for high throughput experimentation, this system was studied in relation to the Vi-cell system in order to validate its reliability for the screening process.

96-well plates were seeded and grown under the conditions specified before, then alternative wells were selected every day. The cultures were analyzed using the CSI and then using the Vi-cell. Finally, the relationships between the confluence of the well and the exact value of total cell concentration, the viable cell contrition and the viability were studied.

3.2.2 Results

3.2.2.1 Cell growth curve and the edge effect

To create a robust system able to produce reliable data it is fundamental to understand how reliable the different components of the system are and how the cell line behaves within itself. In order to do this, plates were tested in order to analyze their intrinsic variability and to identify specific features such as the edge effect. Furthermore, the assessment of the cell line growth behaviour within the conditions of the system was needed in order to obtain incubation times and to decide when to apply the treatment.

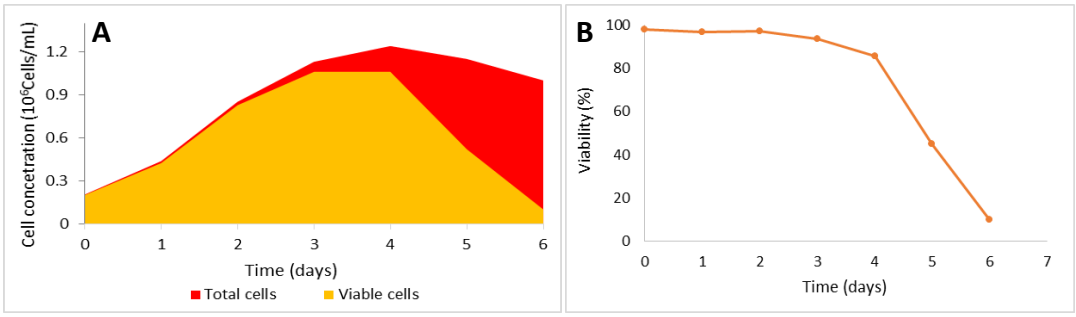

Figure 23 Study of cell growth in 96-well plates
(A) Graph of total (red) viable (orange) cell concentration across time (days). (B) Graph of cell viability (%) across time (days). This data was gathered from CHO cell incubation under static conditions in shallow 96-well plates.

The cell growth curve was studied for six days. Cell population grew exponentially until day 3 with a maximum concentration of 1 million cells per mL at 94% viability. Rapidly after, viability was compromised and dropped to 80% by day four, although the total number of viable cells remained constant (Figure 23).

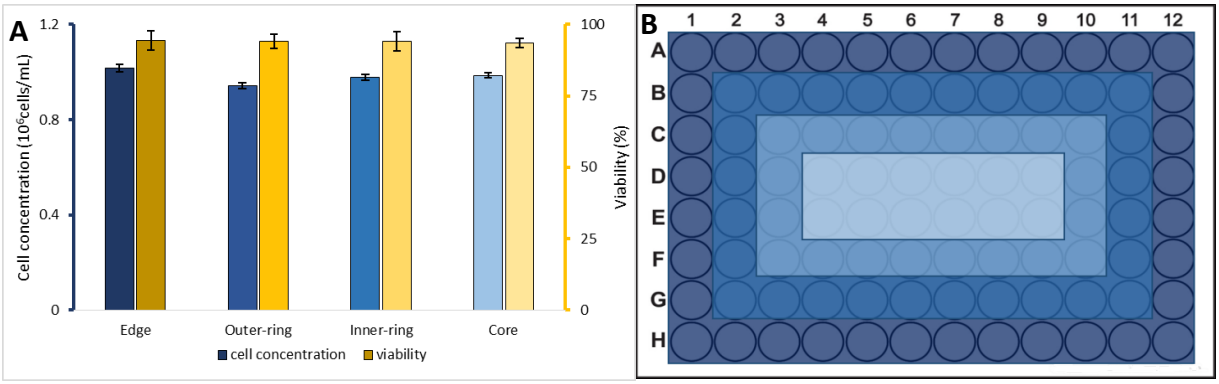

Figure 24 Study of the edge effect in 96-well plates
(A) Graphs of cell concentration (blue) and viability (yellow) for the different sections in a 96-well plate. Cultures were incubated for 3 days under static humid conditions. (B) Representation of the different sections selected from a 96 and a 24-well plate respectively.

The cell concentration and viability measurements in 96-well plates after three days incubation in a static humid incubator, did not show significant differences between the ones taken from the edge and the ones from the rest of the plate sections (Figure 24).

3.2.2.2 Vi-cell vs CSI cell density measurement

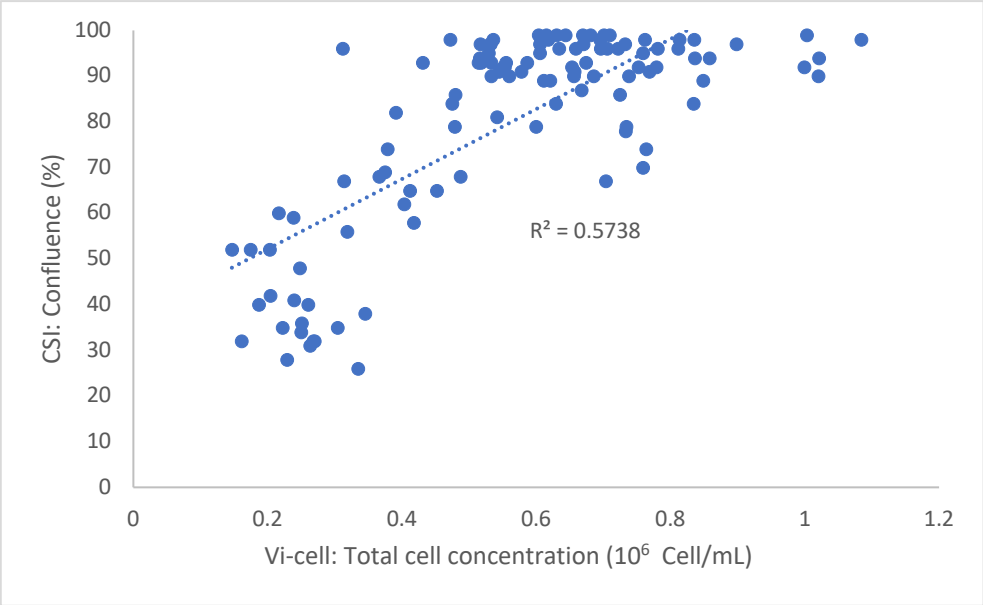

Figure 25 Comparison of Vi-cell vs CSI
The relation between Vi-cell cell concentration readings and confluence readings from a CSI device as the CSI reaches saturation at 0.6 million cells.

There was a linear correlation between the cell growth measured with Vi-Cell and the one measured with the CSI. However, the saturation of the wells was very fast with values close to 95% at concentrations of $0.6 \cdot 10^6$cells/mL. As a result, in order to measure growth in a semi-reliable way, concentrations up to $0.6 \cdot 10^6$cells/mL have to be used. The correlation between total cell concentration and confluence stills had an r^2 of 0.57. As expected, this was the best match for correlation as viability and viable cell density gave worst results (Figure 25).

3.2.2.3 Screening system

Different chemicals with potential chaperone activities were used in a range of concentrations to treat low-density CHO cell cultures for three days in a static humid incubator. These experiments were undertaken in 96 and 24 shallow well plates. From this set of experiments data of total cell concentration, viability and total recombinant IgG production were collected. Later, total recombinant IgG production was divided by its respective cell density to obtain the amount of recombinant protein produced per cell (or relative protein production).

3.2.2.3.1 Viability and cell concentration by CSI

The results from the CSI showed that components such as catechin, epicatechin or epicatechin gallate, were not affecting growth significantly during the first three days of treatment under static conditions. On the other hand, 4-PBA, resveratrol and curcumin inhibited growth at high concentrations while growth at lower concentrations was not affected.

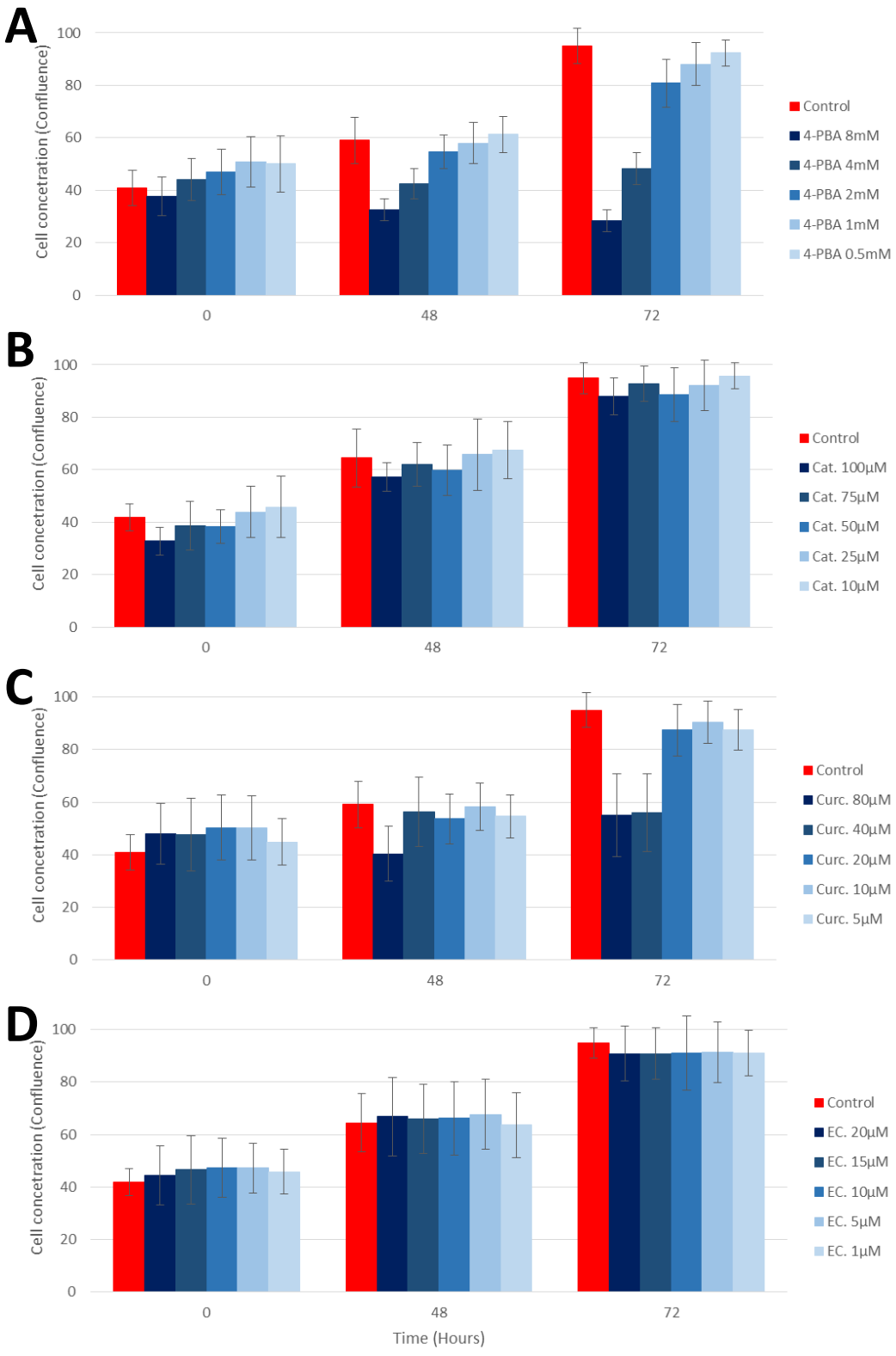

Figure 26 Cell density measurements with CSI I
Display of cell density measurements of confluence by a CSI device for samples grew during 3 days in a static humidified incubator in 96-well plates (section 2.1.2) and treated with (A) 4-PBA, (B) Catechin (Cat), (C) Curcumin (Curc), (D) Epicatechin (EC). The error bars represent ±SD of quadruplicates.

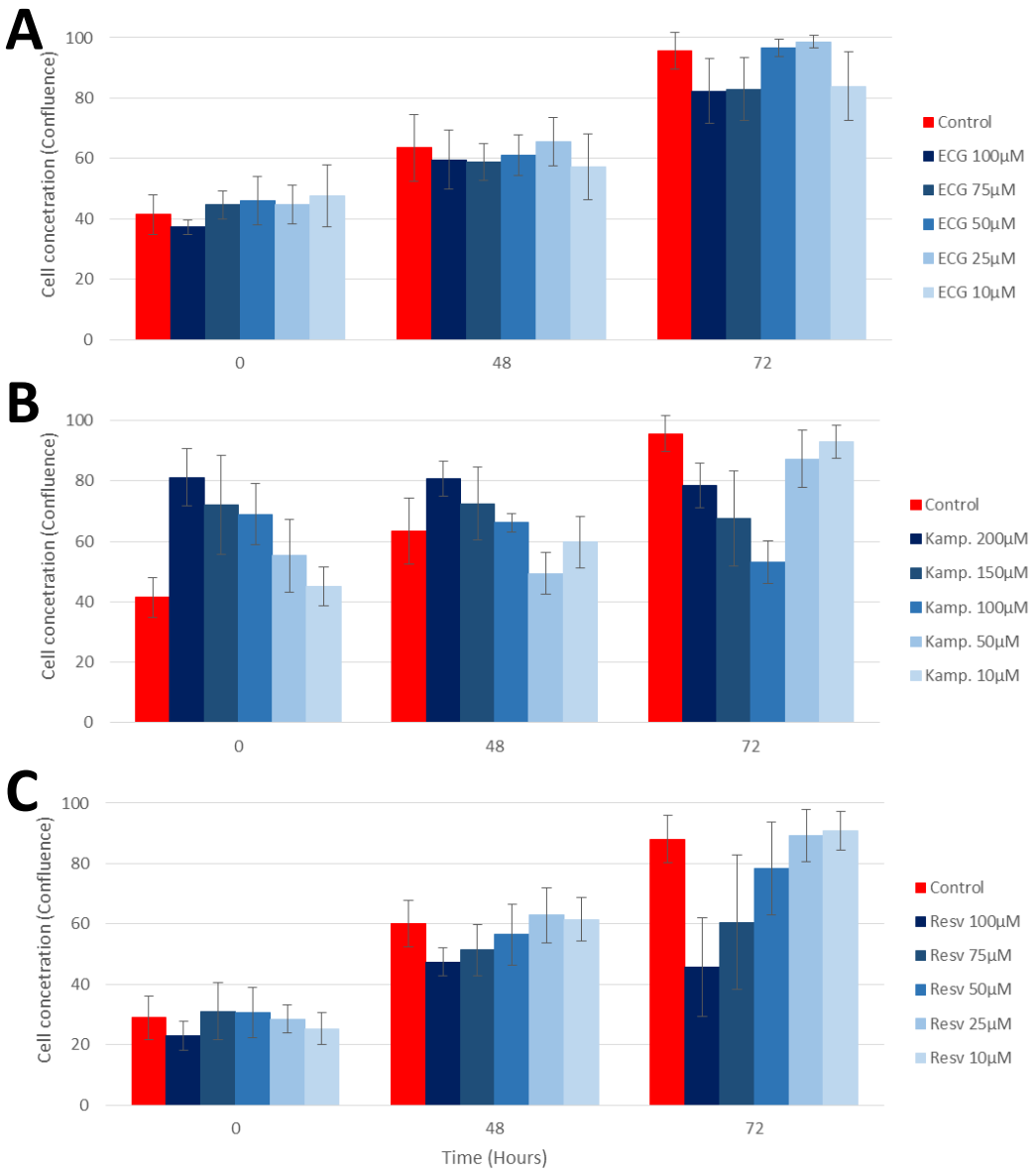

Figure 27 Cell density measurements with CSI II
Display of cell density measurements of confluence by a CSI device for samples grew during 3 days in a static humidified incubator in 96-well plates (section 2.1.2) and treated with (A) Epicatechin gallate (ECG), (B) Kaempferol (Kamp), (C) Resveratrol (Resv). The error bars represent ±SD of quadruplicates.

Kaempferol increased cell concentration at time zero in a concentration-dependent manner. As the time of treatment progressed, the cells treated at high concentrations did not grow, whereas the less concentrated samples were able to grow parallel to the control.

Kaempferol caused the initial cell concentration (confluence) to immediately peak at time zero, whereas the cell concentration in all the wells was the same, further study was done to understand the nature of these results. Images at time zero from the CSI were taken to have an insight into the problem (Figure 28).

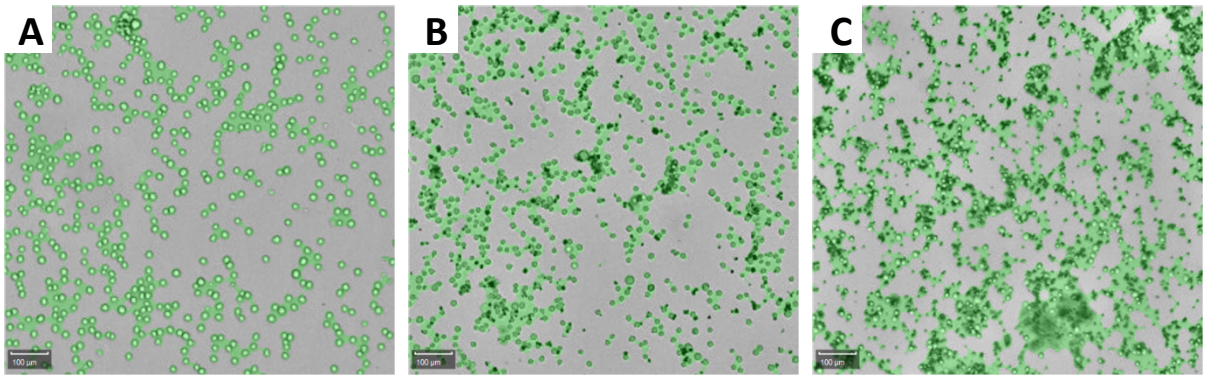

Figure 28 CSI images of kaempferol treatment on cell cultures
Images taken from samples by the CSI at time zero for (A) cells without treatment, (B) cells treated at 100 µM and (C) cells treated at 200 µM of kaempferol.

The images show how the cells treated with kaempferol reacted in a concentration-dependent manner. At 100 µM of kaempferol, the cell surface was not as regular as in the control. Some of the cells started to lose their integrity, bursting open and creating clumps that aggregated. At 200 µM, this reaction was more acute; cells were smaller or broken and the amount of debris was high due to the large number of cells that released their content to the media.

As shown in the graph (Figure 28), there was a correlation between the measurements done by the CSI and the actual concentration obtained by the vi-cell. However, the correlation was weak as stated by the r^2 value. Therefore, the measurements with the CSI could give an approximation of the population dynamics (growing, stationary or decreasing) but could not indicate accurate values.

3.2.2.3.2 Viability and cell concentration by Vi-Cell

Data on cell concentration and viability in 96-well plates showed cell growth inhibition and low viability by 4-PBA and curcumin at high chemical concentrations. In the case of catechin and epicatechin growth was repressed at high concentrations but viability was never compromised. Finally, resveratrol and kaempferol restrained cell growth and viability in a gradient dependent response, causing less effect as chemical concentrations were lower.

Results from Vi-cell™ XR (Beckman-Coulter, Brea, CA, USA) readings in 96-well plates Figure 29) were analogous to those further obtained in the 24-well plates analyses. A more detailed description of the chemical influence on cell concentration and viability can be found in the next section.

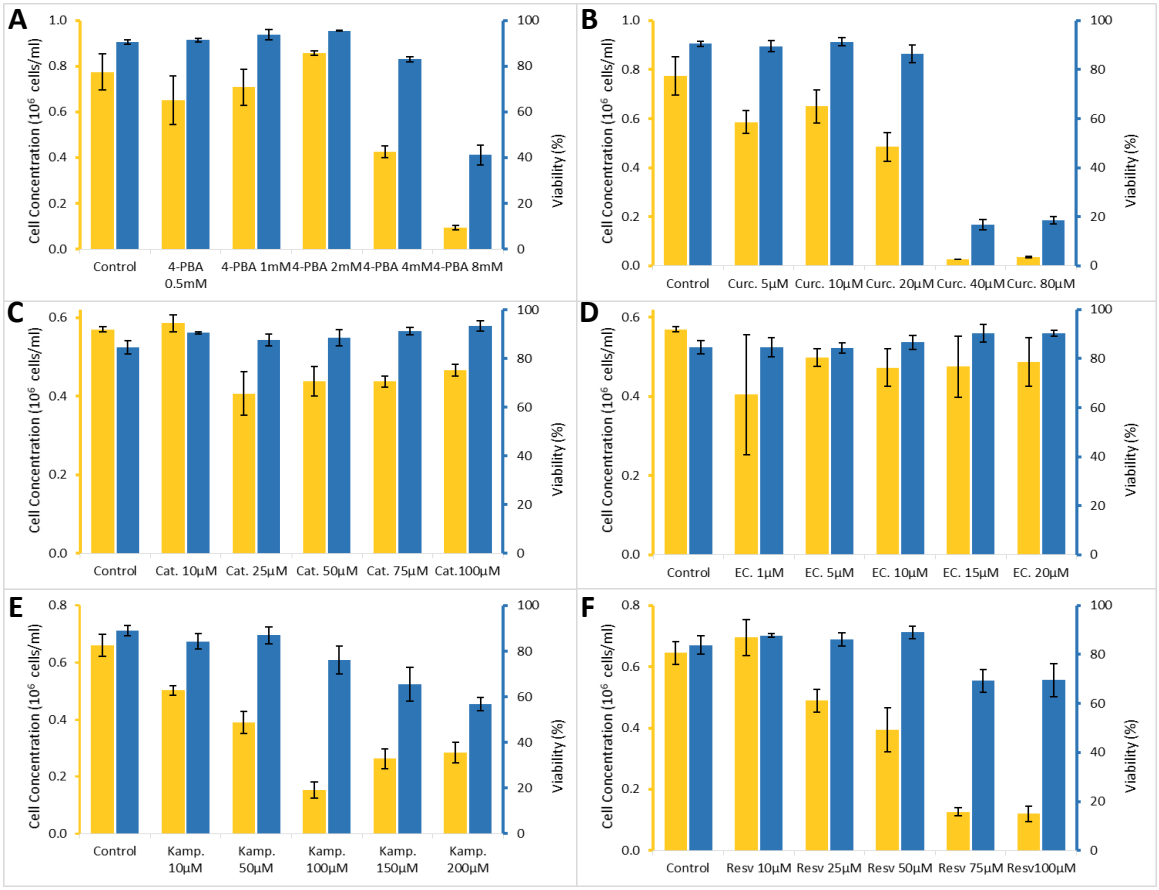

Figure 29 Cell density measurements with Vi-cell
Display of cell density measurements of cell concentration (blue) and viability (yellow) by a Vi-cell device (section 2.1.4) for samples grew during 3 days in a static humidified incubator in 96-well plates (section 2.1.2) and treated with (A)4-PBA, (B) Curcumin (ECG), (C) Catechin, (D) Epicatechin (EC), (E) Kaempferol, (F) Resveratrol. The error bars represent ±SD of quadruplicates.

3.2.2.3.3 Protein production

Protein production was displayed as binding rate and it was directly related to its concentration. Results exhibited a high degree of inconsistency in signal intensity and showed different trends (Figure 29). A clear example of this was epicatechin (Figure 29C) that had different results for each one of the three experimental replicates.

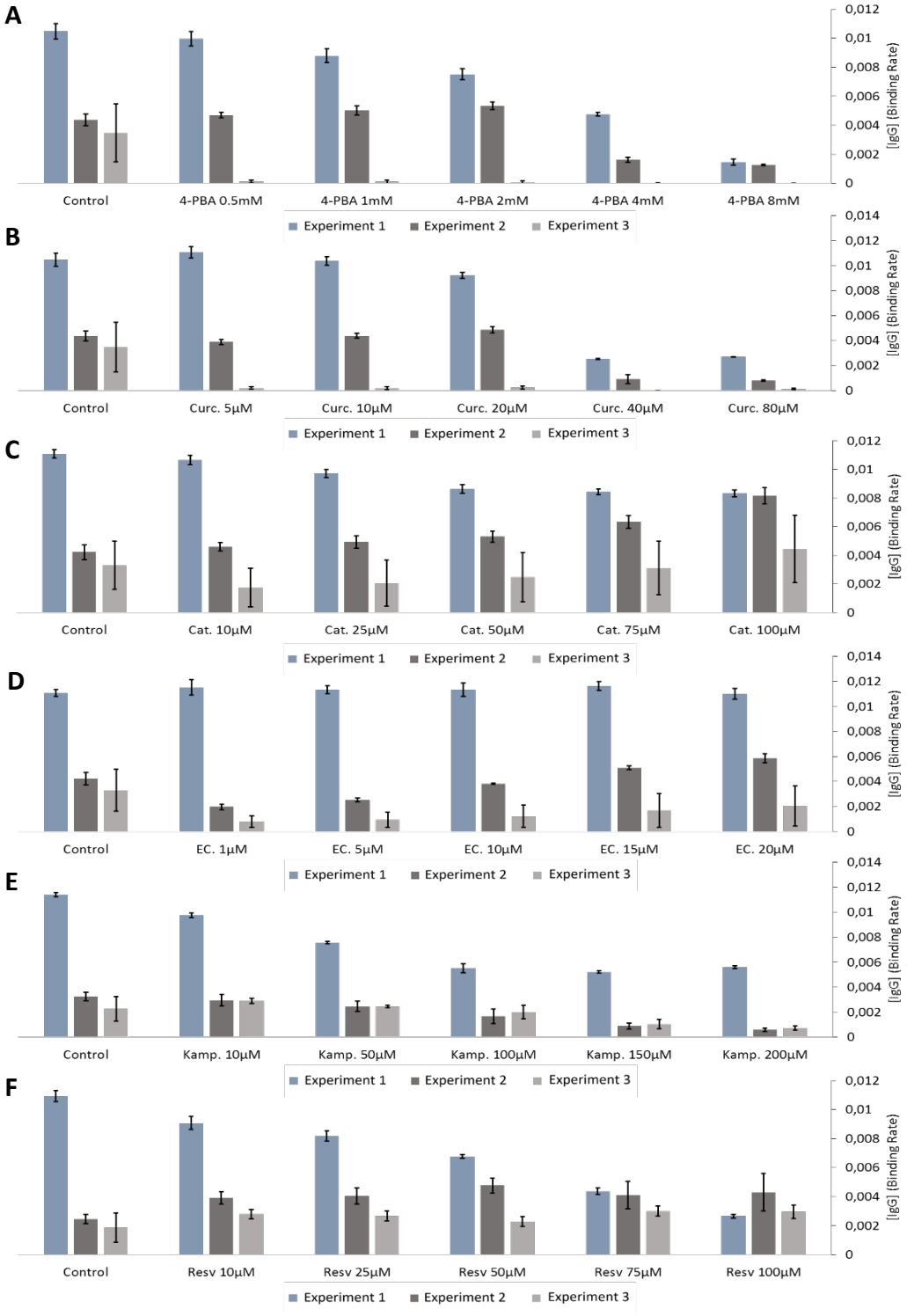

Figure 30 IgG concentration of samples grown in 96-well plates
Graph of total recombinant IgG production measurement (section 2.1.5) in three independent experiments for samples cultured in 96-well plates during 3 days in a static humidified incubator (section 2.1.2) and treated at different concentrations with 4-PBA (A), curcumin (B) catechin (C), epicatechin (D), kaempferol (E) and resveratrol (F). The protein quantity is expressed as binding rate and the error bar is the ±SD of quadruplicates.

3.2.3 Discussion

The growth curve study indicated that the viability in the 96-well started to decrease after the first 48 hours, but the levels were maintained above 90% during the first 3 days. The samples were cultured for 3 days in order to extend the period of effect of the chemical for as long as possible. That had to be done without compromising the level of viability, which is a key feature of the initial toxicological tests. Furthermore, if the cultured was maintained longer, this would allow for a higher concentration of cells and IgG production.

The edge effect was proven to be of no significant impact on cell growth or viability under these conditions. Since edge effect was reported in the literature, well plate companies have started to develop methods and features to minimize this phenomenon. This effect is mainly caused by liquid loss, which originates an increase of cell concentration in the well and variation in the behaviour of cells. It has been described that this effect could lead to a loss of up to 15% of the volume in the corner wells depending on conditions such as the lid used, the time of incubation and the humidity percentage. Our experiments in 96-well plates were performed at 200 µL per well, in plates with lid edge ribs and rings. These were incubated for three days at 95% humidity. Results showed no significant differences in growth across the plate rings. These results are similar to the ones from previous studies using the same conditions; the study showed a difference of evaporation lower than 1% between the edges and the rest of the plate (Esser, P and Weitzmann, 2011).

CSI is easier to adapt to a high throughput system of screening for cell density measurements compared to a Vi-Cell system. The accuracy of the readings was not as good as the ones from the Vi-cell; there was a loss of accuracy as this device uses an indirect method of measuring. When comparing the measurements, it was shown that when cell cultures reached $0.5x10^6$ cells/mL, readings of confluence were often close to 100%. From the growth curve study, it was identified that this concentration was reached after 48 hours. This means that if the cell culture was to be grown under proper conditions, the CSI after the second day would not be able to show any differences. After the first two days, the CSI device became unreliable in measuring the growth, as the culture could overshoot the working range of the apparatus.

The addition of chemicals could have an artifact effect on cell concentration readings. Kaempferol at time zero caused an increase of confluence due to its effect on cells. Finally, CSI was unable to give any information on the viability of the cells in the culture. This limited its usage for the toxicological studies where, both cell growth arrest and the effect over viability are relevant and important features in order to understand the impact on the cell culture.

CSI is a less reliable device to measure the toxic effect of chemicals in CHO cell cultures and could constrain the study considerably as it was not designed to be used for this purpose. This apparatus was built to screen producer desirable cells in a well plate after gene transfection. This method is used in identifying single transformed cells and track their growth. As a result, when the well gets densely populated, the device struggles to give accurate readings, as it was never intended to be used under such circumstances. Newer devices used for the same reason, but with more advanced systems to measure cell density, could be a future possibility

in order to reduce the costs and time of measuring in Vi-cells. The NyONE device has worked around the problems of these devices, such as the loss of focussed images when moving along the well plate.

IgG concentration was very fluctuating and unreliable among the three independent triplicates. There are different reasons why this could be happening. The samples that were obtained from the well plates had low concentrations of the IgG, due to the low cell density and time of culture under these conditions. Furthermore, Octet needs 200 µL volume for reliable readings. The culture volume of 96-well plates is very close to this value, which means that only 100 µL of the final culture had to be taken to ensure that after centrifugation there was only supernatant. This accentuated the low concentration of the culture even further as 100 µL of fresh media had to be added. The samples were taken from different wells and that could cause a small impact when relating to the other measurements.

This system is very dependent on low volumes which increases the uncertainty of the results and small changes in the collection could lead to big changes in the data. As a result, a new system with 24-well plates with 1 mL cultures per well was proposed in order to make the readings more reliable. At the same time, the change of the platform would not result in big differences in the volume of the cell cultures nor time nor resources. That would mean that the experiment could run in a more robust way with almost no increment in cost.

3.3 24-well plates

The previous experiments showed that taking measurements of cell concentration with CSI, has its limitations at high cell densities and that the additions of chemicals could cause

artifacts on the readings. Furthermore, the use of 96-well plates was not found to provide ideal conditions for the experimentation processes. In answer to these findings, a 24-well plate experimentation platform, using a Vi-cell to measure growth and viability, was studied and implemented for the screening of the chemical candidates.

24-well plate cultures were set-up according to section (2.1.2) and wells were treated for each chemical concentration (Table 3). By the end of the culture each treatment was measured for cell concentration viability and morphology (section 2.1.4) and recombinant IgG production (section 2.1.5). The experiment had four biological replicates and was repeated twice independently.

3.3.1 Results and discussion

3.3.1.1 Cell growth curve and the edge effect

To create a robust system able to produce reliable data it is fundamental to understand how reliable the different components of the system are and how the cell line behaves within itself. In order to do this, plates were tested in order to analyze their intrinsic variability and to identify specific features such as the edge effect. Furthermore, the assessment of the cell line growth behaviour within the conditions of the system was needed, in order to obtain incubation times and to decide when to apply the treatment.

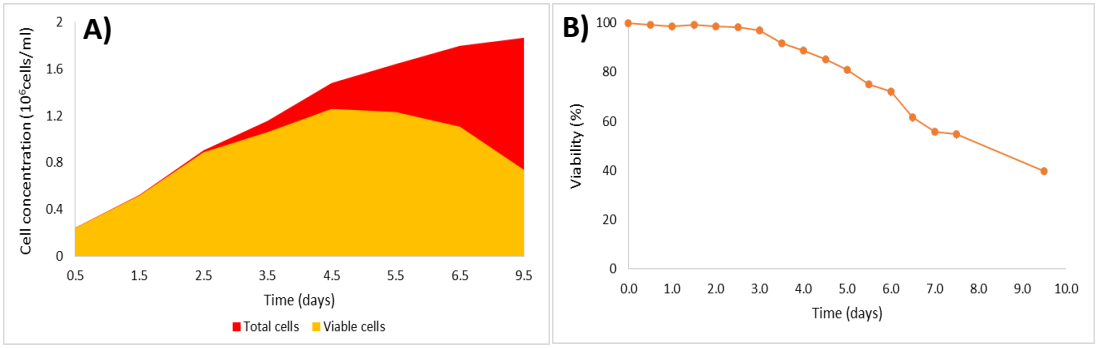

Figure 31 Study of cell growth in 24-well plates
(A) Graph of total (red) viable (orange) cell concentration across time (days). (B) Graph of cell viability (%) across time (days). This data was gathered (section 2.1.4) from CHO cell incubation under static conditions in a 24-well plate (section 2.1.2).

The cell growth curve was studied for 10 days. Cells grew to a cell concentration of 0.9 million cells per mL on day 3 with viability close to 100%. Afterward, the viability dropped by 10% over the following 24 hours and declined constantly for the rest of the experiment. The total cell concentration increased along the entire experiment, while the viable cell concentration reached its peak on day five (Figure 31).

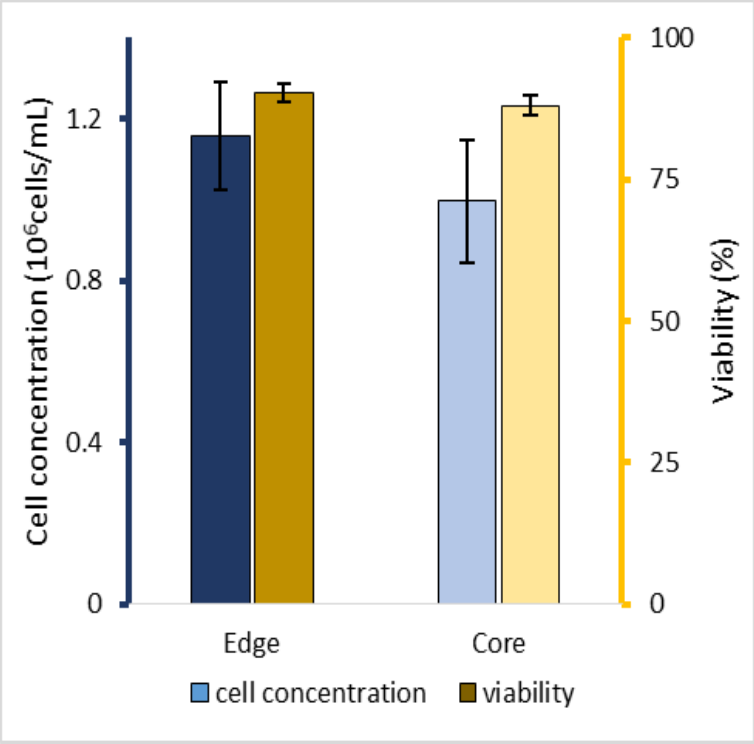

Figure 32 Study of the edge effect in 24-well plates
Graphs of cell concentration (blue) and viability (yellow) (section 2.1.4) for the different sections in 24-well plates respectively. Cultures were incubated for three days under static humid conditions (section 2.1.2). The error bars represent ±SD of quadruplicates.

The cell concentration and viability measurements in 24-well plates after 3 days incubation in a static humid incubator, did not show significant differences between the ones taken from the edge and the ones from the rest of the plate section (Figure 32).

3.3.1.2 Chemical screening results

3.3.1.2.1 4-PBA

4-PBA caused a decrease in cell viable concentration indirectly proportional to the increase of the concentration treatment; this was also observed in other studies (Hwang *et al.*, 2011). As a result, there was a decrease from 1.13 10^6 Viable cells/ mL of 22%, 29% and 52% of viable cells for 0.5, 1 and 2 mM. Higher concentrations of 4 and 8 mM caused complete growth arrest. The GI_{50} was close to 2 mM (Figure 33A).

Viability was preserved at 95% for concentrations of up to 2 mM, while concentrations of 4 mM and 8 mM caused a decrease to 29% viability (Figure 33A). This resulted in an LC_{50} of 4.7 mM, the lethality curve of the component was only comprehended for the drop in viability between the 2 and 4 mM treatments, the lack of data between these two values reduced the confidence of the LC_{50} value obtain.

The difference between the concentrations of GI_{50} (≈2 mM) and LC_{50} (4.7 mM) and the fact that total growth inhibition was reached at 8mM or earlier, indicates that there was a partial separation between the lethal curve and the inhibition curve. The inhibition curve started at 0.5 mM and carried all the way to 4 mM with complete cell arrest. Lethality was a sudden event and happened almost completely between 2 mM and 4 mM. Based on these values, the 2 mM concentration was the limit to where 4-PBA was acting exclusively as a cytostatic, while higher concentrations involved toxic effects on the cells. Nevertheless, CHO cell lines have been shown to have different ranges of tolerance to this chemical (Allen *et al.*, 2008; Hwang *et al.*, 2011).

There seems to be a relationship between the effect of the chemical in culture Cell morphology features and viable cell concentration. Cell size followed the same trend as VCD, with a gradient decrease in cell diameter from control (15.2±0.36 µm) to 2 mM (13.5±0.8 µm); concentrations beyond 2 mM showed a steep drop at around 11.75±0.06 µm (Figure 33C). On the other hand, the circularity of the cell culture had an inverse relationship to VCD, increasing progressively from the control (0.78 ± 0.1) to 4 mM (0.86 ± 0.1) and mainly maintained at 8 mM (Figure 33D).

The IgG total titre showed a direct relationship with the viable cell density; it decreased as the number of cells diminished, dropping from 6.74±0.76 at the control to 0.78± 0.12 µg/mL at 4 mM treatment. The concentration of IgG at 8 mM was so low, that a measurement could not be obtained. The relationship between the decrease in viable cell density and the total IgG produced was proportional, giving no significant differences in the specific protein produced for treatments up to 2 mM. Four mM treatment, on the other hand, had a four-fold increase in q_p when counted for viable cells. This increase in protein in q_p, is likely to be a result of the low viability of the culture (29%) (Figure 33B). The abundant dead cells lose their wall integrity and unfinished IgG products are released to the media increasing the reading on the Octet. The non-mature products in the media, could cause aggregation problems, causing an even bigger loss of the product during purification as 4-PBA does not help to avoid it (Hwang *et al.*, 2011). At the same time, the addition of impurities could lead to overcomplicated downstream processing (Liu *et al.*, 2010).

4-PBA caused cell inhibition and reduction of the cell size at low concentrations, but maintained q_p. This indicates, that although cells were smaller and fewer, they were able to produce more in relation to their biomass.

Allen et al in 2008 and Su-Jeong Hwang et al in 2011, found that 4-PBA at 0.5 and 1 mM respectively, acted over the recombinant CHO cell line flask cultures by: reducing the growth of the viable cell curve, increasing the viability of the culture over the time of incubation and by increasing q_p. However, this q_p increase was always observed after three days of incubation. No improvement in protein production was found during the first 72h of treatment. It is possible that the ineffectiveness of this chemical on the culture was due to the short period of incubation. Other variables that could be involved are the conditions of the culture (volume, agitation), the cell line or the recombinant protein studied.

Other studies found 4-PBA successful at increasing specific protein production and final titre, making it a well-established chemical chaperone. Its main mechanism of action is assisting the folding process at different stages (Chollet *et al.*, 2015; Ma, Goldberg and Goldberg, 2017). Furthermore, a study with a transient difficult to express protein showed an increase of specific productivity while reducing viable cell density (Johari *et al.*, 2015a). However, the present study did not give promising results for further study aligning with other studies in CHO cell recombinant protein (Roth *et al.*, 2012). A possible explanation could be that the cell line did not struggle significantly in the folding and assembly processes and there was not much that 4-PBA could do to increase q_p or total titre. Another explanation could be that the

production was limited by other steps such as insufficient mRNA, etc. Furthermore, the reduction in size by the treatment, is not a desirable feature.

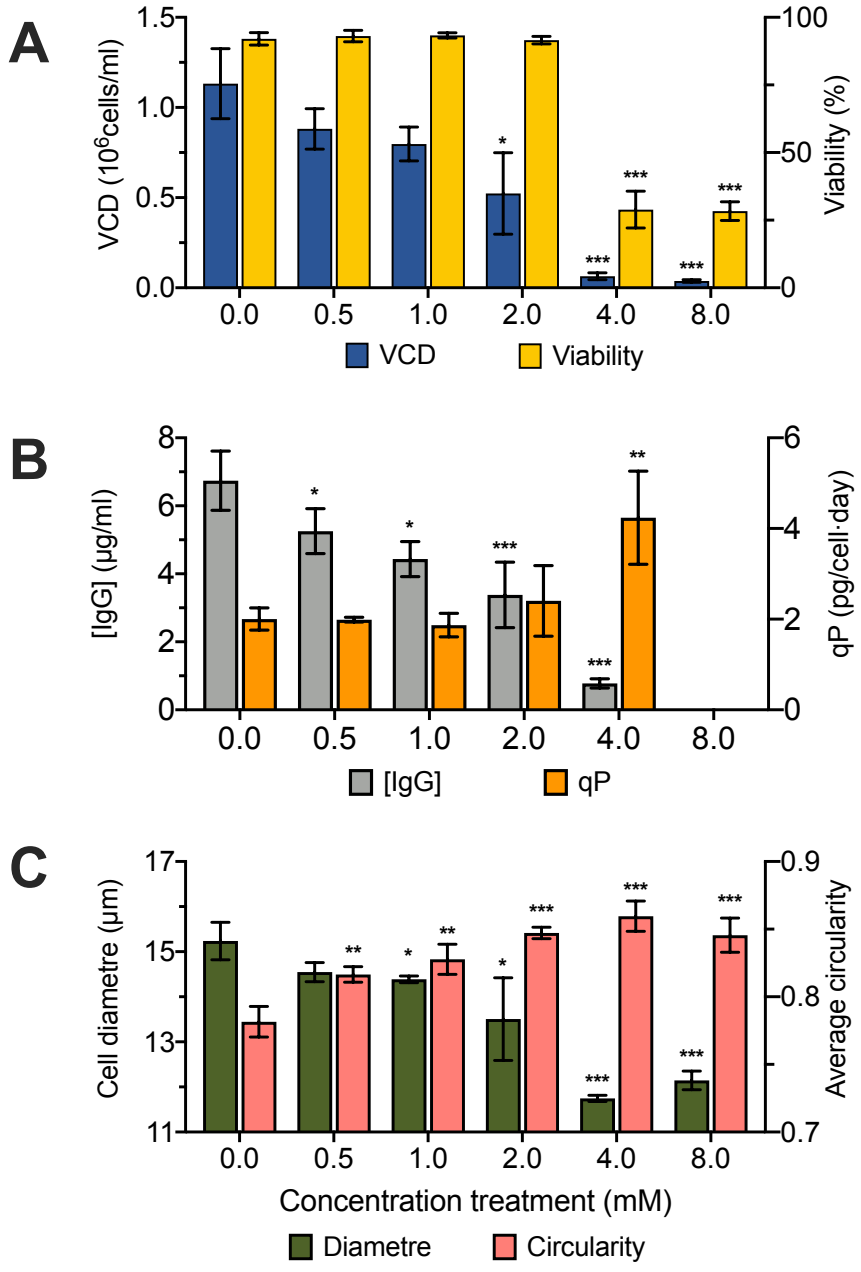

Figure 33 The effect of 4-PBA on the cell culture and IgG production in 24-well plates
Display of measurements for samples treated with 4-PBA (0.5-8 mM) during 3 days in a static humidified incubator (section 2.1.2): (A) viable cell concentration (blue) and cell viability (yellow) (section 2.1.4); (B) total protein production (grey) and relative protein production (orange) (section 2.1.5); (C) cell diameter (green) and cell circularity (red) (section 2.1.4). The error bars represent ±SD of quadruplicates. Statistical t-test was perform to compare treatments with control at p-values: (*)< 0.05, (**) < 0.01 and (***) < 0.001

3.3.1.2.2 Caffeine

Caffeine was able to lower the final viable cell concentration mildly (1.26±0.08 Viable cells/mL at the control level to around 1.0±0.1 10^6 Viable cells/mL at concentrations 13 to 125 µM). Viability was mildly affected with a 3 % drop from control (94.2±0.5 % to 91.3±0.6 % for most of the treatments) (Figure 34A).

Cell size was not affected, while the shape showed an increase in circularity that although not significant indicated a tendency of the cells to be more rounded (Figure 34D). This could be the result of an increase in osmolarity.

Finally, the total IgG produced was reduced slowly as the concentration of caffeine increased. (from 10.88±0.44 µg/mL to a final titre of 7.62±0.69 µg/mL when treated at 125 µM). The difference between the control and the treated samples was significant, but no distinction could be made across them, showing that no main differences could be found between the 13µM and 125 µM treatments (Figure 34B).

Caffeine has been of interest to the scientific community due to its capacity to interact with the cell replication step, by increasing the DNA growing points (Lehmann and Kirk-Bell, 1972; Tatsumi and Strauss, 1979). This capacity was associated with possible changes in the chromatin structure, which also allowed for making the cell less sensitive to DNA damage (Painter, 1980). As a result, caffeine was studied in order to prevent induced toxic conditions with mitoxantrone and was found to revert cell growth inhibition (Traganos, Kaminska-Eddy and Darzynkiewicz, 1991). It was also shown that, the effect over the cell line at 5 mM concentrations caused only a 5-10% decrease in cell growth. A through study of the toxicity

of this component in CHO cells, indicated that concentrations bellow 5 mM were not able to cause any significant inhibition of cell growth aligning with the findings from Traganos et al. Furthermore, this study reported how concentrations higher than 5mM (10 and 16mM) caused DNA fragmentation and increased levels of caspase 8, creating apoptosis (Fernandez 2003). On the other hand, lower concentrations between 1-2.5 mM, were able to induce positive antioxidant effects in stress CHO cells.

A patent with caffeine used in order to enhance recombinant production was created in 2005. The research indicated that caffeine in concentrations between 0.5 mM and 1.4 mM was able to increase the recombinant polypeptide production in CHO cells for different cell lines. Nevertheless, the optimized concentration of the treatment was specific to the cell line and it could only be implemented based on empirical data. This method gave up to a 1.3-fold increase in some cases. The patent study reported that the lowest concentration of caffeine (0.5 mM) resulted in the best production titre. Furthermore, 1.4mM concentrations had titre values close to the control but the viability was compromised. Nevertheless, the relation between cell growth inhibition and an increase in specific productivity was apparent. 2.5mM concentrations on the other hand, were completely toxic for the cultures. Finally, it was pointed out that lower concentrations than 0.5 mM could theoretically cause even better improvements, however they were not studied (Van Ness *et al.*, 2005).

Another study performed with CHO cells using 1 mM of caffeine, showed that the final titre and specific productivity were improved while the viable cell density and viability were kept stable. It was shown that the specific cell line was able to produce more by increasing the mRNA levels that correlated with productivity (Fomina-Yadlin *et al.*, 2015). Although this

could be one of the mechanisms by which caffeine could work in improving production, not all the cells are limited at the transcription level. Therefore, it is likely that more mechanisms are involved.

In the current project, caffeine was studied at lower concentrations than the ones reported in the literature as being active. Our study showed that lower concentrations to those previously studied did not cause any relevant changes, other than a mild inhibition of the cell growth. That was the reason for not including caffeine in the next stages of this study.

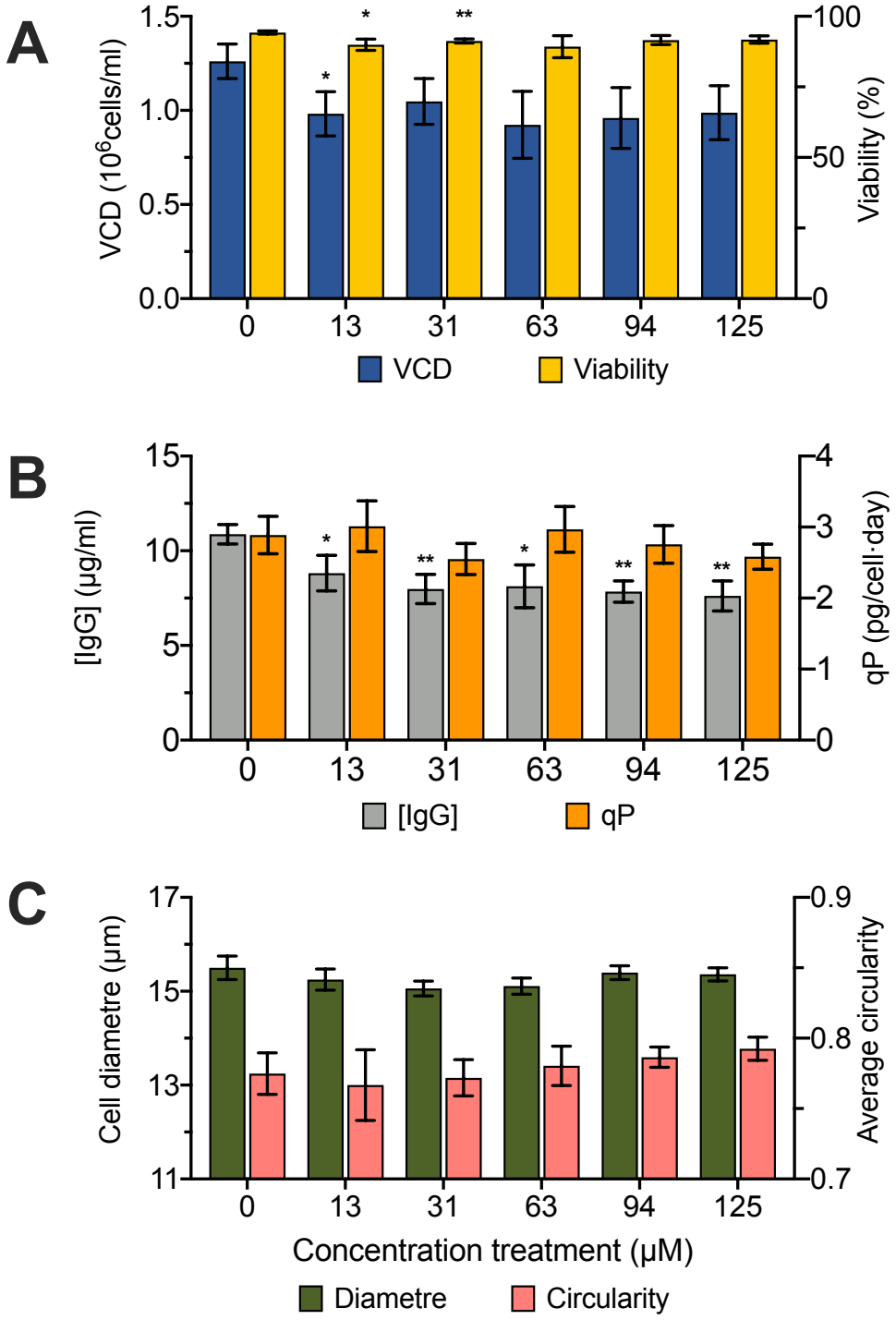

Figure 34 The effect of caffeine on the cell culture and IgG production in 24-well plates
Display of measurements for samples treated with caffeine (Cff) (13-125 µM) during 3 days in a static humidified incubator (section 2.1.2): (A) viable cell concentration (blue) and cell viability (yellow) (section 2.1.4); (B) total protein production (grey) and relative protein production (orange) (section 2.1.5); (C) cell diameter (green) and cell circularity (red) (section 2.1.4). The error bars represent ±SD of quadruplicates. Statistical t-test was perform to compare treatments with control at p-values: (*)< 0.05, (**) < 0.01 and (***) < 0.001

3.3.1.2.3 Caffeic acid phenethyl ester

CAPE was studied in the concentration range of 2 to 40 µM. This chemical had severe effects on viable cell growth arrest, with complete inhibition observed at the lowest concentration studied (0.20±0.04 10^6 viable cells/mL). Higher treatment concentrations had even more severe effects, lowering the final viable cell density bellow the initial value (0.04±0.01 10^6 viable cells/mL) (Figure 35A).

Viability was affected for all treatments when compared to the control (91.76±0.85 %). The lowest concentration used (2 µM), resulted in a value of 61.94±5.14 %. 10 µM treatment caused an even further decrease reaching a value of 24.37±2.77 %. Subsequent increases in chemical concentration, resulted in a partial recovery of viability to around 40% for treatments of 30 and 40 µM (Figure 35A).

The cell diameter was reduced for all concentrations. The diameter at the control level was 14.99±0.10 µm; that was reduced initially to 13.83±0.17 µm at 2 µM, while further increases of the concentration reduced the cell size to 11.79±0.20 µm (Figure 35C). Cell circularity, was only increased at 2µM and 4 µM treatments, from 0.81±0.00 at control level to 0.85±0.01. The rest of the concentrations did not have any significant changes in the circularity of the cells (Figure 35D).

The total recombinant IgG production was also reduced following the same pattern as the viable cell density. Productivity halved from 8.44±0.31 µg/mL at control level to 4.43±0.31 µg/mL at 2 µM, and subsequently decreased to values around 2 µg/mL for further concentrations. Nevertheless, the rate of inhibition of the cell culture by the chemical was

more effective than the one observed in the final titre. This resulted in an increase of the specific productivity for all treatment samples. The average q_p for the control was 3.14 pg/cell·day; treatment with 2 µM doubled the specific productivity to 7.44±0.50 pg/cell·day. Further increments in concentration increased the specific productivity to 17.12±0.70 pg/cell·day (5.45-fold increase) (Figure 35B). This production is associated with very high levels of toxicity; the increase in protein in the media per cell could be an artifact and just being a result of cells losing their cell membrane integrity.

There are no available studies on the effect of CAPE on CHO cells. However, this molecule has been used in medical studies and it has been reported that it interacts with various important regulatory pathways like NF-Kappa B (Wang *et al.*, 2016), nitric oxygen synthetase and has enzyme activity (Song *et al.*, 2002). Overall, the study of this molecule indicates that it has a very strong antiproliferative effect and apoptotic capacity (Ozturk *et al.*, 2012). All this relates to the high levels of toxicity found in this project.

It is unlikely that this chemical could be used for the production process in recombinant CHO cell lines, as the levels of toxicity associated are very high. On the other hand, lower concentration treatments, that could affect the cell without compromising the viability of the culture, might be possible.

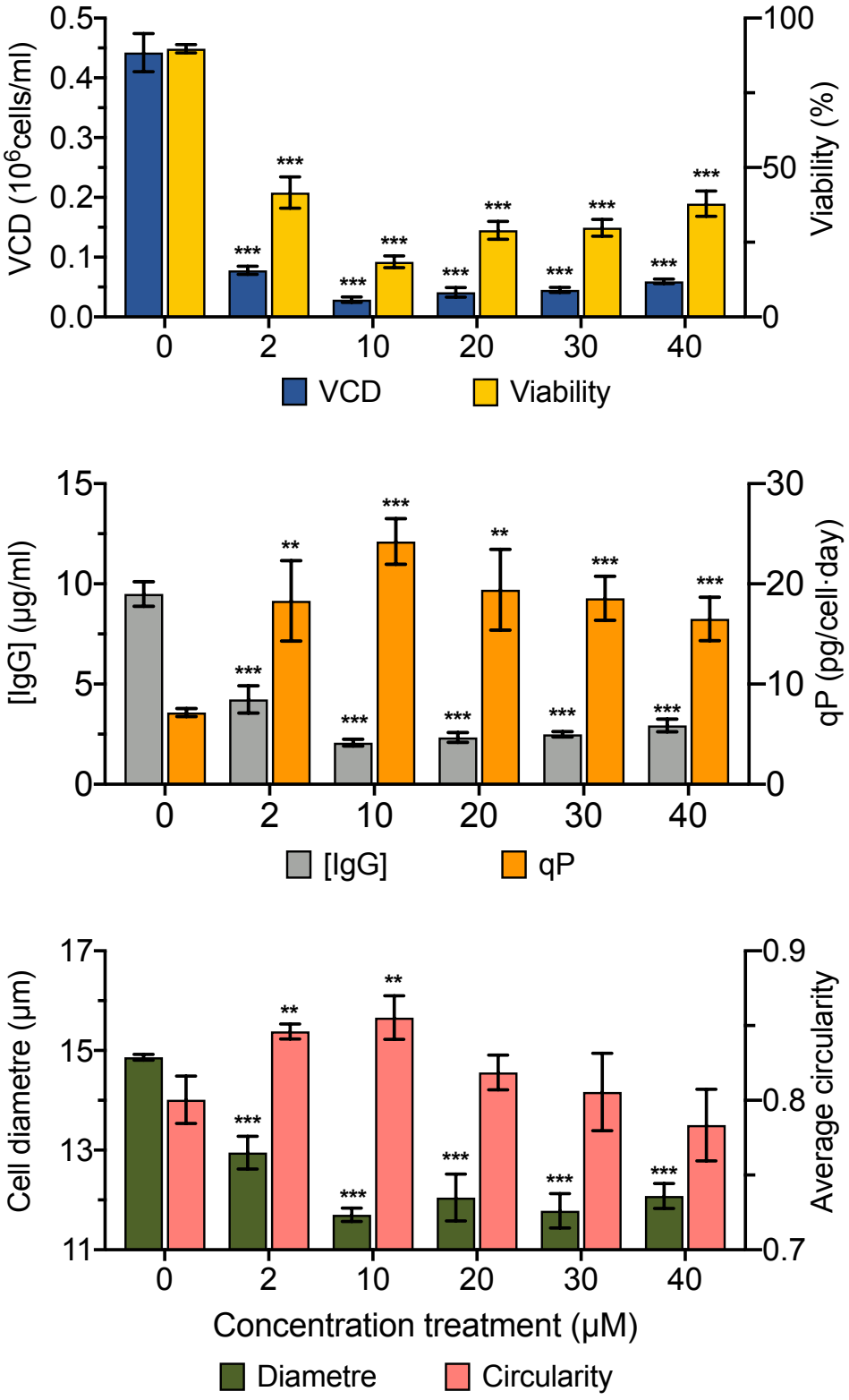

Figure 35 The effect of CAPE on the cell culture and IgG production in 24-well plates
Display of measurements for samples treated with caffeic acid phenethyl ester (CAPE) (2-40 µM) during 3 days in a static humidified incubator (section 2.1.2): (A) viable cell concentration (blue) and cell viability (yellow) (section 2.1.4); (B) total protein production (grey) and relative protein production (orange) (section 2.1.5); (C) cell diameter (green) and cell circularity (red) (section 2.1.4). The error bars represent ±SD of quadruplicates. Statistical t-test was perform to compare treatments with control at p-values: (*)< 0.05, (**) < 0.01 and (***) < 0.001

3.3.1.2.4 Curcumin

Curcumin inhibited viable cell growth in a concentration-dependent manner. Concentrations of 5, 10 and 20 µM caused growth inhibition of the viable cells of 26%, 32% and 56% respectively. Concentrations of 40 and 80 µM resulted in complete inhibition (Figure 36A). The GI_{50} was estimated at 17.2 µM.

Viability was maintained constant, at about 95%, in up to 20 µM treatments. However, treatments of 40 and 80 µM caused the viability to drop drastically down to 31 and 16% respectively (Figure 36A). The LC_{50} was calculated at 47.4 µM.

Only concentrations between 5 and 20 µM seemed to have exclusively cytostatic effects, while increasing the concentration beyond this range caused severe losses of viability and complete arrest. Therefore, the capacity to use this chemical without toxic effects is very narrow.

Cell size was mildly affected when comparing control and treatment at 20 µM, with only a small drop in cell diameter observed (from 15.9±0.20 to 15.3±0.14 µm). On the other hand, the size was considerably reduced to 12.2±0.37 µm for treatments at 40 and 80 µM (Figure 36C). Shape followed a different trend with small changes in circularity from 0.80±0.012 during the control treatment to 0.83±0.012 at 20 µM. This value stabilized as the concentration of the treatment increased (Figure 36D).

The total IgG produced followed the same trend as VCD. There was a reduction in the protein produced from the control (12.1±0.43) compared to the one produced with the 40 µM

treatment (1.15±0.69 µg/mL). The 80 µM treatment caused a mild increase, reaching 2.11±0.29 µg/mL of total IgG (Figure 36B). q_p remained constant (5.80±0.23 pg/cell·day), although for 40 and 80 µM treatments there was an increment of almost two-fold (9.78±2.57 pg/cell·day) and 10-fold (37.3±3.69 pg/cell·day) respectively (Figure 36B). It is very likely that the increase observed in q_p values for higher concentrations, is directly linked to the loss of integrity of the dead cells, causing a release of unwanted unfinished products in the media. Octet measures concentration based on the amount of protein linked to protein A of the measurement tip. It is unable to differentiate between properly folded proteins, partially assembled proteins or mature cases that still link to protein A. This could also explain why there was also an increase in total IgG when doubling the treatment from 40 to 80 µM. Another conclusion could be that although the viability was very low at 40 µM, cells were more likely to preserve the membrane integrity to some extent, as total cell density was very similar between the two (0.12±0.03 for 40 and 0.11±0.02 10^6 total cells/mL for 80µM); the total number of dead cells does not explain the increase in q_p.

Originally, curcumin was identified as a cytotoxic agent because of its capability to cause chromosomal aberrations in CHO cells. Nevertheless, it was found that this effect could be mitigated when in the presence of Fe ions(Antunes *et al.*, 2005). This has driven scientists to think that the toxic behaviour is related to its pro-oxidant nature, which generates free radicals. Media composition in CHO cell cultures is often heavily enriched with ions. A different reaction would be expected under these conditions, as curcumin was also identified to bind with orotein kinase C affecting its assembly and the signaling pathways (Pany, You and Das, 2016).

Park et al studied the effect of curcumin treatment in shaking flasks at a 20 µM concentration (cultured for a period of 16 days). The effect on recombinant CHO cells producing rituximab was similar to the ones observed in the current study. The viable curve was partially inhibited, while the viability was maintained. The protein production was very similar to that of the control (Park *et al.*, 2016).

Curcumin is a very toxic compound whose lethal curve overlapped significantly with the growth inhibition one. This reduces the range of available working concentrations. Furthermore, there was no improvement in the final titre or the specific protein production without a considerable drop in viability. Taking all this data into consideration, it was concluded that curcumin would not be a successful candidate for further research.

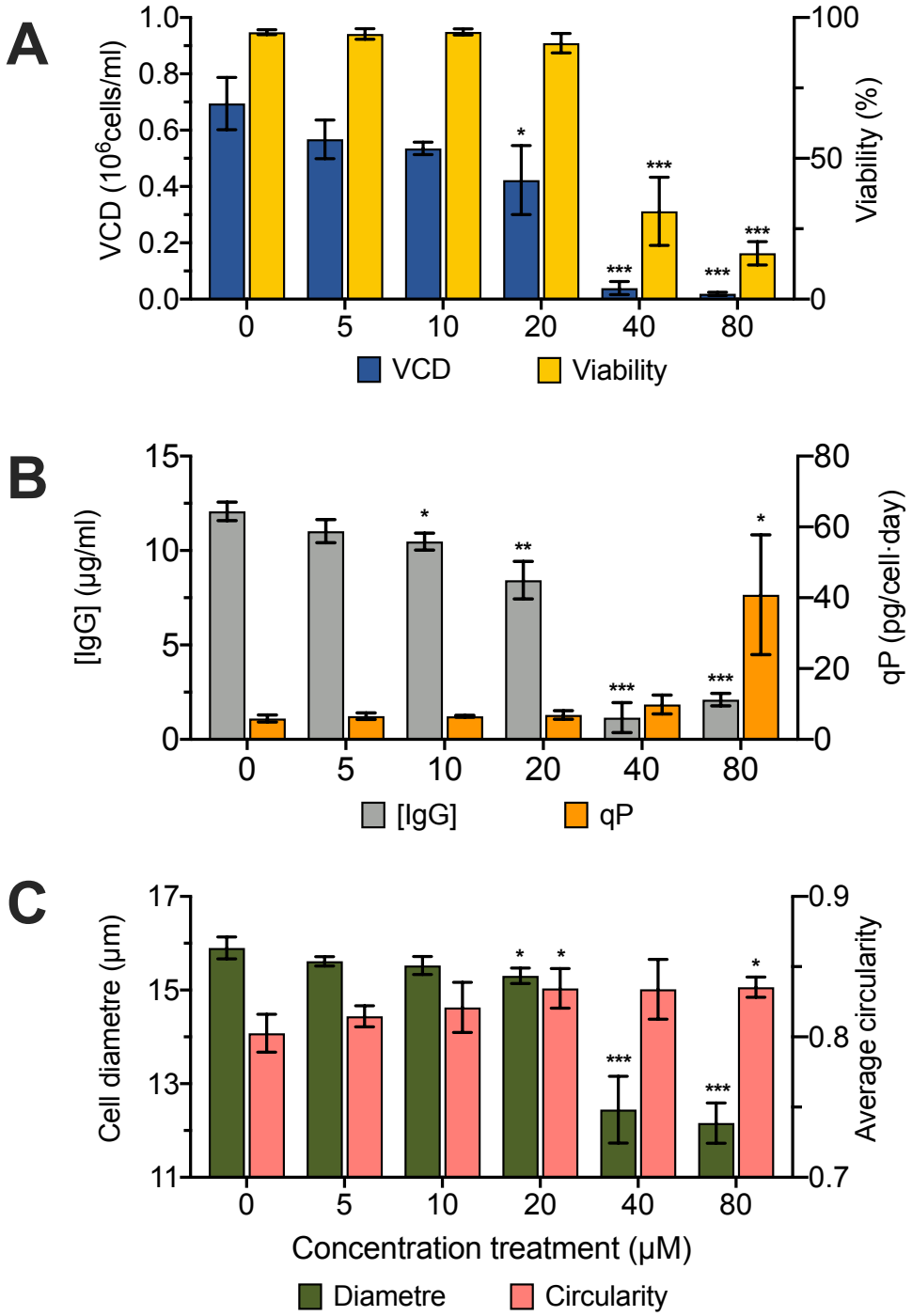

Figure 36 The effect of curcumin on the cell culture and IgG production in 24-well plates
Display of measurements for samples treated with curcumin (Crc) (5-80 µM) during 3 days in a static humidified incubator (section 2.1.2): (A) viable cell concentration (blue) and cell viability (yellow) (section 2.1.4); (B) total protein production (grey) and relative protein production (orange) (section 2.1.5); (C) cell diameter (green) and cell circularity (red) (section 2.1.4). The error bars represent ±SD of quadruplicates. Statistical t-test was perform to compare treatments with control at p-values: (*)< 0.05, (**) < 0.01 and (***) < 0.001

3.3.1.2.5 Catechin

Catechin inhibited viable cell growth in a concentration-dependent manner. Concentrations of 10 and 25 µM caused viable cell growth inhibition of 28% and 51% respectively. Higher concentrations did not increase the inhibition; this remained close to 50% (Figure 37A). The GI_{50} was estimated to be around 55.12 µM.

GI_{50} was only estimated and could not be reliably measured here, as the curve was not complete. In order to produce accurate values with the probit method, the curve needs to be delimited by two completely saturated values before and after, as well as more than one point in the middle. The values were the same for concentrations between 25 and 100 µM.

Viability was stable across the entire range of treatments (Figure 37A). LC_{50} could not be estimated nor calculated. Catechin had exclusively cytostatic effects on the cell culture and could be used for experimentations in a relatively wide range of concentrations without mayor concerns for toxic effects.

During the study of cell morphology, there were no significant changes in the cell diameter (Figure 37C); there was only a small tendency to an increase of circularity. This could be a result of the increase in osmolarity by the addition of the chemical to the media.

The total IgG produced followed the same trend as VCD. There was a reduction of the protein produced from the control (8.18±0.61µg/mL) compared to the one produced with the 25 µM treatment (5.25±0.47 µg/mL). Higher concentration treatments had the same reduced level of production. q_p was constant (2.12±0.11 pg/cell·day), only for the 10 µM treatment, while

the rest of treatments caused a significant increase (13%, 45%, 41% and 17% increase in the q_p for 25, 50, 75 and 100 µM respectively) (Figure 37B).

Previous studies have shown that catechin has the capacity to protect the DNA. It can also inhibit the cell from forming micronucleated toxic components that suppress the cell cycle (Lee Ching *et al.*, 1996). However, not much else is known about the effect of this chemical in CHO cells.

Catechin was further studied recently and was patented along with other potential antioxidants that could be added to the media to improve recombinant protein production (Tian, 2016). This patent studied catechin at 62.5 µM, 250 µM and 1mM concentrations; viability was preserved above 90% for all cases and the final titre was improved to 17%. Furthermore, it was reported that the addition of this chemical to the media, results in a decrease in ammonia and lactate levels. Finally, this experiment showed that this chemical was capable of working in high volumes up to 20 L and the improvement of productivity was maintained (Tian, 2016). Our results look more promising than the patent study data, due to higher increases in final q_p. Scale down studies in this area tend to show big improvements in recombinant protein production, but when scaling up, the gain observed is reduced or insignificant.

Viable cell growth on the other hand, was clearly inhibited in our study at lower concentrations than the ones stated in the patent. This could be the result of the use of different cell lines (aCD137 vs DG44) or different growth conditions (static well plates vs shaker flask fed-batch culture). These parameters could have had an inherent effect on the

sensitivity to the chemical which resulted in the different outcomes. In order to further study this, we would have to create experiments similar to the ones described in the patent, to analyze how the difference in cell line changes the effect of the chemical (Tian, 2016).

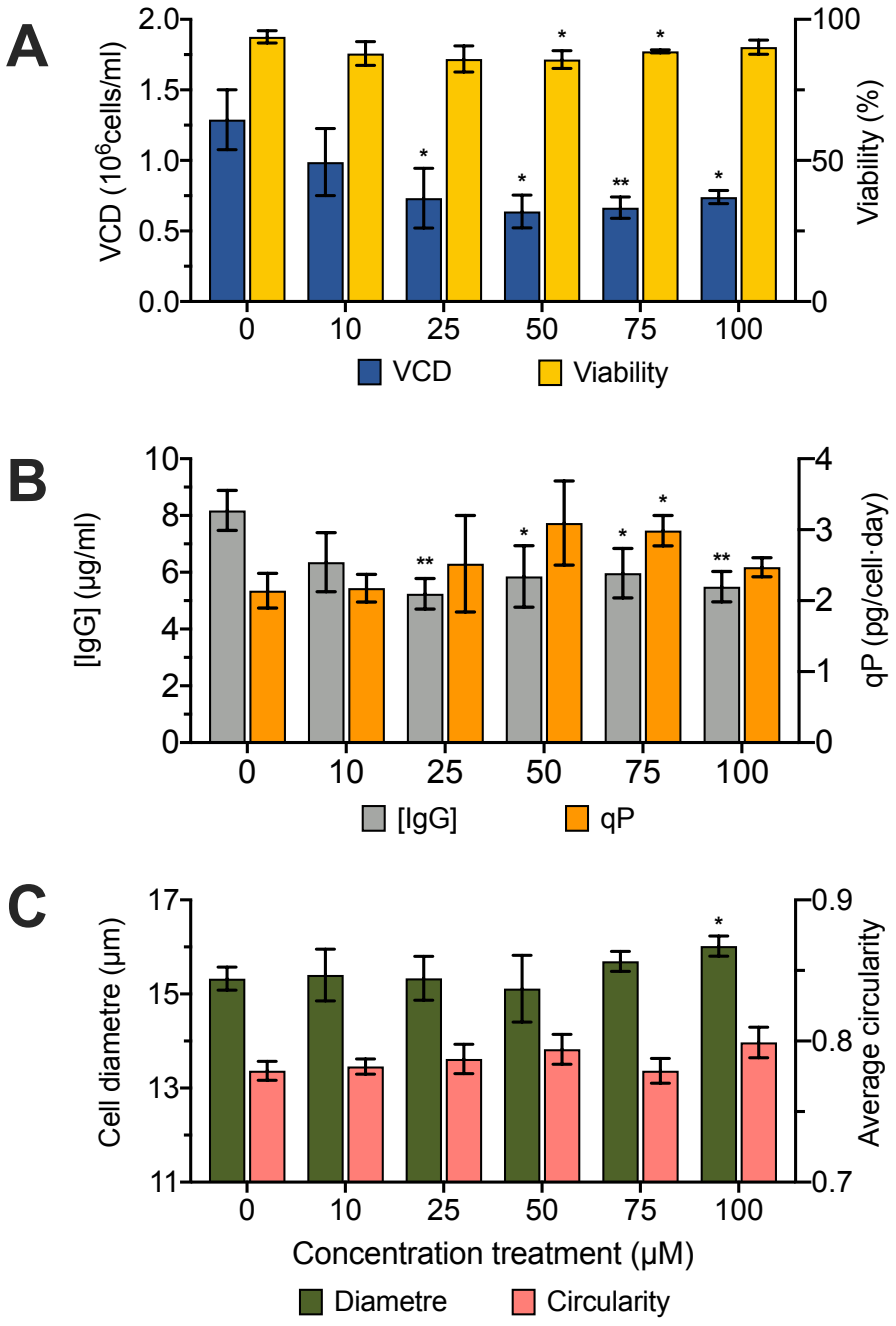

Figure 37 The effect of catechin on the cell culture and IgG production in 24-well plates
Display of measurements for samples treated with catechin (10-100 µM) during 3 days in a static humidified (section 2.1.2): (A) viable cell concentration (blue) and cell viability (yellow) (section 2.1.4); (B) total protein production (grey) and relative protein production (orange) (section 2.1.5); (C) cell diameter (green) and cell circularity (red) (section 2.1.4). The error bars represent ±SD of quadruplicates. Statistical t-test was perform to compare treatments with control at p-values: (*)< 0.05, (**) < 0.01 and (***) < 0.001

3.3.1.2.6 Epicatechin

Epicatechin inhibited viable cell growth in a concentration-dependent manner. There was no effect at lower treatments with 1 and 5 µM (approximately 0.8 10^6 Viable Cells/mL). Concentrations of 10 and 15 µM caused viable cell growth inhibition of 70% and 53% respectively. The highest treatment with 20 µM maintained the same level of inhibition that was found at 15 µM (Figure 38A). The GI_{50} was estimated to be around 15.26 µM.

GI_{50} was only estimated and could not be reliably measured here, as the curve was not complete. In order to produce accurate values with the probit method, the curve needs to be delimited by two completely saturated values before and after, as well as more than one point in the middle. The values were the same for concentrations between 5 and 20 µM.

Viability was stable across the entire range of treatments. LC_{50} could not be estimated nor calculated. Epicatechin has exclusively cytostatic effects on the cell culture and could be used for experimentations in a relatively wide range of concentrations without mayor concerns for toxic effects (Figure 38A).

During the study of cell morphology, there were no differences in shape; circularity was constant across the treatments. On the other hand, there was an increase in cell size when comparing the control treatment (15.75±0.065 µm) to higher concentrations (16.83±0.15 µm) (Figure 38C).

The total IgG produced was constant across the range of concentrations studied and was around 12 µg/mL. This, combined with the reduction of VCD in higher treatments, resulted in

an increase in the q_p. That was true for treatments with 10 μM and above. Maximum production of 8.40±0.32 pg/cell·day was observed at 15 μM (versus 5.22±0.10 pg/cell·day for control). There was an increase in specific protein production by 37%, 61% and 39% for 10, 15 and 20 μM respectively (Figure 38B).

The relationship observed between the increase in cell size and the increase in specific protein production, indicates that the reason for the increase in productivity could the bigger size of the cells. The volume of the cell at control was 205 μm^3 and the volume at 15 μM treatment was 250 μm^3; only a 20% increase in biomass resulted in a 60% increase in production. Therefore, although cells are bigger, they are also more efficient in producing more IgG.

The literature on this chemical and its effect in CHO cells, is to our knowledge inexistent. Most studies looked at other more common or famous chemicals of the same family, such as EGCG or catechin or studied the full range of catechins together by adding extracts of green tea.

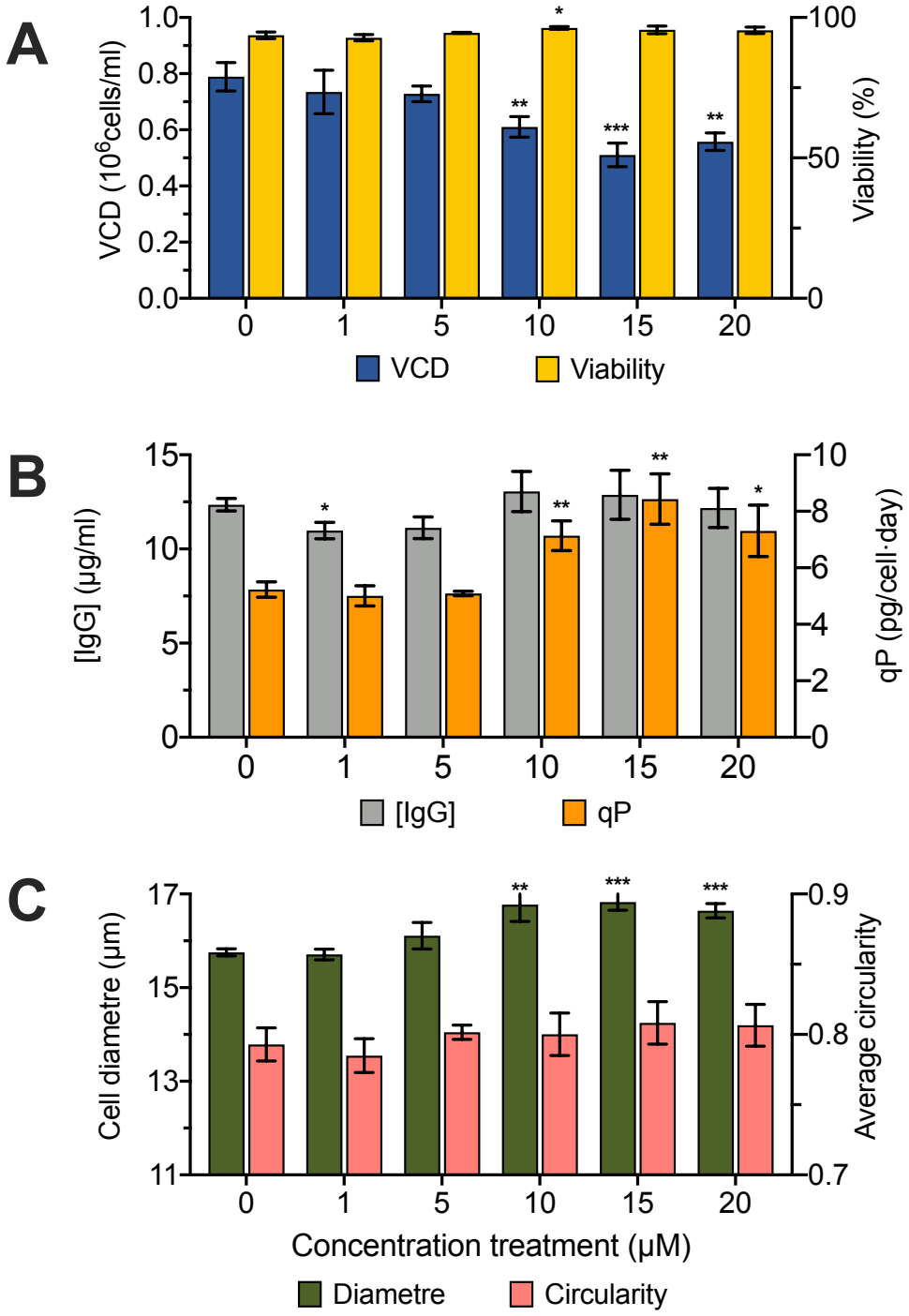

Figure 38 The effect of EC on the cell culture and IgG production in 24-well plates
Display of measurements for samples treated with epicatechin (EC) (1-20 µM) during 3 days in a static humidified incubator (2.1.2): (A) viable cell concentration (blue) and cell viability (yellow) (2.1.4); (B) total protein production (grey) and relative protein production (orange) (2.1.5); (C) cell diameter (green) and cell circularity (red) (2.1.4). The error bars represent ±SD of quadruplicates. Statistical t-test was perform to compare treatments with control at p-values: (*)< 0.05, (**) < 0.01 and (***) < 0.001

3.3.1.2.7 ECG

Epicatechin-gallate was able to inhibit viable cell growth at all the treatment concentrations studied (10-100 µM). The viable cell growth at the control level was preserved at 0.98±0.05 10^6 Viable cells/mL, while treated samples did not grow beyond 0.65±0.02 10^6 Viable cells/mL. Treatment with 100 µM resulted in almost complete inhibition (0.36±0.12 10^6 Viable cells/mL) (Figure 39A).

Concentrations between 25 and 100 µM showed an effect on viable cell density inhibition in a concentration-dependent manner. Treatment at 10 µM seemed to be consistently more effective at inhibiting cell growth than 25 µM, and as inhibiting as the 50 µM treatment. Due to this unusual effect and to the lack of a complete growth inhibition curve we could only estimate the GI_{50} at about 55.7 µM.

Viability was preserved at treatments with concentrations of up to 50 µM. There was a significant 5 % decrease with respect to the control (88.8±0.9 %). Larger concentrations of ECG resulted in a drop in viability (74.4±1.8 and 75.3±6.11 % for 75 and 100 µM respectively) Figure 39A). Although there were only indications of a viability drop at the highest concentrations and the curve of toxicity was not complete, the LC_{50} estimation stood at about 200 µM. This value is just an approximation and a full study of the curve should be done to get precise data.

Nevertheless, it was apparent that there was an overlap between the inhibition curve and the toxicity curve after 50 µM. Concentrations below this limit seemed to have mainly cytostatic effects in the cell culture.

Cell size was increased when comparing the control (14.7±0.12 to 15.4±0.1.8 µm in diameter) with the non-toxic concentrations of 25-50 µM; concentrations above or below this range did not show significant differences (Figure 39C). On the other hand, cell circularity did not show significant differences at low concentrations; there was an increase for treatments of 50 µM and above with respect to the control (0.85±0.01 % vs 0.81±0.02 % respectively) (Figure 39D).

The total IgG produced showed consistent levels of production across all the concentration treatments, which were close to the control value (11.1±0.40 µg/mL). This linked to the capacity of ECG to inhibit growth, causing a considerable increase in the specific productivity of the cell cultures, which was significantly higher for all treatments compared to the control. As a result, while the control had a q_p of 3.75±0.08 pg/cell·day, treated samples increased proportionally to cell inhibition; the specific productivity was close to 10 pg/cell·day for 75 and 100 µM treatments (2.6-fold increase). Non-toxic concentrations on the other hand, resulted in 2-fold increases, with a final specific productivity of 7.42±0.43 pg/cell·day (Figure 39B).The inverse relationship between growth and specific productivity was once again apparent with this chemical.

To our knowledge, epicatechin-gallate is a component for which there is no information on the effect that it could have on CHO cell cultures, as most studies focus on epigallocatechin-gallate.

Overall, ECG looks like a promising candidate for use in recombinant IgG production. While concentrations above 50 µM are toxic and should be avoided, concentrations below this threshold are promising. The most ideal concentration would be 10 µM, as it causes the same

effects as 25 or 50 but there is less risk of toxicity in the long run. The use of 10 µM would also make the process cheaper if it was to be scaled up, as this chemical is very expensive.

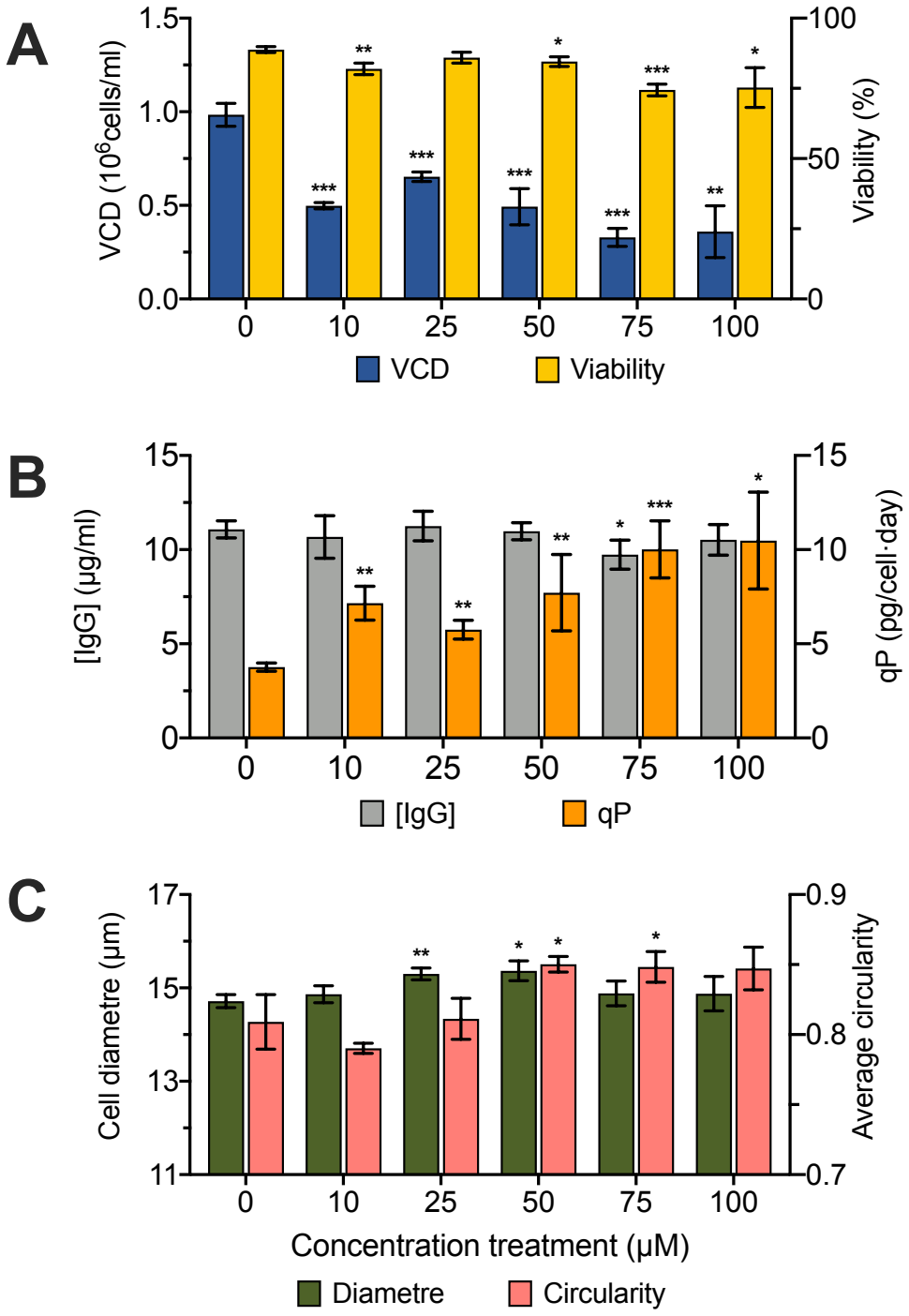

Figure 39 Thd effect of ECG on the cell culture and IgG production in 24-well plates
Display of measurements for samples treated with epicatechin-gallate (ECG) (10-100 mM) during 3 days in a static humidified (section 2.1.2): (A) viable cell concentration (blue) and cell viability (yellow) (section 2.1.4); (B) total protein production (grey) and relative protein production (orange) (section 2.1.5); (C) cell diameter (green) and cell circularity (red) (section 2.1.4). The error bars represent ±SD of quadruplicates. Statistical t-test was perform to compare treatments with control at p-values: (*)< 0.05, (**) < 0.01 and (***) < 0.001

3.3.1.2.8 EGCG

Epigallocatechin-gallate was studied at a range of concentrations from 5 to 100 µM. The effect of this chemical on the viable cell density was consistent across all concentrations after three days of incubation and resulted in a 42% inhibition when compared to control (0.55±0.06 10^6 vs 0.94±0.03 10^6 viable cells/mL) (Figure 40A).

On the other hand, viability remained stable for all samples and there were no significant differences with respect to the control (92.6±1.4%) (Figure 40A).

Cell size remained stable with no significant differences with respect to the control (16.05±0.32 µm) (Figure 40C). There was a concentration-dependent-increase in cell shape (0.76±0.02 at control level to 0.80±0.02 at 50µM) (Figure 40D). The value was maintained at this level for increasing concentrations.

The total IgG produced was kept constant for all treatments up to 50 µM, while higher concentrations resulted in a small decrease of the produced recombinant protein (9.02±0.63 and 7.7±0.27 µg/mL at 75 and 100 µM respectively vs 8.23±0.7 µg/mL at control level). The final titre was reduced by 6% at 100µM. There was more than 40% inhibition of the cell density and an increase of the specific productivity observed at all the tested concentrations. While treatment at the control level produced protein at a q_p of 3.63±0.09 pg/cell·day, treatment at 50 µM caused the biggest increase with 6.90±0.42 pg/cell·day produced (1.9-fold increase) (Figure 40B).

EGCG has the capacity to reduce the toxicity in cultured cells due to aggregation (Bieschke *et al.*, 2010) and the capacity to improve the viability of immortal cell lines at low concentrations (Lu, Ou and Lu, 2013). Nevertheless, this chemical can also cause DNA damage and trigger apoptosis (Lu, Ou and Lu, 2013). The level of toxicity for each cell line is dependent on factors such as the interaction of EGCG with the media (Long *et al.*, 2007) or the permeability of each cell line to the chemical (Zhang *et al.*, 2013).

Parallel studies in recombinant protein production in CHO cells, showed that EGCG can be implemented in growth cell media composition from 44 µM to 1.1 mM concentrations. The chemical had the potential to enhance protein production by 20%. Furthermore, this addition was able to reduce the acidic and basic species of the recombinant IgG, reducing the relative charge heterogeneity of the product consistently across the time of the culture. Finally, this study showed that the half-life of EGCG in the media after the addition was of about six hours (Hossler *et al.*, 2015).

EGCG has been well-researched and has been recently proven to help IgG production (Hossler *et al.*, 2015). This correlates with our observations, since it can improve specific productivity if added under proper conditions. Its capacity to stop the growth and enhance specific recombinant protein production is likely due to the suppression of cell growth and the increase of specific recombinant production associates with it (Vergara *et al.*, 2014). The lack of toxicity also allows for the usage at a wide range of concentrations to promote changes in the metabolic dynamics in cell cultures.

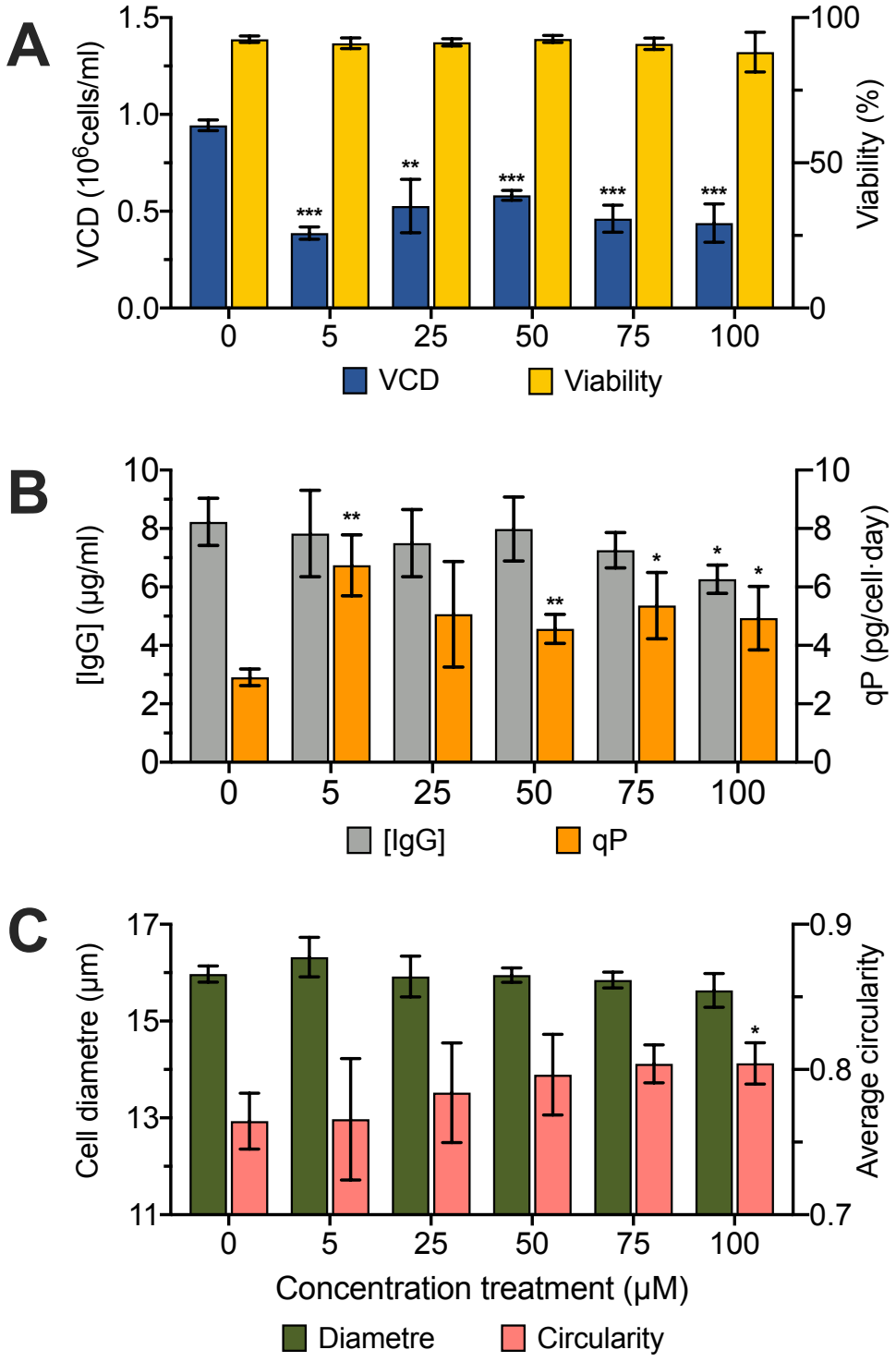

Figure 40 The effect of EGCG on the cell culture and IgG production in 24-well plates
Display of measurements for samples treated with Epigallocatechin-gallate (EGCG) (5-100 µM) during 3 days in a static humidified incubator(section 2.1.2): (A) viable cell concentration (blue) and cell viability (yellow) (section 2.1.4); (B) total protein production (grey) and relative protein production (orange) (section 2.1.5); (C) cell diameter (green) and cell circularity (red) (section 2.1.4). The error bars represent ±SD of quadruplicates. Statistical t-test was perform to compare treatments with control at p-values: (*)< 0.05, (**) < 0.01 and (***) < 0.001

3.3.1.2.9 GCG

Gallocatechin gallate was studied in the range of 5 to 100 µM. The effect of this flavonoid on viable cell density was very similar to the one already observed for EGC; all concentrations caused a decrease in the viable cell density after three days of incubation. There was a 16% inhibition with treatment at 25 µM compared to control (0.67±0.06 10^6 vs 0.80±0.06 10^6 viable cells/mL). At 100 µM concentration, the respective value was 0.44±0.09 10^6 viable cells/mL; this was the most severe inhibition, equivalent to 45% (Figure 41A). Although the viable cell density was affected in a concentration-dependent manner, the first treatment with 5 µM caused a more severe inhibition than expected. This was similar to the behaviour observed when adding structural chemicals of the same family such as EGCG or EGC. As a result of this, GI_{50} was estimated as 41.13 µM.

Viability was affected in a concentration-dependent manner with a small reduction from the control level (91.8.4±1.0 % to 84.3±0.6 % at 100 µM treatment) (Figure 41A). Overall, only concentrations of 50 µM and higher had significantly lower viabilities with respect to control. Nevertheless, viability was not affected by big drops. The lack of severe toxicity in this range of concentrations made it impossible to estimate the LC_{50}.

Cell size was affected by GCG treatments, by significantly increasing the cell diameter at 5 µM (15.9±0.1 µm) in comparison to the control (15.5±0.2 µm). The further increase in concentration, reduced the cell size to a lower, non-significant average (15.2±0.1 µm) at 100 µM treatment (Figure 41C). Cell shape was increased in a concentration-dependent manner with respect to the control (0.75±0.01), with 50 µM treatments and above ranging at the same level of circularity (0.83±0.01) (Figure 41D).

The total IgG production under all conditions was maintained constant with respect to control (7.92±0.63 μg/mL). This together with the inhibitory effect of the chemical, increased the specific productivity of all treated samples in comparison to the control. In more detail, at 25 μM treatment the value was 3.93±0.14 pg/cell·day while at control level the respective value was 3.29±0.12 pg/cell·day (1.2-fold increase). The maximum value observed was 5.66±0.39 pg/cell·day (1.72-fold increase) (Figure 41B).

Gallocatechin-gallate has not been studied much before. Most studies focus on epigallocatechin-gallate which is a more abundant chemical in green tea and other products. Nevertheless, GCG showed an important inhibition capacity with very low toxicity levels, which would allow studies in recombinant production. Furthermore, this chemical was able to enhance specific productivity. Like many other chemicals of the same family, such as ECG or EGCG, GCG was able to shift primary metabolism into secondary metabolism, without compromising cell viability. This characteristic could be useful in recombinant IgG production. Finally, it is important to point out that this chemical acted almost identically as EGCG, and it is likely that the mechanism of action behind is very similar.

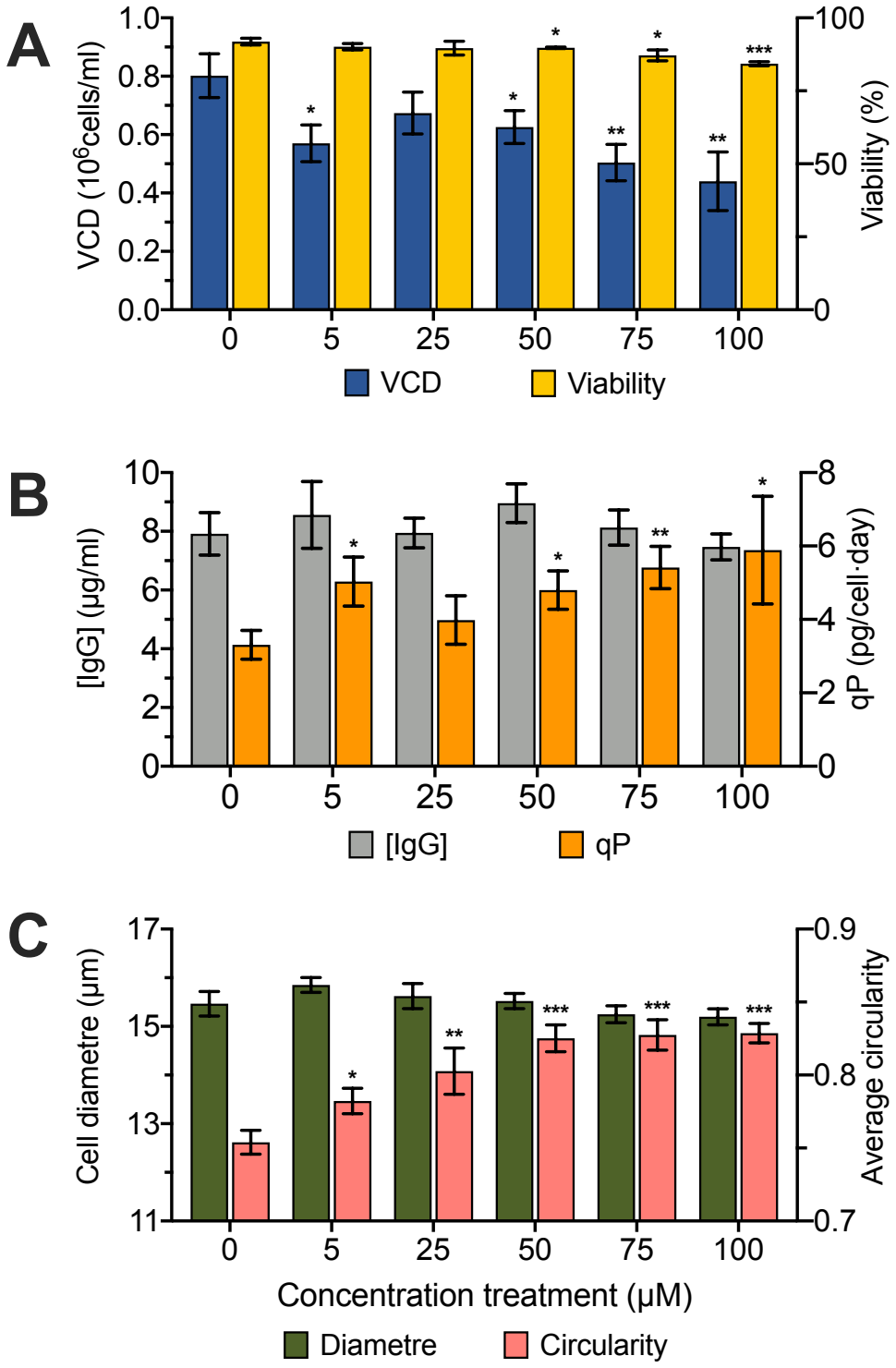

Figure 41 The effect of GCG on the cell culture and IgG production in 24-well plates
Display of measurements for samples treated with gallocatechin-gallate (GCG) (5-100 µM) during 3 days in a static humidified incubator(section 2.1.2): (A) viable cell concentration (blue) and cell viability (yellow) (section 2.1.4); (B) total protein production (grey) and relative protein production (orange) (section 2.1.5); (C) cell diameter (green) and cell circularity (red) (section 2.1.4). The error bars represent ±SD of quadruplicates. Statistical t-test was perform to compare treatments with control at p-values: (*)< 0.05, (**) < 0.01 and (***) < 0.001

3.3.1.2.10 Glycine betaine

Glycine betaine caused an increase in the viable cell density growth in a concentration-dependent manner. The final viable cell density was 40% higher at 100 µM (1.13±0.16 10^6 Viable cells/mL) with respect to the control (0.81±0.03 10^6 Viable cells/mL) (Figure 42A).

Parallel to this, viability was not affected in this range of treatments and it was preserved at a range of 90 to 92% in all cases (Figure 42A).

The cell morphology study did not show any differences; cell size was maintained constant at 14.77±0.14 µm (Figure 42C). On the other hand, circularity showed an increase on average from 0.81±0.02 at the control level to 0.83±0.004 at 100 µM, although this was not significant (Figure 42D).

The total IgG produced was mildly reduced across the study range; at the control level, the IgG was 9.05±0.53 µg/mL, decreasing down to values around 7.5-8.0±1 µg/mL. The reduction of production was not always significant. This was linked to an increase of viable cells, resulting in a decrease in the specific protein production in a concentration-dependent manner (3.75±0.08 at control to 2.24±0.14 pg/cell·day at 100 µM, a 60% decrease) (Figure 42B).

Betaine was able to increase cell proliferation and maintain the viability of the cells, without affecting cell morphology. Unfortunately, this did not result in a direct immediate increase of the total IgG production or an increase in q_p. This could be the result of this chemical fomenting cell growth, which in turn diminishes the number of resources that the cell would

put into IgG production. It is well established that when cells lower their primary metabolism (growth metabolism) they shift into secondary metabolism, which among other things comprises recombinant IgG production. As a result, the relationship between cell growth and specific productivity is often inverse as shown here.

Glycine betaine could be used in the early stages of the culture to promote cell growth, but this would need to be measured carefully. The investigations on CHO cell cultures showed that the faster the culture grows, the faster it enters into late-stage and the stationary phase is shortened. This could lead to premature low viability and a lower quality of the product.

Glycine betaine has been heavily researched before as an osmoprotective agent. When used in combination with sodium chloride it improves recombinant protein production. However, this modification of culture conditions caused simultaneous suppression of cell growth. As a result, this osmoprotective chemical was studied in order to negatively mitigate the effects of high osmolarity conditions. Research showed that the chemical was able to mitigate hyperosmotic stress by increasing cell growth and specific productivity (Ahn *et al.*, 1999). The method used to implement this technology consisted of a two-step culture. During the first step, cells were allowed to grow; during the second one, glycine betaine and sodium chloride were added simultaneously to increase the production of erythropoietin up to 3-fold. Erythropoietin is difficult to express protein (Ahn *et al.*, 1999). Nevertheless, the effects of glycine betaine are not easily transferable, and there are different responses depending on the cell line used (Tae Kyung *et al.*, 2000) or the clone of the same cell line (Ryu *et al.*, 2000). Further studies indicate that, the use of this chemical in combination with cold temperature shifts, is able to enhance productivity by elongating viability on the culture when added at

15mM (Yoon and Ahn, 2007). Although, current experiments in a transient cell line with a difficult to express biologic indicate no positive significant changes in specific productivity nor final titre (Johari *et al.*, 2015a).

The mechanism by which glycine betaine could help protein production is not well understood. Studies have suggested that the effect of the chemical may have to do with translation, as mRNA levels correlate to the productivity of the different cell lines (Tae Kyung *et al.*, 2000). Nevertheless, the mechanism is very complex and difficult to predict, as it involves upregulations of proteins that are part of cellular metabolism, mRNA profiling, protein folding and secretion as well as cellular structure (Kim, Kim and Lee, 2012).

The present results encounter a different context for glycine betaine as, cells were not treated at high osmolarities, shifted to low temperatures or cultivated for long periods of time. This could be the main reason why glycine betaine in the present study did not show improvements in recombinant protein production. Other factors that could have had an impact are the cell line, the recombinant protein or the media used.

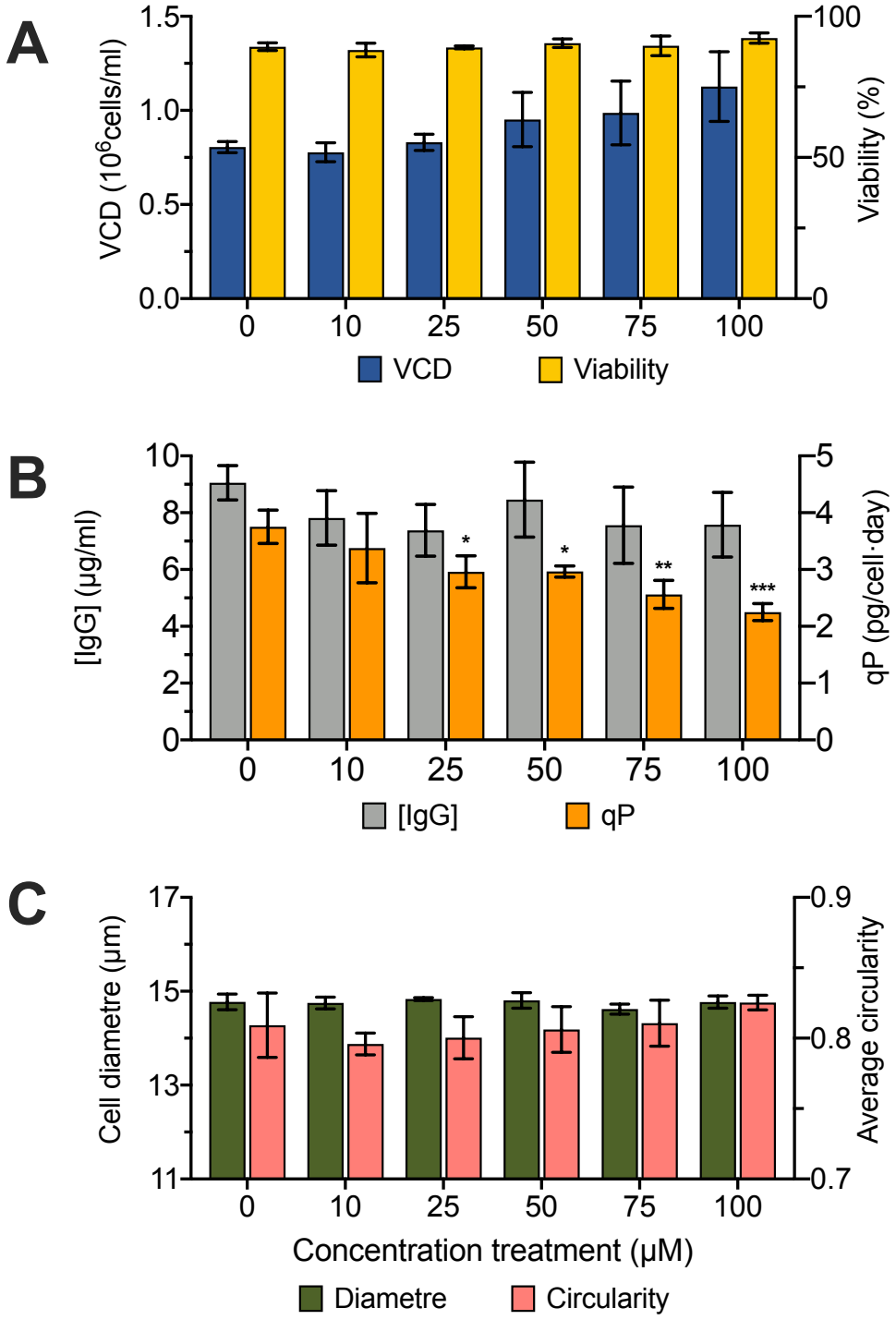

Figure 42 The effect of glycine betaine on the cell culture and IgG production in 24-well plates Display of measurements for samples treated with glycine betaine (Btn) (10-100 µM) during 3 days in a static humidified incubator(section 2.1.2): (A) viable cell concentration (blue) and cell viability (yellow) (section 2.1.4); (B) total protein production (grey) and relative protein production (orange) (section 2.1.5); (C) cell diameter (green) and cell circularity (red) (section 2.1.4). The error bars represent ±SD of quadruplicates. Statistical t-test was perform to compare treatments with control at p-values: (*)< 0.05, (**) < 0.01 and (***) < 0.001

3.3.1.2.11 Kaempferol

Viable cell density dropped consistently and reached full viable growth arrest at 100 µM (0.18±0.1 10^6 Viable cells/mL). Higher concentrations of kaempferol reverted this and a small increase of the viable cell density was seen with subsequent treatments at 150 and 200 µM (0.31±0.02 and 0.44 ±0.08 10^6 Viable cells/mL respectively) (Figure 43A). This recovery effect could be a result of drop out of solution of kaempferol at higher treatment conditions. Kaempferol is a flavonoid. It is soluble in organic solvents and has low solubility in aqueous solutions. The estimated GI_{50} was 56 µM. This value is just a general reference. It might not be accurate as viability came back up as explained previously.

Toxicity was not observed in treatments of 50 µM or bellow. Concentrations above those (100 to 200 µM) caused a decrease in viability to about 67±3.46 % (Figure 43A). The LC_{50} could not be properly calculated nor estimated due to the lack of the complete toxicity curve. Another reason could be the fact that the chemical likely dropped out of solution in the higher concentration treatments. Nevertheless, the overlap between the inhibition curve and the toxic curve was considerable and the range of concentrations that could be effective but not toxic is narrow.

The study of the morphology showed that there was no significant change in size for concentrations that were not affecting viability. In more detail, treatment with the control and treatments with concentrations up to 50 µM, had an average size of 15.8±0.26 µm, while treatments with concentrations above 50 µM, caused a big decrease in cell diameter (12.8±0.29, 10.8±0.26 and 10.4±0.32 µm for 100, 150 and 200 µM respectively) (Figure 43C).

There was a tendency for an increase in cell circularity as concentrations increased from 0 (control) to 50 µM. On the other hand, there was a big drop in circularity at 50 (0.81±0.01) and 100 µM (0.74±0.01). Higher successive concentrations only resulted in small increases in circularity (Figure 43D).

The total IgG concentration decreased slowly and in a proportional way to viable cell density in 10 and 50 µM treatments, resulting in a specific protein production of 3.85±0.15 pg/cell·day. The total protein production for the 100 µM treatment, had a big drop to 3.24±0.19 µg/mL. This reduction in the IgG produced was not as significant as the reduction of the viable cell density. Specific protein production was increased by 60% (5.91±0.16 µg/mL) with respect to the original control value. Higher concentrations of the treatment resulted in a decrease of q_p with respect to the control, but the total production was maintained to the levels observed at 100 µM treatment (Figure 43B). The viable cell density observed was recovered as explained before.

In summary, kaempferol treatment did not cause toxic effects in concentrations up to 50 µM; it reduced the viable cell concentrations, it did not change cell size, but it increased circularity, probably due to an increase in osmolarity. There were no changes in the relative production and the total IgG was reduced. Overall, it was not apparent how kaempferol could be used for protein production in this range of concentrations and within this set of conditions.

The 100 µM treatment showed complete cell growth arrest; viability was compromised. Cell shape and size changed drastically. Although there were signs of an increase in the specific

productivity, this is linked to low viability; the increase could be a result of cell death and loss of cell membrane integrity causing non-mature IgG leakage into the media.

Overall, kaempferol seems to be a very cytotoxic component that does not improve specific protein production without compromising viability. It causes radical changes in cell morphology (eg. diameter). It is unlikely that kaempferol could be used in this set of conditions for the improvement of recombinant protein production.

Kaempferol was found to affect CHO cells by causing chromosomic aberrations for concentrations between 87 to 157 mM (Carver, Carrano and Macgregor, 1983). Little else has been studied about the effects of this chemical in CHO cells.

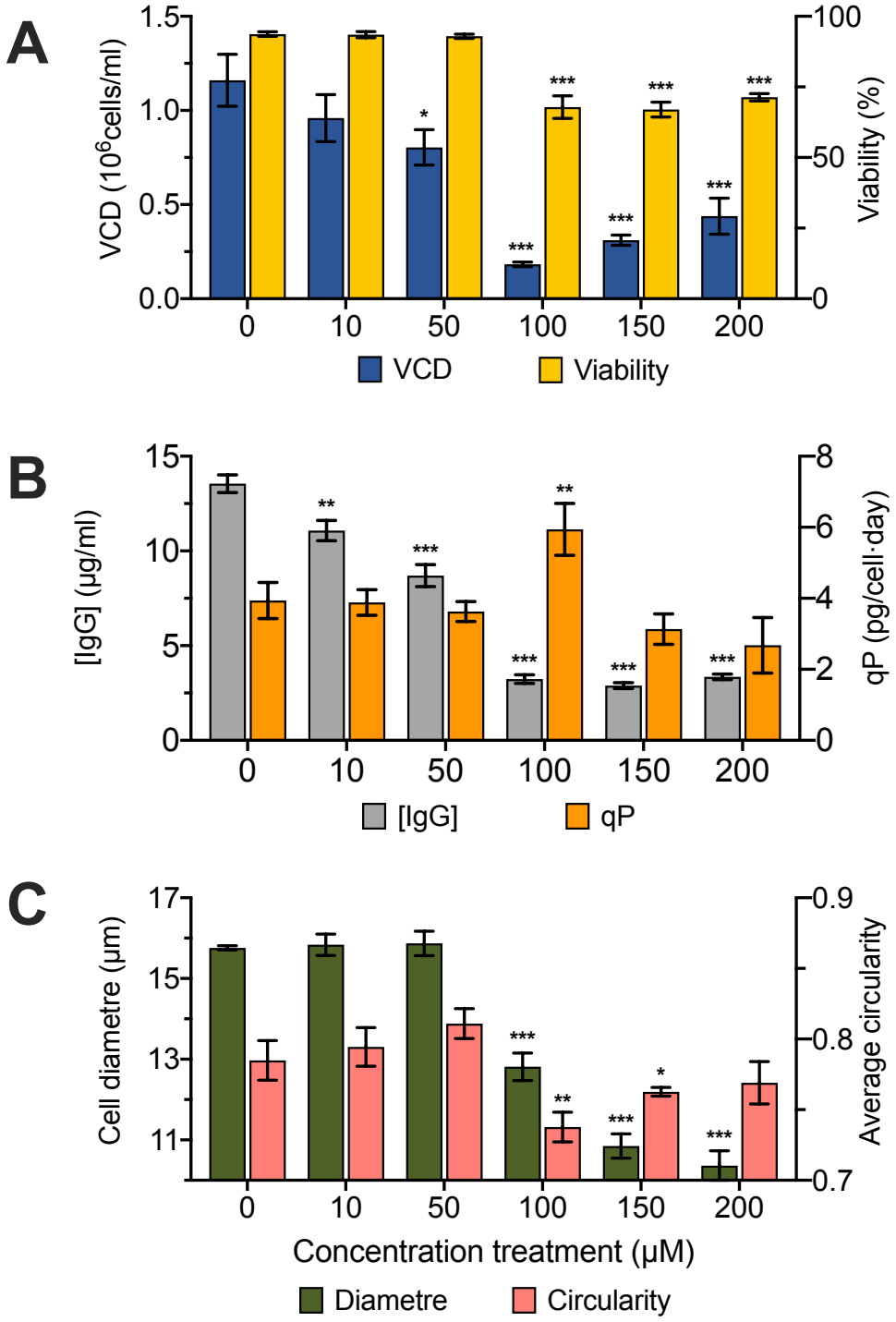

Figure 43 The effect of kaempferol on the cell culture and IgG production in 24-well plates
Display of measurements for samples treated with kaempferol (Kmp) (10-200 µM) during 3 days in a static humidified incubator (section 2.1.2): (A) viable cell concentration (blue) and cell viability (yellow) (section 2.1.4); (B) total protein production (grey) and relative protein production (orange) (section 2.1.5); (C) cell diameter (green) and cell circularity (red) (section 2.1.4). The error bars represent ±SD of quadruplicates. Statistical t-test was perform to compare treatments with control at p-values: (*)< 0.05, (**) < 0.01 and (***) < 0.001

3.3.1.2.12 Luteolin

Luteolin was studied in a range of concentrations from 2 to 20 µM. Treatment for three days resulted in a concentration-dependent decrease in viable cell density from 0.93±0.13 10^6 viable cells/mL at control level to 0.52±0.06 10^6 viable cells/mL at 20 µM (equivalent to a 45% decrease) (Figure 44A). The estimated GI_{50} was 13.15 µM although the curve was not completely studied.

Viability was preserved above 90% for all cases, with no significant differences with respect to the control (94.87±1.07%). The only exception was the 20 µM treatment, which is significant with viability of 91.1±0.58% (Figure 44A).

Cell size followed the same trend as viability and was maintained constant (14.78±0.15 mµ) regardless of the treatment (Figure 44C). At the same time, cell shape was maintained (Figure 44D).

The total recombinant protein produced remained stable at all treatments on levels close to the control (11.75±0.46 µg/mL). This resulted in a steady increase in specific protein production in a concentration-dependent manner, with a final q_p of 7.13±0.27 pg/cell·day for the highest concentration of luteolin treatment (20 µM). This was equal to a 1.72-fold increase with respect to the control (3.29±0.12 pg/cell·day) (Figure 44B).

There is limited information about the effect of luteolin in CHO cells. Most studies performed used this cell line as a recombinant factory in order to study the medical effects of the chemical in functional pathways, such as the ones of dopamine transporter interaction with

this flavonoid (J. Zhang *et al.*, 2010; Zhao *et al.*, 2010). This indicates bioactivity of the component, but does not relate to the study circumstances described here.

Other studies carried out, used a plant extract including luteolin and not the isolated chemical. As a result, it is difficult to correlate any of the effects described (Gemelli *et al.*, 2015; Jaramillo-García *et al.*, 2018).

To our knowledge there is no study available on the effect of luteolin on non-producer or recombinant CHO cell lines. Our hypothesis is that luteolin could be a good candidate for further research in recombinant production, as this molecule is able to shift primary metabolism into secondary, without having main toxic effects. Moreover, it can increase the specific productivity without main alterations in the cell morphology.

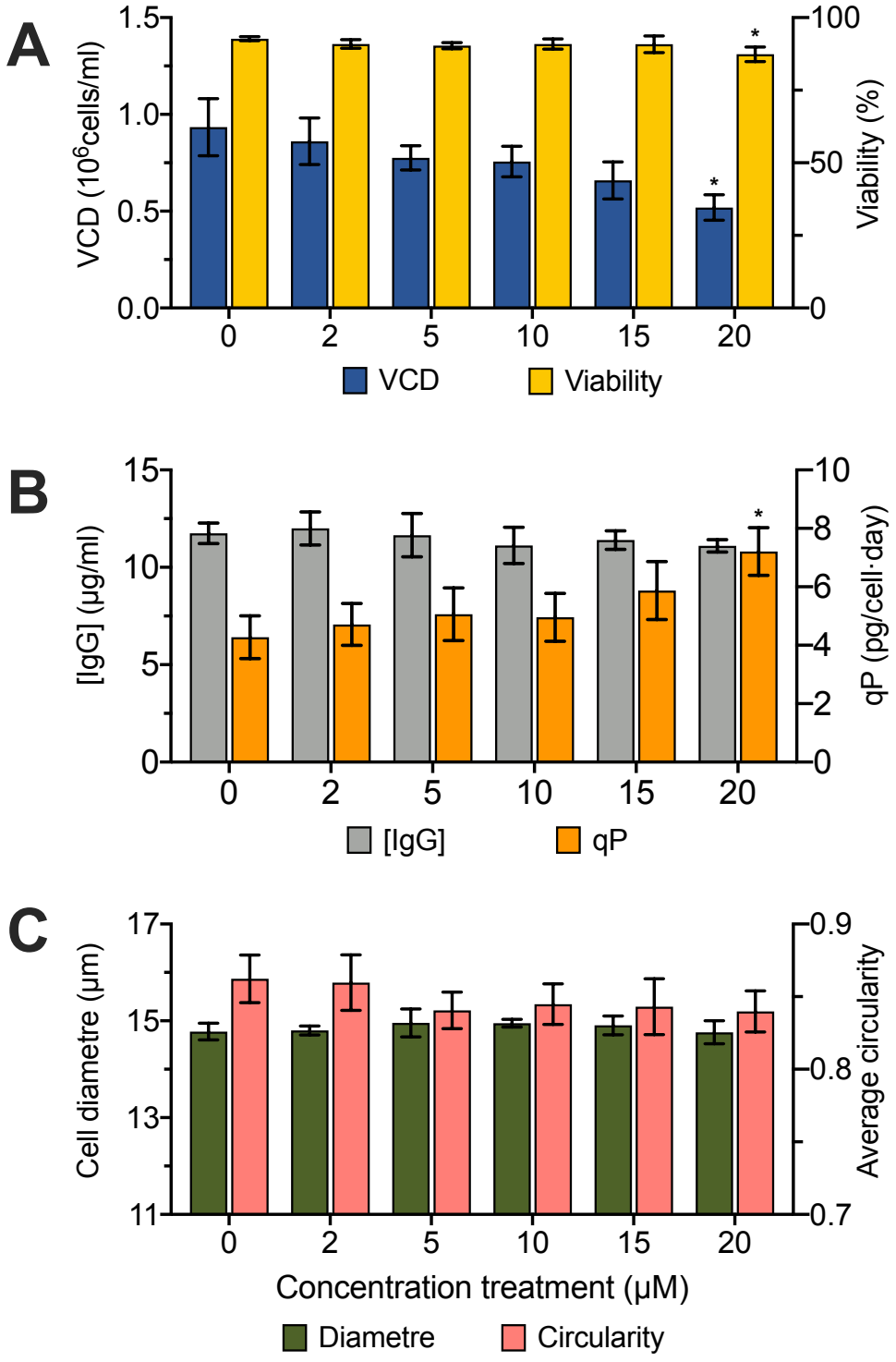

Figure 44 The effect of luteolin on the cell culture and IgG production in 24-well plates
Display of measurements for samples treated with luteolin (Ltl) (2-20 µM) during 3 days in a static humidified incubator (section 2.1.2): (A) viable cell concentration (blue) and cell viability (yellow) (section 2.1.4); (B) total protein production (grey) and relative protein production (orange) (section 2.1.5); (C) cell diameter (green) and cell circularity (red) (section 2.1.4). The error bars represent ±SD of quadruplicates. Statistical t-test was perform to compare treatments with control at p-values: (*)< 0.05, (**) < 0.01 and (***) < 0.001

3.3.1.2.13 Piceid

Piceid was studied in the concentration range from 10 to 100 µM. The chemical was found not to affect the viable cell concentration (0.85±0.05 10^6 Viable cells/mL) nor the viability (93.0±1.2 %) (Figure 45A). Furthermore, the morphology of the cells was kept constant with no significant changes in cell size (diameter 15.03±0.09 µm, circularity around 0.82±0.01) (Figure 45C&D).

The total IgG produced decreased from 14.55±0.26 µg/mL to about 11.3±0.55 µg/mL (32% reduction). The specific productivity also decreased from 5.7±0.1 pg/cell·day at the control level to 4.04±0.12 pg/cell·day at 100 µM (Figure 45B).

Piceid is the major precursor of resveratrol, which is a well-studied bioactive compound. Most of the studies performed were carried out using the final form. A study performed on cancer cells showed that it had a higher scavenging capacity than resveratrol, but caused less biological activity (Su *et al.*, 2013). Finally, the only study available on the effect of this component on CHO cells reported that piceid was not able to bind to CHO cells at the same concentrations as resveratrol (Xue, Dong and Liang, 2016). This correlates with the lack of bioactivity observed in our study when investigating the same concentrations of resveratrol and piceid. This difference in bioactivity could be linked to the difficulty of the cell to uptake the molecule (Xue, Dong and Liang, 2016).

Piceid is unlikely to be considered as a potential chemical additive as it caused no apparent benefits to the producing cell line in the current examination. Further research into higher concentrations may be needed in order to properly assess the capabilities of this molecule.

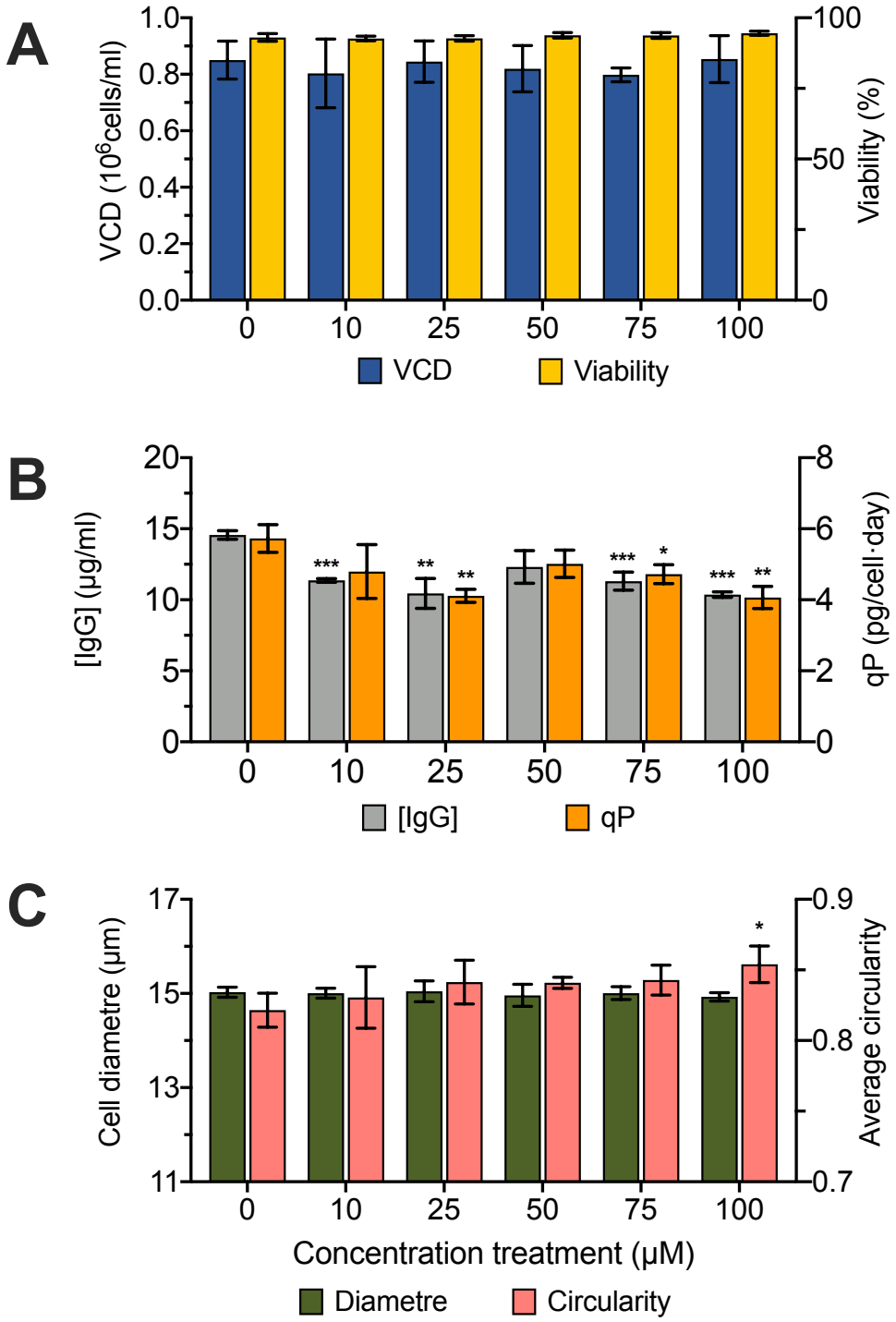

Figure 45 The effect of piceid on the cell culture and IgG production in 24-well plates
Display of measurements for samples treated with piceid (Pcd) (10-100 µM) during 3 days in a static humidified incubator (section 2.1.2): (A) viable cell concentration (blue) and cell viability (yellow) (section 2.1.4); (B) total protein production (grey) and relative protein production (orange) (section 2.1.5); (C) cell diameter (green) and cell circularity (red) (section 2.1.4). The error bars represent ±SD of quadruplicates. Statistical t-test was perform to compare treatments with control at p-values: (*)< 0.05, (**) < 0.01 and (***) < 0.001

3.3.1.2.14 Resveratrol

The effect of resveratrol treatment at 10 µM resulted in a marginal reduction of VCD while the rest of the parameters were not significantly different. Total protein production showed some tendency to drop from 12.05 ±0.5 at the control level, but that was not significant. The small drop was consistent with the drop of viable cells. As a result, the specific protein production q_p, remained constant as did the morphology of the cells (both the circularity and the diameter were constant).

VCD diminished as treatment concentration increased. 25 and 50 µM treatments caused 42% and 78% decrease of viable cells respectively, while higher concentrations resulted in complete viable cell growth arrest (Figure 46A). GI_{50} for these conditions was calculated at 28 µM.

Resveratrol started to affect viability at concentrations of 50 µM. While resveratrol had a mild effect at 50 µM, concentrations of 75 µM and 100 µM resulted in drops of up to 70% (Figure 46A). The estimated LC_{50} for resveratrol was 163 µM, but this is out of the range of treatments, it can only be used as an indication.

The GI_{50} (28 µM) and the LC_{50} (eligibly 163 µM) estimations were considerably distanced, which indicates that the overlap between the cell inhibition and cell toxicity is minimal and resveratrol could be used under the concentrations where it has cytostatic properties. We considered that 50 µM concentrations of resveratrol should be the study upper limit as values above it could geoparticle cell integrity.

The effect of resveratrol on the morphology of the cells showed that there are two main responses from the cell population depending on the concentration.

Cell size: Concentrations between 10 and 50µM caused an increase in cell diameter in a concentration-dependent manner. At the control level, the size was 15.7±0.1 µm whereas at 50 µM the average diameter was 16.3±0.3 µm. That was the only significant increase observed. On the other hand, concentrations above 50µM caused a significant drop of the diameter (more than 1 µm), reaching 14.4±0.8 µm at 100 µM (Figure 46C).

Cell shape: There was an increase in the circularity as the concentration increased. There was a peak at 25 and 50 µM. Concentrations of 75 and 100 µM did not cause any changes (Figure 46D).

There was an inverse relationship between IgG total titre and resveratrol concentration, causing approximately a 3-fold decrease at 100 µM. The cell growth was inhibited more heavily than IgG production. This resulted in an increase of q_p from 3.3 pg/cell·day at the control level, to almost 4 times increase at 75 and 100 µM concentrations (12.3 pg/cell·day) (Figure 46B).

The impact of resveratrol treatment on cells, indicated that the cultures react in two main ways depending on the concentration of the treatment.

For concentrations up to 50 µM, the viable cell concentration decreased but viability was mainly preserved. This caused an increase in both the cell size and the average circularity of the cells, which is likely to be the cause of the increase in the specific protein production.

Estimation of the average size of the cells was done considering circularity insignificant; at the control level the volume was 2.03 mm^3, while at 50 µM the volume was 18.1 mm^3. The nine-times increase of the cell volume only gave a 3.17 increase in q_p, which showed that cells were producing 3 times less per biomass volume.

On the other hand, at 75 µM and 100 µM concentrations, cells behaved in a completely different manner. Cell growth was completely arrested, viability was reduced by up to 20% and cells were diminished in size although they preserved their cell shape. It is likely that the increase of the specific protein production at these concentrations was due to a very different mechanism that is likely to do with the chemical's toxic effect. If this was the case, a change in the characteristics of the IgG produced would be expected.

Recent work done on the effect of resveratrol in recombinant CHO cell lines indicates that concentrations of 10 µM were not able to affect the viability, cell density or final recombinant protein titre (Baek et al. 2016). These results correlate with the findings of this experimentation which showed that there were no significant differences in these parameters when comparing the control with the 10 µM treatment.

Resveratrol has been recently studied and included in a patent in order to be used as an additive for recombinant protein production in CHO cells. The chemical was studied at 62.5 µM, 250 µM and 1 mM. It was found to increase the viable cell density in some circumstances, although it was not clear that this phenomenon was significant on a regular basis. Furthermore, resveratrol was able to cause up to a 1.44-fold increase in production when added at 1mM concentration (Tian, 2016).

The disparity in the effects of the chemical in the different experimentations has to be addressed and checked whether it is significant. Resveratrol in the current study was found to be toxic at concentrations above 50 µM and was estimated to cause considerable toxic effects at concentrations around 163 µM. On the other hand, concentrations around 1000 µM were not reported as very toxic in the patent study. Furthermore, other studies done with different CHO cell lines, identified toxic effects at concentrations as low as 80 µM (Basso *et al.*, 2013). This discrepancy can only be possible if the cell line has been adapted to withstand such high concentrations of the chemical or if the cell line is inherently resistant.

In order to further clarify the real differences across the studies, a scale-up method where comparable methods could be assessed needs to be implemented (static well plates vs shaker flask fed-batch culture) (Tian, 2016).

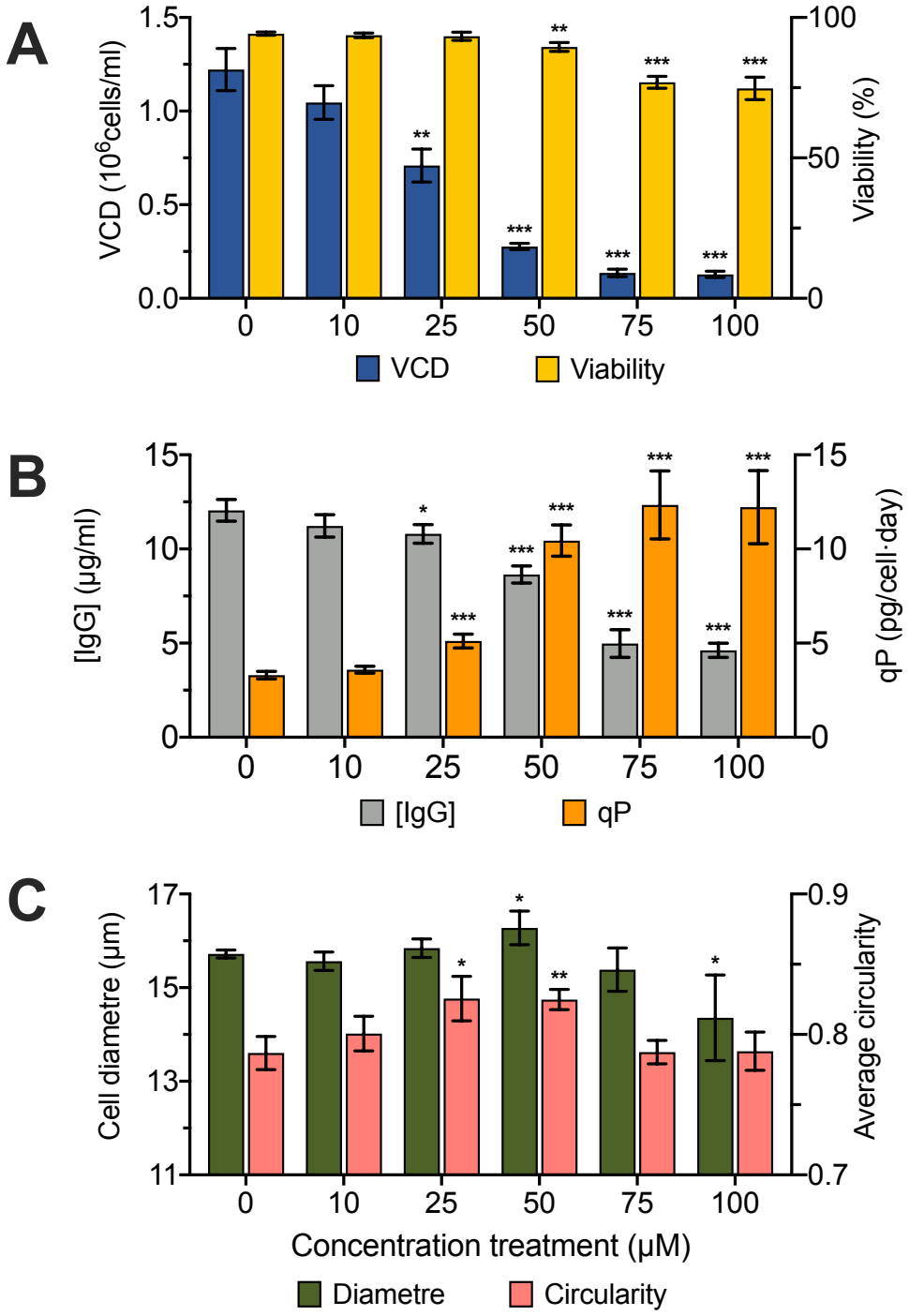

Figure 46 The effect of resveratrol on the cell culture and IgG production in 24-well plates
Display of measurements for samples treated with resveratrol (Rsv) (10-100 µM) during 3 days in a static humidified (section 2.1.2): (A) viable cell concentration (blue) and cell viability (yellow) (section 2.1.4); (B) total protein production (grey) and relative protein production (orange) (section 2.1.5); (C) cell diameter (green) and cell circularity (red) (section 2.1.4). The error bars represent ±SD of quadruplicates. Statistical t-test was perform to compare treatments with control at p-values: (*)< 0.05, (**) < 0.01 and (***) < 0.001

3.3.1.2.15 Tocopherol

Tocopherol was studied in a wide range of concentrations from 35 to 700 µM, and the experiments showed that the concentration had no effect on the results.

Tocopherol affected the viable cell density by decreasing it from 0.58±0.004 10^6 Viable cells/mL at control, to values around 0.36±0.04 10^6 Viable cells/mL for all treated samples (Figure 47A). This represents a 38% inhibition after three days of incubation. Due to the fact that tocopherol was not studied in concentrations before inhibiting or after complete inhibition, plus all the concentrations studied showed the same level of inhibition, there was no way of assessing GI_{50} not even by approximation.

Viability was not significantly changed when compared with the control and all values were found to be between 92 to 88 % (Figure 47A). LC_{50} was not considered.

Cell size was maintained constant across the range of study, with no significant differences with respect to the control (average cell diameter of 14.88±0.13 µm) (Figure 47C). Furthermore, the cell shape was also unaltered significantly, with an average circularity of 0.84±0.02 (Figure 47D).

The total IgG was reduced for all treated samples and was found to be around 11.9±0.2 mg/mL; the respective control value was 13.85±0.35 µg/mL. This 14% decrease in IgG produced is lower than the general 38% decrease in viable cell density. As a result, all treated

samples had increased specific productivities of approximately 1.6-fold (13.32±0.71pg/cell·day) compared to the control (8.06±0.08 pg/cell·day) (Figure 47B).

Tocopherol was found to affect growth without causing any toxic effects at any of the concentrations studied. Furthermore, it was able to enhance specific protein production. This chemical is likely to be a good candidate for supplementation strategies. However, this chemical is very difficult to manipulate due to its high viscosity and it is difficult to preserve in proper conditions as it undergoes oxidation at a very high rate.

Fazzio and colleagues found tocopherol to a cause slight inhibition of the cell growth and linked this to gene expression activation of Kinase C (Fazzio, Marilley and Azzi, 1997). Vitamin E has been researched heavily for its capacity to help mitigate stress and toxic conditions in CHO cells (Soloneski, Reigosa and Larramendy, 2003; Kmetič *et al.*, 2009).

This chemical was found to be useful in assisting CHO cell lines to adapt to short-term hypothermic preservation (Byoun and Park, 2006). It is also present in well-described media compositions for biopharmaceutical production (Krishnan, Rendeiro and San-Dadi, 2010). However, its effect as an additive to the media has not been studied.

The results of our investigation indicate that tocopherol affects growth at all the studied concentrations, without causing any toxic effects. Furthermore, it is able to enhance specific protein production. This chemical is likely to be a good candidate for supplementation strategies.

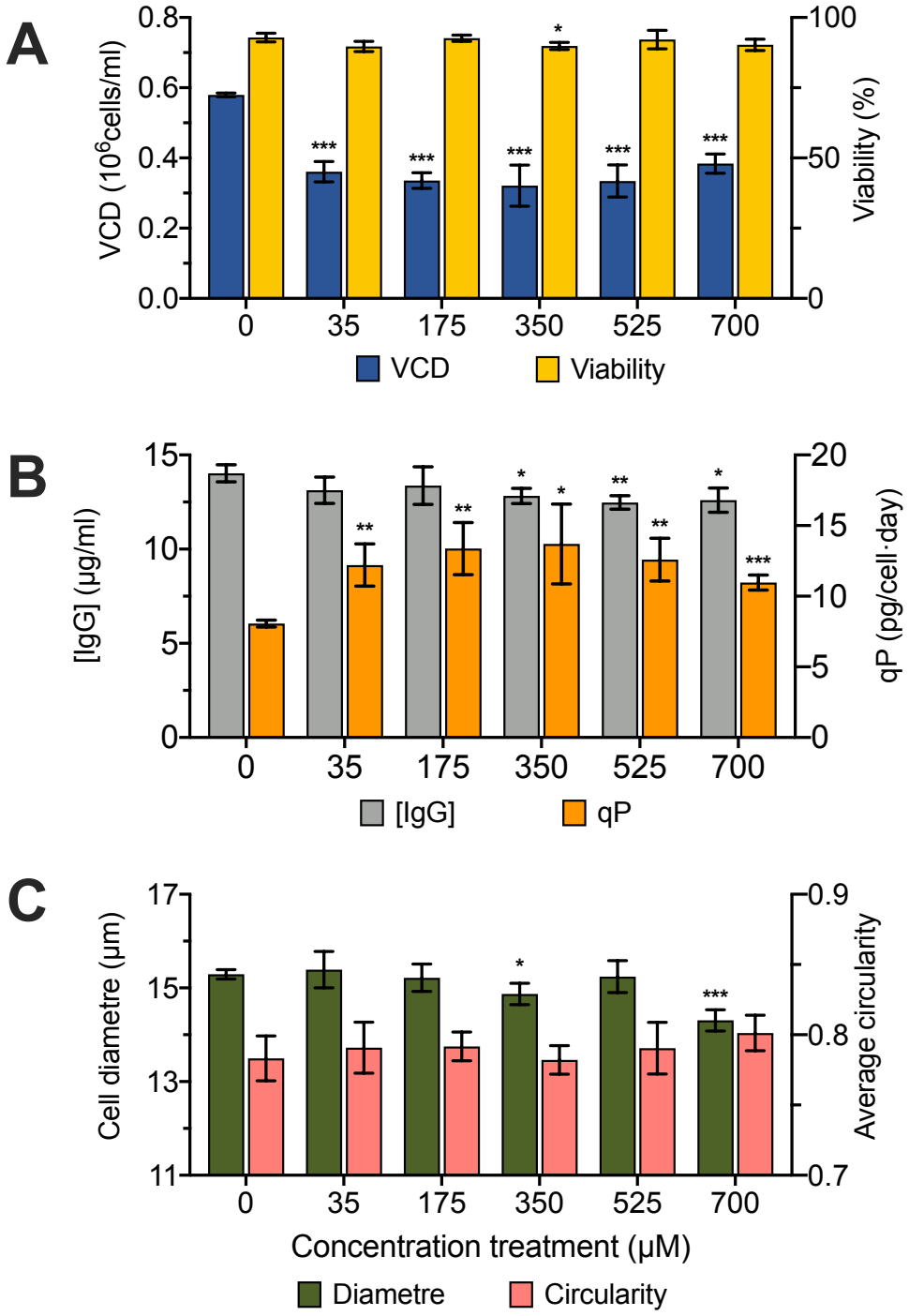

Figure 47 The effect of tocopherol on the cell culture and IgG production in 24-well plates
Display of measurements for samples treated with tocopherol (Tcp) (35-700 µM) during 3 days in a static humidified incubator (section 2.1.2): (A) viable cell concentration (blue) and cell viability (yellow) (section 2.1.4); (B) total protein production (grey) and relative protein production (orange) (section 2.1.5); (C) cell diameter (green) and cell circularity (red) (section 2.1.4). The error bars represent ±SD of quadruplicates. Statistical t-test was perform to compare treatments with control at p-values: (*)< 0.05, (**) < 0.01 and (***) < 0.001

3.3.2 Conclusions

The 24-well plate screening method was found to be reliable and had high reproducibility. There was no edge effect. However, the process was limited to three days of incubation, to preserve the viability of the cell culture across the experiment. This platform was very efficient in identifying chemicals able to shift cell growth into specific IgG production, but was limited in identifying other mechanisms of action. Furthermore, the data obtained, although indicative, are not directly transferable to scale up conditions, as cells were incubated for a short period of time and under static conditions.

From all the chemicals studied, 4-PBA, glycine betaine, caffeine and piceid did not cause any improvements in the production process. Other compounds such as curcumin, kaempferol and CAPE, showed drastic toxic effects and an increase of q_p was only linked to low levels of viability. Based on this investigation, these compounds will not be considered for further research, as it seems unlikely that they could help the protein production.

Finally, catechin, epicatechin, resveratrol, EGC, tocopherol, EGCG and GCG, showed positive effects on the recombinant IgG production. Some of these chemicals were also patented and data from those studies correlate with our findings. However, little information on the mechanism of action of the chemicals was identified. The present study showed that most of the chemicals with positive features are able to improve the specific protein production by inhibiting cell growth without lowering viability.

Table 4 Effect of chemical treatments in CHO cell culture growth and IgG production

Chemical candidates	VCD	[IgG]	Viability	q_P	Score
Catechin	- -	-	=	+	+
Epicatechin	- -	-	=	+	+
ECG	- -	=	=	+	+
EGCG	- -	-	=	+	+
GCG	-	=	=	+	+
Kaempferol	- -	- -	=	=	-
Luteolin	-	=	=	+	+
Piceid	=	=	=	-	-
Resveratrol	- -	-	=	+++	+++
CAPE	- - -	- - -	- - -	- - -	- - -
Curcumin	-	-	=	=	-
Tocopherol	-	=	=	++	++
Btn	+	=	=	-	-
4-PBA	- -	-	=	=	-
Caffeine	-	-	=	=	-

Effect of cytostatic conditions of chemical candidates on viable cell density (VCD) IgG recombinant titre (IgG) viability and specific IgG production (q_p) for producing CHO cell cultures. (ECG) Epicatechin gallate, (EGCG) Epigallocatechin gallate, (GCG) Gallocatechin gallate, (CAPE) Caffeic acid phenethyl ester, (Btn) glycine betaine, (4-PBA) 4-phenylbutyrate. Minus symbol (-) represent the a decrease in the variable, an equal (=) indicates that the variable stais the same and a plus symbol (+) indicates a increase on the variable. The over all score represent an arvitrari measurement to assess the capacity of the chemicals to increase productivity in the recombinant cell line.

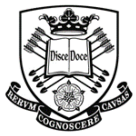
Disce Doce
Rerum Cognoscere Causas

Chapter 4

The effect of flavonoids over time on culture behaviour and cell cycle

4.1 Initial remarks

The results from the previous chapter (Chapter 3) showed that some of the initial chemical candidates screened (resveratrol and the catechin family compounds) were able to increase q_p by slowing cell growth without lowering cell viability. This indicated that their capacity to improve recombinant IgG production is probably linked to their cytostatic nature. In order to better understand the effect of those conditions, cell cultures were followed over time to study their viability, cell growth, cell morphology and cell cycle composition.

24-well plate cultures were set-up as specified in section 2.1.2. Measurements of viability, cell concentration (section 2.1.4) and cell cycle phase analysis (section 2.2) were performed every 24 hours for catechin group treatments and every eight hours for resveratrol treatments. All the measurements were done in quadruplicates and were repeated twice independently.

4.2 Results and discussion

4.2.1 Protocol optimization for fixation and propidium iodide staining

The resveratrol cultures had to be studied after eight hours of incubation, as described in the previous section. The problem with this, is the fact that the cell density would be limited. Flowcytometry requires large numbers of cells to produce reliable data and this could jeopardize the quality of the readings. The fixing protocol of cell cultures is a very long process that requires many intermediate steps; each step can reduce the number of cells. The present study intended to analyze the buffer exchange steps, which are critical for the loss of cells and

to minimize this loss without compromising the results by studying the changes in concentration of the sample across the protocol

The experiment was carried out in six different chemicals for three concentration treatments, at three different time points and in triplicates. The protocol needed to be adapted to minimize the waste of chemicals and the time to run it.

The cell fixation and propidium iodide stain protocol, is a robust method that has been implemented in the flow cytometry cell cycle study, since its very early stages of development (Krishan, 1975). Due to the advantages of this technique, a standard method optimizing the process followed shortly after (Fried, Perez and Clarkson, 1976). Since then, the protocols have diversified and been adapted to new technologies and needs, in order to reduce the time and money put into the process (Pozarowski and Darzynkiewicz, 2004; Kumar *et al.*, 2014). The first implementations of this method were performed in the field of medicine. In these cases, the amount of sample was the limiting factor.

In the present set up, the process is not limited by a reduced number of samples. On the contrary, the samples were many and required a very long process of fixation and staining, making the high throughput capability the main concern. Furthermore, some samples had limited low cell concentration. This was critical, as the protocol requires many steps and samples could be lost in the process.

The standard conservative protocols tend to wash the sample several times in order to preserve them and ensure that they have correct fixation and stain (Table 5). This is a problem in terms of time and reagents used. Moreover, it could cause problems with the final cell

density measured, especially when having to deal with a big number of samples, some of them with very low cell concentrations.

In order to optimize time reagents and deal with low cell concentration samples, a study of the protocol with a smaller number of washes was looked into. PBS buffer washes in steps 3 and 4 were reconsidered, as previously described (Yeh *et al.*, 2009; Kumar *et al.*, 2014). At the same time, step 7 was reduced to two washes (steps 12 and 13), as some manufacturer protocols indicate two or even one wash (Molecular Probes, 1999; Abcam, 2012; H. Zhu, 2012). The study protocol was assessed at four main checkpoints in order to track the loss of cells (steps 2, 8, 9 and 10).

The experiments showed, as was expected, that the steps which included buffer exchange or supernatant removal were associated with a considerable loss of cells. The study protocol resulted in a loss of 94% of the cells. The disposal of the supernatant media in step 3, resulted in an initial cell loss of 29.4%. Step 8 was less critical and only resulted in a 19.4% loss of the cells when discarding ethanol. Subsequent washes with PBS buffer at steps 9 and 10, were identified as the most critical ones, with a loss of 56.3 and 76.1 % respectively (Table 6).

Table 5 Propidium iodide fixation and stain protocol adaptation

	Initial protocol	Study protocol	Final protocol
1	Collection of sample in vial	Collection of sample in vial	Collection of sample in vial
2	Cell centrifugation and disposal of media supernatant	*Cell centrifugation and disposal of media supernatant	*Cell centrifugation and disposal of media supernatant
3	1st PBS wash centrifugation and supernatant disposal	---	---
4	2nd PBS wash centrifugation and supernatant disposal	---	---
5	PBS resuspension to minimal volume	PBS resuspension to minimal volume	PBS resuspension to minimal volume
6	Fixation with 70% ethanol	Fixation with 70% ethanol	Fixation with 70% ethanol
7	Incubation for 30 minutes	Incubation for 30 minutes	Incubation for 30 minutes
8	Centrifugation and disposal of the ETOH supernatant	*Centrifugation and disposal of the ETOH supernatant	*Centrifugation and disposal of the ETOH supernatant
9	1st PBS wash centrifugation and supernatant disposal	*1st PBS wash centrifugation and supernatant disposal	*1st PBS wash centrifugation and supernatant disposal
10	2nd PBS wash centrifugation and supernatant disposal	* 2nd PBS wash centrifugation and supernatant disposal	---
12	3rd PBS wash centrifugation and supernatant disposal	---	---
13	4th PBS wash centrifugation and supernatant disposal	---	---
14	Addition of RNAase	Addition of RNAase	Addition of RNAase
15	Addition of propidium iodide	Addition of propidium iodide	Addition of propidium iodide
16	Incubation in dark for 5-10 minutes	Incubation in dark for 5-10 minutes	Incubation in dark for 5-10 minutes

* Steps after which cell concentration was studied

Table 6 Cell loss along the steps of propidium iodide fixation and stain protocol

Step	Cell concentration (Cells 10^6/mL)			Cell loss (%)		Supernatant	Cell state
	Mean		SD	by step	accumulative		
Initial	1.9	±	0.12	--	--	--	--
Step 3	1.34	±	0.13	29.4	29.4	Media	Non-fixated
Step 8	1.08	±	0.09	19.4	43.1	70% ethanol	Fixated
Step 9	0.47	±	0.06	56.3	75.1	PBS	Fixated
Step 10	0.11	±	0.02	76.1	94	PBS	Fixated

The steps of the protocol contemplated in this study were only the ones of buffer exchange and supernatant removal

Pellet formation and integrity are key components when removing the supernatant. Two main factors that affect the pellet formation are the nature of the liquid phase and the state of the cells. If pellet formation is compact and maintains integrity, the supernatant collection can be done easily without perturbing the sediments, thus reducing cell loss to a minimum. On the other hand, loose pellet formation hinders the collection of the liquid phase, without perturbating the pellet and often results in a considerable cell loss or an incomplete removal of the supernatant.

When cells are fixed with ethanol, they lose their membrane integrity and a decrease of both the cytoplasmic content as well as the cell diameter can be observed (Gusnard and Kirschner, 1977; Hobro and Smith, 2017). These physiological changes make the cells more buoyant and more difficult to centrifuge, thus making the pellet less consistent.

The liquid phase also plays an important role. Non-fixed cells were easy to centrifuge out of the solution. Fixed cells were also easily spin out of solution when in ethanol, thus resulting in a very compact pellet. On the other hand, fixed cells formed very loosed pellets in PBS

buffer and this resulted in a big loss of cells when exchanging buffers. This condition is to be avoided when there is concern about samples with a low number of cells. As a result, the protocol was further adjusted by dropping the wash at step 10.

All the previous experimentations resulted in the formation of the final protocol:

1. Cells to be collected from 24-well plate cultures and transferred into a 1.5 mL Eppendorf
2. Cells to be centrifuged at 300 g for 5 minutes and then pellet to be discarded

   Note: CHO cells are very robust and stand high centrifugation speeds. This centrifugal force was selected based on empirical data from previous work done with this cell type in the laboratory. More extreme centrifugation at 400 g, had the same results in terms of pellet formation and cells were able to maintain integrity. These conditions can be adapted when cells are more difficult to collect in the early stages, but if not needed it is better to use 300g as a conservative measurement to preserve the cell's integrity until fixation
5. Cell pellet to be resuspended gently into 30 µL of ice-cold PBS buffer

   Note: This step was performed in order to avoid clumps of cells and facilitate the fixation of cells that would follow. If the pellet was to be very abundant at this step, then 60 µL of PBS buffer instead of 30 µL could be used. However, this would also mean that the amount of ethanol in the subsequent steps should also be doubled
6. Cell fixation: Ice cold ethanol at 70% to be added drop by drop to the cell suspension, while vortexing the Eppendorf at medium intensity

Note: Vortexing allows for the fast dissolution of the ethanol in the media. It also allows the ethanol to act on the cells homogenously, thus avoiding the formation of clumps and aggregates

7. Incubation to be performed for at least 30 minutes at 4^{o}C

   Note: The time of incubation could be adjusted starting from 20 minutes and up to overnight, depending on the protocol

8. Centrifugation to be performed at 400 g for 5 minutes followed by removal of the ethanol supernatant

   Note: At this stage centrifugation should not be a problem; cells come out from the solution easily and form a very compact pellet. In order to avoid future PSB passages without compromising the removal of ethanol, the maximum amount of supernatant possible, has to be removed at this stage

   As ethanol is removed, the pellet would be exposed and rapidly dried due to the fast evaporation of the ethanol remaining in the pellet. That is why, the immediate subsequent addition of PBS buffer to the pellet in order to avoid the formation of aggregates and lumps, is crucial

9. A. 1000 µL of PBS buffer to be added and the pellet to be resuspended gently in the new buffer. Cells should be left to rehydrated for at least 15 minutes. The volume of the PBS buffer wash is to be maximized in order to counteract the lack of future washes and reduce the amount of ethanol left in the vial

   B. Centrifuging should be performed at 400 g for 5 minutes

   Note: At this stage cells tend to rehydrate and lose density, thus forming very fussy pellets. Therefore, this could result in considerable cell loss. For that reason, it is

recommended to use high speed when centrifuging in order to obtain the best pellet possible

C. Supernatant to be removed

Note: If there was a doubt regarding the amount needed to be removed, then leaving a small quantity of the supernatant behind would be allowed; the opposite could easily lead to loss of the sample

14. Addition of 30 µL of RNAase (100µg/mL)

15. Addition of 200 µL of propidium iodide (50 µg/mL)

16. Incubation of the sample for 5 - 10 minutes

This protocol is able to minimize the cell sample loss over the fixation and stain process, and reduces the time of performance. The subsequent experiments of this chapter were performed following this protocol with no loss of sample quality at the flow cytometry readings. As a result, we believe that this strategy is robust and could be useful for future studies.

4.2.2 Resveratrol time course study and cell cycle

The time course study undertaken in 24-well plates, showed that resveratrol treatment delayed the exponential phase of the cell culture in a concentration-dependent manner

(Figure 48A). Control and 10 µM treatments showed a stationary phase, that lasted less than 16 hours before the CHO cells started to grow with a steady increase in VCD for 72 hours. 25 µM treatment lengthened the stationary phase by approximately 32 hours. However, the growth after that point was of the same rate as the control, indicating that after the cells had adapted to the media, the presence of resveratrol did not affect growth. Treatment with 50 µM resveratrol lengthened the stationary phase by approximately 32 hours, but the growth after that point and up to the end of the experiment (72 hours) was sluggish. The effects on viability (Figure 48B). in the untreated control and the 10 µM resveratrol, both remained high around 97-98%, dropping to 95% after 72 hours in culture. The 25 µM resveratrol treatment showed a temporary dip in viability, to around 93±0.95% between 24 and 40 hours, but recovered to mirror the control after 40 hours in culture. The 50 µM resveratrol treatment showed a temporary dip in viability after 40 hours in culture, down to around 90.24±0.83%, but then showed signs of recovery after 48 hours. Resveratrol treatment caused a temporary increase in cell diameter from around 14.5 µm to 16.5 µm (Figure 48C). This peaked at 32

hours for the 25 µM (16.62±0.17 µm) treatment and at 48 hours for the 50 µM treatment (16.43±0.12 µm). The cell diameter then dropped to match the control values.

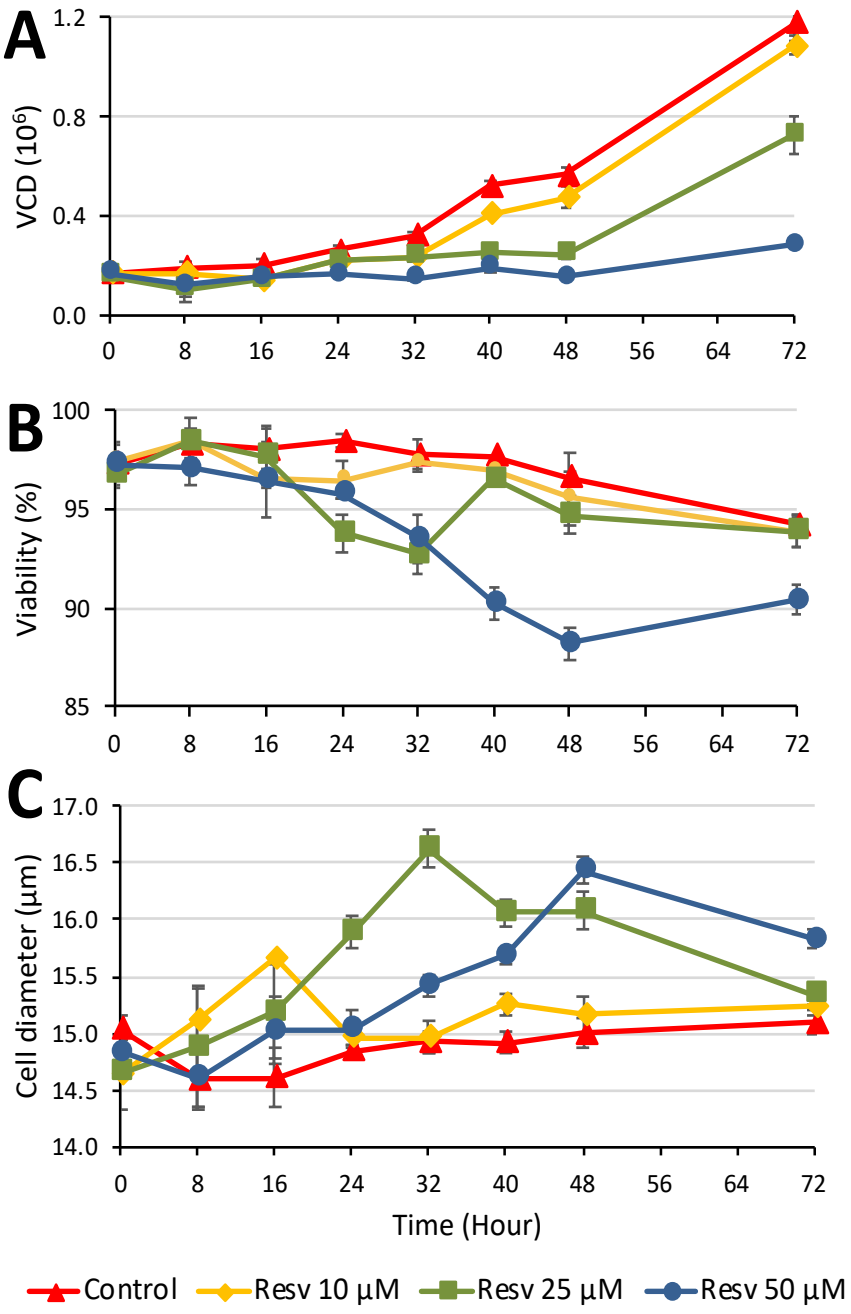

Figure 48 Time course study effect of resveratrol over cultures in 24-well plates
Effect of resveratrol (Resv) on viable cell density (VCD) (A), viability (B) and cell diameter (C) (section 2.1.4) at 10 µM (yellow), 25 µM (green) and 50 µM (blue) treatments for CHO cells grown in 24-well plates (section 2.1.2). Each data point represents the average from a triplicate, and the error bars correspond to ±SD. These experiments were repeated independently.

The cell cycle analysis of the samples from the time course study (Figure 49 and Table 7), showed that the presence of resveratrol had an impact on the population of the cells at different parts of the cell cycle. The untreated control showed a rise in the G_1/G_0 phase cells at 8 hours and S phase cells at 16 hours after inoculation. The control then returned to a stable population with around 40% of the cells at G_1/G_0 phase, 40% at S phase and 15 to 20% at G_2/M phase. The cells with 10 µM resveratrol treatment behaved very similarly to the control. The cells with 25 µM resveratrol treatment displayed some perturbation to the cell cycle with elevated levels of cells in the S phase at 8, 16, 32 and 40 hours after inoculation; at 48 and 72 hours the cell population returned to levels similar to the untreated control. The cells with 50 µM resveratrol treatment showed no marked changes in their population for the first 24 hours after inoculation, but by 32 hours there was a peak in the S-phase cells and a corresponding collapse in the G_1/G_0 phase cells. The cells in this treatment group did not return to a normal population as seen in the untreated control over the 72 hours of the experiment, but had elevated levels of G_2/M phase cells at 40 and 48 hours and elevated S phase cells at 72 hours.

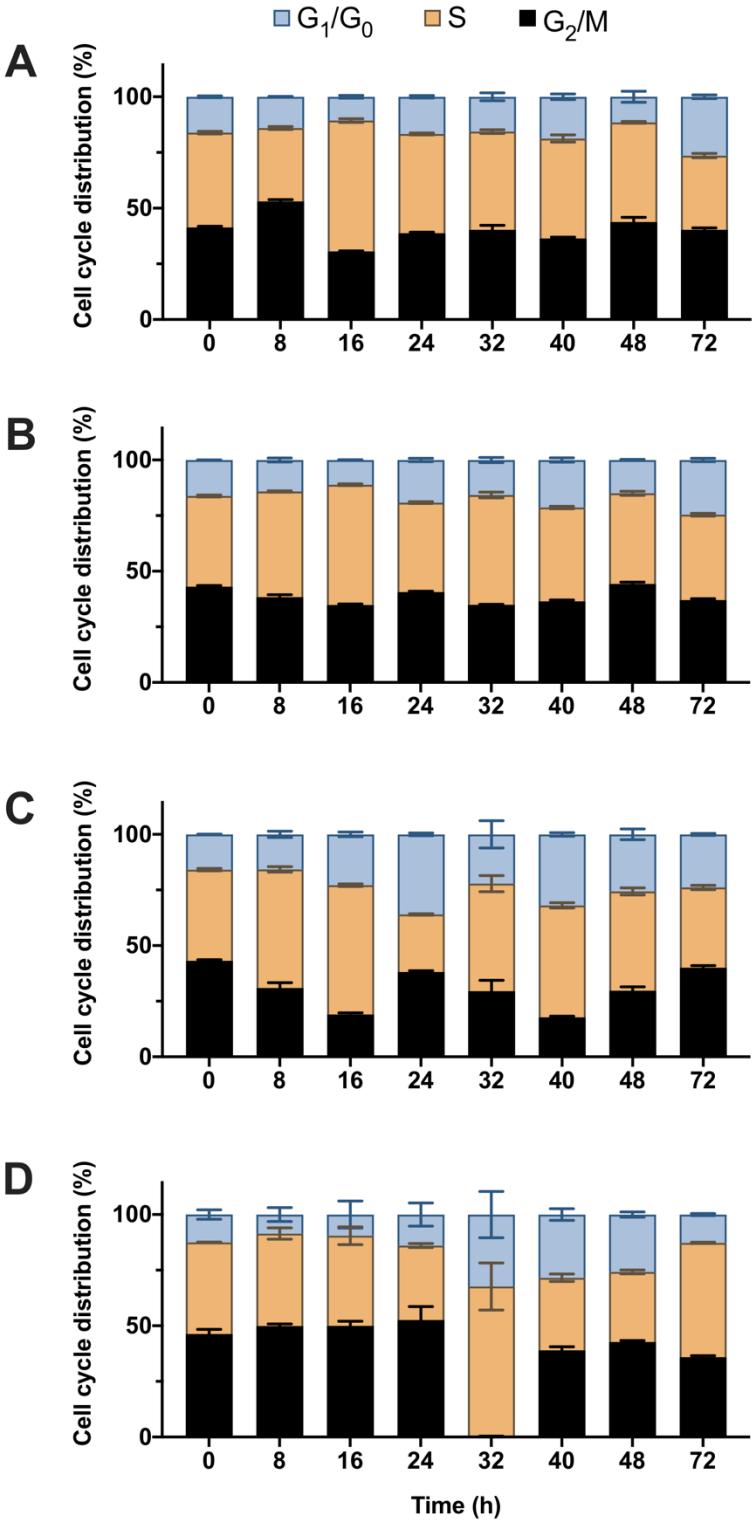

Figure 49 Cell cycle distribution under resveratrol treatment
Cell cycle distribution for G_1/G_0 (grey), S (orange), and G_2/M (black) phases under resveratrol treatments at 0 µM (A), 10 µM (B), 25 µM (C) and 50 µM (D) for CHO cells grown in 24-well plates for three days (section 2.1.2). Each data point represents the average from a triplicate, and the error bars correspond to ±SD. These experiments were repeated independently.

Table 7 Cell cycle distribution at different time points under resveratrol treatment

Treatment	G_1/G_0			S			G_2/M		
0 h									
Cont.	41.33 ± 0.43			42.58 ± 0.48			16.09 ± 0.33		
Resv 10 µM	43.11 ± 0.37	ns		40.74 ± 0.36	ns		16.15 ± 0.01	ns	
Resv 25 µM	43.19 ± 0.39	ns		40.96 ± 0.41	ns		15.85 ± 0.09	ns	
Resv 50 µM	46.32 ± 1.67	**		41.18 ± 0.13	ns		12.51 ± 1.70	ns	
8 h									
Cont.	53.06 ± 0.66			32.92 ± 0.53			14.02 ± 0.14		
Resv 10 µM	38.36 ± 0.88	***		47.49 ± 0.24	***		14.16 ± 0.72	ns	
Resv 25 µM	30.93 ± 1.93	***		53.32 ± 0.99	***		15.75 ± 1.14	ns	
Resv 50 µM	49.92 ± 0.76	ns		41.54 ± 2.08	***		8.54 ± 2.54	ns	
16 h									
Cont.	30.61 ± 0.17			58.74 ± 0.68			10.65 ± 0.52		
Resv 10 µM	34.81 ± 0.35	*		54.07 ± 0.33	*		11.12 ± 0.06	ns	
Resv 25 µM	19.04 ± 0.62	***		58.12 ± 0.47	ns		22.85 ± 0.88	***	
Resv 50 µM	49.94 ± 1.71	***		40.53 ± 3.26	***		9.53 ± 4.93	ns	
24 h									
Cont.	38.78 ± 0.34			44.52 ± 0.35			16.70 ± 0.42		
Resv 10 µM	40.66 ± 0.30	ns		40.18 ± 0.32	ns		19.17 ± 0.61	ns	
Resv 25 µM	38.16 ± 0.42	ns		25.83 ± 0.25	***		36.00 ± 0.50	***	
Resv 50 µM	52.61 ± 4.90	***		33.47 ± 0.72	***		13.91 ± 4.26	ns	
32 h									
Cont.	40.30 ± 1.64			44.08 ± 0.67			15.62 ± 1.43		
Resv 10 µM	34.93 ± 0.15	**		49.32 ± 1.07	*		15.76 ± 0.94	ns	
Resv 25 µM	29.51 ± 3.98	***		48.35 ± 2.97	ns		22.14 ± 5.00	*	
Resv 50 µM	0.19 ± 0.16	***		67.48 ± 8.66	***		32.33 ± 8.49	***	
40 h									
Cont.	36.40 ± 0.49			44.88 ± 1.33			18.72 ± 1.01		
Resv 10 µM	36.46 ± 0.47	ns		42.17 ± 0.43	ns		21.37 ± 0.80	ns	
Resv 25 µM	17.76 ± 0.39	***		50.29 ± 0.97	*		31.95 ± 0.64	***	
Resv 50 µM	39.02 ± 1.24	ns		32.58 ± 1.36	***		28.40 ± 2.14	***	
48 h									
Cont.	43.83 ± 1.69			44.66 ± 0.32			11.51 ± 2.01		
Resv 10 µM	44.33 ± 0.61	ns		40.69 ± 0.72	ns		14.98 ± 0.23	ns	
Resv 25 µM	29.72 ± 1.41	***		44.66 ± 1.28	ns		25.63 ± 1.99	***	
Resv 50 µM	42.71 ± 0.52	ns		31.49 ± 0.72	***		25.80 ± 0.95	***	
72 h									
Cont.	40.25 ± 0.75			33.32 ± 0.79			26.42 ± 0.69		
Resv 10 µM	37.04 ± 0.47	ns		38.36 ± 0.51	*		24.60 ± 0.62	ns	
Resv 25 µM	40.08 ± 0.77	ns		36.04 ± 0.81	ns		23.87 ± 0.36	ns	
Resv 50 µM	35.88 ± 0.58	**		51.40 ± 0.21	***		12.73 ± 0.39	***	

Numbers correspond to the relative quantity of cells (%) for each of the cell cycle phases ± the SD of triplicate samples treated with resveratrol (Resv). Statistical two-way ANOVA was perform to compared treatments with control at p-values: (ns) ≥ 0.05, (*)< 0.05, (**) < 0.01 and (***) < 0.001.

Resveratrol acted by lengthening the stationary culture phase trough, causing cell growth arrest and a small slope of decreasing viability. This stationary stage was more apparent and lengthened as resveratrol concentration increased. This was characterized by a peak of cells in the S phase at the end of this stage, which aligned with a drop in viability and an increase in the diameter. Then, cell growth was restored and parameters tended to normalize towards the control values. This suggests that a significant part of the big drop in viability, is associated with the end of this stage and synchronized with the accumulation of cells in the S phase. This process can be related to the capacity of resveratrol to interfere with DNA duplication, repair and segregation (Basso *et al.*, 2013; Traversi *et al.*, 2016) accumulating cells in the S phase through direct (N'soukpoé-Kossi *et al.*, 2015) and indirect (Leone *et al.*, 2010) mechanisms late in the culture (Subramanian, Soundar and Mangoli, 2016). Previous studies report that DNA damage occurs at high concentrations with a subsequent possibility of apoptotic events (Basso *et al.*, 2013; Uchiumi *et al.*, 2016). However, not all studies reported the same results (Sainz *et al.*, 2003). One of the mechanisms of the toxicity of resveratrol on CHO cell dividing cultures, could be its interaction with topoisomerases during the S phase (Leone *et al.*, 2012; Basso *et al.*, 2013).

Regardless of all this, the connection between the arrest at S phase from the viability drop and the growth inhibition should not be assumed. During treatment with the highest concentration of resveratrol (50 μM), not many cells were found in the S phase during the culture; the peak was observed at 48h. On the other hand, the growth arrest and the drop in viability took place consistently for the first 48 hours of the culture. This disparity between the three effects suggests that the previous mechanism of S phase arrest cannot fully explain the growth arrest or the drop of viability that took place previous to 48 hours. Therefore, it is

likely that another mechanism is also involved. This is in line with other findings (Della Ragione *et al.*, 1998). Furthermore, other studies have shown that the cell growth stops in other phases (Rubiolo *et al.*, 2012; Gokbulut *et al.*, 2013) or stops in a non-specific way (Pozo-Guisado *et al.*, 2002).

We hypothesize that the results observed by resveratrol treatment in CHO cell cultures under these conditions are due to complex effects, giving different outcomes depending on the concentration of the treatment or the moment of it. Due to its bioactive characteristics, resveratrol is more likely to be causing a pleiotropic effect on CHO cells by interfering with signaling and metabolic pathways in many different ways. This could lead to different effects by introducing small changes in concentration (Hahnvajanawong *et al.*, 2011; Rubiolo *et al.*, 2012; Bosutti and Degens, 2015).

Overall, resveratrol caused cell growth arrest in a concentration-dependent-manner. The effect was observed in the stationary phase of the cell culture, with a small drop in viability and a sudden increase of cells in the S phase. The toxic behaviour seen in this study is related partially to resveratrol's interference with DNA replication, repair and segregation mechanisms, indicating that highly dividing cells could be more affected. This hypothesis correlates with cancer studies where resveratrol was identified to have anti-tumour effects due to its capacity to selectively cause higher toxic effects in highly dividing tissues (Zhou *et al.*, 2011; Trung *et al.*, 2015).

Based on this investigation, we suggest that resveratrol should be considered and further studied for the use in recombinant IgG production. In order to improve protein production

under scale-up conditions, the effect of toxicity and cell division should be investigated as well as the capacity of this chemical to stop growth.

4.2.3 Catechins time-course study and cell cycle

4.2.3.1 Catechin

The time-course study of cell cultures in 24-well plates under static conditions indicated that cells adapted and started to grow before 24 hours (from 0.2 at time zero to 0.3 10^6 cells/mL after 24 hours for all concentrations). Control reached specific cell growth (μ) of approximately 1 $days^{-1}$ for the next 48h to up to 0.97±0.06 10^6 cells/mL. Treatment with catechin at 10 μM caused no changes in the growth curve. Higher concentrations of 25 and 50 μM caused inhibition of the specific growth rate to half (0.53 $days^{-1}$) but did not elongate the cells in the stationary phase as all readings after 24 hours were similar for all conditions (approximately 0.3±0.02 10^6 cells/mL) (Figure 50A).

Cell viability was not really affected at any point during the culture or under any given treatment concentration. The measurements ranged from 95 to 99%. There was a small trend of higher viability of the treated samples with respect to control, at any given concentration after the initial 24 hours. Treatment at 50 μM resulted in an increase in viability of approximately 2% over the control after the first 24 hours. This increase could be related to a delay in the cell concentration of the well plate. As well plates become more densely populated, cell cultures become less hospitable. as there is a fast consumption of the nutrients and accumulation of toxic components. Nevertheless, the cells treated with control were growing at the fastest doubling time until day three, so it is unlikely that the conditions

in the culture cause stress at that. Catechin was able to cause conditions in the culture which increase viability minimally, although the mechanism by which this happens is unclear (Figure 50B).

Cell diameter was increased by the addition of catechin in the culture. Cell size in the control samples was initially 15.16±0.30 µm, with no significant differences observed at the treated samples. By day 3, non-treated cells increased slightly in size up to 15.52±0.16 µm. On the other hand, catechin was able to increase the cell size to 16.70±0.29 µm for treatments at 25 and 50 µM concentrations, after three days of incubation. Treatment with 10 µM caused a less severe increase with a final diameter of 16.23±0.11 µm (Figure 50C). The increase in size during the first 24 hours indicates that this parameter does not have to be strictly linked to cell growth arrest, since the 10 µM treatment caused considerable cell size increment with no apparent cell growth arrest. Another possible reason for cell size increase could be an increase in homeostasis when adding this chemical to the media.

Overall, the cell cycle study showed significant differences between the non-treated samples and the treated samples. Nevertheless, all concentrations of the treatment seemed to have a very similar effect on the cell cycle. Catechin reduced the relative population of cells in G_1/G_0 phase and in return increased the number of cells in the S and G_2/M phases. Furthermore, the G_2/M increase was more evident after 72 hours. It is difficult to elucidate the reason by which catechin is able to elongate the cell cycle at these two stages (Figure 51).

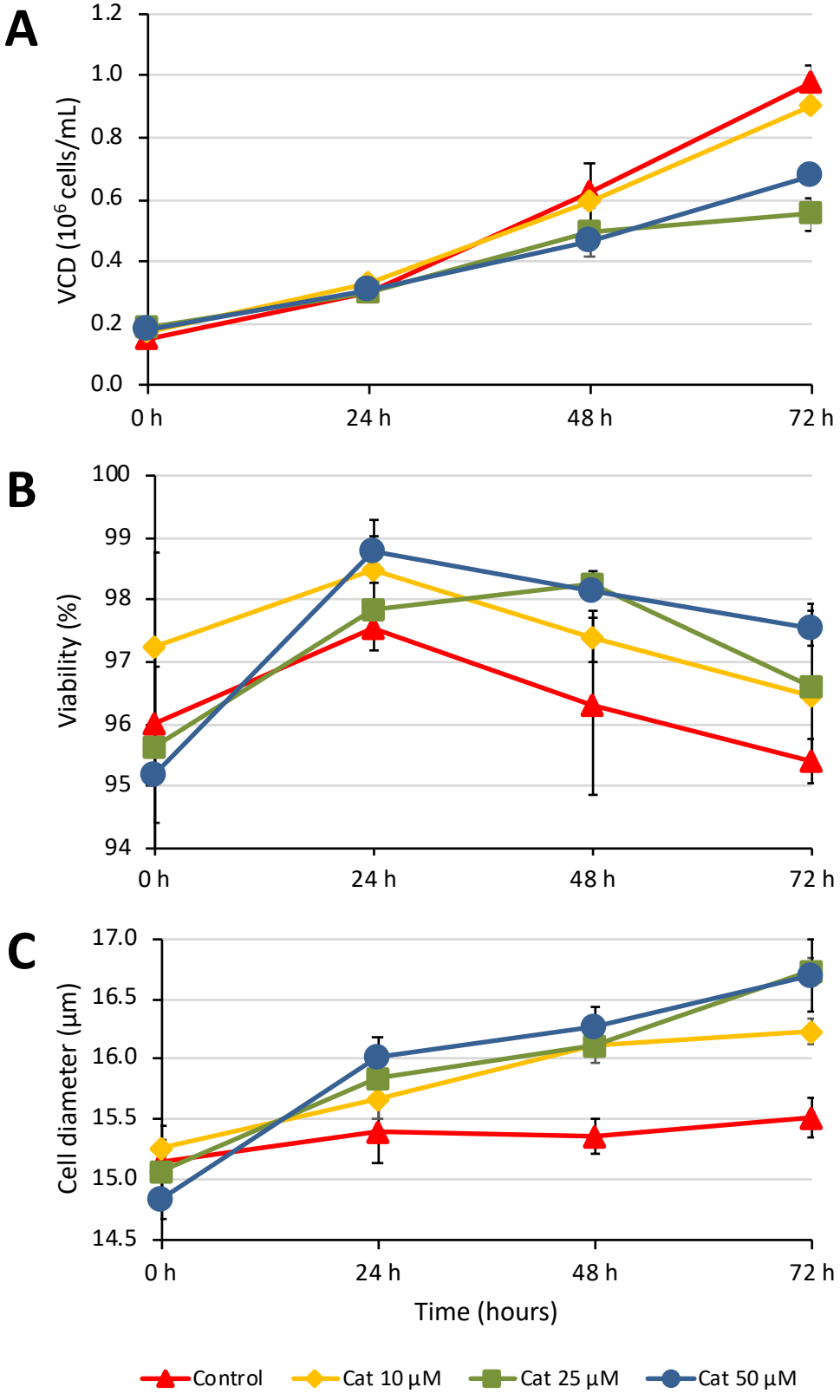

Figure 50 Time course study effect of catechin over cultures in 24-well plates
Effect of catechin (Cat) on viable cell density (VCD) (A), viability (B) and cell diameter (C) (section 2.1.4) at 10 µM (yellow), 25 µM (green) and 50 µM (blue) treatments for CHO cells grown in 24-well plates (section 2.1.2). Each data point represents the average from a triplicate, and the error bars correspond to ±SD. These experiments were repeated independently.

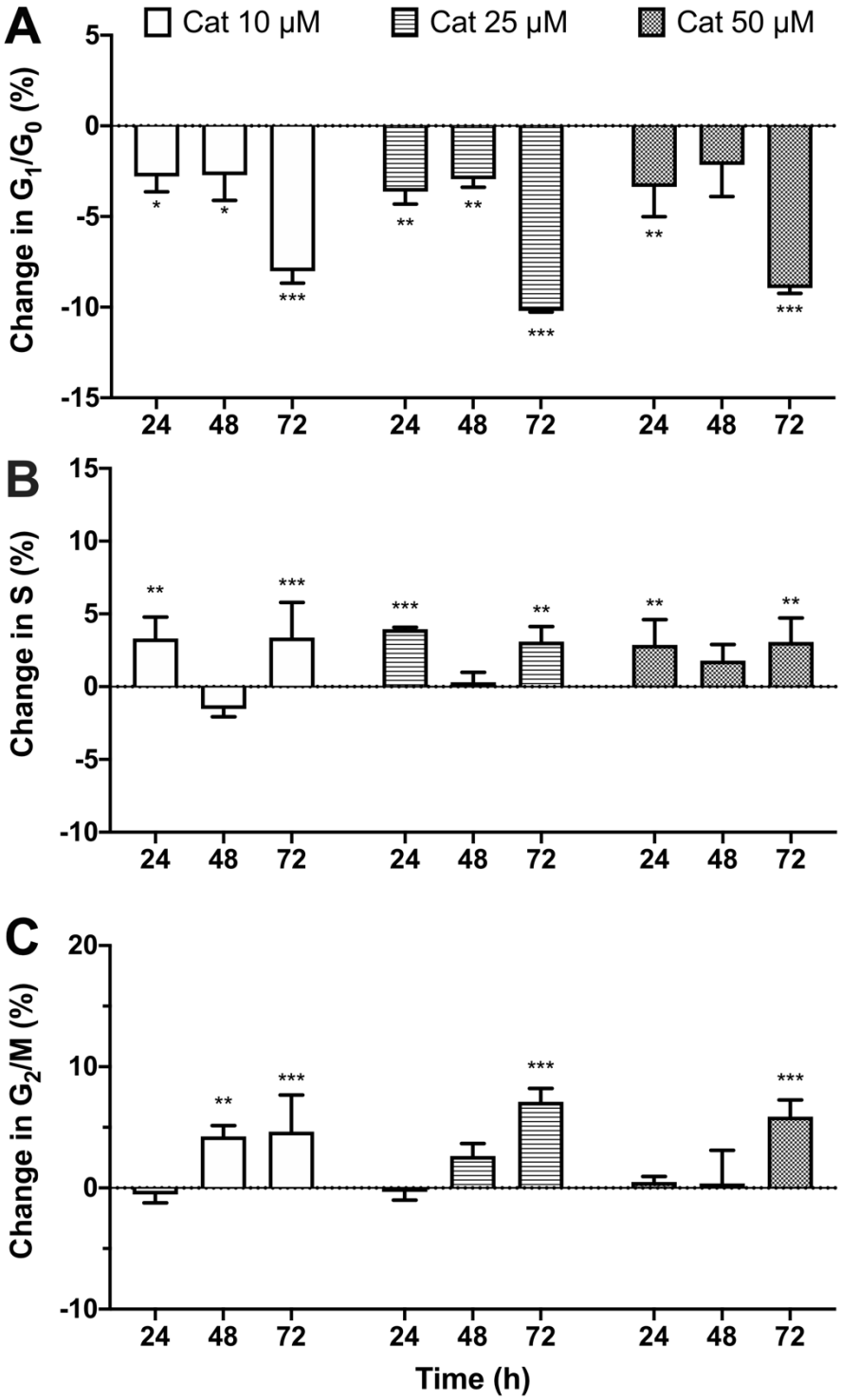

Figure 51 Relative cell cycle distribution under catechin treatment
Relative change in cell cycle distribution compared to the control for G_1/G_0 (A), S (B), and G_2/M (C) phases under catechin (Cat) treatments at 10, 25 and 50 µM for CHO cells grown in 24-well plates for three days (section 2.1.2). Each data point represents the average from a triplicate, and the error bars correspond to ±SD. These experiments were repeated independently. Statistical two-way ANOVA test was perform to compare treatments with control at p-values: (*)< 0.05, (**) < 0.01 and (***) < 0.001.

4.2.3.2 Epicatechin

The time-course study of cell cultures in 24-well plates under static conditions, indicated that cells adapted and started to grow before 24 hours (from 0.14±0.01 at time zero to 0.33±0.01 10^6 cells/mL after 24 hours for all concentrations). Control reached specific cell growth (μ) of approximately 1 $days^{-1}$ for the next 48h (up to 0.97±0.04 10^6 cells/mL). Treatment with 5 μM did not cause any change in the growth curve. 10 μM concentration treatment caused decay in growth rate after 48 hours and the 15 μM treatment caused a continuous steady increase, equal to the one observed during the first 24 hours. Epicatechin was able to arrest cell growth in a concentration-dependent manner (Figure 52A), as described in previous results mentioned in Chapter 2.

Viability was maintained along the three days of incubation, with values ranging between 92 and 99%. Addition of the chemical seemed to cause toxicity in the culture at time zero since the average values dropped to 93.49±0.14% for 10 μM and 92±1.50% for 20 μM treatments with respect to the control (95.90±0.76%). During the first 24 hours, viability increased to then steadily decrease during the next 48 hours of culture. This trend was consistent across all samples, both treated and untreated (Figure 52B).

Cell diameter was equal for all samples at time zero and increased over time under all conditions. Samples treated with control, increased their cell diameter from 14.82±0.20 μm at time zero, to 15.62±0.04 μm after three days of incubation. Treated samples increased their cell size more, up to 16.73±0.20 μm for 20 μM, 16.26±0.10 μm for 10 μM and 16.31±0.09 μm for 5 μM treatments. That was observed after three days of incubation. Epicatechin's effect on cell size, is not linked to its growth inhibition, as treatment at 5 μM caused an

increase in cell size, with no cell growth inhibition associated. Furthermore, the trends of growth arrest and cell diameter increase did not much at all data points (Figure 52C).

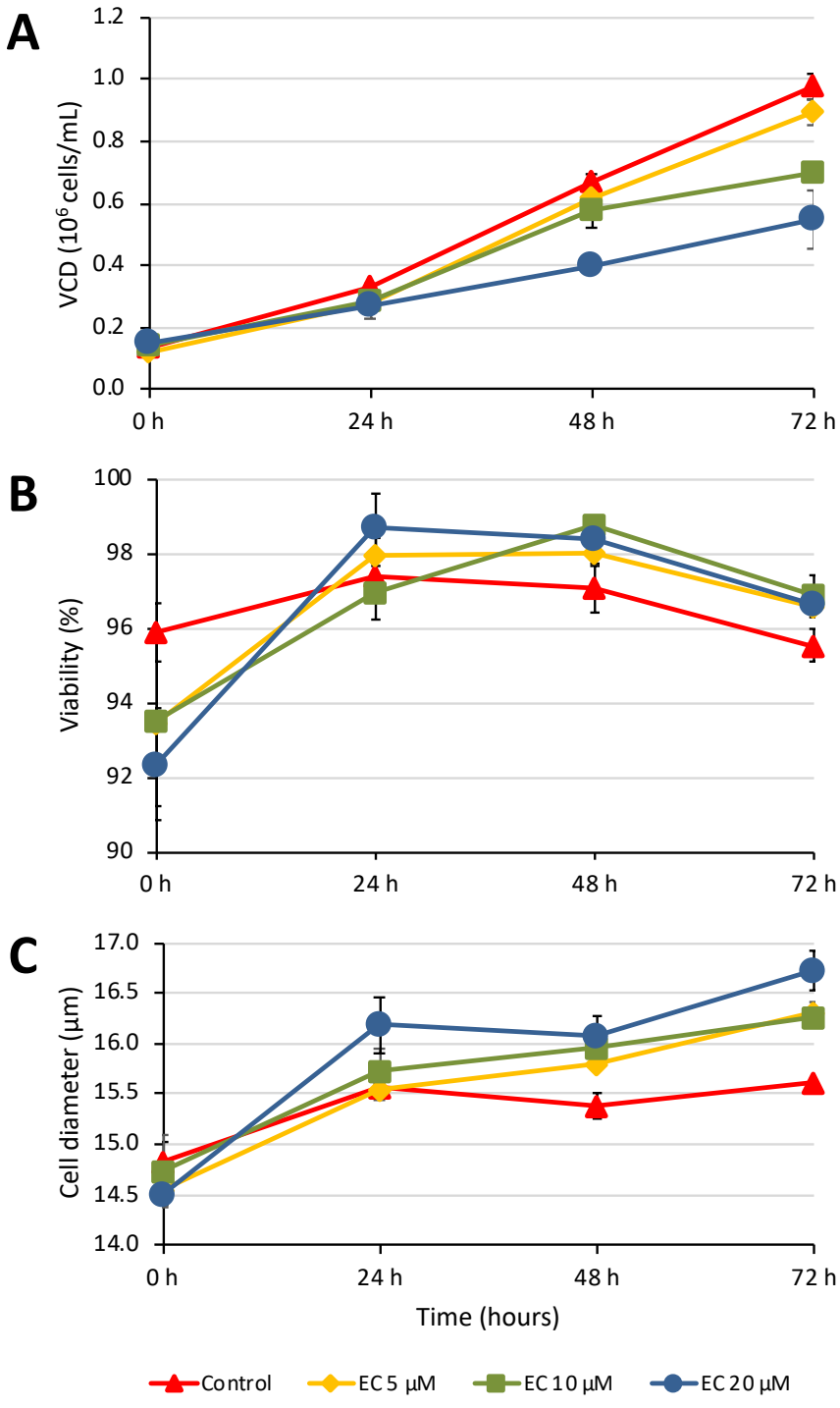

Figure 52 Time course study effect of EC over cultures in 24-well plates
Effect of epicatechin (EC) on viable cell density (VCD) (A), viability (B) and cell diameter (C) (section 2.1.4) at 10 µM (yellow), 25 µM (green) and 50 µM (blue) treatments for CHO cells grown in 24-well plates (section 2.1.2). Each data point represents the average from a triplicate, and the error bars correspond to ±SD. These experiments were repeated independently.

Overall, the cell cycle study showed significant differences between the non-treated samples and the treated samples. Nevertheless, all concentrations of the treatment seemed to have a very similar effect in the cell cycle. Epicatechin reduced the relative population of cells in G_1/G_0 phase and in return increased the number of cells in the S and G_2/M phases. Furthermore, G_2/M increase was more evident after 72 hours. It is difficult to elucidate the reason by which epicatechin is able to elongate the cell cycle at these two stages (Figure 53).

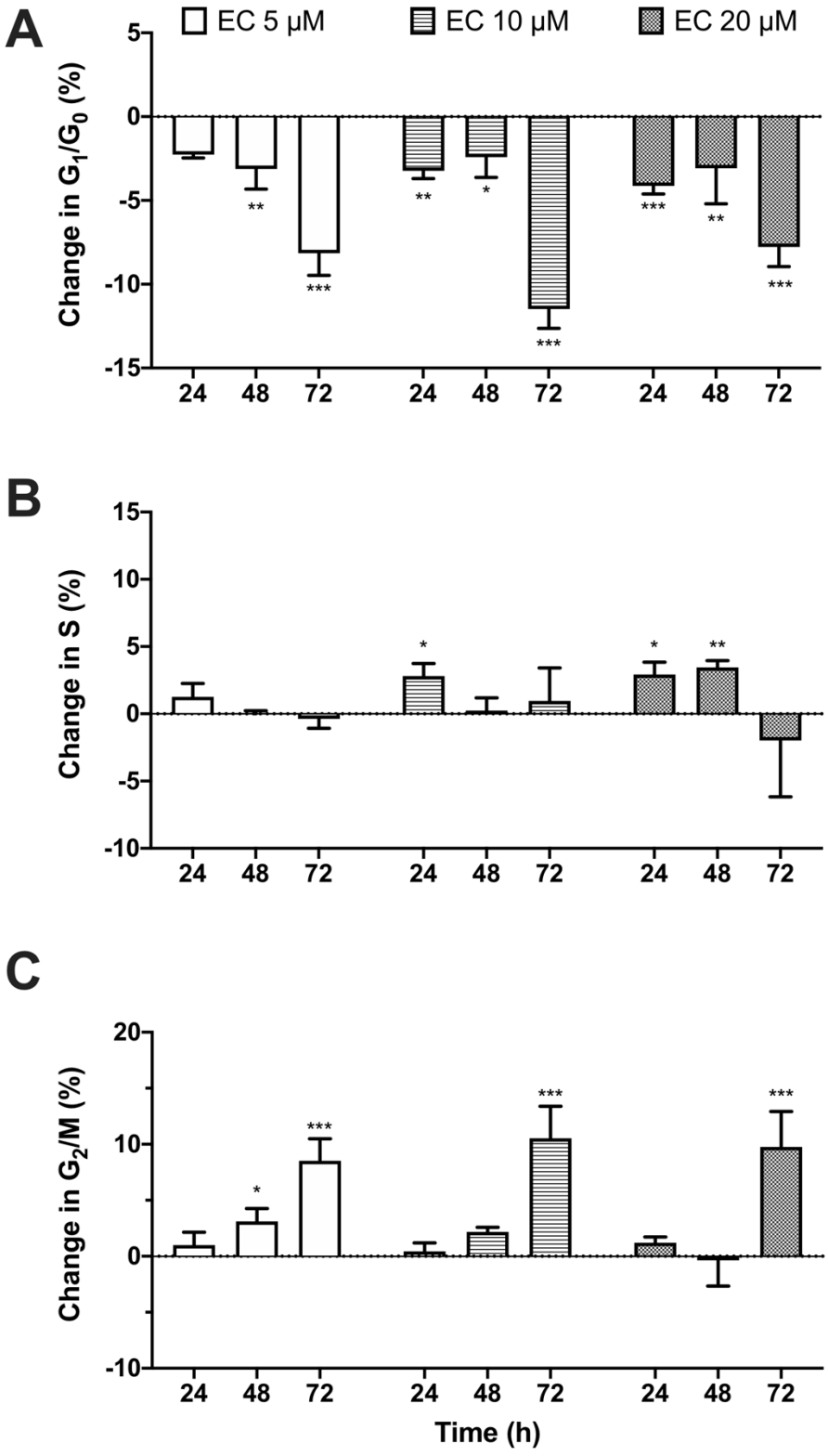

Figure 53 Relative cell cycle distribution under epicatechin treatment
Relative change in cell cycle distribution compared to the control for G_1/G_0 (A), S (B), and G_2/M (C) phases under epicatechin (EC) treatments at 5, 10 and 20 µM for CHO cells grown in 24-well plates for three days (section 2.1.2). Each data point represents the average from a triplicate, and the error bars correspond to ±SD. These experiments were repeated independently. Statistical two-way ANOVA test was perform to compare treatments with control at p-values: (*)< 0.05, (**) < 0.01 and (***) < 0.001.

4.2.3.3 Epicatechin-gallate

The time-course study of cell cultures in 24-well plates under static conditions indicated that cells adapt and start to grow way before 24 hours. With growth from 0.150±02 at time zero to 0.30±0.04 10^6 cells/mL after 24 hours for all concentrations. Control reached specific cell growth (μ) of approximately 1 $days^{-1}$ for the last 48h of the culture reaching 1.01± 10^6 cells/mL after 72h of culture. All the treatments of epicatechin-gallate (5, 25 and 50 μM) caused very similar responses on the cell culture (Figure 54A). Under these conditions cell growth is partially repressed with an overall cell growth rate of 0.78 $days^{-1}$.

Cell viability was maintained between 94 and 97% for all samples at all times, this indicates that regardless the inhibitory effect of the chemical over the population, these concentrations do not cause severe toxic effects in the cultures under these conditions (Figure 54B).

Epicatechin-gallate caused no significant changes in cell size under these conditions with values close to the control (15.2-15.3 μm). Cell diameter is maintained very similar to the control although after 72h there is a consistent increase in size to 16.06±0.23 μm for all treatments with respect to the control at 15.62±0.12± μm (Figure 54C).

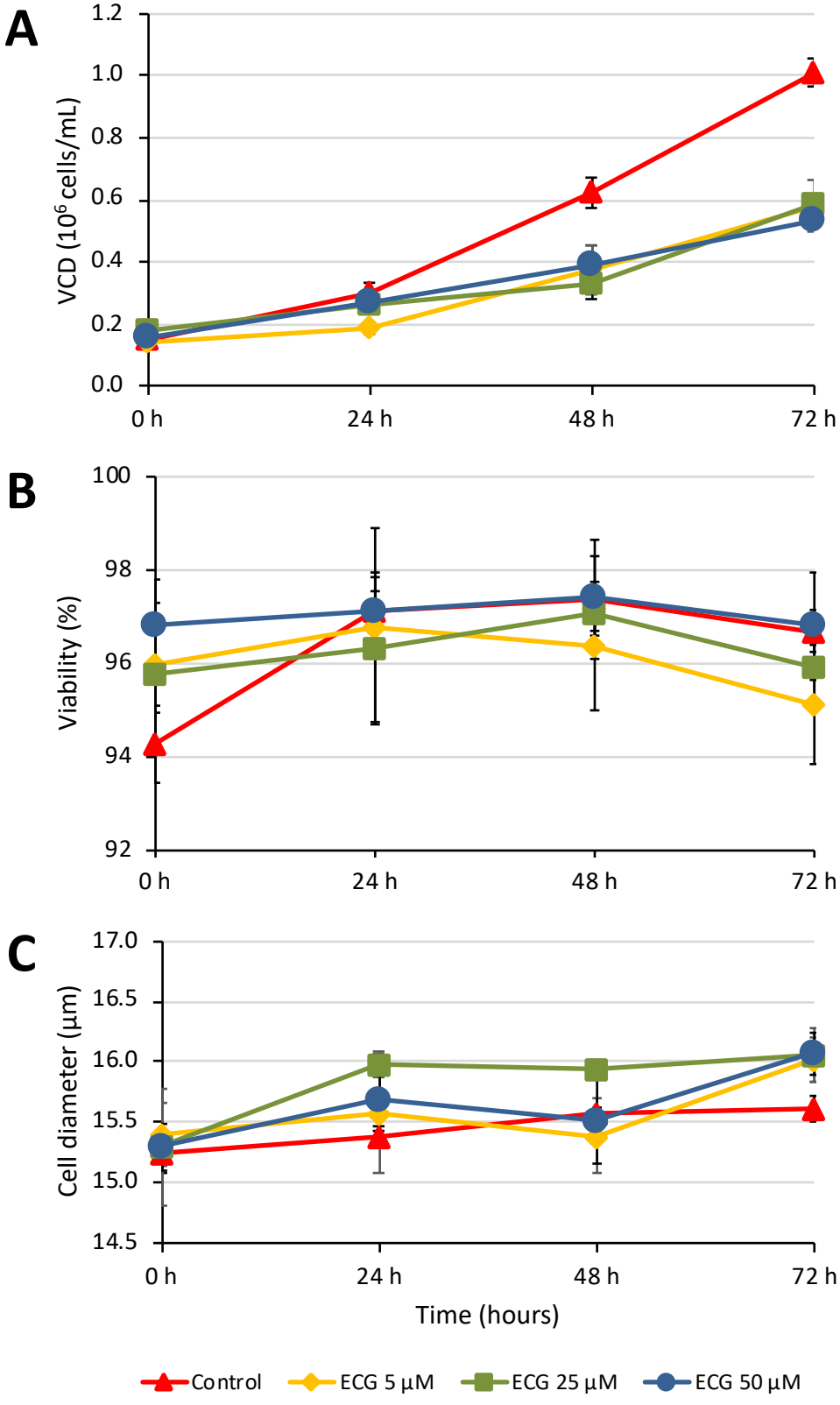

Figure 54 Time course study effect of ECG over cultures in 24-well plates
Effect of epicatechin gallate (ECG) on viable cell density (VCD) (A), viability (B) and cell diameter (C) (section 2.1.4) at 10 µM (yellow), 25 µM (green) and 50 µM (blue) treatments for CHO cells grown in 24-well plates (section 2.1.2). Each data point represents the average from a triplicate, and the error bars correspond to ±SD. These experiments were repeated independently.

The concentration of 5 µM epicatechin-gallate causes no main changes in cell cycle composition after 24 hours. Accumulation of cells in the G_2/M phase appears after 48 and 72 hours of treatment in detriment of mainly G_1/G_0.

Concentrations of 50 µM have a very different effect with a consistent significant increase in S phase. While at the beginning this cell increase in the S phase accounts mainly from loss of cell in the G_2/M phase, as time passes by the cells missing in the G_1/G_0 phase are more numerous. After 72 hours the accumulation of cells in the S phase accounts exclusively from cells in the G_1/G_0 phase and there is also a consistent increase in G_2/M. It is likely that the missing cells under different phases of the cell cycle are due to partial synchronization taking place as cells are immediately partially arrested in S phase as early as 24 hours after treatment. This could explain the depletion of cells in G_2/M phase as cells cannot move further from the S phase. As the culture elongates in time, cells pass to G_2/M phase but they don't reach G_1/G_0.

The concentration of 25 µM is a mix in between. This indicates that the chemical is likely able to elongate both phases of the cell culture S and G_2/M. Furthermore, the face that is more affected shifts as the concentration increases (Figure 55).

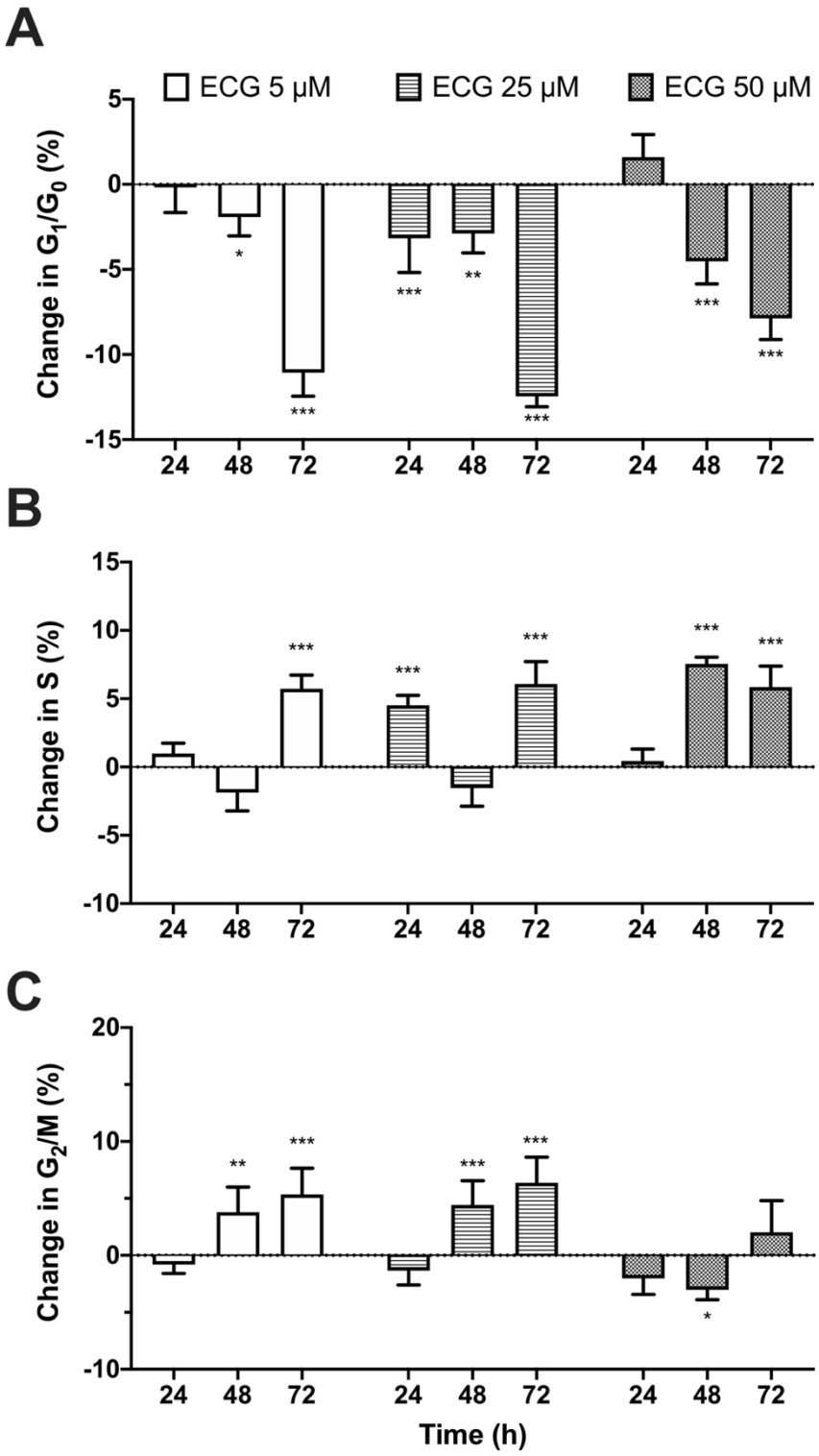

Figure 55 Relative cell cycle distribution under epicatechin gallate treatment
Relative change in cell cycle distribution compared to the control for G_1/G_0 (A), S (B), and G_2/M (C) phases under epicatechin gallate (ECG) treatments at 5, 25 and 50 µM for CHO cells grown in 24-well plates for three days (section 2.1.2). Each data point represents the average from a triplicate, and the error bars correspond to ±SD. These experiments were repeated independently. Statistical two-way ANOVA test was perform to compare treatments with control at p-values: (*)< 0.05, (**) < 0.01 and (***) < 0.001.

4.2.3.4 Epigallocatechin-gallate

The time-course study of cell cultures in 24-well plates under static conditions indicated that cells adapted and started to grow before 24 hours (from 0.16 at time zero to 0.35 10^6 cells/mL after 24 hours for all concentrations). Control reached specific cell growth (μ) of approximately 1 $days^{-1}$ for the last 24h of the culture (up to 0.98±0.03 10^6 cells/mL). Treatment with epicatechin-gallate at 5 μM caused severe inhibition of the cell growth, although this was taking place at a lower rate, with a specific growth rate close to 0.64 day^{-1}. Higher concentration treatment at 25 μM, caused a considerable inhibition of cell growth at the first 48 hours of the culture, close to the one observed during the 5 μM treatment. The last 24 hours however, caused complete cell growth arrest, with a final total cell density of 0.37±0.06 10^6 cells/mL. Treatment with 50 μM, caused the complete arrest of the cell culture over the entire period of cultivation, with a final density of 0.23±0.03 10^6 cells/mL. These results, are not identical to the ones obtained during the initial screening of the chemicals. During this investigation, EGCG seems to have a stronger inhibition effect (Figure 56A).

Cell viability was maintained between 92 and 96% for all samples at all times. This indicates that, regardless of the sudden inhibitory effect of the chemical over the population, these concentrations do not cause severe toxic effects in the cultures under these conditions. There were no main differences in the initial viability values. However, this does not ensure that this chemical does not have minimal cytotoxic effect when added to the culture, since the variation at time zero was considerable. This effect can be observed at time zero, since the Vi-cell readings take place at very low concentrations, close to the limit of resolution of the device. This is further confirmed as the error bars diminished as the cell culture grew (Figure

56B). The final viability numbers, indicated that this chemical caused a small drop in viability (3.3-1.5±0.54%) in the last 24 hours, with significant differences from the control (95.57±0.24%). This may indicate that epigallocatechin-gallate could have adverse effects on the culture if recorded for longer.

Epigallocatechin-gallate caused no significant changes in cell size under these conditions with values close to the control (15.1-15.5 μm) (Figure 56C).

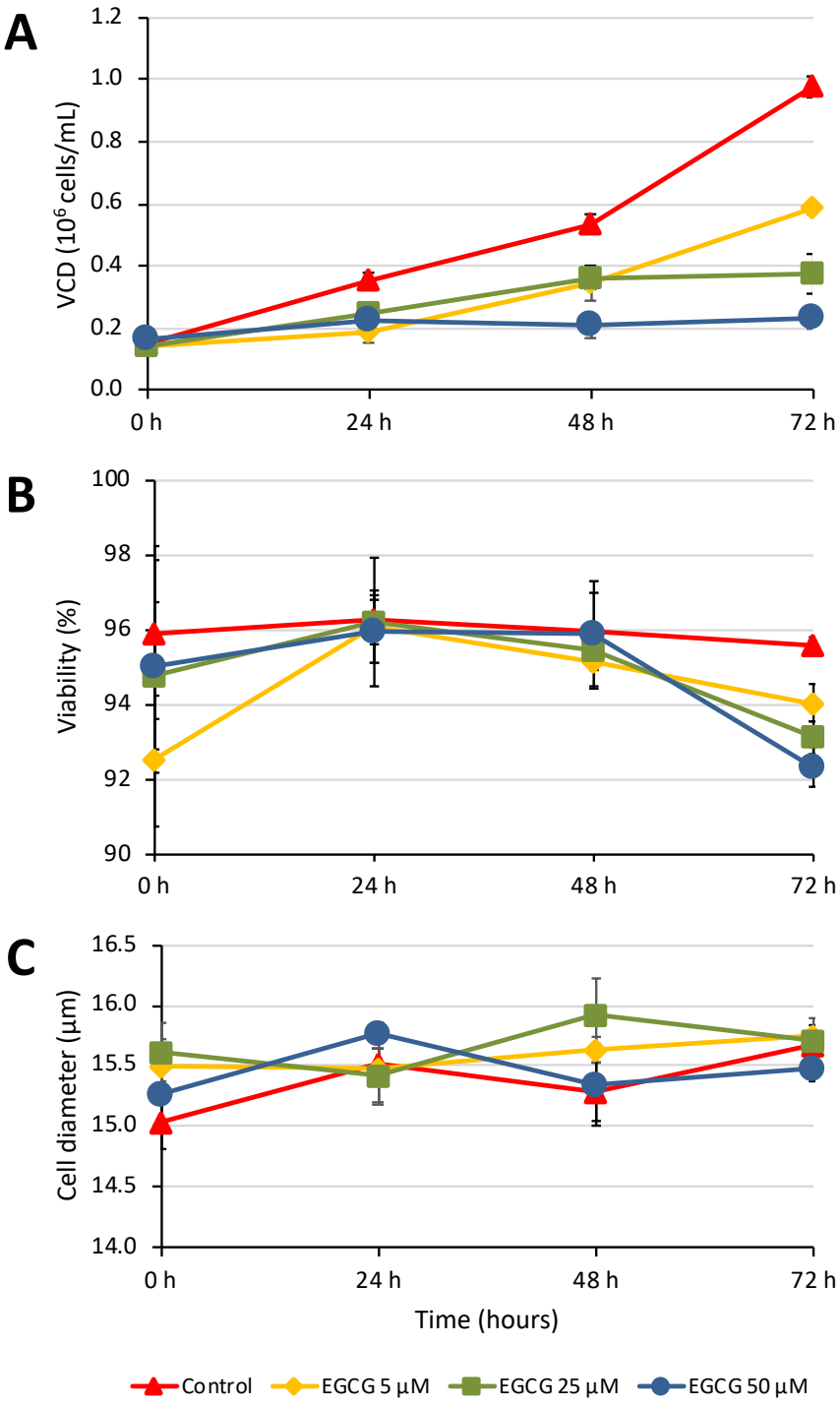

Figure 56 Time course study effect of EGCG over cultures in 24-well plates
Effect of epigallocatechin gallate (EGCG) on viable cell density (VCD) (A), viability (B) and cell diameter (C) (section 2.1.4) at 10 µM (yellow), 25 µM (green) and 50 µM (blue) treatments for CHO cells grown in 24-well plates (section 2.1.2). Each data point represents the average from a triplicate, and the error bars correspond to ±SD. These experiments were repeated independently.

The cell cycle experiment did not show a clear pattern. The 5 µM concentration of epigallocatechin-gallate, caused accumulation of cells in the G_2/M phase after 72 hours of treatment, in detriment of G_1/G_0. Concentrations above (25 and 50 µM) had a very different effect, with a consistent significant increase in S phase. In the beginning, this cell increases in the S phase accounted mainly from the loss of cells from the G_1/G_0 phase. However, as time passed by, the cells missing from the G_1/G_0 phase were more numerous. After 72 hours, the accumulation of cells in the S phase accounted exclusively from cells in the G_1/G_0 phase and there was also a consistent increase in G_2/M. It is likely that the missing cells under different phases of the cell cycle, are due to partial synchronization taking place, as cells were partially arrested in S phase as early as 24 hours. This could explain the depletion of cells in G_2/M phase as cells cannot move further from the S phase (Figure 57). As the culture elongated in time, cells passed to G_2/M phase, but they did not reach G_1/G_0.

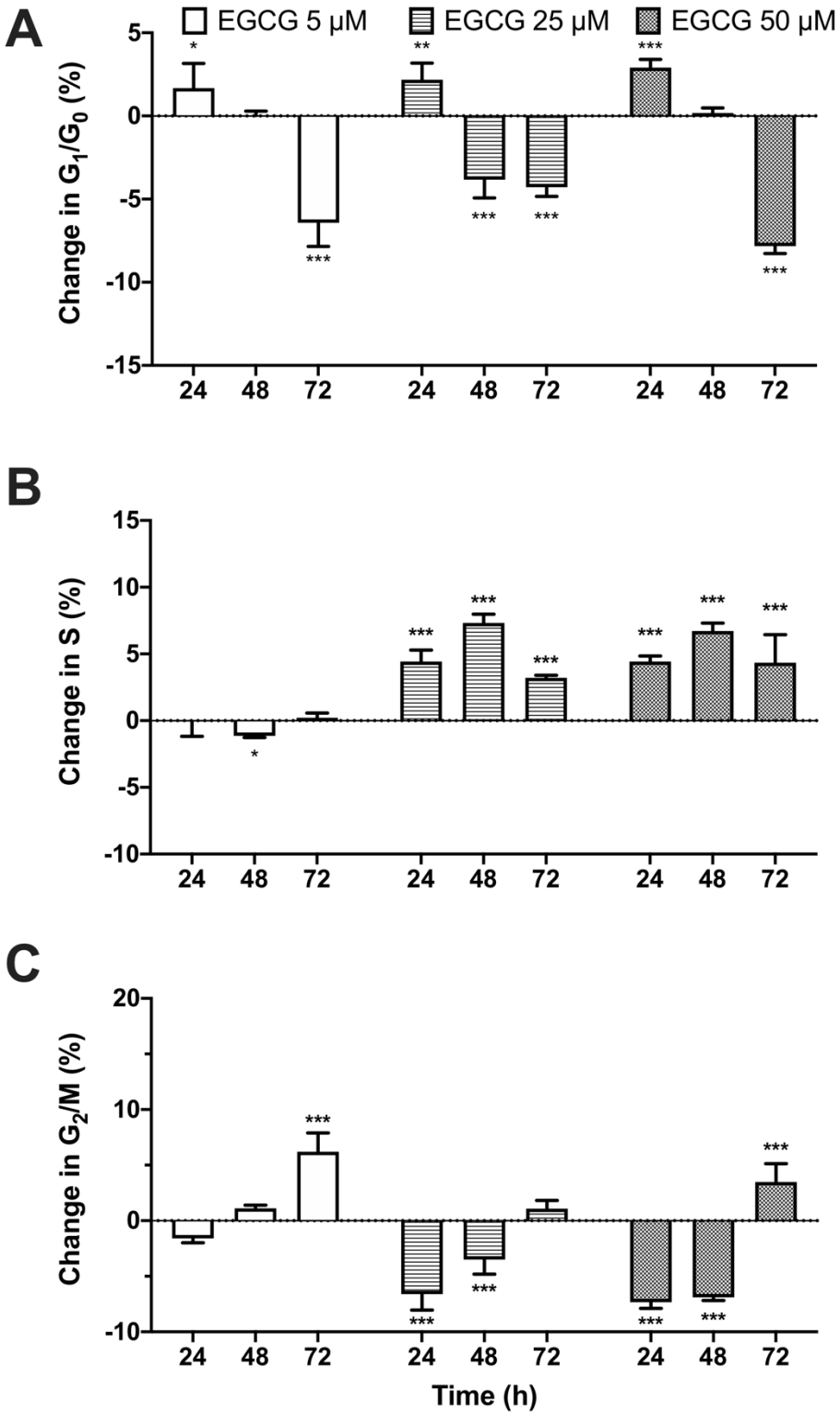

Figure 57 Relative cell cycle distribution under epigallocatechin gallate treatment
Relative change in cell cycle distribution compared to the control for G_1/G_0 (A), S (B), and G_2/M (C) phases under epigallocatechin gallate (EGCG) treatments at 5, 25 and 50 µM for CHO cells grown in 24-well plates for three days (section 2.1.2). Each data point represents the average from a triplicate, and the error bars correspond to ±SD. These experiments were repeated independently. Statistical two-way ANOVA test was perform to compare treatments with control at p-values: (*)< 0.05, (**) < 0.01 and (***) < 0.001.

4.2.3.5 Gallocatechin-gallate

The time-course study of cell cultures in 24-well plates under static conditions indicated that cells adapt and start to grow way before 24 hours. With growth from 0.16±0.01 at time zero to 0.29±0.03 10^6 cells/mL after 24 hours for all concentrations. Control reached specific cell growth (μ) of approximately 1 $days^{-1}$ for the last 48h of the culture reaching 1.02±0.04 10^6 cells/mL after 72h of culture (Figure 58A). All the treatments of gallocatechin-gallate (5, 25 and 50 μM) cause very similar responses on the cell culture. Under these conditions, cell growth is partially repressed with an overall cell growth rate of 0.79 $days^{-1}$.

Cell viability was maintained between 93 and 97% for all samples at all times, this indicates that regardless of the inhibitory effect of the chemical over the population, these concentrations do not cause severe toxic effects in the cultures under these conditions. The increase in the average viability of the samples in a concentration-dependent manner is consistent. Treatments at 5 μM concentrations have overall viabilities (94.3-95.1 %) lower than 25 μM (95.1-96.7 %), and this one lower than 50 μM (96.5-97.1 %)(Figure 58B). Regardless of the consistent trend, there are no significant differences and these treatments do not seem to cause any effect in viability under these conditions.

Gallocatechin-gallate caused no significant changes in cell size under these conditions with values close to the control (15.1-15.5 μm). Cell diameter is maintained very similar to the control except for 25 μM (16.05±0.15 μm) and 50 μM (15.97±0.11 μm) at 72h which have a significant increase in size with respect to the control at 15.5 μm (Figure 58C).

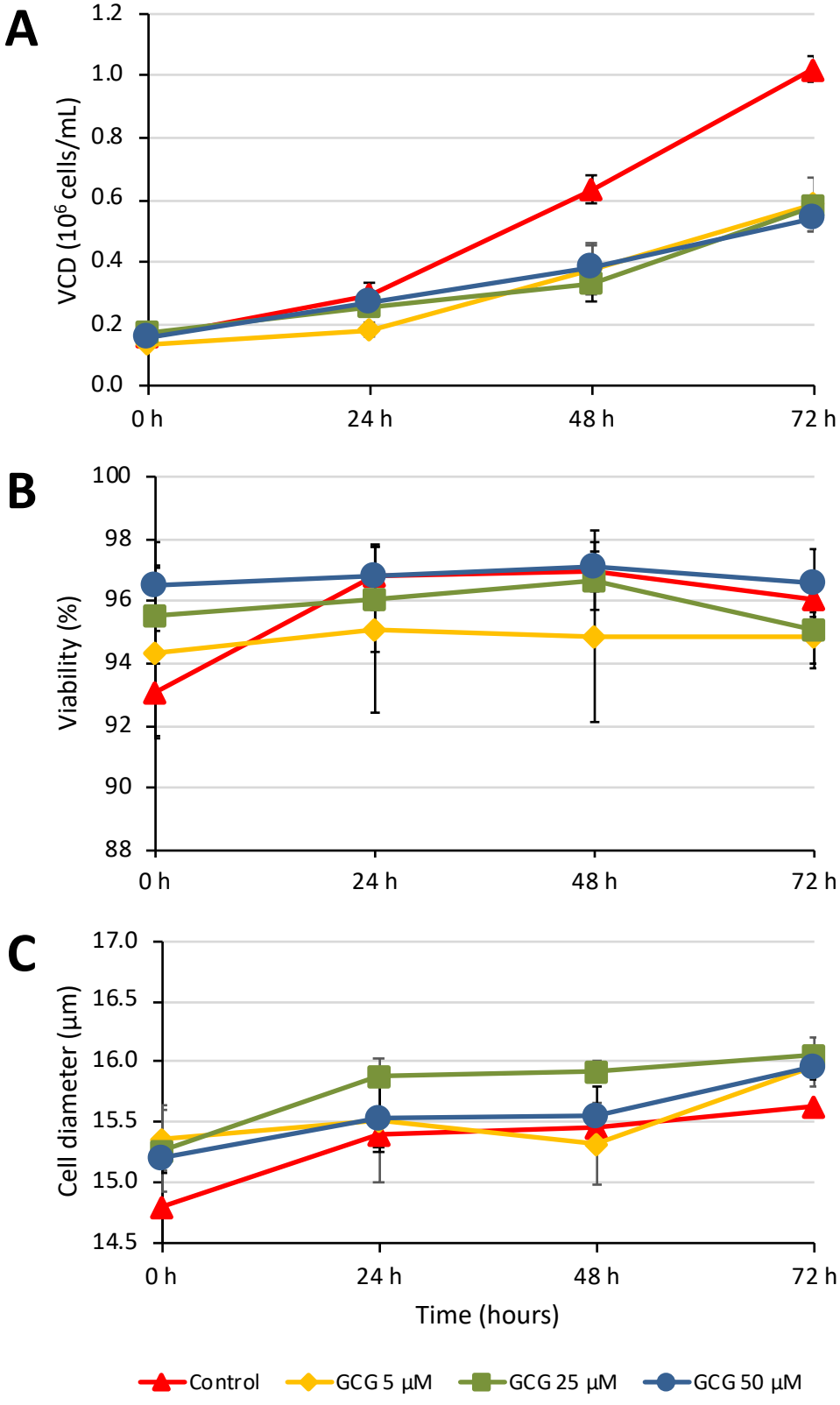

Figure 58 Time course study effect of GCG over cultures in 24-well plates
Effect of gallocatechin gallate (GCG) on viable cell density (VCD) (A), viability (B) and cell diameter (C) (section 2.1.4) at 10 µM (yellow), 25 µM (green) and 50 µM (blue) treatments for CHO cells grown in 24-well plates (section 2.1.2). Each data point represents the average from a triplicate, and the error bars correspond to ±SD. These experiments were repeated independently.

The cell cycle experiment does not show a clear pattern. The concentration of 5 µM epigallocatechin-gallate causes accumulation of cells in the G_2/M phase after 72 hours of treatment in detriment of G_1/G_0 (+7.24%). Concentrations above (25 and 50 µM) have a very different effect with a consistent significant increase in S phase. While at the beginning this cell increase in the S phase accounts mainly from loss of cell in the G_2/M phase, as time passes by the cells missing in the G_1/G_0 phase are more numerous. After 72 hours the accumulation of cells in the S phase accounts exclusively from cells in the G_1/G_0 phase and there is also a consistent increase in G_2/M (Figure 59). It is likely that the missing cells under different phases of the cell cycle are due to partial synchronization taking place as cells are immediately partially arrested in S phase as early as 24 hours after treatment. This could explain the depletion of cells in G_2/M phase as cells cannot move further from the S phase. As the culture elongates in time, cells pass to G_2/M phase, but they don't reach G_1/G_0.

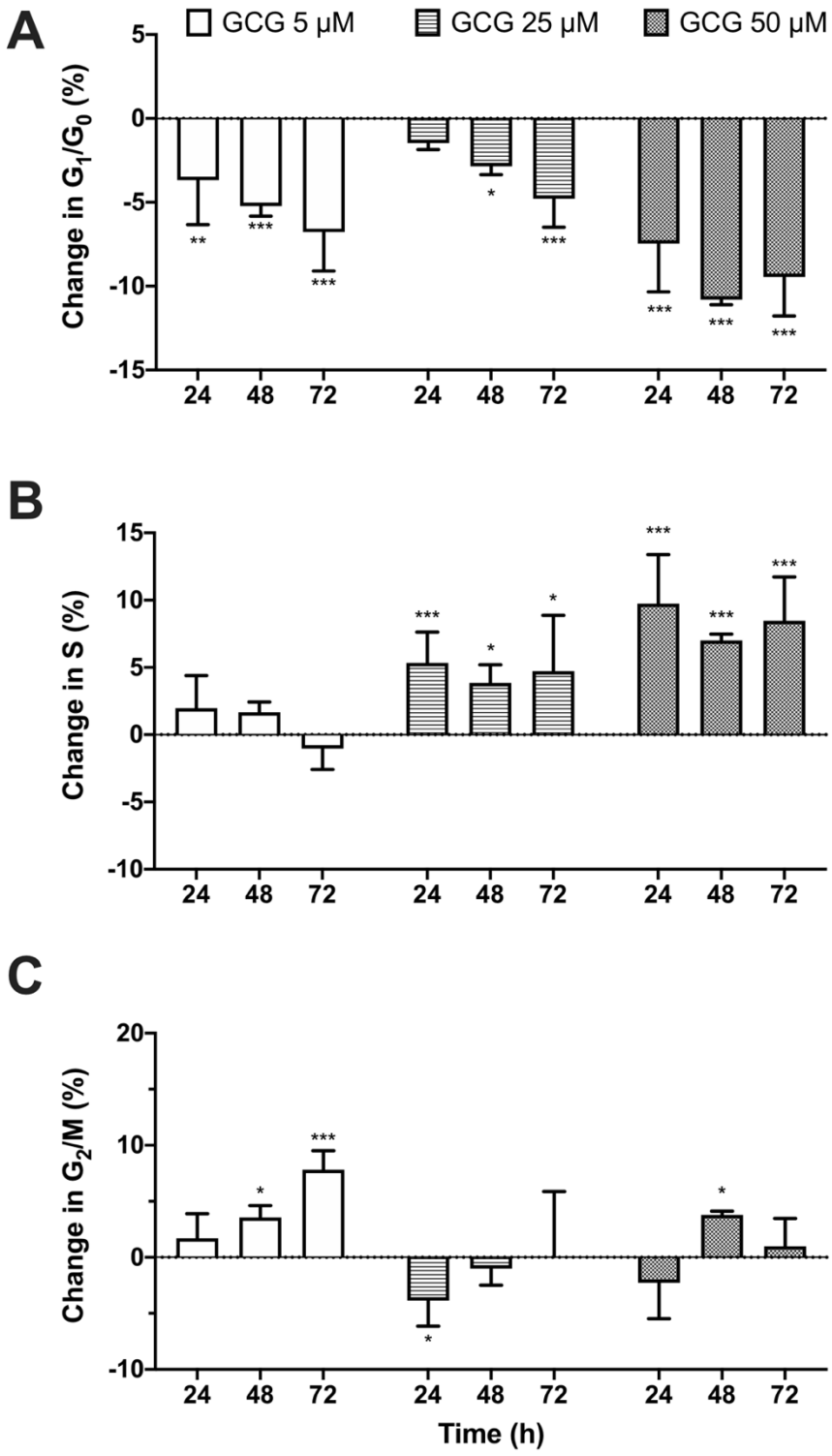

Figure 59 Relative cell cycle distribution under gallocatechin gallate treatment
Relative change in cell cycle distribution compared to the control for G_1/G_0 (A), S (B), and G_2/M (C) phases under gallocatechin gallate (GCG) treatments at 5, 25 and 50 µM for CHO cells grown in 24-well plates for three days (section 2.1.2). Each data point represents the average from a triplicate, and the error bars correspond to ±SD. These experiments were repeated independently. Statistical two-way ANOVA test was perform to compare treatments with control at p-values: (*)< 0.05, (**) < 0.01 and (***) < 0.001.

4.2.3.6 Discussion

Catechins cause an inhibitory effect on cell cultures in a concentration-dependent manner. The degree of cell arrest seems to be linked to the structure. Catechin is the less effective in reducing cell growth, while epigallocatechin-gallate is the one that affects more severely, ECG and GCG have very similar trends that are in between both extremes. EC is difficult to compare as the concentration range is different, it is less toxic than EGCG or GCG and ECG and seems to cause a slightly more severe effect on cell inhibition than catechin.

The structure of the compounds seems to be key in the different effects over cell growth inhibition as the chemicals with the galloyl group (EGCG, GCG and ECG) seem to have an overall more severe effect. Furthermore. The epimerization disposition of the molecule also seems to be important as epimeric compounds such as EC or EGCG are prone to inhibit growth more effectively than their counterparts catechin and GCG.

No main changes in viability were observed under all conditions, overall catechin compounds are non-toxic regardless of their cell inhibition capacity.

Cell shape is affected differently depending on the structure of the chemical, while Catechin and epicatechin are able to cause severe increases in cell diameter, bigger compounds fail to do so and only a small increase after three days can be observed. The addition of the galloyl group to the compound again causes a very different effect. In this case the epimeric disposition of the molecule does not seem to cause a big difference in the change of size as GCG, EGCG and ECG all have a very similar trend, at the same time catechin and epicatechin

seem to be doing very similar changes as both treatments with 10 µM cause very similar changes in size.

Catechins affect cell cycle in a different way depending on the presence of the galloyl group, Catechin and epigallocatechin mainly cause increases in the G_2/M phase after 3 days incubation. For compounds with the galloyl group there is a difference between the lowest treatment, and the high concentrated treatment. While treatments at 5-10 µM cause an increase to G_2/M phase very similar to the one observed in catechin and epigallocatechin, higher concentrations tend to cause a bigger accumulation in the S phase after three days of incubation.

EGCG is the most studied compound of the catechin family. Research indicates that this compound is able to inhibit the cell cycle in the S phase (Shabana *et al.*, 2014; Shen *et al.*, 2014). The chemical affects the regulation of many different cell cycle proteins up-regulating p21, p27 and inhibiting Nf-κB (Shabana *et al.*, 2014; Shen *et al.*, 2014) among many others. It is likely that the effect of the chemical is very complex and that although looking into one mode of action there might be pleiotropic mechanisms linked to the high bioactive capability of the compound (Ye *et al.*, 2017).

Although most of the research done has been in EGCG as the main compound, an exception to this was the study by Huang et al. 2005 that researched the effect of catechin in murine microglial cells. Catechin causes cell cycle arrest in S phase under induced toxic conditions when treated with catechin at 500 µM (Q. Huang *et al.*, 2005). This is similar to the effect seen

in compounds with galloyl group, it is possible that the effect of catechin at very high concentrations could be similar to those of the compounds with galloyl group.

Comparative studies of the effect of different catechin compounds on the cell cycle were consistent in identifying different behaviours depending on the presence of the galloyl group. The studies indicate that. While EGCG (500 μM) and ECG (1 mM) cause increases in G_1/G_0 with the respective decreases in S and G_2/M phases, EC (1 and 2 mM) causes S phase arrest (Tan *et al.*, 2000). Although the arrest happens in a different phase of the cell cycle when compared to the present study, the indication of a different behaviour linked to the structure is reinforcing in our previous observations.

A further comparative study of compounds with galloyl groups indicated that ECG, gallocatechin (GC) and EGCG cause very similar responses in cell cycle arrest. All the chemicals inhibit cell growth in a concentration-dependent manner and cause inhibition of Nf-κB and also an increase in S phase while decreasing in G_1/G_0.

Showed that different chemicals form the catechin family show different effects in human pancreatic ductal adenocarcinoma cell lines. All the chemicals inhibit cell growth in a concentration-dependent manner (20-80 μM) and also elongated the S phase of the cell cycle in detriment of the G_1/G_0 phase. Furthermore, all the chemicals caused inhibition of Nf-κB. Nevertheless, other markers were not even for all the chemical treatments. GC and ECG increase p21 and p27 while EGCG increases p21 but decreases p27 (Kürbitz *et al.*, 2011). This reinforces the idea that the galloyl group is relevant and causes changes in the way the

chemicals act over the cells, but that small changes in the structure of the catechin even with the presence of the galloyl group can account for changes at different levels.

The mechanism by which catechins may be acting on the cell cycle could include their inhibitory effect over the topoisomerase enzymes. EGCG the most studied molecule of the family was found to inhibit topoisomerase I and II (Bandele 2008) by sequestrating the enzyme in a complex that seems to be mediated by hydrogen peroxide (Lopez-Lazaro 2011). Topoisomerases are enzymes that cut one or two strands of DNA to unwind it and access it for replication and segregation. This inhibition of topoisomerases leads to G_2/M and S phases arrest (Cliby 2002). This extends to catechins in general with all indicating certain topoisomerase inhibition capability depending in their structure with EGCG being the most effecting in inhibiting topoisomerases followed by ECG while compounds such as EC show very low inhibitory capacity (Suzuki 2001). This could explain the differences between catechin and epicatechin when compared with the compounds with a galloyl group. It is possible that EC and Catechin act in a completely different way to the other compounds and that most likely the differences in cell size, cell growth inhibition or cell cycle arrest between them and the catechins with galloyl groups is due to the capacity of the last ones to interact with topoisomerases.

Two main parameters that seem indicative of the activity of the catechins' effect on cells are the galloyl group mainly and the epimeric disposition to a lesser degree. In order to further validate if this group of chemicals can be used as chemical tools for biopharmaceutical production improvement as additives, catechin, epicatechin, gallocatechin-gallate and epigallocatechin were selected for scale-up studies.

Overall, all catechins compounds caused a significant decrease of the relative quantity of cells in the G_1/G_0 phase, refuting the initial hypothesis that this chemicals were able to assist in increase in the specific IgG production by specific cell cycle arrest described in previous literature (Hendrick *et al.*, 1999; Carvalhal, Marcelino and Carrondo, 2003; Bi, Shuttleworth and Al-Rubeai, 2004; Dutton, Scharer and Moo-Young, 2006). It is likely that the method of action of these chemicals over the CHO cell culture and specific recombinant antibody production is different and could be of use as a tool in industry as an alternative method to increase the final titre.

4.3 Conclusions

During the present investigation, a protocol for fixation and propidium iodide stain of CHO cells with only three washes was developed. This protocol was able to reliably treat cells for further flow cytometry studies. Moreover, cell cycle flowcytometry data, indicated that resveratrol was able to stop the cell cycle in an aphasic way and elongate the stationary stage. Furthermore, resveratrol caused cell growth arrest during S phase in the first cell divisions; this phenomenon seems to be linked is to resveratrol's toxic effect on CHO cells, suggesting that the toxic effect over dividing cells may be partially linked to an effect on the topoisomerases. All the present results provide a better understanding of how this chemical interacts with CHO cell cultures and could help to develop strategies for further scale-up and recombinant protein optimization experiments.

The experiments with components from the catechin family, showed that the galloyl group is fundamental in determining the effect of the chemical over the CHO cell culture. Catechin

compounds with the galloyl group inhibited cell growth more and the cell arrest was more prominent in the S phase. The different levels of cell growth arrest caused by the catechin compounds seemed to correlate with their capacity to inhibit the topoisomerase activity. Based on the current information, catechins are good candidates for further scale-up and recombinant protein optimization experiments.

In the light of the results of these experiments, resveratrol, catechin, epicatechin, gallocatechin-gallate and epigallocatechin-gallate will be taken forward for scaling up and optimization.

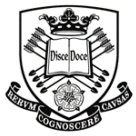
Disce Doce
Rerum Cognoscere Causas

Chapter 5

Scale-up and optimization of recombinant IgG production

5.1 Initial remarks

Previous results indicated that resveratrol and catechins are able to improve q_p while causing cytostatic conditions (Chapter 3). Further experimentation revealed that these chemicals stop the cell growth by specific cell phase arrest of the G_1/G_0 in the case of the catechins (Chapter 4). Resveratrol, on the other hand, had a a more complex effect on cell growth arrest with an aphasic cell cycle arrest (Chapter 4). The increases in q_p studied so far did not translate into a final increase in titre. In the current chapter we aimed to investigate the effect of resveratrol, catechin, epicatechin, gallocatechin-gallate and epigallocatechin-gallate over the cell culture in scale-up conditions, with 33 mL cultures under different feeding regimes.

To optimize the process of chemical addition to the culture and study the effect that this could have in the cell population and the protein production, feed batch Erlenmeyer flask cultures were run as specified in section 2.1.3. Cultures were treated at days 0, 3 and 6 with 25 and 50 µM concentrations of resveratrol, catechin, epicatechin, gallocatechin-gallate and epigallocatechin-gallate. Everyday measurements of viability and concentration (section 2.1.4) and IgG recombinant IgG production (section 2.1.5) were collected for a period of ten days. The experiment was run in triplicates and was repeated twice independently.

5.2 Results and discussion

5.2.1 Resveratrol feeding optimization strategy and effect on cell culture

5.2.1.1 Viable cell curve and growth rate

The viable cell density curve of the control indicated that the cells were able to grow immediately after inoculation. Twenty four hours of incubation resulted in an increase of 0.34±0.02 10^6 viable cells/mL which almost doubled the initial seeding concentration of 0.18±0.00 10^6 viable cells/mL. The fast adaptation of the cells to the culture is expected as the cells are seeded into the same conditions, and the only change is the fresh media. Cells under control conditions grew in cell concentration until day seven, reaching a maximum concertation of 12.34±0.20 10^6 viable cells/mL. After this, the number of viable cells decreased drastically to 3.52±011 10^6 viable cells/mL.

Treatments with 25 µM concentrations caused a reduction of growth at any given time, and did not reach the high concentrations seen for the control at day seven. In contrast, the peaks were milder and more elongated in time, creating a stationary phase. When adding resveratrol at time zero, the viable cell curve was delayed by one day and the stationary phase was between days seven and nine, with a maximum viable cell density observed at day eight (9.10±0.61 10^6 viable cells/mL). Addition of 25 µM of resveratrol at day three, caused a very similar delay in the cell curve, but less severe, with maximum viable cell concentration at day eight (10.13±0.76). Furthermore, a shorter stationary phase was observed (days seven and eight). 25µM of resveratrol at day six, caused an immediate arrest of the cell growth and there

was a stationary stage for the next 48 hours. The pattern of the cell culture was the same and the viable cell density decayed after incubating for eight days (Figure 60A).

The effects with 50 µM treatments were more dramatic and the different time of addition resulted in clearer differences in the viable cell curve. The addition of 50 µM of resveratrol at time zero, caused a severe arrest of the cell culture. This resulted in a delay in the maximum viable cell density of three days at 7.55±1.08 10^6 viable cells/mL by day nine. This curve did not show signs of decay for the ten days of incubation studied. A few samples were studied under these conditions at days eleven and twelve, and the viable cell density was heavily compromised. The 50 µM treatment at day three caused an immediate stop of the viable cell growth for 24 hours at 1.65±0.06 10^6 viable cells/mL. Although cell growth was restored, the culture grew slower for the rest of the incubation time, with a delay in respect to the control. This treatment resulted in a stationary phase of the viable cell curve during days seven and nine (6.86±0.57 10^6 viable cells/mL). The addition of resveratrol at 50 µM on the sixth day, caused cell growth arrest, with a 48 hours stationary phase at 8.95±0.16 10^6 viable cells/mL. Nevertheless, the behaviour of the cell curve was preserved and after day eight, there was a decay in viable concentration (Figure 60B).

The culture under control conditions seemed to grow during the first seven days of the culture at an average rate of 0.87±0.09 $days^{-1}$. The addition of 25 µM of resveratrol did not seem to cause a delay in the growth phase nor a change in length maintaining the seven-day period. The average of the growth during this period was not significantly compromised, but there was a tendency to lose overall growth rate the sooner the chemical was added. The treatment with the most inhibitory effect was the one where the chemical was added at time zero

(0.75±0.06 days^{-1}). Treatment at day six was the less repressive (0.81±0.17). On the other hand, the addition of 50 µM to the media had a very significant effect on the growth phase length. The addition of the chemical at day six immediately inhibited the growth, but there was no significant difference in the growth rate (0.91±0.19 days^{-1}). Addition on day three had a similar effect, with the treatment truncating the growth of the culture for the rest of the incubation time. This caused a significant increase in the average growth rate (1.09±0.10 days^{-1}) as the decay phase was avoided. If 50 µM of resveratrol were added at the initial time of the cell culture, the growth phase was longer elongated, up to the ninth day. This is probably because the growth rate of the culture significantly decreased with an average of 0.54±0.11 days^{-1}. Under these conditions cells divided at a slower rate and this extended the growing phase mainly because the rate of media consumption was lower (Table 8).

Table 8 Growth rate of feed-batch cultures treated with resveratrol

Treatment	µ (days^{-1})			Growth phase (days)	
	Mean		SD	Start	Finish
Control	0.87	±	0.09	1	7
Resv Day0 25 µM	0.75	±	0.06	1	7
Resv Day3 25 µM	0.78	±	0.05	1	7
Resv Day6 25 µM	0.81	±	0.17	1	7
Resv Day0 50 µM	0.54	±	0.11	1	9
Resv Day3 50 µM	1.09	±	0.10	1	3
Resv Day6 50 µM	0.91	±	0.19	1	6

(Resv) resveratrol, (SD) standard deviation

5.2.1.2 Viability

Control samples kept very high levels of viability (above 94%) until day seven. Viability was highly compromised as the cell culture reached the death phase and then dropped to

78.06±0.78%. After 48 hours, most of the cells in the culture were dead, with a viability of 33.90±0.75% by day nine. Treatment with 25 µM of resveratrol at time zero resulted in a delay of the decay by day one. Viability was preserved at day eight (90.08±0.57%) and day nine, having more cells alive than dead (72.78±1.87%). The cell culture was mostly dead again by day ten, with a viability of 41.97±2.78%. The viability behaviour of the cell culture did not change under these conditions and was mainly delayed. This aligns with the viable cell density curve results. Treatment with 25 µM of resveratrol at day three, caused a less sudden drop of viability after day seven, reaching 30.08±0.58 % by day ten. There were no meaningful differences between adding 25 µM of the chemical at day three or six (Figure 60C).

50 µM concentration treatments caused more distinguishable effects on the viability of the culture, in a time-dependent manner. Adding the chemical at time zero resulted in an initial, steady drop in viability until day four (86.71±1.54%). After that, viability recovered until day eight (95.06±0.52%). Finally, viability dropped at the end of the culture (88.05±1.95%), although it did not drop as drastically as the control; measurements two days beyond the ten days of incubation showed fast drop and viability values below 50%. Addition of 50 µM of resveratrol at day three, caused a less severe effect on viability over time; It originated an immediate drop in viability at 24 hours (from 97.39±0.30% to 92.44±0.67%) and this level was maintained until the decay phase at day eight, which was not delayed. The drop in viability at the end of the culture was less severe. Adding resveratrol at the highest concentration (50 µM) at day six, did not cause any main changes in the behaviour of the culture viability and only made the decay curve milder (Figure 60D).

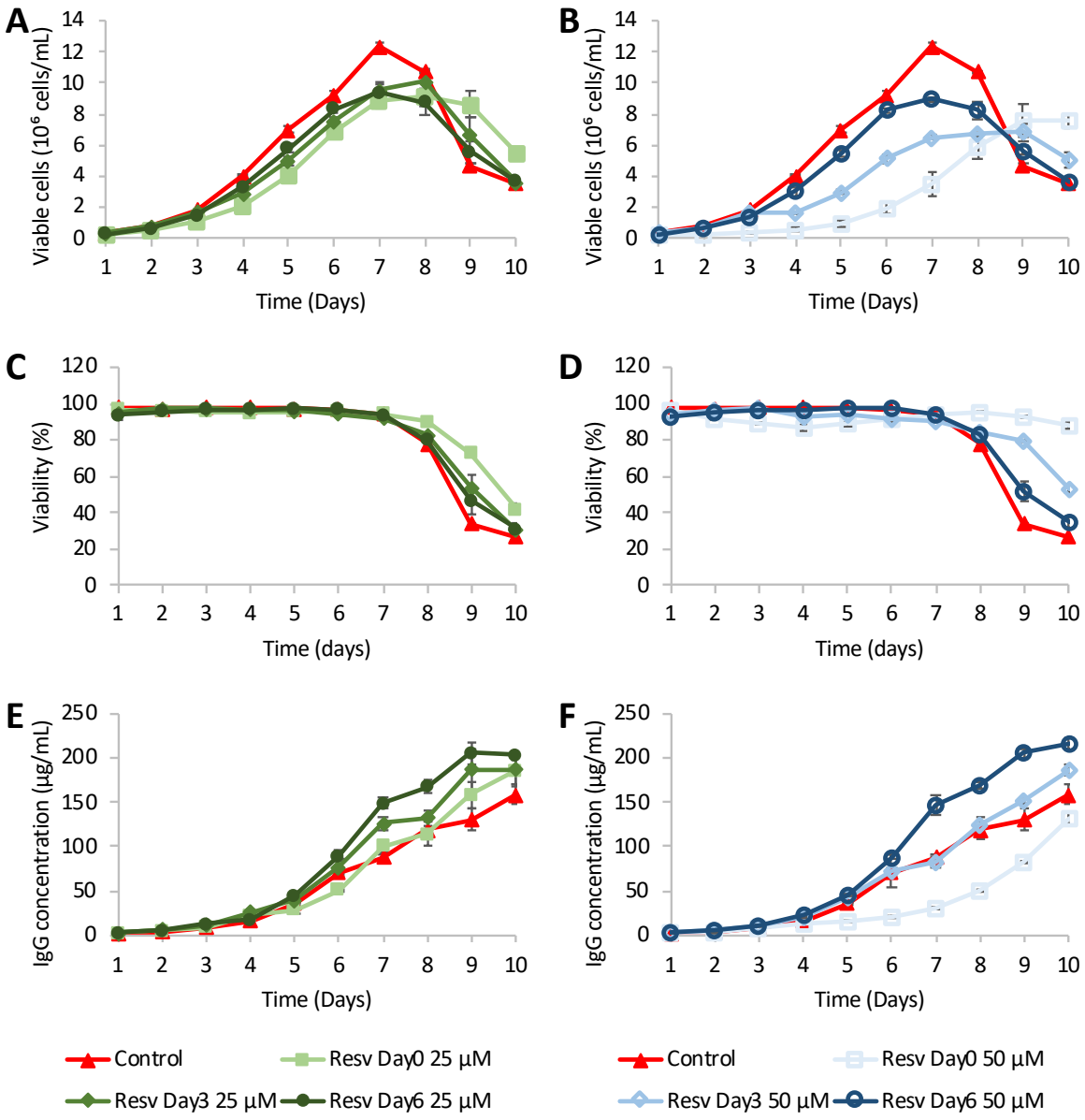

Figure 60 Effect of resveratrol over growth and IgG production in flask cultures
Effect of resveratrol (Resv) treatments in viable cell density (A,B), viability (C,D) and IgG concentration (E,F) when added at days 0 (squares), 3 (diamonds) and 6 (circles) for 25 µM (green) and 50 µM (blue) concentrations. Cells were incubated in 125mL Erlenmeyer flasks with an initial 33 mL volume for 10 days under shaking conditions (section 2.1.3). The error bars represent the standard deviation of triplicates and the experiment was carried twice independently.

5.2.1.3 IgG final titre and specific productivity

The cell line under control conditions was able to produce at a constant rate that reached a final titre of 158.6±11.2 μg/mL. The addition of 25 μM of resveratrol at time zero, did not cause any main changes in the production profile of the cell culture over the ten days of incubation. The IgG produced reached a non-significant increase in the average final titre (186.8±17.5 μg/mL). The addition of 25 μM at day three showed the same response, with a non-significant increase (187.4±16.7 μg/mL). Finally, the addition of 25 μM of resveratrol at day six, resulted in a significant, 1.28-fold increase of the final titre (203.1±12.0 μg/mL). Overall, the chemical seemed to be increasing IgG production in a steady manner (Figure 60E).

The addition of a 50 μM concentration to the culture at different time points, caused important changes to the production process in the cell culture. Resveratrol in this concentration at time zero, caused a delay in the production during the first six days. After that, the prolonged static period production of the recombinant protein accelerated, until it reached a final titre close to that of the control, but significantly lower (131.9±6.7 μg/mL). The addition of 50 μM of resveratrol at day three, did not cause any changes in the pattern of the production and slightly increased the productivity over the last two days, reaching 187.5±6.1 μg/mL (1.18-fold increase). Addition at day six, caused the cell culture to increase its productivity with a fast increase observed during the last four days (final titre 216.8±6.29 μg/mL, equivalent to 1.37-fold increase) (Figure 60F).

Cell specific productivity was increased for all the treatments of resveratrol compared to control (2.21±0.17 pg/cell·day). The addition of 25 μM of resveratrol at different time points did not cause any significant changes in the increase of $q_{p,}$ with averages between 3-3.5

pg/cell·day. All treatments with 25 µM caused lower q_p increases when compared to those using 50 µM. This is due to the concentration-dependent effect of cell growth inhibition of the chemical. This condition was not paired with a reduction in the productivity of the cells. On the contrary, the opposite was often observed. The time of addition of higher treatment concentrations of resveratrol, was associated with the increase in q_p. Late addition on day six, showed the lowest increase (3.88±0.21 pg/cell·day). Addition at time zero (50 µM) caused the highest increase in specific productivity (4.74±0.59 pg/cell·day), doubling the effect seen by the control. This 2-fold increase, was possibly related to the fast recovery of IgG production during the last section of the culture, while cell concentrations never peaked under this treatment (Figure 61).

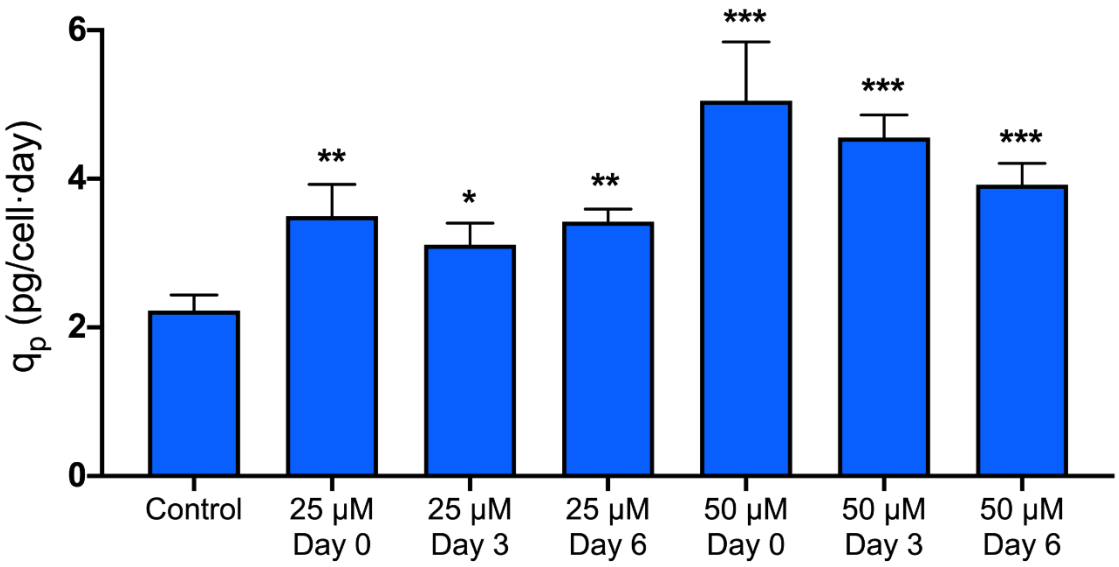

Figure 61 Effect of Resv on relative protein production in flask cultures
Relative protein production (q_p) of 33 ml batch recombinant CHO cell cultures in 125 ml Erlenmeyer flasks after a period of 10 days (section 2.1.3) and treated with resveratrol (Resv) at 25 and 50 µM on days 0, 3 or 6. q_p was calculated by dividing final protein production by the integral of the VCD curve. Each data point represents the average from a triplicate, and the error bars correspond to ±SD. These experiments were repeated independently. One way ANOVA statistical test was perform for the treatment compared to the control for p-values: (*)< 0.05, (**) < 0.01 and (***) < 0.001.

5.2.1.4 Discussion

Resveratrol added at time zero, was associated with non-desirable traits of the chemical, under the conditions studied. As a result, the cell culture lost its viability and cell growth was inhibited considerably. All this elongated the adaption phase of the feed-batch culture. This was associated with low specific cell productivity. Moreover, it resulted in levels of final IgG concentration equal to control in the best-case scenario. A reasonable hypothesis is that by elongating the culture for more days, the stationary phase would extend beyond day ten and productivity would increase. Samples analyzed at days eleven and twelve showed a fast decay of viability under 50% and indicated that the culture cannot be extended in time. Extension of the culture is not a desired feature, because it does not elongate the production phase of the culture, which is often found in the deceleration and stationary phase. The extension of the culture also requires more time and energy. Finally, the drop in viability of the culture could jeopardize the quality of the product, as dead cells lose the integrity of their cell membrane; the longer they are in the media, the more likely this is to happen.

When adding resveratrol at day six, the properties of the chemical were more desirable. Under these conditions, cell culture growth was maximized in time, and cells were healthy with high viability. Furthermore, at the end of the growth phase, the addition of the chemical, stopped uncontrolled cell growth and enhanced the specific protein production. This resulted in a considerable increase of the final titre. The chemical is a potent agent for the development of biphasic feed-batch strategies in recombinant CHO cell lines. It possesses many traits that are associated with successful process engineering strategies (Du *et al.*, 2015).

Intermediate addition of the chemical at day three, caused an intermediate effect compared to the ones observed at days zero and six. Furthermore, the higher concertation of the chemical caused a more pronounced effect.

Parallel studies done with resveratrol in recombinant CHO cells, indicated that treatment with 10 µM had no significant effects (Baek *et al.*, 2016). The screening process of the current project identified the same phenomenon and this concentration was discarded. Some feeding strategies described in this protocol, using the 25 µM concentration, did not results in any main changes in the cell culture or protein production, thus supporting the findings by Baek and colleagues.

Other data available, show how resveratrol can be used as an initial media additive at a very high concentration (1 mM), with no negative effects (Tian 2016). Our study showed that resveratrol, in concentrations as low as 50 µM, causes a considerable delay on the cell curve when added at the beginning of the culture. This is accompanied with a significant, but not drastic drop in viability and a decay in the final titre. These differences in the effects of resveratrol are difficult to reconcile. Other studies performed with CHO cells (Basso *et al.*, 2013; Mallebrera *et al.*, 2015) and different mammalian host systems (Lu, Ou and Lu, 2013; Quoc Trung *et al.*, 2013) identified a much lower tolerance of the compounds than what claimed by Tian and colleagues. This indicates that it is likely that the results from this study are an exception, and that most likely, the range of sensitivity of most mammalian cells and more specifically CHO cells, is lower than claimed.

Resveratrol caused drops in viability when added at time zero; addition at the end of the growth phase did not result in any toxic effect. This indicates, as stated in the previous chapter on the cell cycle, that the toxic effect of the chemical and the drop in viability, is strongly related to the division of cells.

These results also highlight the capacity to extrapolate general mechanisms of action of resveratrol, from the initial screening set-up to the flask scale-up conditions. The same effects described in previous chapters were also found in this chapter; these are the inhibition of the cell culture combined with the improvement of the IgG specific productivity. Changing from a static 3-day incubation system of 1 mL volume, to a shaking ten-day incubation system of 33 mL was a success. There is still a long way to go to reach a full scale-up 2000L reactor used in industry. However, the conditions are closer to the final intended conditions and there are many parameters that are relevant when scaling up further. Shear stress, pH and dissociation of relevant gases such as CO_2 or O_2, are some of the principal variables that could affect the cell population and the quality of the product when changing the cell culture conditions (Brunner *et al.*, 2017). Therefore, these experimentations should be taken as promising indicators. Further scaling up should be done to ratify that the compound is adaptable for production scale-up processes.

The effect of the addition of resveratrol at the end of the exponential phase proves that this chemical is best used as a late growth phase inhibitor, in order to modulate growth and improve final titre during the stationary phase. This ratifies the initial hypothesis that the optimal use of the chemical is when cell growth has already been completed.

Nevertheless, in order to further consider resveratrol as a possible tool for the production of recombinant protein in CHO cells, the quality of the product needs to be assessed, in order to ensure that it is not compromised.

Resveratrol was selected for further studies regarding the quality of the product. This was due to the fact that it resulted in the fewest adverse events amongst all the studied chemicals and yielded in a considerable increase in the final IgG production.

5.2.2 Catechins feeding optimization strategy and effect in cell culture

The effects of the addition of catechins at different time points, in cultures incubated for ten days under shaking conditions, were studied to identify proper feeding regimens of the compounds and to identify any differences amongst these compounds.

5.2.2.1 Catechin

5.2.2.1.1 Viable cell curve and growth rate

The viable cell curve did not show any major changes compared to the control when adding catechin at 25 µM. The cell curve was preserved during the exponential phase for all adding treatments until day six. The main change in behaviour appeared after the sixth day. In more detail, the maximum viable cell density was observed at day seven under control conditions (12.34±0.20 10^6 viable cells/mL). On the other hand, this was shifted to day eight when adding the compound on the third day (11.08±1.66 10^6 viable cells/mL) or on the sixth day (11.45±0.68 10^6 viable cells/mL). There were no significant differences in the maximum density reached. Addition of 25 µM of catechin at time zero, did not cause a delay in time for

the maximum viable density, but significantly lowered it to 80% (9.80±0.91 10^6 viable cells/mL) (Figure 62A).

On the other hand, the addition of catechin at a 50 μM concentration, caused significant changes in the overall behaviour of the viable cell density curve. Addition at the late stage of the growth phase (day six), caused minimal changes. The changes observed were a flattening of the growth that took place until day seven, and a reduction in the maximum viable cell density to 10.61±0.40 10^6 viable cells/mL. This treatment timing did not cause any further changes and the decay phase happened in identical terms to that of the control. When the chemical was added at day three, more severe growth repression was observed, similar to the one observed before; the sooner the inhibition of cell growth was induced, the lower the maximal viable cell density was (the lowest being 9.28±0.41 10^6 viable cells/mL). Regardless of the change in the exponential phase, the decay of the cell culture was maintained identical to that of the control from day eight onwards. Finally, the early addition of the chemical at time zero, caused the culture to grow slowly, reaching a prolonged stationary phase at day six. This was maintained until day nine at a very low viable cell density (5.55±0.57 10^6 viable cells/mL) (Figure 62B).

The growth rate and period of growth under the presence of catechin did not change significantly from the control (0.87±0.09 day^{-1}). This was observed in all treatments studied (Table 9).

Table 9 Growth rate of feed-batch cultures treated with catechin

Treatment	μ (days^{-1})			Growth phase (days)	
	Mean		SD	Start	Finish
Control	0.87	±	0.09	1	7
Cat Day0 25 μM	0.81	±	0.11	1	7
Cat Day3 25 μM	0.81	±	0.07	1	7
Cat Day6 25 μM	0.82	±	0.09	1	7
Cat Day0 50 μM	0.78	±	0.16	1	6
Cat Day3 50 μM	0.79	±	0.08	1	7
Cat Day6 50 μM	0.82	±	0.17	1	7

(Cat) catechin, (SD) standard deviation

5.2.2.1.2 Viability

Viability at 25 μM treatments was maintained at the control level and there were no significant differences depending on the addition time. The cell culture preserved its initial viability, with values close to 95% and above. The decay phase of the cell culture and the drop in viability was evident between day seven and eight, as the values dropped to 78.06±0.78% after 24 hours. By day ten values were as low as 26.66±0.78% (Figure 62C).

On the other hand, treatments with 50 μM of catechin, showed differences in their effect in relation to the supplementation time. Treatments at days three and six did not cause any significant changes in behaviour. When catechin was added to the media at time zero, this resulted in high values similar to the ones observed with the control culture for the first 6 days. After day six, viability started to drop sooner, but at a lower rate. Finally, by day ten, the viability of the culture was significantly higher (52.6±16.0%) (Figure 62D).

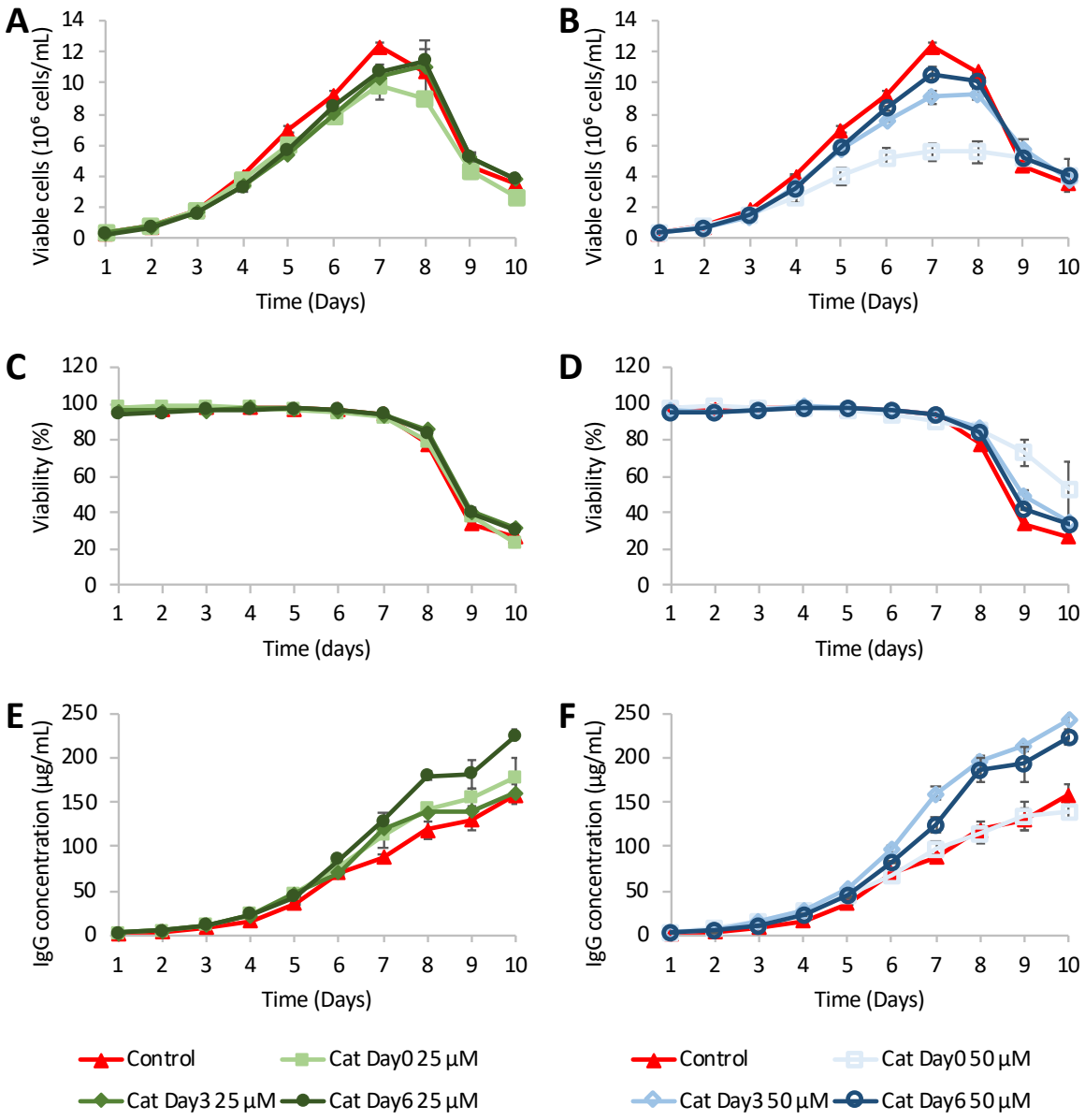

Figure 62 Effect of catechin over growth and IgG production in flask cultures
Effect of catechin (Cat) treatments in viable cell density (A,B), viability (C,D) and IgG concentration (E,F) when added at days 0 (squares), 3 (diamonds) and 6 (circles) for 25 µM (green) and 50 µM (blue) concentrations. Cells were incubated in 125mL Erlenmeyer flasks with an initial 33 mL volume for 10 days under shaking conditions (section 2.1.3). The error bars represent the standard deviation of triplicates and the experiment was carried twice independently.

5.2.2.1.3 IgG final titre and specific productivity

Control conditions indicated that the cell was able to produce recombinant IgG at a constant rate, reaching final titres of 158.6±11.2 μg/mL. The addition of catechin at 25 μM at time zero, did not cause any changes in the profile of the production curve and productivity reached values up to 179.2±20.7 μg/mL. Addition on day three had the same effect as the previously described treatment, with a final titre of 161.8±0.9 μg/mL. The addition of the chemical on day six, on the other hand, had a massive effect on IgG production. Cells under these conditions were able to maintain productivity at a higher rate during the last five days of the culture. This resulted in a final titre of 226.3±7.1 μg/mL (1.43-fold increase) by the end of the culture (Figure 62E).

The addition of catechin at 50 μM, was more successful at improving titres under different feeding time regimes. Treatment at day zero had a very similar IgG production profile compared to control, but caused a significantly lower final IgG concentration, with a final titre of 138.4±8.3 μg/mL (0.87-fold change). On the other hand, treatments at day three and six behaved very similarly to the 25 μM treatments, having positive effects. Cells were able to maintain high levels of production beyond day six (unlike the control) and caused considerable increments in the final titre. Addition of the chemical after three days of incubation, resulted in a final titre of 243.6±12.3 μg/mL, while the respective value with supplementation at day six was 224.2±9.6 μg/mL (1.54 and 1.42-fold increase respectively) (Figure 62F).

The specific protein production of the cells under control conditions was 2.21±0.17 pg/cell·day. All treatments with catechin showed an improvement over the control value.

There was a mild increase at the specific productivity of the cells treated with 25 µM of catechin at day three, (2.53±0.12 pg/cell·day). This was the result of a small change in the viable cell curve towards a lower area, and no changes in the production of the recombinant protein. On the other hand, treatment with 50 µM at the same incubation time, resulted in a completely opposite effect, resulting in the most efficient production (4.21±0.25 pg/cell·day), almost doubling the level of the control. Treatments at days zero and six were not significantly different amongst each other. This indicates that cells were equally productive over the ten-day culture for both situations, but the suppression of the cell growth when adding the chemical at time zero limited the final titre (Figure 63).

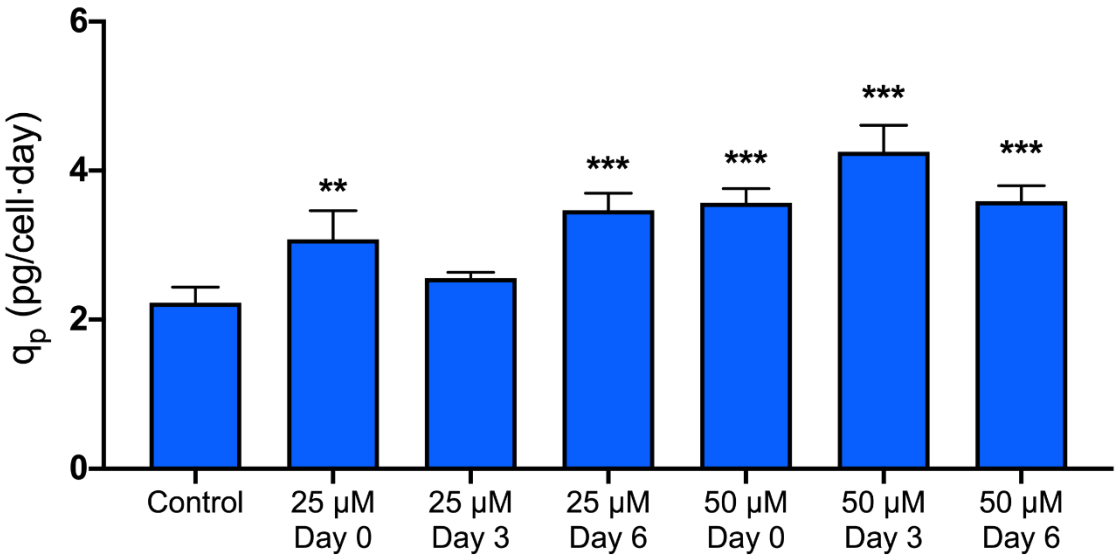

Figure 63 Effect of Cat on relative protein production in flask cultures
Relative protein production (q_p) of 33 ml batch recombinant CHO cell cultures in 125 ml Erlenmeyer flasks after a period of 10 days (section 2.1.3) and treated with catechin (Cat) at 25 and 50 µM on days 0, 3 or 6. q_p was calculated by dividing final protein production by the integral of the VCD curve. Each data point represents the average from a triplicate, and the error bars correspond to ±SD. These experiments were repeated independently. One way ANOVA statistical test was perform for the treatment compared to the control for p-values: (*)< 0.05, (**) < 0.01 and (***) < 0.001.

5.2.2.2 Epicatechin

5.2.2.2.1 Viable cell curve and growth rate

There was a steady increase in viable cell density during the first eight days under control conditions, reaching a maximum viable cell density of 10.87±0.14 10^6 viable cells/mL. After that, the viability decreased abruptly for the next 48 hours, finishing at 3.74±0.07 10^6 viable cells/mL by day ten.

The addition of 25µM of epicatechin at time zero caused considerable changes in the viable cell density curve; cell growth was repressed and the maximum value observed was 7.63±0.99 10^6 viable cells/mL. This only occurred after day four, indicating that the effect is linked to the deceleration section of the growth phase. This is similar to the behaviour observed in catechin treatments (Figure 64A).

The addition of 25 µM of epicatechin at day six did not cause any main changes in the curve at any point in the culture. The maximum viable cell density remained very close to the one under control conditions (10.65±0.36 10^6 viable cells/mL). When epicatechin was added to the cultures at day three, the viable cell density did not change; it had an increase until day eight and then decreased over the last two days with very similar slopes to control. The maximum viable cell density was 9.43±0.17 10^6 viable cells/mL.

The addition of epicatechin at a higher concentration (50 µM), caused a more severe difference, depending on the supplementation time. When epicatechin was added at time zero, the inhibition of the cell growth was persistent during the ten days of incubation; cells

were not able to divide under these conditions and the maximum viable cell density was 1.32±0.38 10^6 viable cells/mL at day five. On the other hand, the addition of the chemical on day six, caused no main changes to the viable cell curve. The addition of the chemical at day three, caused an intermediate effect. The cells grew close to the control until day seven, but then the cell culture remained static until day eight and decayed similarly to the control afterward (Figure 64B).

The growth phase of the culture lasted for the first eight days of incubation under control conditions, with an average growth rate of 0.74±0.14 $days^{-1}$. The addition of 25 µM of epicatechin at different time points did not cause any changes in the period of growth nor in the average growth rate. 50 µM treatments did not have any significant effects on the average growth rate either, regardless of the time of addition. Supplementation at days zero, three and six resulted in growth rates of 0.68±0.11, 0.79±0.10 and 0.72±0.14 $days^{-1}$ respectively. The addition of 50 µM at early stages, caused the growth phase to stop sooner. The addition of this concentration at time zero made the growth phase stop after the fourth day, while addition at day six caused it to stop on the sixth day (Table 10).

Table 10 Growth rate of feed-batch cultures treated with epicatechin

Treatment	µ ($days^{-1}$)			Growth phase (days)	
	Mean		SD	Start	Finish
Control	0.74	±	0.14	1	8
EC Day0 25 µM	0.81	±	0.43	1	7
EC Day3 25 µM	0.71	±	0.14	1	8
EC Day6 25 µM	0.72	±	0.18	1	8
EC Day0 50 µM	0.68	±	0.11	1	4
EC Day3 50 µM	0.79	±	0.10	1	7
EC Day6 50 µM	0.72	±	0.14	1	8

(EC) epicatechin, (SD) standard deviation

5.2.2.2.2 Viability

Viability for the control was preserved until day eight; at that point the cell culture had an initial 8% drop in viability, to subsequently drop further at a rapid rate. At the end of the incubation period, viability reached values as low as 29.6±1.5%. Almost none of the conditions caused changes in the viability of the culture across time. The only treatment that caused viability changes was epicatechin at a 50 µM concentration when added at time zero. Under these conditions, viability started to drop slowly during the last six days of the culture, to reach values close to the control by the end of the ten-day incubation period (44.4±3.5%) (Figure 64C&D).

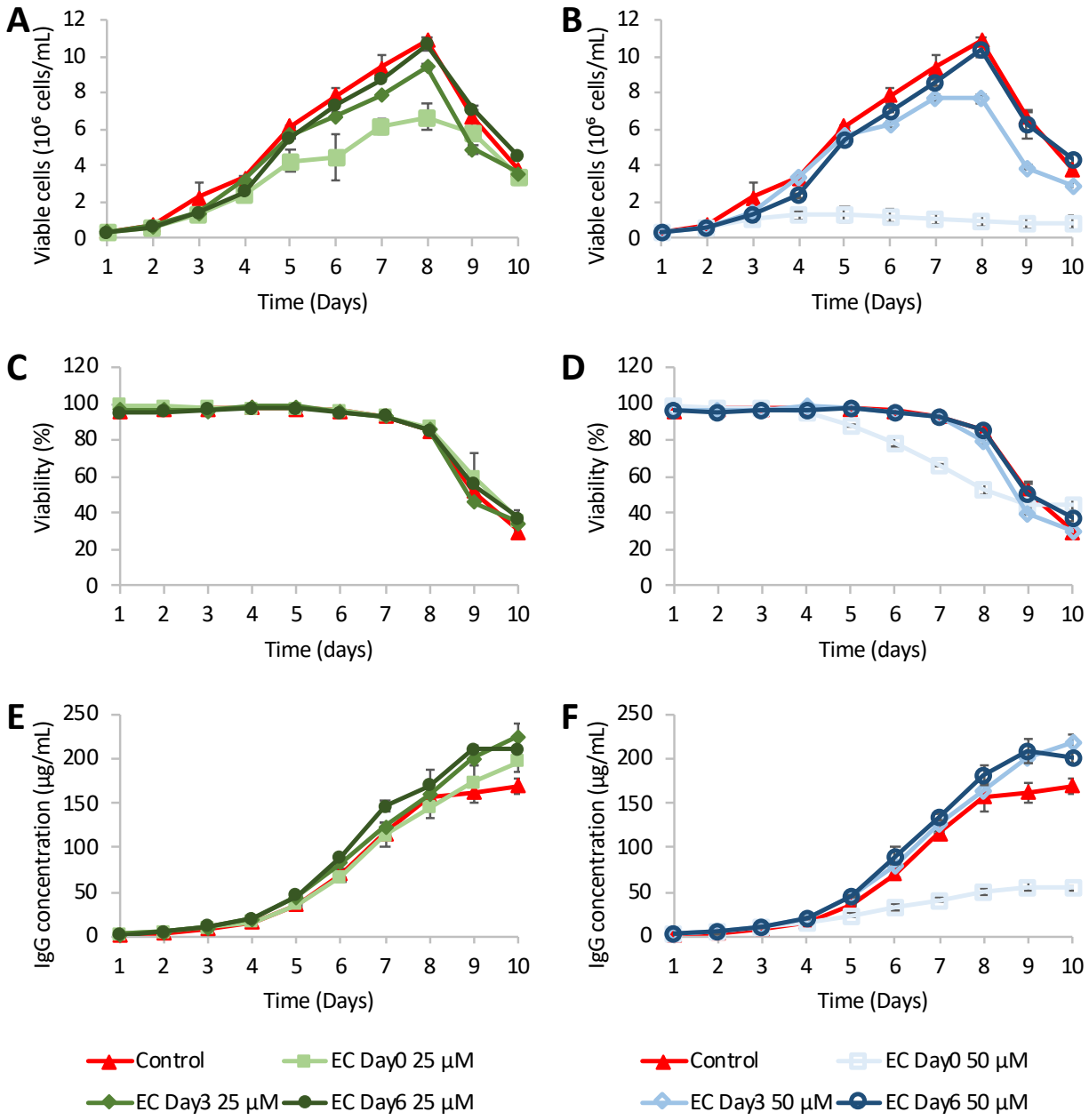

Figure 64 Effect of EC over growth and IgG production in flask cultures
Effect of epicatechin (EC) treatments in viable cell density (A,B), viability (C,D) and IgG concentration (E,F) when added at days 0 (squares), 3 (diamonds) and 6 (circles) for 25 µM (green) and 50 µM (blue) concentrations. Cells were incubated in 125mL Erlenmeyer flasks with an initial 33 mL volume for 10 days under shaking conditions (section 2.1.3). The error bars represent the standard deviation of triplicates and the experiment was carried twice independently.

5.2.2.2.3 IgG final titre and specific productivity

IgG production in feed-batch cultures under control conditions delivered a constant increase in the monoclonal antibody production for the first eight incubation days. During the last two days, the production slowed down, yielding a final titre of 167.7±10.8 µg/ mL.

Treatment with 25 µM of epicatechin at any given time point caused considerable increases in production compared to control. This was mainly seen after day eight. The highest yield was acquired when the treatment was administrated on day three. This resulted in 226.0±13.7 µg/mL final product (1.35-fold increase) (Figure 64E).

Treatments with 50 µM caused similar results. The addition of the chemical at either day three or six caused an improvement in the recombinant antibody final titre, up to 218.8±9.9 µg/mL (1.30-fold increase). On the other hand, addition at time zero caused consistent IgG production arrest, reducing the productivity of the culture to 32% of the control (53.9±2.2 µg/mL) (Figure 64F).

The specific productivity observed under these conditions, indicated that each cell was able to produce more protein under treatment conditions when compared to the control (2.65±0.22 pg/cell·day). In general, there seemed to be a trend in treatments; the earlier the chemical was added, the greater the increase in the specific productivity observed. The highest value was seen with the 25 µM concentration added at time zero (4.62±0.48 pg/cell·day), almost doubling the one of the control (1.74-fold increase). On the other hand, adding 50 µM at day six caused the smallest improvement in q_p (3.51±0.12 pg/cell·day), with a 1.32-fold increase. Finally, there were no main differences in q_p improvement due to

concentration. Samples treated at the same incubation time, caused the same level of improvement in q_p, regardless of the treatment concentration (Figure 65).

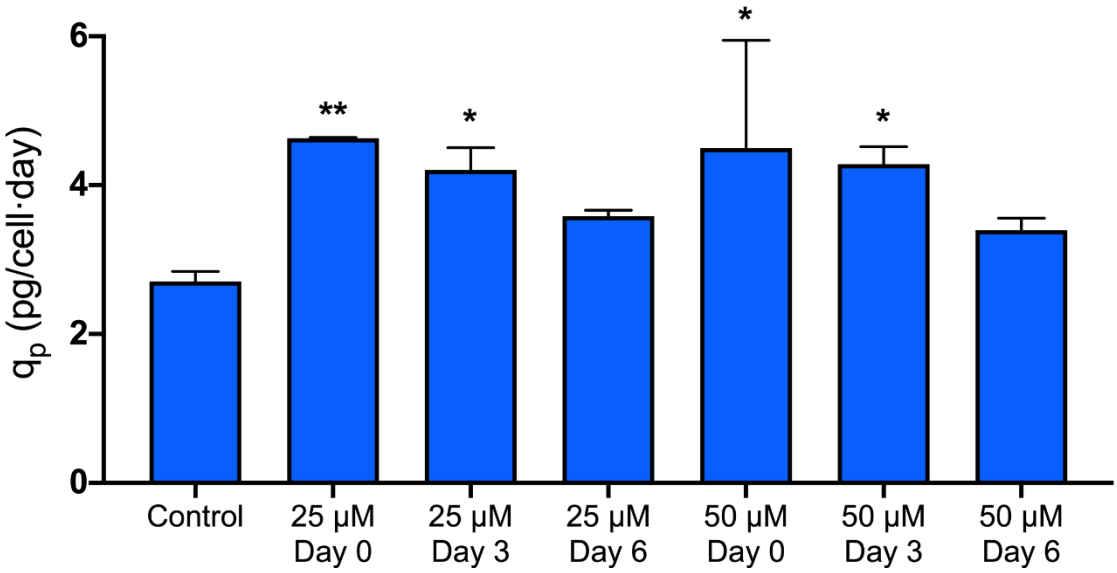

Figure 65 Effect of EC on relative protein production in flask cultures
Relative protein production (q_p) of 33 ml batch recombinant CHO cell cultures in 125 ml Erlenmeyer flasks after a period of 10 days (section 2.1.3) and treated with epicatechin (EC) at 25 and 50 µM on days 0, 3 or 6. q_p was calculated by dividing final protein production by the integral of the VCD curve. Each data point represents the average from a triplicate, and the error bars correspond to ±SD. These experiments were repeated independently. One way ANOVA statistical test was perform for the treatment compared to the control for p-values: (*)< 0.05, (**) < 0.01 and (***) < 0.001.

5.2.2.3 Gallocatechin-gallate

5.2.2.3.1 Viable cell curve and growth rate

There was a steady increase in viable cell density during the first eight days of the culture under control conditions, reaching a maximum viable cell density of 10.87±0.14 10^6 viable cells/mL. After that, the viability decreased abruptly for the next 48 hours, finishing at

3.74±0.07 10^6 viable cells/mL by day ten. All the treatments caused changes in the growth, profile and behaviour of the viable cell curve.

Treatment with the 25 µM concentration at day zero, caused complete repression of the cell growth for the first three days; the maximum concentration was 0.59±0.05 10^6 viable cells/mL. After that and for the rest of the incubation time, there was a slow decay. The same was observed when adding 50 µM at time zero, only that the peak of the viable cell density was at day two and at a lower concentration (0.41±0.04 10^6 viable cells/mL) (Figure 66A&B).

The addition of 25 µM on day three caused the viable cell growth to decrease considerably after day four with respect to control. The growth was constant and slow, and there was no decay of the culture until day ten. The maximum viable cell density was 5.50±0.40 10^6 viable cells/mL; this was reached by the ninth day. The addition of 50 µM at day three, caused the cell culture to grow for the next 24 hours, close to the control rate. From day four onwards, the cell culture reached a stationary phase and the viable density stop increasing, remaining constant for the remaining of the culture at 2.57±0.15 10^6 viable cells/mL (Figure 66A&B).

When cell cultures were treated with gallocatechin-gallate at the late stage of the growth phase (day six), the decay phase was not omitted as seen previously. Treatment with 25 µM caused the growth to slow down considerably, reaching a stationary phase that lasted until day nine with a concentration peak of 8.41±0.67 10^6 viable cells/mL. When adding 50 µM, cell growth was maintained for 24 hours. At day seven, the cell population started to decay. As the culture did not grow between days seven and eight, the maximum viable cell density

was lower and equal to that of the control at day seven (8.84±0.19 10^6 viable cells/mL) (Figure 66A&B).

The average rate of growth of the different samples did not show significant differences when compared to control (0.74±0.14 $days^{-1}$). Nevertheless, the addition of the chemical had an effect on the length of the growth phase. Early additions of gallocatechin-gallate at 25 µM and 50 µM concentrations at day zero, caused an arrest of the growing phase at day three and day two respectively. Later addition of the chemical, at days three and six, caused a stop of the cell growth at approximately day six (Table 11). This probably indicates, that the chemical is more efficient in stopping cell growth before the growth phase starts (time zero) or when it is about to end (day six). On the other hand, if the cell culture is dividing rapidly, then the chemical needs more time to stop the growing population.

Table 11 Growth rate of feed-batch cultures treated with gallocatechin-gallate

	µ ($days^{-1}$)			Growth phase (days)	
Treatment	Mean		SD	Start	Finish
Control	0.74	±	0.14	1	8
GCG Day0 25 µM	0.54	±	0.17	1	3
GCG Day3 25 µM	0.75	±	0.11	1	6
GCG Day6 25 µM	1.07	±	0.38	1	6
GCG Day0 50 µM	0.57	±	0.12	1	2
GCG Day3 50 µM	0.72	±	0.20	1	6
GCG Day6 50 µM	0.92	±	0.19	1	7

(GCG) gallocatechin gallate, (SD) standard deviation

5.2.2.3.2 Viability

The viability under control conditions was maintained at high levels for the first seven days of incubation with values above 90%. After that, it suddenly dropped to 29.6±1.5%. This aligned with the decay phase observed in the viable cell curve data, indicating that after day eight cells find inhospitable conditions in the culture and are not able to proliferate or maintain their population.

Gallocatechin-gallate added at the beginning of the culture caused the most severe impact on the viability profile. Cultures treated with 25 µM, start to present a drop in viability after day three and this trend continued until the loss of viability remained stationary at 43.2±0.6% by day nine. Adding the 50 µM concentration, caused the same behaviour as explained previously, with a decrease of viability right after day three. In this case, the decay stabilized sooner, approximately at day six, at a higher viability level (67.0±1.5%) (Figure 66C&D). This probably indicates that there are fewer severe events at a higher concentration in the long run. The reasons for this phenomenon however are unclear; this could be a result of less media consumed or the chemical dropping out of solution when at high concentrations. A similar phenomenon was seen in the screening process, at which the lowest concentration treatment would often yield more viable cell growth arrest than the ones of 25 µM or 50 µM. It is possible that under these conditions something similar could have occurred.

The viability of the cell culture was initially compromised under both time-zero treatments, but the viability values at day ten were never as low as the control (two to three folds higher). This may be a result of an incomplete consumption of the media and a lower concentration of toxic metabolites such as lactic acid.

The addition of 25 µM of gallocatechin-gallate at day three, did not inherently change the viability with respect to the control until day eight. After that, instead of a rapid decay in viability in the last 48 hours, there was a constant decay until 75.5±6.4% at day ten. The addition of 50 µM, also resulted in a constant slow decay of viability. The only difference, was that the drop started to occur at day five, reaching lower final viability (65.7±3.6%) than the one observed at 25 µM (Figure 66C&D). Nevertheless, the viability was always higher than the control, with an almost threefold increase. Again, the lack of a sudden drop in viability, could be a result of the slower consumption of the media and the accumulation of undesirable metabolites.

Treatments on day six cause the less dramatic changes in viability. Addition of 25 µM caused a delay in the viability drop after day seven and mildly slowed the drop. On the other hand, treatment at 50 µM did not cause any significant changes (Figure 66C&D). Overall, the behaviour of viability in the culture did not change under these conditions, and the abrupt decay of the culture during the last 40 hours was preserved.

The addition of gallocatechin-gallate, heavily affected the viability profile of the culture over the ten days of incubation. The time of addition of the chemical was the most important parameter; the earlier the supplementation, the more predominant the effect on viability. This is expected as gallocatechin-gallate is a cell growth inhibitor and its effect should be more predominant the sooner it is implemented in the growing phase.

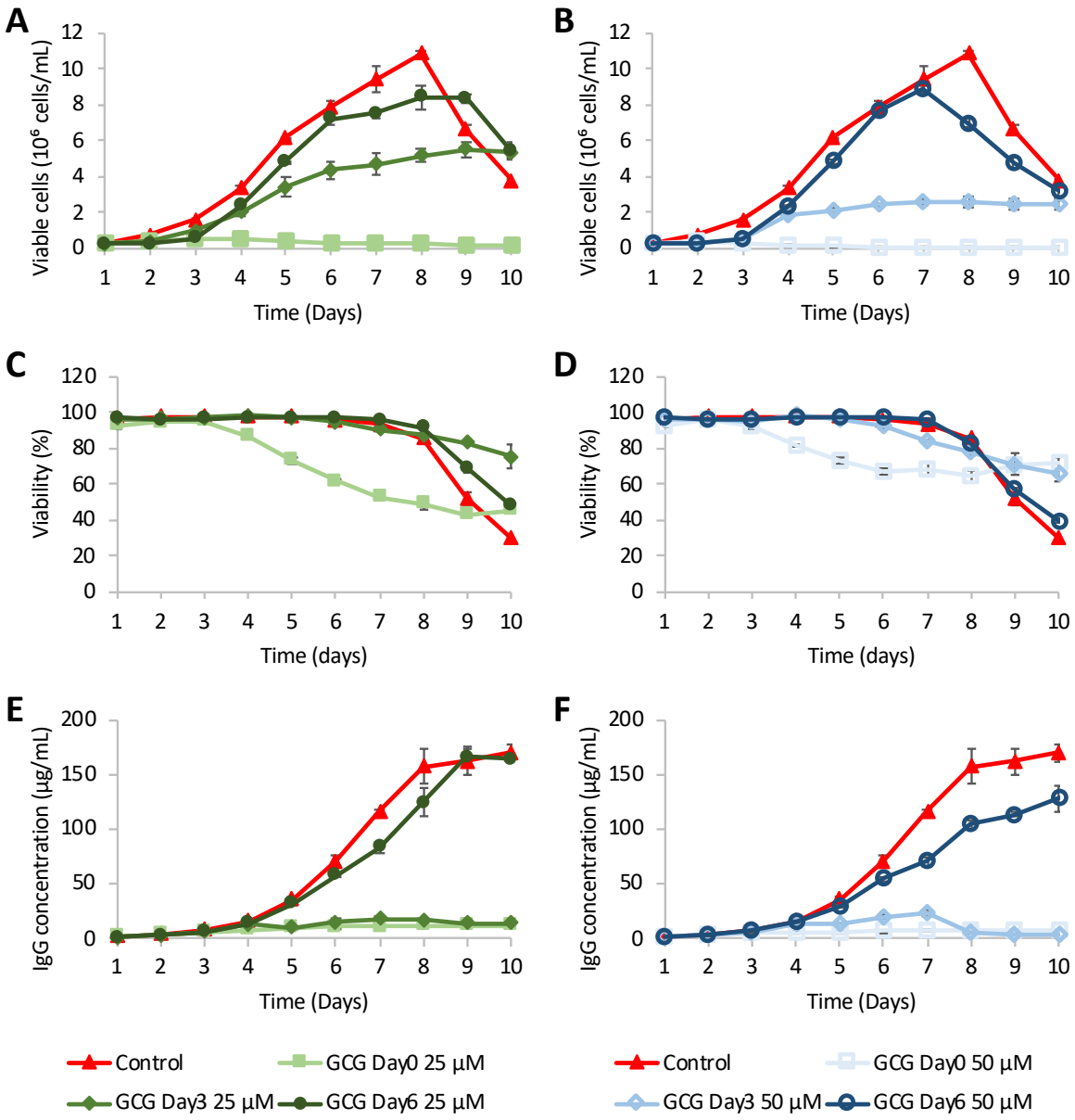

Figure 66 Effect of GCG over growth and IgG production in flask cultures
Effect of gallocatechin-gallate (GCG) treatments in viable cell density (A,B), viability (C,D) and IgG concentration (E,F) when added at days 0 (squares), 3 (diamonds) and 6 (circles) for 25 µM (green) and 50 µM (blue) concentrations. Cells were incubated in 125mL Erlenmeyer flasks with an initial 33 mL volume for 10 days under shaking conditions (section 2.1.3). The error bars represent the standard deviation of triplicates and the experiment was carried twice independently.

5.2.2.3.3 IgG final titre and specific productivity

Control conditions in feed-batch cultures delivered a constant increase in monoclonal antibody production for the first eight incubation days. During the last two days, the production slowed down yielding a final titre of 167.7±10.8 µg/ mL.

Adding gallocatechin-gallate at time zero and three, resulted in complete repression of the production of IgG. There is no actual growth with treatments at time zero and a lack of production was to be expected. On the other hand, treatment at day three, resulted in some cell growth; however, the antibody production was close to zero by the end of the ten days of incubation.

The addition of 25mM at the latest stage of the growth phase (day six) caused a delay in the IgG produced, but it did not cause a reduction of the final titre; the values were identical to the control. This is thanks to the slowing down of IgG production by the control in the last 48 hours. The addition of a higher concentration (50 µM) caused the cells to produce less over the next 4 days and a considerable decrease (23.8%) was observed by the end of incubation (128.1±11.8 µg/mL) (Figure 66E&F).

Specific protein production was also heavily influenced. Control had a final q_p of 2.68±0.13 pg/cell·day. Treatment at day three, regardless of the concentration, caused an almost complete arrest in specific productivity with values as low as 0.14±0.02 pg/cell·day. This was the result of the complete arrest of the antibody production, while retaining a discrete viable cell concentration through the incubation time. This indicated that cells under these conditions are not able to produce IgG, regardless of successfully surviving to some degree.

The addition of 25 µM of gallocatechin-gallate at time zero did not result in any differences with respect to control. On the other hand, the 50 µM treatment resulted in a considerable 1.34 fold increase in q_p (3.60±0.015 pg/cell·day). Either way, small changes in the final IgG production, could lead to big changes in specific productivity due to its low values. The addition of 25 µM at day six, caused a 1.20-fold increase of q_p (3.21±0.09 pg/cell·day). This was due to slower growth of the cell culture after day six whilst the final titre being constant. The addition of 50 µM, did not cause any main changes in specific productivity, as the viable cell concentration and final titre were reduced proportionally (Figure 67).

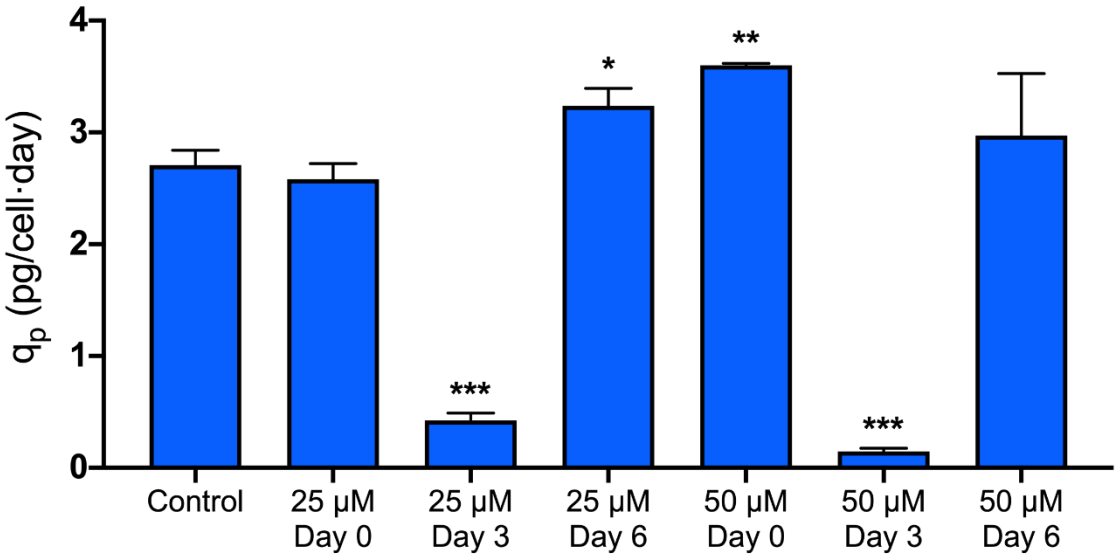

Figure 67 Effect of GCG on relative protein production in flask cultures
Relative protein production (q_p) of 33 ml batch recombinant CHO cell cultures in 125 ml Erlenmeyer flasks after a period of 10 days (section 2.1.3) and treated with gallocatechin gallate (GCG) at 25 and 50 µM on days 0, 3 or 6. q_p was calculated by dividing final protein production by the integral of the VCD curve. Each data point represents the average from a triplicate, and the error bars correspond to ±SD. These experiments were repeated independently. One way ANOVA statistical test was perform for the treatment compared to the control for p-values: (*)< 0.05, (**) < 0.01 and (***) < 0.001.

5.2.2.4 Epigallocatechin-gallate

5.2.2.4.1 Viable cell curve and growth rate

There was a steady increase in viable cell density during the first eight days of the culture, reaching a maximum of 10.87±0.14 10^6 viable cells/mL. After that, the viability decreased abruptly for the next 48 hours, finishing at 3.74±0.07 10^6 viable cells/mL by day ten. All the treatments caused changes in the growth, profile or behaviour of the viable cell curve.

The addition of epigallocatechin-gallate at time zero caused complete inhibition of the cell growth for the entire period of incubation, regardless of the concentration of the treatment. Treatment with 25 µM reached maximum viable cell concentration at day three, with 0.58±0.07 10^6 viable cells/mL, to then slowly decay to 0.24±0.02 10^6 viable cells/mL by day ten. Although the behaviour of the culture was the same, higher treatment concentrations caused even more severe inhibition. At 50 µM, the peak of viable cell density was reached sooner, at day two (0.41±0.02 10^6 viable cells/mL). Once again, there was a decay until day ten (0.10±0.02 10^6 viable cells/mL) (Figure 68A&B).

The addition of epigallocatechin-gallate on day three caused partial inhibition of viable cell growth. When added at 25 µM, cells were partially inhibited and growth was maintained at a lower rate until day nine, with a peak at day eight (7.02±0.57 10^6 viable cells/mL). After day nine, there was a normal decay that correlated with the one observed at control. When adding 50 µM, the inhibitory effect on cell growth was more relevant; cells grew at a much slower rate from supplementation until day six. After that, the culture reached a stationary phase and the viable cell concentration was maintained for the rest of the culture at

3.87±0.73 10^6 viable cells/mL (Figure 68A&B). This means that by the end of incubation the viable cell density was close to that of the control.

Adding 25 µM epigallocatechin-gallate at day six, did not cause any main changes in the viable cell concentration curve. There was only some small repression of cell growth, which led to a maximum viable cell density of 9.16±0.80 10^6 viable cells/mL by day eight. Finally, the decay phase was identical over the last 24 hours. Higher concentration treatments (50µM), caused a more immediate response to the adverse conditions. As a result, after 24 hours from supplementation, the culture reached a maximum concentration at day seven (9.36±0.05 10^6 viable cells/mL). Immediately after, the viable cell density started to decay and continued to do so for the remaining three days (Figure 68A&B).

The average rate of growth of the different samples did not show significant differences when compared to the control (0.74±0.14 $days^{-1}$). Nevertheless, the chemical addition had an effect on the length of the growth phase. Early addition of epigallocatechin-gallate at day zero, caused a stop of the growing phase at day two, for both concentration treatments (25 and 50 µM). Later addition of the chemical at days three and six, caused a stop of the cell growth approximately at day six-seven (Table 12). This seems to indicate that the chemical is more efficient in stopping cell growth before the growth phase starts (time zero) or when it is about to end (day six). On the other hand, if the cell culture is dividing rapidly, the chemical needs more time to stop the growing population. This behaviour is identical to the one observed in GCG.

Table 12 Growth rate of feed-batch cultures treated with epigallocatechin-gallate

Treatment	μ (days^{-1})		Growth phase (days)	
	Mean	SD	Start	Finish
Control	0.74	± 0.14	1	8
EGCG Day0 25 μM	0.81	± 0.11	1	2
EGCG Day3 25 μM	0.71	± 0.10	1	7
EGCG Day6 25 μM	0.80	± 0.23	1	7
EGCG Day0 50 μM	0.61	± 0.08	1	2
EGCG Day3 50 μM	0.72	± 0.20	1	6
EGCG Day6 50 μM	0.83	± 0.27	1	7

(EGCG) epigallocatechin gallate, (SD) standard deviation

5.2.2.4.2 Viability

Under control conditions, viability was maintained at high levels for the first seven days of incubation, with values above 90%. After that, it suddenly dropped to 29.6±1.5%. This aligned with the decay phase observed in the viable cell curve data, indicating that after day eight cells find inhospitable conditions in the culture and are not able to proliferate or maintain their population.

When epigallocatechin-gallate was added at day zero, the viability profile of the culture over the ten days of incubation changed drastically. The addition of 25 μM caused the cell viability to start dropping at a constant rate since day three, to reach the final viability of 37.2±4.2%. When adding 50 μM of epigallocatechin-gallate, viability dropped even earlier on day two. After that, the viability lost was contained during the last part of incubation reaching an evident stationary viability level after day six (62.6±7.2%). Similar to gallocatechin-gallate, this seemed to indicate that higher concentrations on the long run had less drastic effects. The reasons for this phenomenon however were unclear. This could be a result of less media consumed or the chemical dropping out of solution when at high concentration. A similar

phenomenon was seen in the screening process; the lowest concentration treatment would yield a more viable cell growth arrest than 25 µM or 50 µM. It is possible that the culture has the same behaviour, regardless of the different conditions in the screening and the flask study (Figure 68C&D).

The addition of EGCG on day three caused a different effect, depending on the concentration. Lower concentrations of 25 µM did not cause any changes in viability during the first eight days. The decay phase, on the other hand, was slightly delayed. 50 µM of the treatment caused more severe effects; viability started to decay after day six, slowly avoiding the abrupt decay seen at control and reaching the lowest viability at day ten (69.0±3.9%) (Figure 68C&D).

Treatments at day six did not cause any main changes in the viability profile at any point during the incubation process. This indicates that at this point in the culture, the addition of the chemical compound (EGCG) does not have a significant toxic effect. The differences observed in the viable cell density curves were therefore a result of cell growth inhibition, which makes epigallocatechin-gallate mainly cytostatic under these conditions (Figure 68C&D).

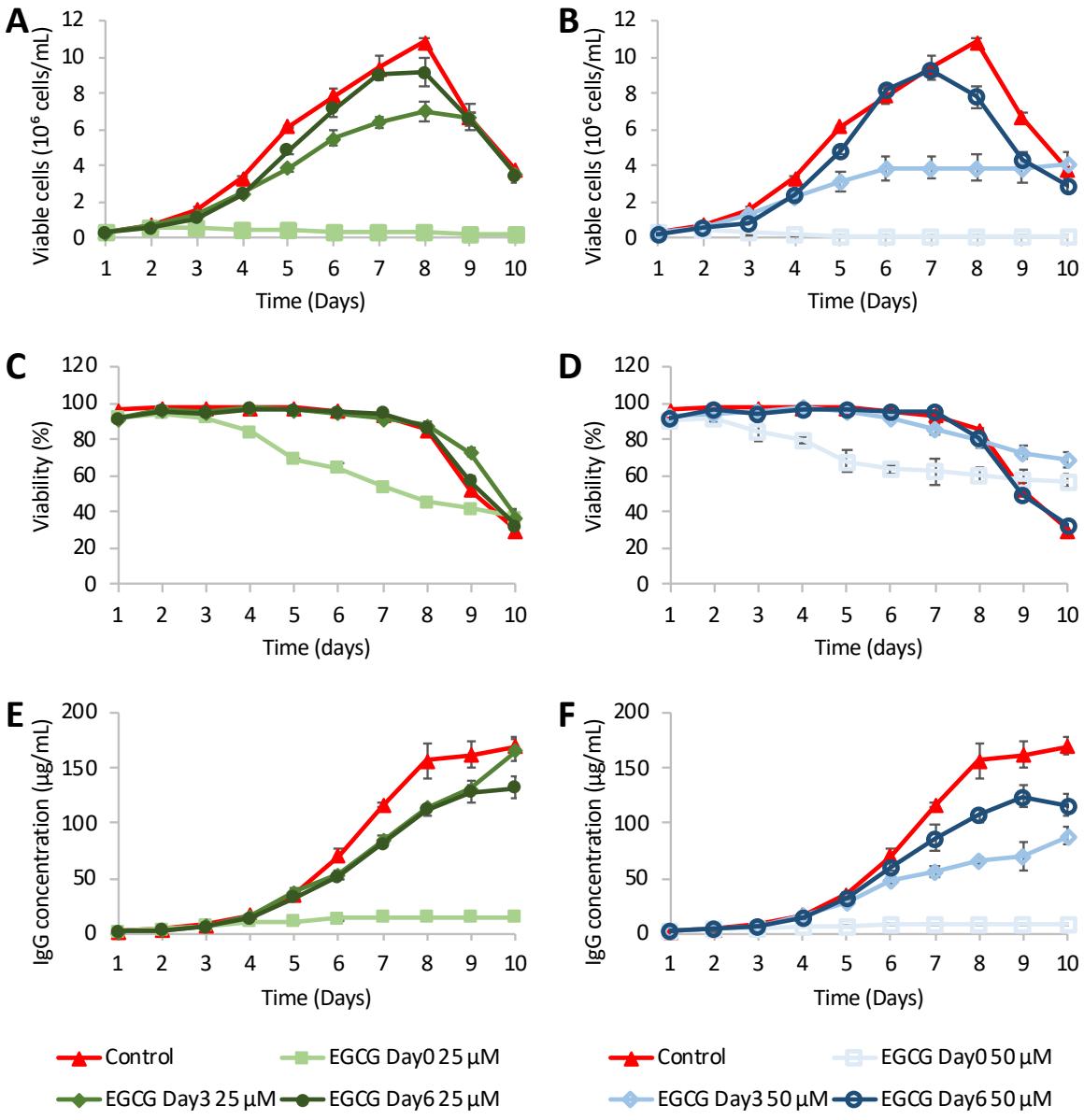

Figure 68 Effect of EGCG over growth and IgG production in flask cultures
Effect of epigallocatechin-gallate (EGCG) treatments in viable cell density (A,B), viability (C,D) and IgG concentration (E,F) when added at days 0 (squares), 3 (diamonds) and 6 (circles) for 25 µM (green) and 50 µM (blue) concentrations (section 2.1.3). Cells were incubated in 125mL Erlenmeyer flasks with an initial 33 mL volume for 10 days under shaking conditions. The error bars represent the standard deviation of triplicates and the experiment was carried twice independently.

5.2.2.4.3 IgG final titre and specific productivity

Under control conditions, feed-batch culture delivered a constant increase in monoclonal antibody production for the first eight incubation days. During the last two days, the production slowed down, yielding a final titre of 167.7±10.8 µg/ mL. Protein titre was compromised at some point under all conditions, and most of them caused a decrease in the final titre.

A complete arrest of production regardless of the concentration treatment was observed when adding the chemical at time zero. At 25 µM, the antibody concentration increased to 14.60±0.33 µg/mL and stayed constant. The 50 µM concentration caused even more IgG repression, allowing it to increase only up to day five (7.25±0.65 µg/mL) to then remain constant. Intermediate supplementation of 25 µM of epigallocatechin-gallate (day three) caused a delay in antibody production. Nevertheless, the production continued during the ten days of incubation, reaching final IgG concentration equal to control (166.1±10.5 µg/mL). When the concentration was increased to 50 µM, the inhibition of IgG production was irreversible, and the culture produced at a considerably lower rate during the last five days. The final titre was 88.4±7.9 µg/mL, corresponding to a 48% decrease. Once more, when EGCG was added on day six, there was a decrease in the final titre observed. The parameter of the concentration did not make significant changes in the production profile of the antibody. As a result, after supplementation, the production of antibody was heavily reduced, showing a slower increase in production with a final titre of 132.7±9.8 µg/mL and 116.6±10.0 for 25 and 50 µM respectively (Figure 68E&F).

The capacity of the cells to produce IgG was affected by the treatment of EGCG. Addition of the compound at day six, led to lower average specific productivity for 25 µM (2.42±0.18 pg/cell·day) and 50 µM (2.27±0.20 pg/cell·day) when compared to the control (2.68±0.13 pg/cell·day). Treatment with 25 µM at day three, caused a considerable increase in specific productivity (3.76±0.26 pg/cell·day). This was a result of the culture's capacity to maintain productivity until the end of the incubation time. Adding 50 µM at time zero also resulted in a significant increase in q_p (3.22±0.20 pg/cell·day), but in this case the reason for that was the lack of cells along the incubation time. The q_p for the rest of the treatments remained at levels close to control (Figure 69).

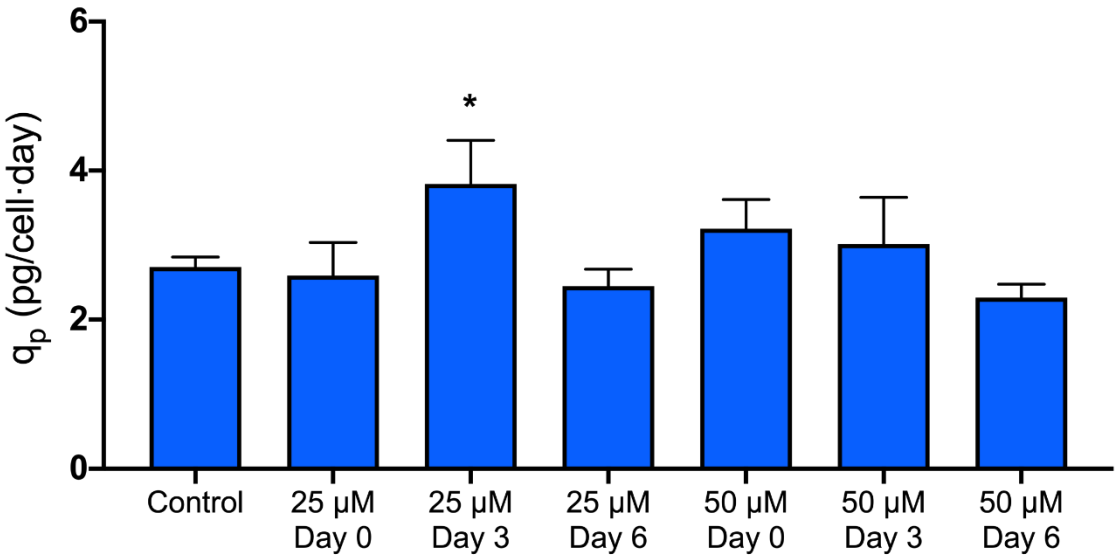

Figure 69 Effect of EGCG on relative protein production in flask cultures
Relative protein production (q_p) of 33 ml batch recombinant CHO cell cultures in 125 ml Erlenmeyer flasks after a period of 10 days (section 2.1.3) and treated with epigallocatechin gallate (EGCG) at 25 and 50 µM on days 0, 3 or 6. q_p was calculated by dividing final protein production by the integral of the VCD curve. Each data point represents the average from a triplicate, and the error bars correspond to ±SD. These experiments were repeated independently. One way ANOVA statistical test was perform for the treatment compared to the control for p-values: (*)< 0.05, (**) < 0.01 and (***) < 0.001.

5.2.2.5 Discussion

There were two main reasons for cell death and viability decay under these conditions. The first one was the addition of the chemicals; catechin seems to be only a cytostatic compound; the others caused severe toxicity depending on the concentration and the time of addition. This caused a slow drop in viability along the incubation time. On the other hand, cultures that are not heavily inhibited, grow to their maximum potential and deplete the media while increasing toxic metabolites (Kumar, Gammell and Clynes, 2007). This situation causes a stipe drop in viability during the last two-three days of the culture.

Toxicity was not immediate and it required at least two days to have an effect on the viability of the culture. The more drastic the effect of the treatment over the culture, the sooner the viability drop starts to appear. There is no sign of toxicity until day five when adding epicatechin at time zero. EGCG at 50 µM, added at time zero, affected viability after two days of incubation.

In general, addition at time zero caused more severe effects; these related to cell inhibition, increase in toxicity and in many occasions decrease of the antibody production. The later the chemical was added, the less effective it was at lowering the viability of the culture. This is because the toxicity effect is a slow process that needs time. If the chemical is added later, the cells have less time in contact with it and thus suffer less from its toxic effects. Furthermore, the toxicity of these chemicals could be linked to dividing cells and more importantly to topoisomerase inhibition, as discussed in Chapter 2. The present results indicate that this could be the case, as the cultures treated at the end of the growth phase

(day six) did not show any additional loss of viability compared to a normal decay phase. This was true for all chemicals at all concentrations.

The present studies indicate that the effect of the chemicals on the cell culture departs from each other in a very similar trend to the results from viable cell cycle. Catechin seems to be very different to the rest, followed close by epicatechin which is an intermediate into catechins with galloyl group and being GCG and EGCG the closes match.

Results showed that the effect of epigallocatechin-gallate and gallocatechin-gallate are very close to each other with similar viable cell growth inhibition and viability profiles. Interestingly enough, independently of this similarity, gallocatechin-gallate was able to arrest specific productivity more efficiently than epigallocatechin-gallate. The reason for this difference is not clear.

All the chemicals were used under the same conditions in order to better compare the different effects of the molecules. The results indicate that catechins without the galloyl group have a positive effect on the optimization of IgG production. The negative effects of GCG and EGCG however, do not imply that these chemicals do not have the possibility to be used as additives. Lower concentrations of epigallocatechin-gallate or gallocatechin-gallate could cause similar results to the ones observed with catechin and epicatechin. The presence of the galloyl group seems to increase the toxicity of the chemical and lower concentration treatments may palliate the severity of the effect and increase the chance of positive results. Parallel studies in recombinant protein production in CHO cells, showed that EGCG can be implemented in growth cell media composition from 44 μM to 1.1 mM concentrations. The

chemical had the potential to enhance protein production by 20% (Hossler *et al.*, 2015). The discrepancy with the current study could be due to a different cell line, recombinant protein or culture conditions. The study by Hossler et al. showed that the half-life of EGCG in the media was of about six hours (Hossler *et al.*, 2015). This, in relation to the results presented here, seems to indicate that the chemical is able to penetrate the cells and accumulate inside. The less cell density there is, the more the accumulation of EGCG there would be in each cell increasing the toxicity of the chemical the sooner it is added.

Furthermore, the compounds without the galloyl group were able to increase the IgG production when added along the growth phase (day three and six). Adding these chemicals at time zero rarely caused any improvement in production. This validates the hypothesis that if chemicals were to be used at a later stage of the culture, it would be more likely that they would help the productivity by modulating growth and increasing specific protein production; this would lead to a higher antibody titre. Nevertheless, the addition of catechins to the media can result in changes in the quality of the recombinant antibody produced. Previous studies on the effect of EGCG in recombinant antibody characteristics by media supplementation, indicated that there is a reduction of the acidic and basic species of the protein of interest, reducing the product's relative charge heterogeneity consistently across the time of the culture (Hossler *et al.*, 2015).

In order to further consider catechins as possible tools for the production of recombinant proteins in CHO cells, the quality of the product needs to be assessed in order to ensure that it is not compromised. Catechin was selected to further study the quality of the product as it

is the compound that had the fewest adverse effects and resulted in a considerable increase in the final IgG production.

5.3 Conclusions

The sooner the chemicals were added, the more intense the negative traits observed (lower viable cell density, lower viability and lower IgG produced). Resveratrol, catechin and epicatechin caused an improvement in the final antibody titre. On the other hand, GCG and EGCG were too toxic under these conditions and they did not cause any improvements in the final IgG production. Since catechin and epicatechin are quite similar, catechin and resveratrol were selected to be studied further, in order to test their effect on the quality of the recombinant antibody.

Chapter 6

Recombinant IgG product characterization and quality assessment

6.1 Initial remarks

It has already been described in previous chapters, that catechin and resveratrol were able to enhance the specific productivity of the recombinant IgG product in a CHO cell line (Chapter 3). When scaled up and optimized feeding, these chemicals also succeeded in increasing the final titre (Chapter 5) through the use of biphasic strategies. However, in order for these chemicals to be considered as appropriate additives, their effect on the quantity should not affect negatively the quality. The aim of this chapter was to study whether the addition of these chemicals to the media would change the characteristics of the product. The structural integrity of the heterologous protein was assessed by size exclusion chromatography, while charge heterogeneity was assessed by cation exchange chromatography (CEX). Mass spectrometry was used to study the specific modifications.

Flask cultures were performed under similar conditions specified in chapter 5 following section 2.1.3 of the matherials and methods, with the exception of being treated at day 3 with catechin at 10, 25 and 50 µM concentrations and resveratrol at 10, 25, 50, 100, 250 µM and 500 µM concentrations (Appendix 2). Final IgG production was assessed on day ten (section 2.1.5). Cultures were purified (section 2.3.1) and purity was assessed by SDS-PAGE (section 2.3.2) (Appendix 3). The purified IgG was studied by size exclusion chromatography (section 2.4.1) and cation exchange chromatography (section 2.4.2). The IgG was digested (section 2.5.1), the fragments were run through LC-MS/MS (section 2.5.2) and later analyzed (section 2.5.3). The experiment was run in four independent replicates.

6.2 Results

6.2.1 Size exclusion chromatography

6.2.1.1 Peak identification

The samples were run in a high-performance liquid chromatography (HPLC) system, using the size exclusion chromatography technique, in order to quantify the relative abundance of the different components of the IgG in the purified product.

Firstly, the peaks for the different possible fragments of the recombinant product were identified. Spectra from bovine serum albumin (BSA) were used to correlate the time of retention with the molecular weight. The spectra were characterized by four main peaks evenly separated, ranging from lower to maximum levels of absorbance (Figure 70A). This spectrum indicated that the sample was composed of a single protein that interacts with itself. This resulted in the monomer peak which was the highest and latest, but it also resulted in peaks corresponding to the dimer, trimer and tetramer. This theory explains the consistent increase of the peaks observed with increased elution time. The monomer was the most relevant form of the protein in the solution, followed by the dimer and so on. This has been previously described in previous studies done in bovine serum albumin (Ombelli *et al.*, 2011). The logarithmic molecular weight of each peak was linearly associated with their specific elution time (Figure 70B). The equation (Equation 5) of the linear fit was used to estimate the molecular weight of the different fragments of the IgG spectrum. The data was underestimating the size of the molecules (Table 13). The main peak of the IgG chromatogram

(Figure 70C), appeared at 13.68 min of elution time. The elution time calculated with Equation 1 was 95.5 KDa, instead of the 144 KDa expected.

$$log_{10}(molecular\ weight) = -0.2115(elution\ time) + 4.8729$$

Equation 5

The differences in the molecular weight, could be a result of the differences in structure between the proteins. Bovine serum albumin is a compact globular protein, while IgG or its chains are less globular and have a different relative size. We hypothesized that the capacity of the column to separate different fragments of the IgG is maintained and therefore, the slope should be very similar independently of the molecule. However, the elution times could vary due to the different structure of the antibody.

The main peak of the size exclusion chromatogram (144 KDa after 13.68 minutes), was used to determine the intersection of the new equation (Equation 6).

$$log_{10}(molecular\ weight) = -0.2115(elution\ time) + 5.0517$$

Equation 6

The molecular weight values were then calculated with the adapted IgG linear equation. Values seemed to be aligning consistently with the expected ones (Figure 70B). The most deviated values were the ones coming from molecules that had a single heave chain in their

structure. Structures associated with a single heavy chain or a heavy chain associated with a light chain, gave lower calculated values than expected (7.9 and 5.6 KDa respectively) (Table 13). It seems that single heavy chains have a different conformation that causes them to collapse on themselves, thus reducing their hydrodynamic radius with respect to a completely assembled heavy chain. This causes the underestimation of the molecular weight when a monomer is used as a point of reference.

Table 13 Calculation of molecular weight of IgG peaks from size exclusion chromatograms

Peak struture	Elution time (minutes)	Expected (KDa)	Calc BSA (KDa)	Calc IgG (KDa)	Diff (KDa)
2 mAb	12.23	288	191.5	290.8	-2.8
1 mAb	13.68	144	94.8	144.0	0.0
2 HC	14.45	98.2	65.3	99.1	-0.9
1HC 1LC	15.26	72.3	43.9	66.7	5.6
1HC	16.24	49.2	27.2	41.3	7.9
1LC	17.33	23.1	16.0	24.3	-1.2

Monoclonal antobody (mAb), heavy chain (HC), light chain (LC), bovine serum albumin (BSA)
(‡)Calcuations of the peak molecular weight based on the BSA linear equation (Calc BSA),
(†)Calcuations of the peak molecular weight based on the IgG linear equation (Calc IgG),
(*) difference between the expected and calculated values from IgG linear equation (Diff)

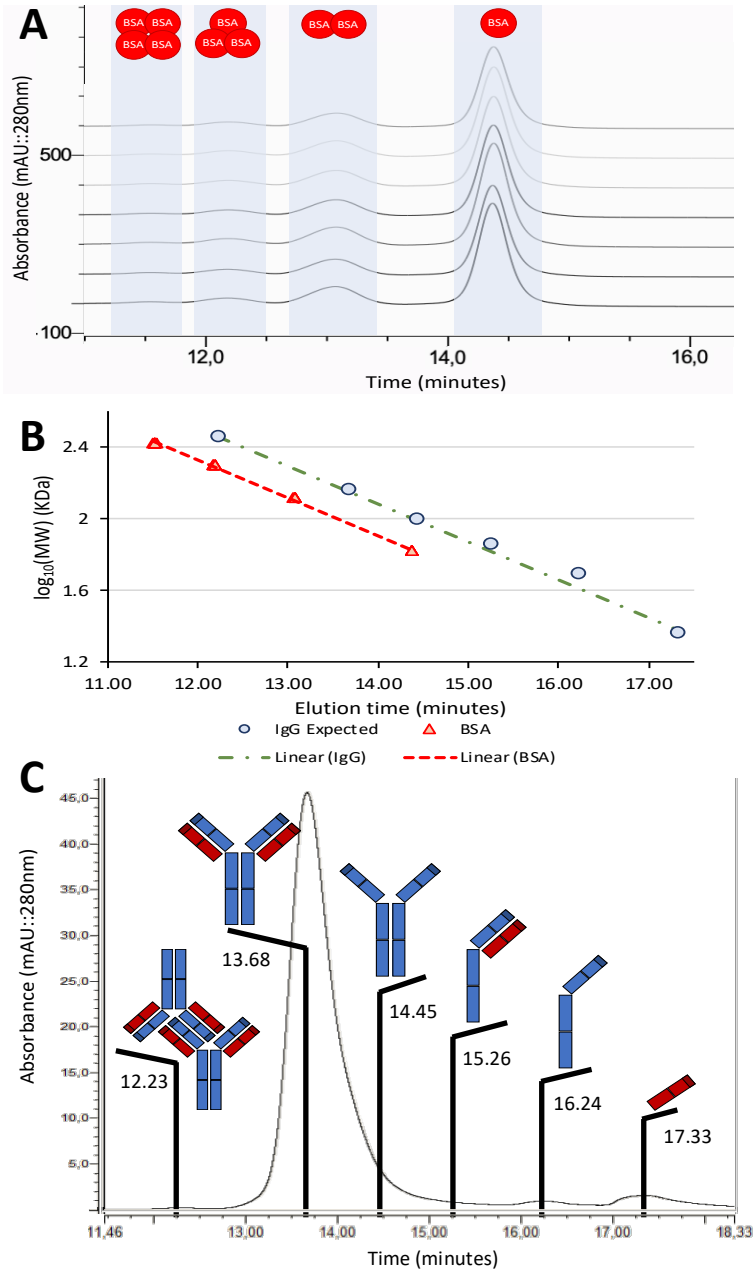

Figure 70 Peak identification of purified IgG proteins in a size exclusion chromatogram (A) Identification of the peaks of a known component; bovine serum albumin (BSA) in its monomer, dimer, trimer and tetramer form in a size exclusion chromatogram spectrum. (B) Correlation between the elution time and the logarithm of the molecular weight (MW) for BSA (red). Extrapolation of the linear relationship to an IgG molecule (green line). The expected values of the IgG chromatogram for each peak (blue circles). (C) Identification of the molecular structures of the IgG in a size exclusion chromatogram based on their elution time.

6.2.1.2 Peak quantification

Some peaks identified by SEC were often lost in the noise of the spectrum or other more intense signals, due to the overlap between them and due to the lower concentrations of these species (Figure 70C). The only signals that were consistent across the spectra were the ones corresponding to the monomeric form (retention time 13.68 minutes), the one corresponding to the heavy chain (16.24 minutes) and the one of the light chain (17.33 minutes). This indicates that rituximab, produced under these conditions was not prone to aggregation, with or without the chemical addition. These findings are very similar to those previously recorded (Beck *et al.*, 2013).

The fragmentation of the molecule was not massive, with values of the monomer always being at 96% or above. The addition of resveratrol in the media feed increased the relative concentration of the purified monomer, in a concentration-dependent manner (from 96.2 ± 0.04 % at level control to 97.6 ± 0.9 % at 100 µM treatment) (Figure 71A). As the monomer increased in a relative quantity, there was a trend of a decrease in the relative quantity of the light chain (Figure 71E). However, the heavy chain did not follow this trend and remained static with quantities below 1% at all times. Resveratrol at 100 µM caused the peak to disappear. This could be a result of the signal not being intense enough, as the concentration of the antibody is considerably lower than in the previous cases.

Catechin did not cause any main changes in the relative quantity, however, there was a consistent trend of decrease (1% reduction) (Figure 71B). Overall, none of the light or the heavy chains showed any significant changes in quantity (Figure 71D&F).

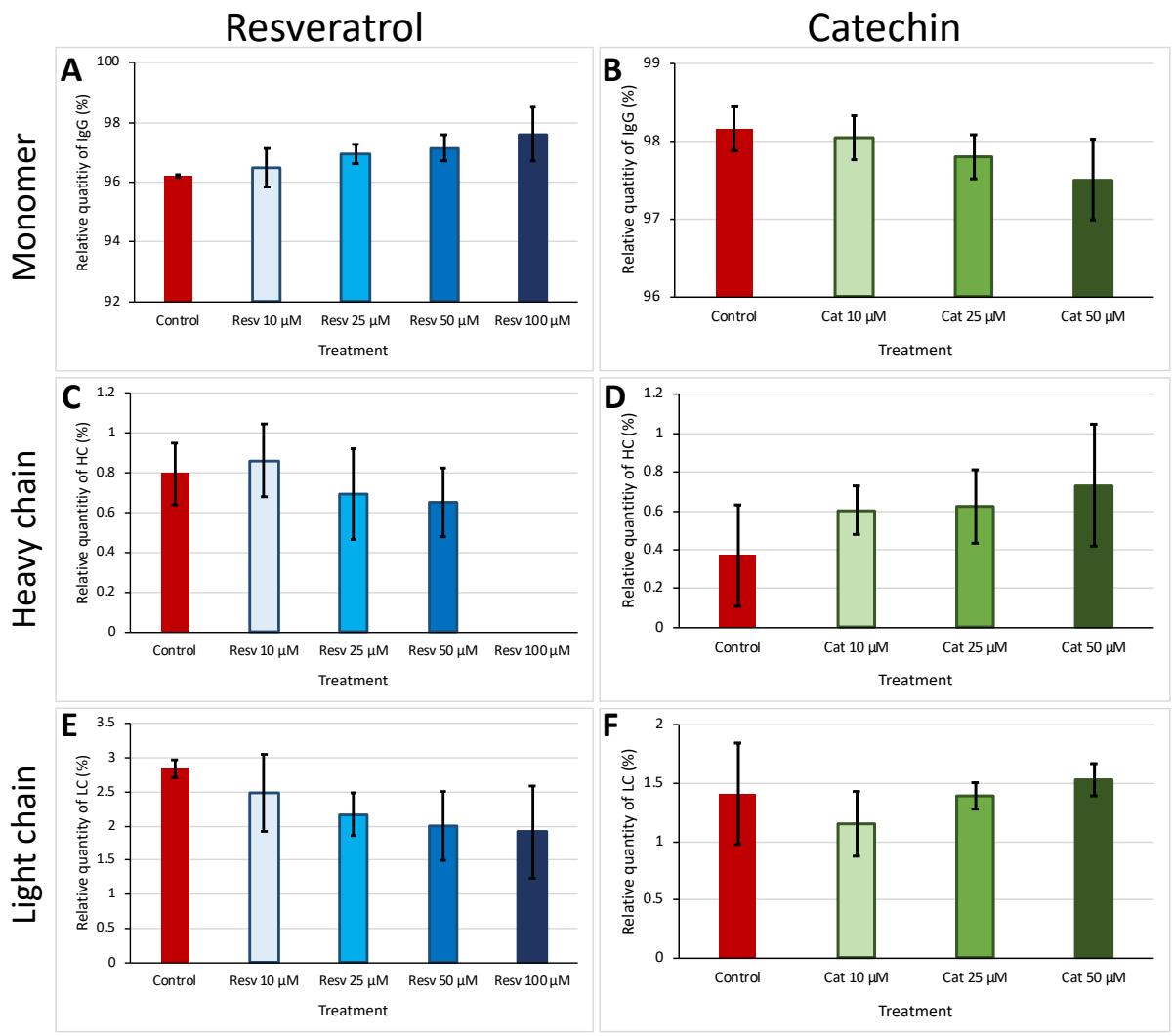

Figure 71 Relative quantification of the SEC peaks for purified IgG
The monomeric (A, B), heavy chain (LC) (C, D) and light chain (LC) (E&F) peaks were assessed (section 2.4.1) under resveratrol and catechin culture addition. Recombinant CHO cells were grown for 10 days in flask cultures and treated on day 3 (section 2.1.3). The IgG was then collected and purified (section 2.3). The error bars displayed here correlate to ± SD. The experiment was run 4 times independently.

There were no changes in the product quality, based on the size exclusion chromatography analysis and there were no main changes in the profile. Furthermore, the absence of aggregates and fragments confirmed that there were no changes in the behaviour of the production process or the protein. As a result, based on the current findings, the addition of these chemicals under these conditions is not contraindicated.

6.2.2 Cation exchange chromatography

The distribution of the charge species for the purified antibody was studied by ion-exchange chromatography. Spectra results were in line with previous studies (Andrasi, Gyemant and Gaspar, 2014). The current study showed that resveratrol treatments up to 50 µM did not cause any main changes in the charge heterogeneity of the product. High concentrations of resveratrol (100 µM) on the other hand, caused changes in the relative amount of charge species of IgG, as the acidic species dropped by 6.75 ± 3.91 % and the acidic species increased by 15.91 ± 5.71%. At the same time, the main peak also had an average decrease of 9.16 ± 9.46 % (Figure 73 A). These big deviations were the result of the low-intensity signals of the spectra; small deviations have bigger changes in the overall relative abundance of the charge groups. Further correction of the spectra was performed in order to diminish the variability due to variations at baseline. Although the variability across the replicates could not be completely eliminated, it seemed clear that resveratrol treatment at high concentrations changes the charge heterogeneity of the IgG and result in a more basic product (Figure 72).

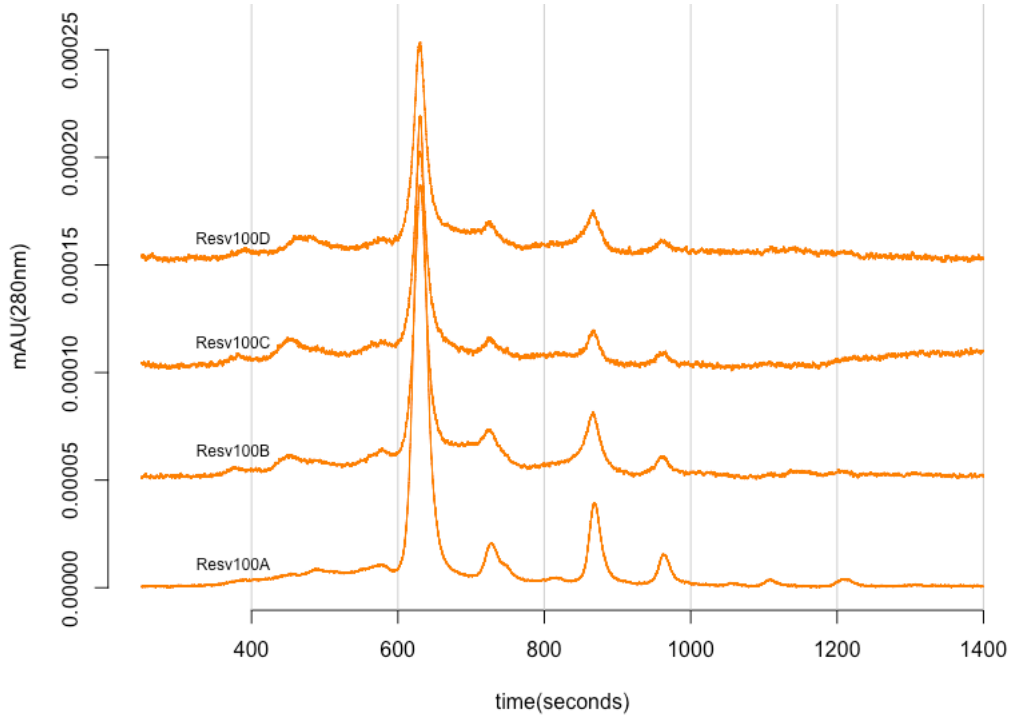

Figure 72 Normalized spectra of purified IgG for samples treated at 100 µM Resv
The graph shows the normalized four replicates results of the cation exchange chromatography of recombinant monoclonal purified IgG for treatment at 100 µM of resveratrol. Recombinant CHO cells were grown for 10 days in flask cultures and treated on day 3 (section 2.1.3).

Catechin treatment caused changes in the charge heterogeneity of the recombinant product, in a concentration-dependent manner. The addition of catechin caused an increase in the main peak while reducing the acidic species. Treatments with 25 µM resulted in a 1.80 ± 1.10 %, decrease in acidic species, while causing a 2.04 ± 0.77 % increase of the main peak. Treatments with 50 µM, caused more severe changes, with a 3.58 ± 0.28% decrease observed in acidic species and a 3.64 ± 0.23% increase of the main peak (Figure 73B). Net changes in the basic species of the IgG seemed to result in proportional increases in the main peak. As a result, the basic species of the protein remained constant under these treatment conditions.

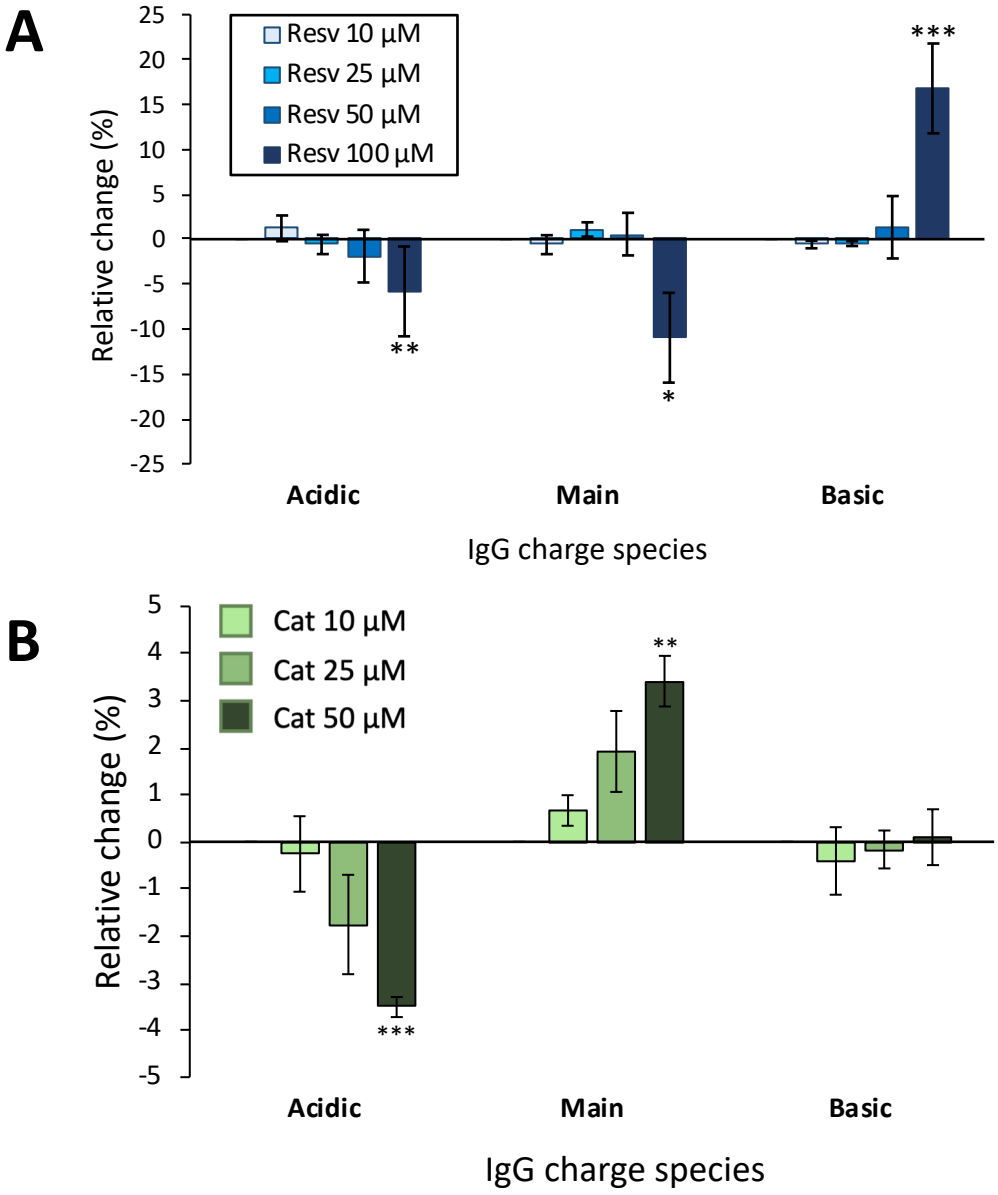

Figure 73 Relative quantification (%) of charge species for purified IgG
Data from cation exchange chromatography (section 2.4.2). The acidic (left), main (center) and basic (right) species were assessed under resveratrol (A) and catechin (B) culture additions at different concentrations. Recombinant CHO cells were grown for 10 days in flask cultures (section 2.1.3) and treated at day 3 The IgG was then collected and purified (section 2.3). The error bars displayed here correlate to ± SD. The experiment was run 4 times independently. One-way ANOVA statistical test was perform for the treatment compared to the control for p-values: (*)< 0.05, (**) < 0.01 and (***) < 0.001.

6.2.2.1 Discussion

Catechins were able to cause a relative reduction of the acidic species in the purified IgG product and an increase in the amount of protein with main charge. This was a significant change (although it was only 4%), as approximately 20% of the IgG fell in this category. As a result, the fold change was 16.5 ± 1.2 % when compared to control. The same can be stated for the main species, although most of the molecules belong to this category; a more moderate change was observed, as a 3.64 ± 0.23% change relates to a 6.59 ± 0.4 % fold increase. In the same manner, treatment with 100 µM of resveratrol had a drastic change in charge species, causing a 24.4 ± 13.1 % decrease of the acidic species and, more importantly, a 73.3 ± 25.5 % increase of the basic species that almost doubled the relative amount found in the control.

Epigallocatechin-gallate was studied as an additive for recombinant protein expression by Hossler and colleagues in 2015. It was found to have very similar effects to the ones observed using catechin in our study. When the chemical was added to the CHO culture media, it caused changes in the charge heterogeneity of the purified product (decrease of the acidic species of up to 4%, a decrease of the basic species of 2% and a consequent increase of the main peak charge of 6%) (Hossler *et al.*, 2015). Although the changes described in the paper are very similar to ours, the range of concentrations that resulted in significant changes, varied between 100-450 µM. Treatments with 10 or 50 µM on the other hand, did not have any impact. The studies conducted, also showed that the mechanism by which epigallocatechin gallate reduces the acidic species was transferable; similar effects were observed on other proteins, cell line expression level or scale-up conditions. The decrease in the acidic species,

was not linked to any phase of the culture; as the culture fermented, the acidic species become more abundant. The addition of epigallocatechin gallate caused a decrease of the acidic species during the first stages of the culture, but after 48 hours, the relative increase of the acidic species was the same as observed using control. This explains why the reduction of acidic species in the current experiment, is still effective regardless of addition on day three.

Cation exchange chromatograms can be indicative of the distribution of the general charge of the population of recombinant proteins. However, this view is a bit simplistic. Cation exchange chromatography is more related to localized surface charges. As a result, studies have found different shifts in chromatograms, although the same modifications were located in a different residue (Perkins *et al.*, 2000). Furthermore, modifications that do not cause any change in the overall charge or do not involve charge residues, could cause shifts in the chromatogram, because they can change the structural conformation of the IgG and expose charge areas (Saphire *et al.*, 2002).

While the above is true, most of the changes in the heterogeneity of the IgG cation exchange chromatogram, are associated with a well-known group of modifications. Basic species can be explained by modifications such as N-terminal glutamine cyclization, C-terminal lysine clipping and oxidation. Acidic species shifts are more difficult to interpret and can be explained by deamidation and glycan profiles with sialic acid or high mannose content although more modifications can cause it. Acidification of the product, although very common, is more difficult to interpret because it is the result of aging and degradatory pathways (Gandhi *et al.*, 2012; Leblanc *et al.*, 2017) on top of the post-translational modification.

Both chemicals showed the capacity to reduce acidic species when compared to the control indicating that they could add important characteristics to the product such as increase if shelf-life against depredatory pathways of degradation.

In order to identify the specific modifications, the mass spectrometry technique was used.

6.2.3 Mass spectrometry

6.2.3.1 Sequence coverage

The raw data was used to study the sequence coverage of the molecule, previous to analyzing the data obtained from mass spectrometry. The light chain was covered almost in its entirety, with only amino acids 207 to 213 missing. This was consistent for all the samples as lysine in position 206 and arginine in position 210 were actively cleaved by trypsin. This fragmentation is possibly efficient due to the exposure of the end of the peptide chain (Figure 74A).

This leaves two fragments of 523 and 307 Da within the range of molecular mass studied (up to 6.6 KDa) but the length is 4 and 3 respectively which is below the limit of minimum peptide length studied (seven amino acids).

The heavy chain missed a considerable fragment of its sequence (from 152 to 221 amino acid). This fragment possesses no arginine or lysine. This resulted in a peptide of 69 amino acids, with a molecular weight of 7555 Da when treated with trypsin. The molecular weight exceeded the range stated for the experimentation and was not analyzed. To study this region

an alternative protease could be used, which would cleave the sequence at a different amino acid.

Furthermore, regions 323-330 and 338-344 of the amino acid sequence were often missing. This is because the region is rich in lysine residues, resulting in small peptides bellow seven residues. Although reducing the peptide length of study would result in bigger sequence coverage, this would also imply the need for higher computational power. More importantly, it would create a staggering number of short peptide spectra, for which the assignment of the sequence might be dubious. In conclusion, although an expansion of the sequence coverage would be desirable, the reliability of the spectra sequence matching is the most important feature and should not be compromised.

Another section missing from the mass spectrometry spectra sequence identification was 293-305. There was no apparent reason for this 13-amino acid peptide (molecular weight 1.67 KDa) to be missing from the mass spectrometry analysis. This region is characteristic in rituximab, as it contains a glycosylation site in the asparagine in position 301. The presence of glycosylation in the area complicates the identification of the spectrum, and sequence could not be found for these spectra. Control treatment only resulted in one sample out of four to which there was coverage of the sequence. This was due to a peptide (amino acids 293-324, molecular weight 3.88 KDa), which avoided the cleavage at arginine 305. The elongated peptide sequence resulting from the miscleavage, allowed for a better interpretation of the spectrum, despite the glycosylation pattern (Figure 74B).

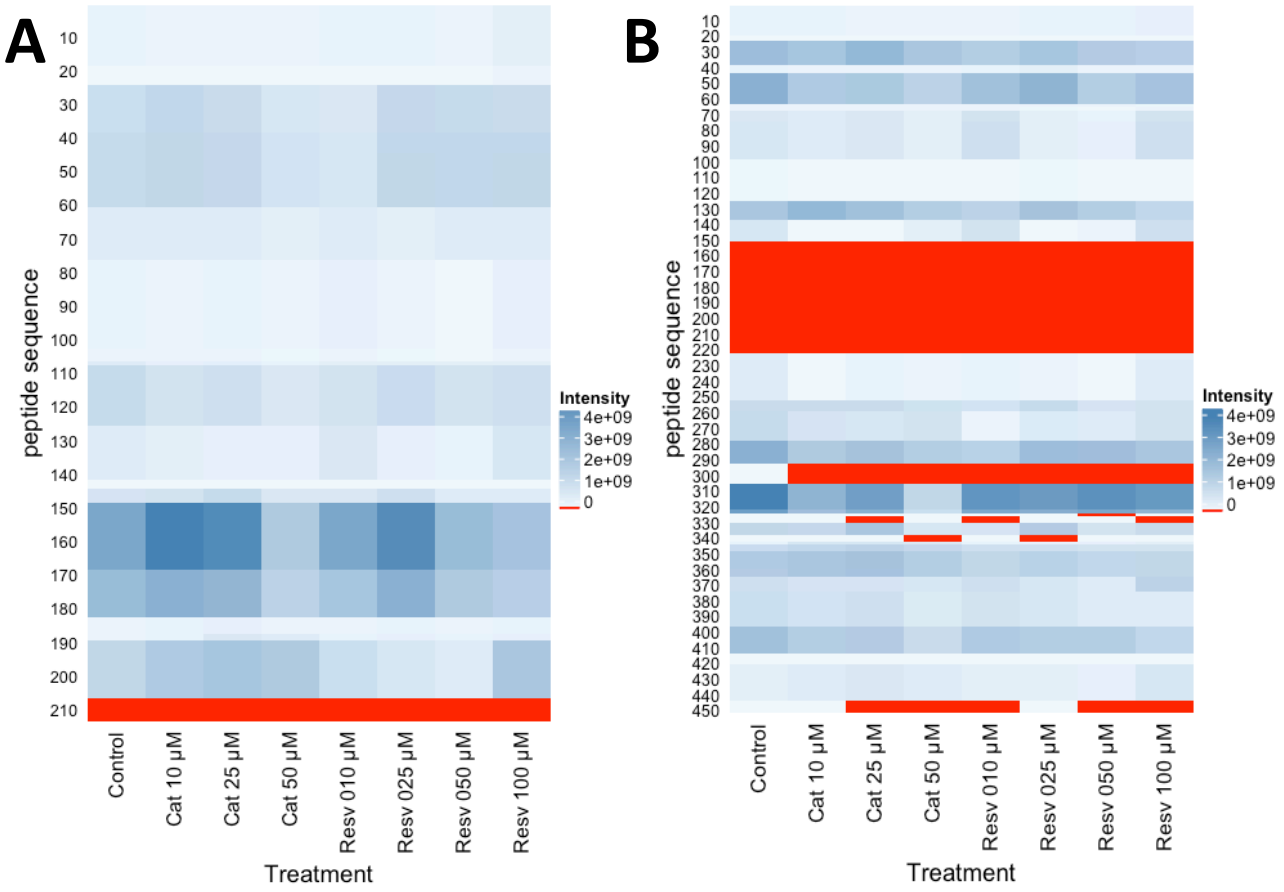

Figure 74 Heatmap of sequence coverage from the mass spectrometry study of Rituximab
The heatmaps show the accumulative intensity across the amino acid sequence for the light chain (A) and the heavy chain (B). Red colour indicates a complete absence of the region when mass spectrometry was performed, blue colour shows the presence of the region; darker blue indicates more signal intensity. Rituximab was produced in recombinant CHO cells grown cultures incubated for 10 days in flasks (section 2.1.3) and treated at day 3 with resveratrol and catechin at different concentrations. The IgG was purified by protein A affinity chromatography (section 2.3) and digested with trypsin (section 2.5.1) for mass spectrometry analysis (section 2.5.3). The intensities shown here are the additives of 4 independent replicates.

Finally, the C-terminal fragment (444-451) was also often missing. The last eight amino acid sequence (SLSLSPGK) has an ionizable amino acid and a molecular weight of 788 Da. The peptide was only observed consistently across the four independent replicates of the control conditions, although this happened in relatively low intensities (10^6). It was also present in two out of four samples during the treatments with resveratrol at 25 µM and catechin at 10

µM. While all these samples represented the unmodified peptides, a specific search for C-terminal truncated peptides (SLSLSPG_) was performed, but with no result. It is possible that the absence of the sequence coverage in most of the treated samples had to do with this fragment not being identifiable, although the reason for this is unknown. Cation exchange chromatography, with and without carboxypeptidase treatment, was also used to investigate further and verify whether there was any main change in the peak profile. There were not main changes observed in the profile. This result was similar to previous experiments studying the C-terminal lysine heterogeneity (Laurence 2008). This seems to indicate, that this cell line is very consistent in cleaving C-terminal lysine residues efficiently, but that does not give an answer for the absence of this fragment in the sequence coverage analysis. It is likely that a modification of the region could be responsible for the absence.

These results showed that the addition of resveratrol and catechin to the media causes modifications of the C-terminal region. Modifications that include changes in the C-terminal region of the heavy chain do not affect the antibody's function in general; this is due to the fact that its antigen recognition site and the recruitment site for the immune response are far away from the C-terminal. It has been shown that modifications such as lysine clipping to those regions, do not cause structural changes (Tang *et al.*, 2013). However, a recent study showed that terminal lysine residues, lower the complement-dependent cytotoxicity (CDC) response, by inhibiting the formation of hexametric rings (van den Bremer *et al.*, 2015).

The addition of resveratrol and catechin to the product caused changes to the C-terminal region of the heavy chain and maybe of the light chain, but the nature of these modifications is unknown and it is unlikely that it would have a meaningful impact on the potency of the product.

Finally, 97% of the sequence of the light chain was studied by mass spectrometry. However, only 77% of the heavy chain was studied in the worst-case scenario. This was consistent amongst the different treatment conditions. This indicates that the sequence coverage was robust across samples (although not complete) and further investigations could take place.

Table 14 General information on amino acids

Name	3-Letter Symbol	1-Letter Symbol	MW (Da)	Isoelectric Point	Type
Alanine	ALA	A	89.09	6	Non-polar
Isoleucine	ILE	I	131.17	5.94	Non-polar
Leucine	LEU	L	131.17	5.98	Non-polar
Valine	VAL	V	117.15	5.96	Non-polar
Phenylalanine	PHE	F	165.19	5.48	Non-polar aromatic
Tryptophan	TRP	W	204.23	5.89	Non-polar aromatic
Tyrosine	TYR	Y	181.19	5.66	Non-polar aromatic
Asparagine	ASN	N	132.12	5.41	Polar uncharge
Glutamine	GLN	Q	146.15	5.65	Polar uncharge
Methionine	MET	M	149.21	5.74	Polar uncharge
Serine	SER	S	105.09	5.68	Polar uncharge
Threonine	THR	T	119.12	5.64	Polar uncharge
Arginine	ARG	R	174.2	11.15	Positive charge
Histidine	HIS	H	155.16	7.47	Positive charge
Lysine	LYS	K	146.19	9.59	Positive charge
Aspartic Acid	ASP	D	133.1	2.77	Negative charge
Glutamic Acid	GLU	E	147.13	3.22	Negative charge
Glycine	GLY	G	75.07	5.97	Special
Proline	PRO	P	115.13	6.3	Special
Cysteine	CYS	C	121.16	5.02	Special

Molecular weight (MW)

6.2.3.2 Dependent peptide search and unspecific search for IgG modifications by overall mass shift differences

A dependent peptide search, with a follow-up search for significant differences in the presence of mass shifts, was performed in order to try and identify the causes of the changes in charge variants in the IgG. The study showed that most mass shifts were exceptional when compared to the control, and only three modifications were consistent across most treatments (Table 15).

Table 15 Mass shift differences for recombinant IgG samples treated with resveratrol and catechin compared to control

Resveratrol				Catechin		
10 µM	25 µM	50 µM	100 µM	10 µM	25 µM	50 µM
-57.02	-57.02	-57.02	---	---	-57.02	-57.02
---	---	---	---	-9.04*	---	---
---	21.98	21.98	21.98	---	21.98	---
---	27.99	27.99	27.99	---	27.99	---
---	---	52.92*	---	---	---	---
---	57.99*	---	---	---	---	---
---	---	190.08*	---	---	---	---

**Non-consistent mass shift differences across samples. These values only appear in one treatment and only for one chain*

All consistent modifications seem to be the result of artifacts during the preparation of the samples. A 27.99 mass shift could be the result of formylation, which is a modification that can occur under a high concentration of formic acid present in the suspension. As the protocol stopped the trypsin reaction with 100% formic acid added to the sample, it is likely that this could have caused formylation. It seems treatment with resveratrol and catechin causes an increase in this phenomenon, as it was more present under these conditions than in the control.

The 21.98 Da mass shift could not be easily linked to any specific modification. It could be related either to the incorporation of magnesium or to sodium adduction. Both mass shifts described seem to be linked to each other, as they were always missing or appearing together (Table 15).

Finally, the -57.02 Da mass shift is a modification that could be associated with several changes. Firstly, it could be the result of asparagine to glycine or glutamine to alanine

substitution. What was apparent from the experiment, is that under treatment conditions the IgG seems to be suffering more of these substitutions than under control conditions.

On the other hand, the difference could be an artifact from sample processing. Alkylation of samples with iodoacetamide, causes peptides with cysteine residues to be carboxy-methylated and thus increasing the mass of the peptide by 57.02 Da. If a sample is not modified at cysteine, then a molecular shift of -57.02 can be observed. If this was the case, then samples under treatment conditions, would be less likely to suffer carboxyamidomethylation. In order to further check which process took place, substitutions associated with this mass shift were studied by a specific modification search. However, the shift from polar neutral amino acids to polar amino acids did not explain the shifts in acidic and basic species.

Overall, the present results do not seem to explain the changes observed during the cation exchange experimentation.

6.2.3.3 Modification search by LFQ

Specific modification search showed that most modifications were not affected when treated with either resveratrol or catechin. Only a few modifications showed differences with respect to the control.

6.2.3.3.1 Oxidation

Oxidation was studied in methionine, histidine and proline residues. Proline oxidation was not detected in this experiment, unlike histidine and methionine. Oxidation of methionine was found in 10% of the peptides (Figure 75). Histidine was a less prone modification and appeared at a much lower rate (0.025-0.075%).

Methionine was the most predominant modification, with four consistent residues at sites 34, 81, 256 and 432 of the heavy chain. Most of the modifications were commonly shared for all treatments. One exception was position 432; this was only found in catechin treated samples and at samples treated with 10 µM and 100 µM of resveratrol (Table 16). Another exception was histamine modification at site 433; most conditions did not cause a modification, however high concentrations of catechin and resveratrol caused oxidation of the amino acid. We think that resveratrol at high concentrations is likely to interact directly with this region and induces oxidation of both sites. This can also be true for catechin treatments, but it is less clear.

The residues in positions 256 and 432, have been identified as the most susceptible ones when exposed to stress incubating conditions such as high temperature and addition of chemicals (Shen *et al.*, 1996). This is thought to be a result of exposure, as these residues are not imbedded inside the chain domains; Met^{256} is located between the C_{H2}-C_{H3} and Met^{432} is situated in the final part of the heavy chain. Residues 34 and 81 of the heavy chain were also consistently oxidized. This was probably a result of their exposure, as they are part of the variable region. This effect on Met^{34} has been previously described (Wei *et al.*, 2007). On the other hand, the effect on Met^{81} has not been previously reported. The increase of molecules

with oxidized residues, resulted in an increase of the basic species in the ion exchange chromatogram.

Table 16 Oxidation modification sites for rituximab

		Catechin			Resveratrol			
Position	Control	Cat 10 µM	Cat 25 µM	Cat 50 µM	Rsv 10 µM	Rsv 25 µM	Rsv 50 µM	Rsv 100 µM
HC-34-OxiM	Yes	Yes	Yes	Yes	Yes	Yes	Yes	Yes
HC-81-OxiM	Yes	Yes	Yes	Yes	Yes	Yes	Yes	Yes
HC-256-OxiM	Yes	Yes	Yes	Yes	Yes	Yes	Yes	Yes
HC-432-OxiM	---	Yes	---	---	---	---	---	Yes
HC-433-OxiH	---	---	---	Yes	---	---	---	Yes

Presence (Yes) or absence (---) of oxidation modification in methionine(M) and histidine (H) residues of the light (LC) and heavy (HC) chain of rituximab

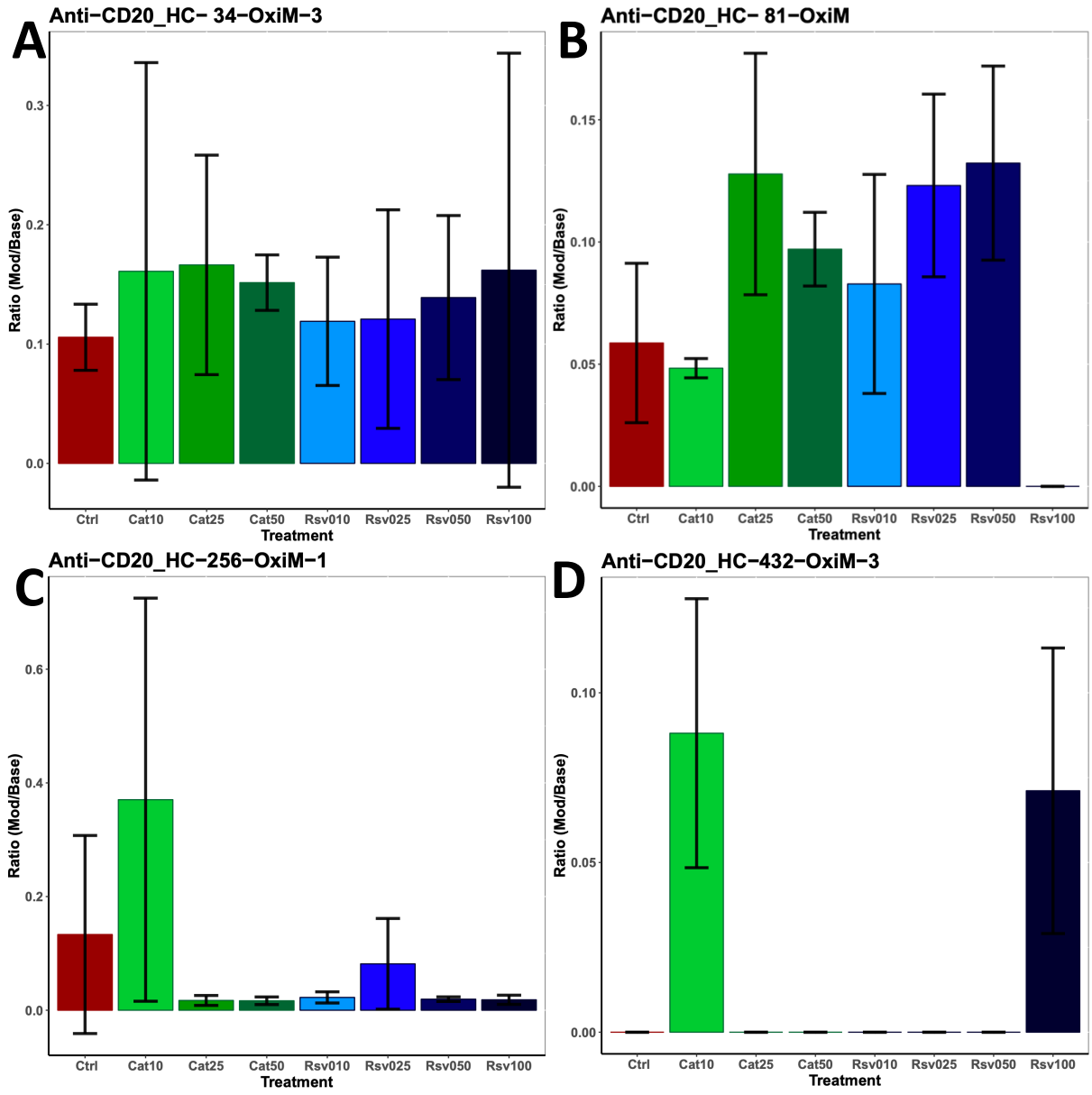

Figure 75 Oxidation ratio in the recombinant IgG
Modified peptide (oxidation) to non-modified peptide ratio in methionine residues 34(A), 81(B) 256(C) and 432 (D) of the heavy chain (HC) of rituximab. Data are shown for treatments under control conditions (red) and treatments with catechin (green) and resveratrol (blue). Samples were purified (section 2.3), and trypsin-digested (section 2.5.1) previous to LC-MS/MS (section 2.5.2). Modifications were looked for with the targeted approach and the label-free quantification method with MaxQuant software (section 2.5.3)

6.2.3.3.2 Tri-oxidation

Rituximab was found to have four sites that suffered tri-oxidation consistently; One in the light chain at Cys193, and the other three located at the heavy chain at Cys positions 148, 265 and 371. This pattern of tri-oxidation is not very clear. Control had three modifications out of four presented consistently (Table 17). Catechin treatment at 10 µM also resulted in three out of four modifications, however, these were different than the ones observed at control. Treatments with higher concentrations of the chemical (50 or 100 µM) led to only one tri-oxidation site. Resveratrol treatments were also very inconsistent, with 50 µM being the treatment with more modification sites (four), while the others had lower counts.

Table 17 Tri-oxidation modification sites for rituximab

		Catechin			Resveratrol			
Position	Control	Cat 10 µM	Cat 25 µM	Cat 50 µM	Rsv 10 µM	Rsv 25 µM	Rsv 50 µM	Rsv 100 µM
LC-193-TrOx	Yes	Yes	---	---	Yes	Yes	Yes	---
HC-148-TrOx	Yes	---	---	---	---	---	Yes	---
HC-265-TrOx	Yes	Yes	---	Yes	---	---	Yes	---
HC-371-TrOx	---	Yes	Yes	---	Yes	---	Yes	Yes

Presence (Yes) or absence (---) of tri-oxidation modification in rituximab light chain (LC) and heavy chain (HC)

When looking into the abundance of the modification, tri-oxidation was found only in small proportions, with 2% rates observed in the best-case scenario. This was to be expected, as tri-oxidation is a rare event. There was a tri-oxidation at site 371 of the heavy chain with most catechin treatments, but not with control (Figure 76D); the rate of oxidation of the amino acid was close to 0.3%. It is quite possible that the absence of tri-oxidation when treating with control, was due to chance, since the event itself is rare. Resveratrol treatment had similar

results for site 371 (Figure 76 D). On the other hand, an opposite effect was observed in the other sites, with control having the modifications and resveratrol and catechin showing no significant increase in them (Figure 76 A, B & C). This modification is rare as most cysteines are forming disulphide bonds and later are modified by carboxy-methylation the preparation of the samples.

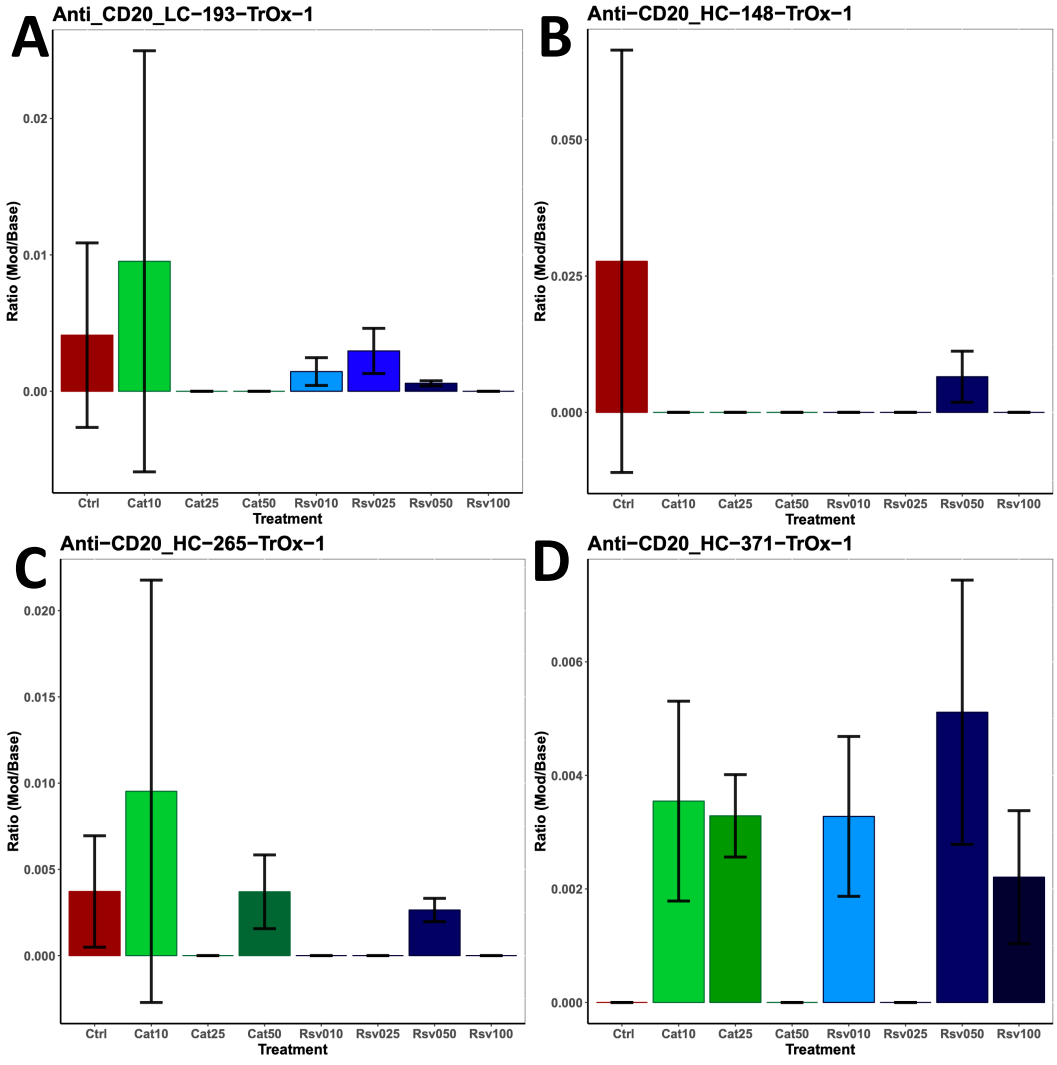

Figure 76 Tri-oxidation ratio of the recombinant IgG
Modified peptide (tri-oxidation) to non-modified peptide ratio in residue Cys193(A) of the light chain(LC) of rituximab and residues Cys148(B) Cys265 (B) and Cys371(C) of the heavy chain (HC). Data are shown for treatments under control conditions (red) and treatments with catechin (green) and resveratrol (blue). Samples were purified (section 2.3), and trypsin-digested (section 2.5.1) previous to LC-MS/MS (section 2.5.2). Modifications were looked for with the targeted approach and the label-free quantification method with MaxQuant software (section 2.5.3)

6.2.3.3.3 Carboxy-methylation

Carboxy-methylation, was the most relevant modification, as expected, with a total of thirteen modified sites on a consistent basis (Table 18). The light chain was found to possess four main cysteine residues susceptible to alkylation (23, 87, 133 and 193). The four sites were associated with the disulphide bonds in the two domains of the light chains; the variable region (Cys^{23} and Cys^{87}) and the constant region (Cys^{133} and Cys^{193}). Another region with a disulphide bond is the Cys^{214} residue, which connects the light chain to the heavy chain. However, the last section of the peptide could not be properly assessed, as mentioned in the sequence coverage section.

There were nine carboxymethylated sites at the studied section of the heavy chain; these were found in positions 96, 148, 224, 230, 233, 265, 371 and 429. Only three sites were consistently carboxymethylated across all treatments (224 230 and 233). These areas in the peptide chain are located in the hinge of the heavy chain and correspond to the three main sulphide bonds that link the four peptide chains together. Cys^{224} links the heavy chain to the light chain and Cys^{230} and Cys^{233} link the heavy chains between them. Internal peptide disulphide bonds of the heavy chain are also present in the variable domain of the heavy chain, between Cys^{22} and Cys^{96}. However, only the latter was found modified in the present experimentation. Furthermore, it is known that cysteine at position 148 bounds to cysteine at position 204, but we could not screen this position, as it was not found in the sequence coverage. Cysteines in charge of stabilizing the second constant domain of the constant region of the antibody, are located at positions 265 and 325; the latter was missing as the area is rich in lysine and prone to excessive digestion cleavage. Finally, the third constant domain of the

heavy chain is held by cysteines 371 and 429, both of which were identified and modified during the alkylation process.

Table 18 Carboxy-methylation modification sites for rituximab

		Catechin			Resveratrol			
Position	Control	Cat 10 µM	Cat 25 µM	Cat 50 µM	Rsv 10 µM	Rsv 25 µM	Rsv 50 µM	Rsv 100 µM
LC-23-Ctyl	Yes	*Yes	Yes	Yes	Yes	Yes	Yes	*Yes
LC-87-Ctyl	Yes	Yes	Yes	Yes	Yes	---	Yes	*Yes
LC-133-Ctyl	Yes	Yes	Yes	Yes	Yes	Yes	Yes	*Yes
LC-193-Ctyl	Yes	Yes	Yes	Yes	Yes	Yes	Yes	*Yes
HC-96-Ctyl	Yes	Yes	Yes	Yes	Yes	Yes	Yes	Yes
HC-148-Ctyl	Yes	---	Yes	Yes	Yes	Yes	Yes	Yes
*HC-224-Ctyl	Yes	Yes	Yes	Yes	Yes	Yes	---	Yes
*HC-230-Ctyl	Yes	Yes	Yes	Yes	Yes	Yes	---	Yes
*HC-233-Ctyl	Yes	Yes	Yes	Yes	Yes	Yes	---	Yes
HC-265-Ctyl	Yes	Yes	Yes	Yes	Yes	Yes	Yes	*Yes
HC-371-Ctyl	Yes	*Yes	Yes	*Yes	Yes	Yes	Yes	*Yes
HC-429-Ctyl	Yes	Yes	Yes	Yes	Yes	Yes	Yes	Yes

Presence (Yes) or absence (---) of carboxy-methylation modification in rituximab light chain (LC) and heavy chain (HC)

**Sites that had 100% of their peptides modified*

Interestingly, resveratrol treatment at 50 µM, caused complete inhibition of the carboxy-methylation, but only for cysteines in the hinge area, suggesting that the effect must be localized in this region and is related to sulphide bonds between different chains. This was the only exception as all the other treatments including control had different results, as mentioned above. It is possible that this is due to resveratrol being able to bond with the region and interact. It is highly possible that traces of resveratrol were still present in the media after purification. More interesting is the fact that this treatment also caused tri-oxidation of the adjacent cysteine residues consistently at HC 96, 148, 265 and 371. This is

paradoxical, as treatment with 100 µM of resveratrol caused the opposite effect and almost all the studied sites become permanently modified (Figure 77).

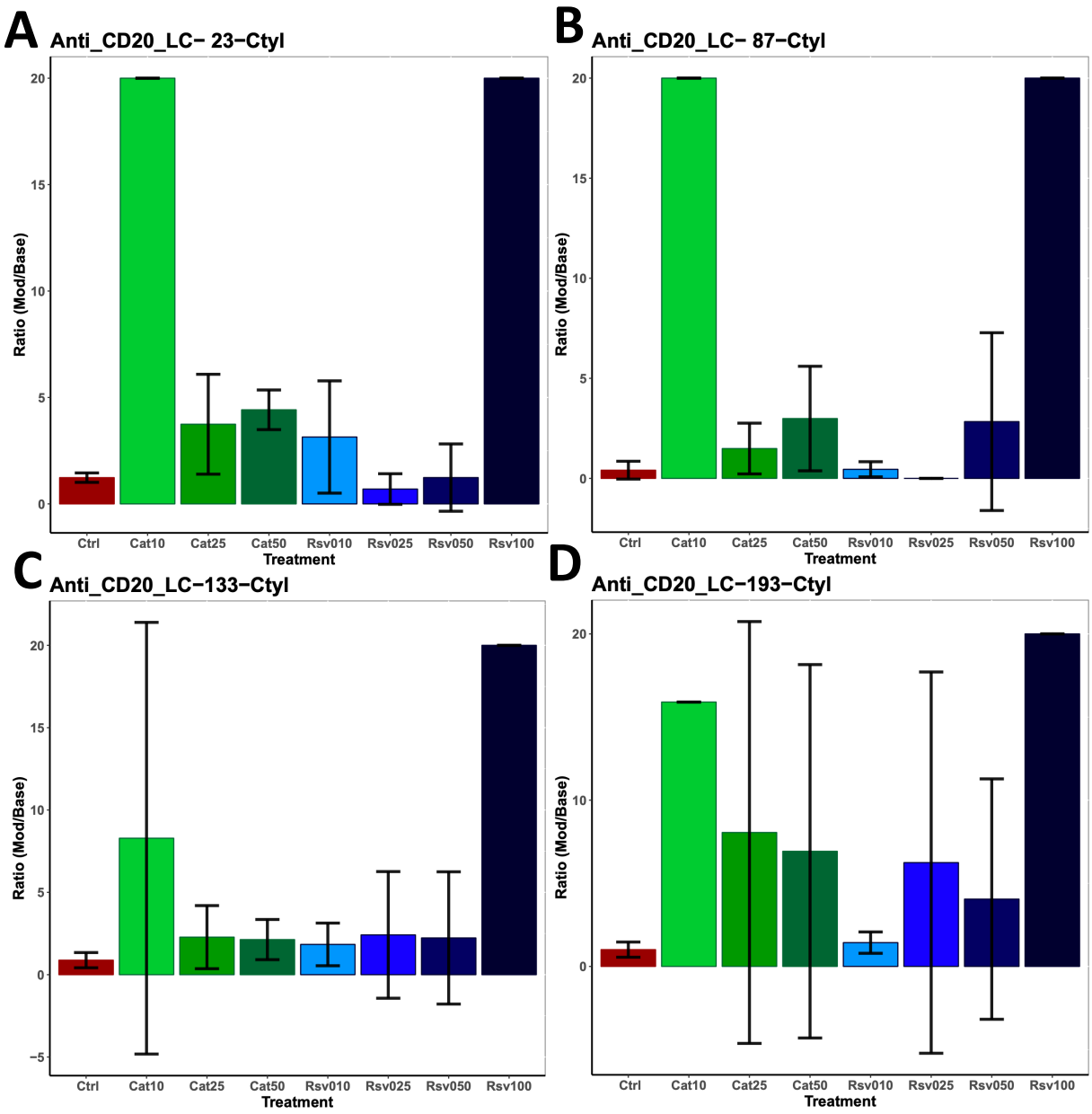

Figure 77 Carboxy-methylation ratio of the recombinant IgG
The ratio of carboxy-methylation modification in cysteine residues 23(A), 87(B) 133(C) and 193 (D) of the light chain (LC) of rituximab. Data are shown for treatments under control conditions (red) and treatments with catechin (green) and resveratrol (blue). Samples were purified (section 2.3), and trypsin-digested (section 2.5.1) previous to LC-MS/MS (section 2.5.2). Modifications were looked for with the targeted approach and the label-free quantification method with MaxQuant software (section 2.5.3)

Furthermore, and in line with the dependent peptide search, there was a clear dichotomy between the treated samples. One group included catechin treatments at 25 and 50 µM as well as resveratrol at 10, 25 and 50 µM. These treatments had little effect on the changes of carboxy-methylation. The second group included resveratrol at 100 µM and catechin at 10 µM, which caused a considerable increase in the ratio of carboxy-methylations (Figure 77). These results further ratify the previously identified modifications of the samples found by the dependent peptide search.

Furthermore, other possible modifications with the same mass shift, like the substitution of glutamine by alanine and asparagine by glycine, were examined but were not found. Therefore, it is apparent that the changes observed are due to carboxy-methylation.

6.2.3.3.4 Reduction

Only one reduction site was found during the current experimentations (Ser84 at the heavy chain). This modification was common during the control treatments; 10% of the peptides were substituting Ser, an amino acid with a polar neutral side chain to Ala, a smaller amino acid with a hydrophobic side chain. Growth of the culture under catechin concentrations repressed the modification completely. Resveratrol treatments, on the other hand, were less efficient, but still caused some repression (Figure 78). This modification did not cause any direct changes in the overall charge of the IgG. However, alanine is highly hydrophobic, while serine possesses a polar chain. This substitution could cause some structural changes that could induce local charges on the molecule and cause shifts in the cation exchange chromatogram. Residue 84 appertains to the variable region of the heavy chain, as such

changes in this region could cause changes in the affinity of the biologic for the target molecule, in this case CD20. The repression of this modification could render the product more efficient as potentially 15% of the product will not carry this modification under some of the treatment conditions, but further research needs to be undertaken about the effect of this modification in the monoclonal antibody to clarify this.

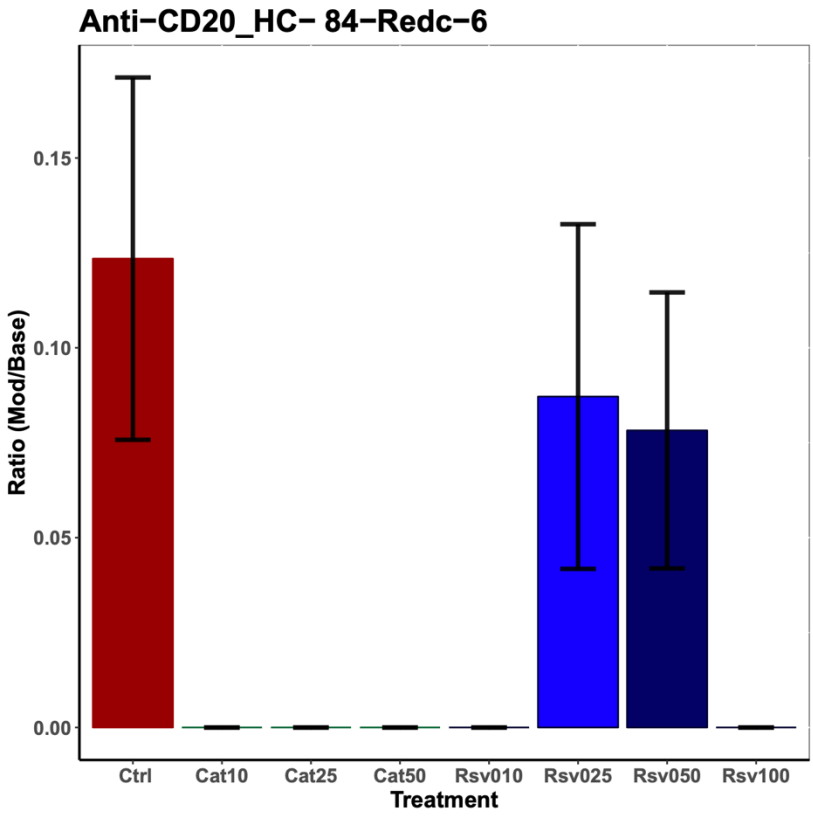

Figure 78 Reduction ratio of the recombinant IgG
Modified peptide to non-modified peptide ratio in residue Ser84 of the heavy chain (HC) of rituximab. Data are shown for treatments under control conditions (red) and treatments with catechin (green) and resveratrol (blue). Samples were purified (section 2.3), and trypsin-digested (section 2.5.1) previous to LC-MS/MS (section 2.5.2). Modifications were looked for with the targeted approach and the label-free quantification method with MaxQuant software (section 2.5.3)

6.2.3.3.5 Deamidation

Deamidation of asparagine to aspartate was found only in one residue, at position 136 of the light chain. However, this modification only occurred during treatment with high concentrations of resveratrol (100 µM) and accounted only for 0.3% of the peptides in the sample. This modification has been previously described (Chelius, Rehder and Bondarenko, 2005). Deamidation causes the relative number of acidic species to increase and it is a process that occurs at a very low rate. This phenomenon is often observed in late cultures and is symptomatic of the degradation and age of the product. Non- enzymatic deamidation is among the most common modifications that cause charge heterogeneity (Ponniah *et al.*, 2017). It can result in a considerable effect in the ion exchange chromatograms, leading to distinguishable peaks in some cases (Perkins *et al.*, 2000; Vlasak *et al.*, 2009). Although deamidation contributes to the charge heterogeneity, the shift in charge species observed by cation exchange chromatography, is unlikely to be mainly due to this.

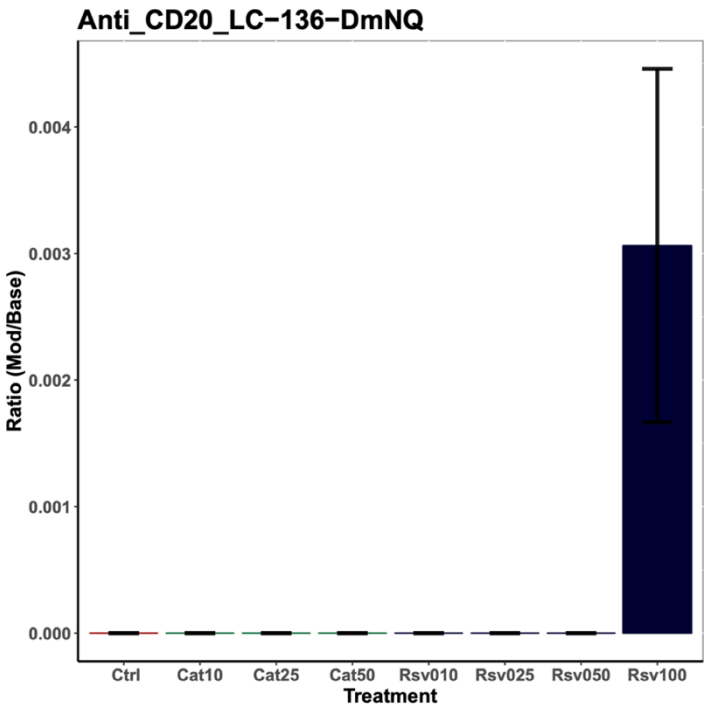

Figure 79 Deamidation ratio of the recombinant IgG
Modified peptide to non-modified peptide ratio in residue Asn[136] of the light chain (HC) of rituximab. Data are shown for treatments under control conditions (red) and treatments with catechin (green) and resveratrol (blue). Samples were purified (section 2.3), and trypsin-digested (section 2.5.1) previous to LC-MS/MS (section 2.5.2). Modifications were looked for with the targeted approach and the label-free quantification method with MaxQuant software (section 2.5.3)

6.2.3.3.6 Loss of ammonia

The loss of an ammonia group from asparagine, was found in four different locations (Table 19). One was found in the light chain at position 157, although this modification was only present when the sample was treated with 10 µM of resveratrol (affected 0.15% of the peptides). On the other hand, modified sites at positions 55, 319 and 388 of the heavy chain, were consistent for all samples and affected double or more peptides than the previously described one. The modifications were constant across all samples and differences were not apparent (Figure 80).

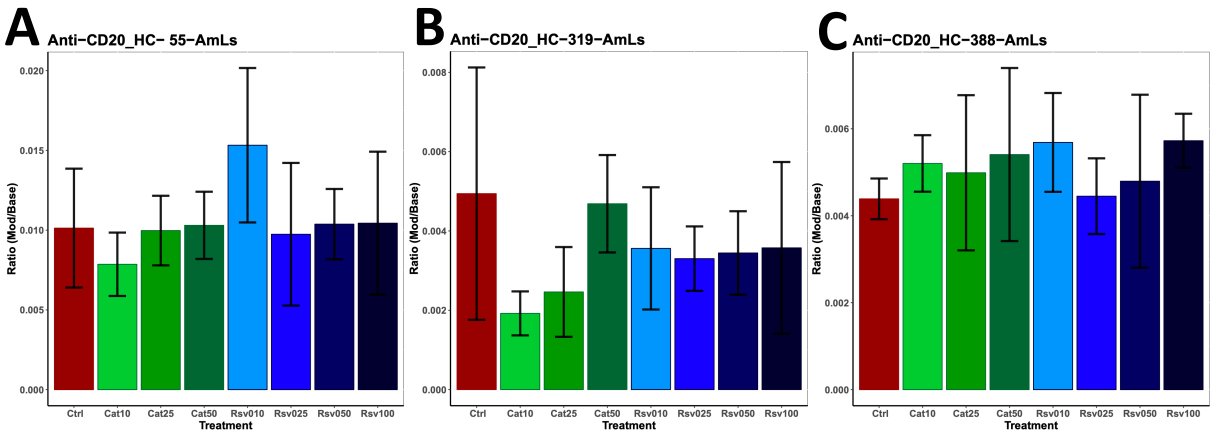

Figure 80 Ammonia loss ratio of the recombinant IgG
The ratio of loss of ammonia in asparagine residues 55(A), 319(B) and 388(C) of the heavy chain (HC) of rituximab. Data are shown for treatments under control conditions (red) and treatments with catechin (green) and resveratrol (blue). Samples were purified (section 2.3), and trypsin-digested (section 2.5.1) previous to LC-MS/MS (section 2.5.2). Modifications were looked for with the targeted approach and the label-free quantification method with MaxQuant software (section 2.5.3)

Table 19 Loss of ammonia sites for rituximab

Position	Control	Catechin			Resveratrol			
		Cat 10 µM	Cat 25 µM	Cat 50 µM	Rsv 10 µM	Rsv 25 µM	Rsv 50 µM	Rsv 100 µM
LC-157-AmLs	---	---	---	---	Yes	---	---	---
HC-55-AmLs	Yes	Yes	Yes	Yes	Yes	Yes	Yes	Yes
HC-319-AmLs	Yes	Yes	Yes	Yes	Yes	Yes	Yes	Yes
HC-388-AmLs	Yes	Yes	Yes	Yes	Yes	Yes	Yes	Yes

Presence (Yes) or absence (---) of ammonia loss in rituximab light chain (LC) and heavy chain (HC)

6.3 Conclusions

The addition of catechin or resveratrol to the media did not cause any changes in IgG aggregation or fragmentation, at any of the studied concentrations. Treatment with catechin caused a decrease of the acidic species and an increase of the main species in a concentration-dependent manner. Treatment with resveratrol caused a decrease of the acidic species and an increase of the basic species in a concentration-dependent manner. This deacidification of the product caused by both chemicals could be a positive trait towards the stability of the product and the shelf-life. The addition of flavonoids was able to stop changes in the hydrophobicity of the variable region, by avoiding reduction in specific residues (Ser^{24}); this could enhance the IgG binding to the antigen. Furthermore, modification patterns suggest that resveratrol compounds can target specific regions of the IgG, such as the hinge section. Overall, resveratrol and catechin did not cause any modifications that could negatively affect the quality of the product.

Chapter 7

Final discussion

Out of fifteen chemicals studied, this research has shown that resveratrol and catechins are plausible chemicals to use for the improvement of recombinant IgG production as they do not compromise the quality of the product (Figure 81). The key results are summarized below and compared with the available literature.

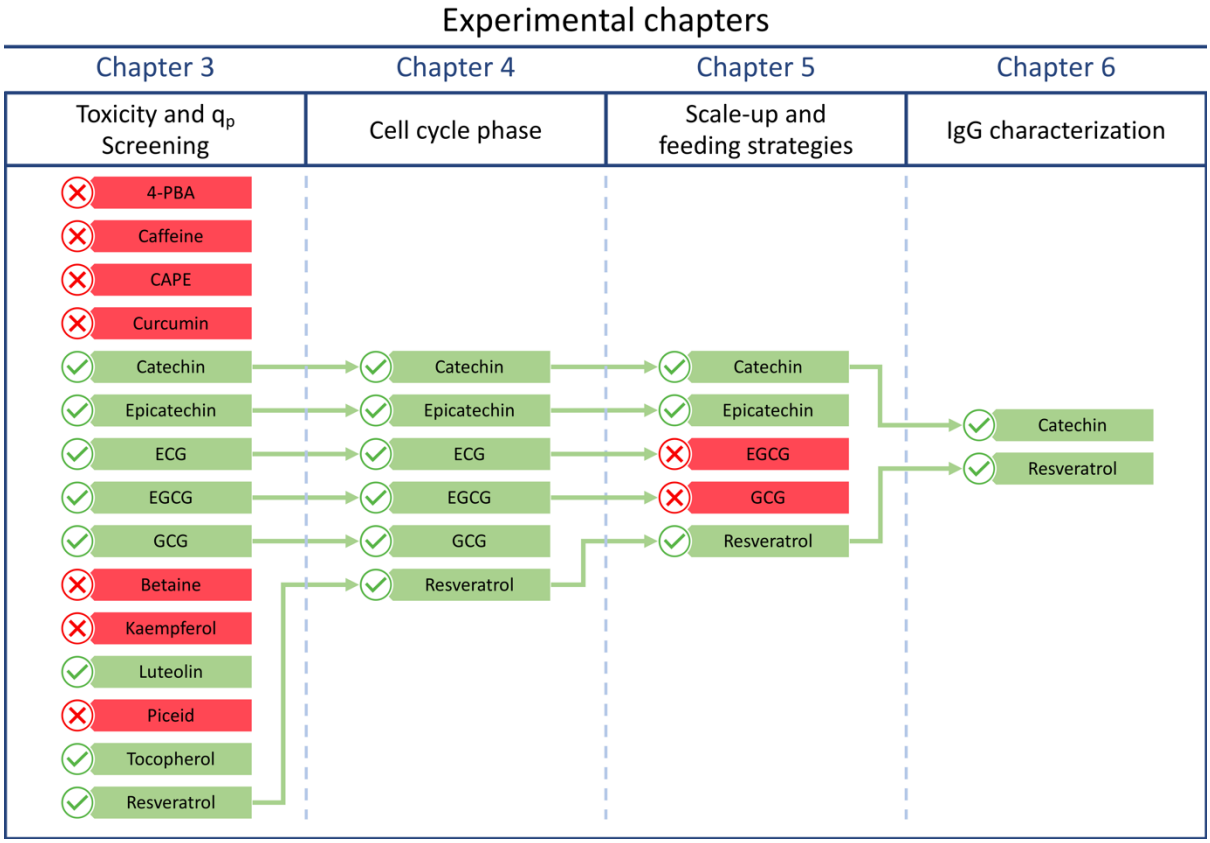

Figure 81 Flow chart of chemicals studied across the project.
Flow chart of chemicals studied across the project; green represents positive results while red represents undesirable traits found during experimentation across the four stages of research of this project. Of the initial 15 chemicals screened, only two were taken to the final experimentation chapter. Chemical acronyms stand for: 4-PBA (sodium 4-phenylbutyrate), CAPE (caffeic acid phenethyl ester), ECG (epicatechin gallate), EGCG (epigallocatechin gallate), GCG (gallocatechin gallate).

7.1 Key results

7.1.1 Initial toxicological and recombinant production screening

- The screening method using 24-well plates, was very efficient at identifying chemicals able to shift cell growth into specific protein production, but it is uncertain whether it has the capacity to assess other mechanisms of improvement of recombinant IgG production

- Among the chemicals screened, 4-PBA, betaine, caffeine and piceid caused no improvements in the production process. Curcumin, kaempferol and CAPE showed drastic toxic effects and the increase of q_p was only present at low levels of viability. Catechin, epicatechin, resveratrol, EGC, tocopherol, EGCG and GCG all showed positive effects on recombinant IgG production

- Most of the chemicals with positive features were able to improve the specific protein production by inhibiting cell growth without lowering viability

7.1.2 The effect of flavonoids over time on culture behaviour and cell cycle

- Resveratrol stopped cell cycle in an aphasic way and elongated the stationary stage. Resveratrol caused cell growth arrest during the S phase in the first cell divisions of the culture; this phenomenon is linked to its toxic effect in CHO cells

- Catechin compounds caused an increase of the cells in the G_2/M and S phases of the cell cycle, while reducing the number of cells in G_1/G_0. The galloyl group was identified

as a fundamental part of the catechins structure resulting in an increase of the cell growth arrest

7.1.3 Scale-up and optimization of the recombinant IgG production

- Flask culture early feeding strategies caused an increase of the negative traits observed (lower viable cell density, lower viability and lower IgG produced) for all the chemicals studied

- Feeding the culture at later stages with resveratrol, catechin and epicatechin caused an improvement of the final antibody titre

- GCG and EGCG were too toxic under these conditions and they did not cause any positive improvements in the final IgG production

7.1.4 Recombinant IgG product characterization and quality assessment

- Treatment with catechin and resveratrol did not cause any changes in the IgG aggregation or fragmentation at any of the studied concentrations

- Treatment with catechin caused a decrease of the acidic species and an increase of the main species in a concentration-dependent manner

- Treatment with resveratrol caused a decrease of the acidic species and an increase of the basic species in a concentration-dependent manner

- Overall, resveratrol and catechin did not cause any modifications that could negatively affect the quality of the product

From the results displayed, it is apparent that the principal goals stated at the beginning of this project have been achieved (section 1.8). In addition to the aims, a list of questions was established which is considered during the overall discussion.

7.2 Overall discussion

7.2.1 How does resveratrol help with the production of recombinant IgG in CHO cell cultures?

Present results from experimentation with resveratrol showed that this chemical was able to increase q_p with different setups (section 3.3.1.2.14) and when added to the culture at the late stages of the exponential phase it was able to enhance recombinant production (section 5.2.1.3). Resveratrol was able to cause cytostatic conditions that enhanced the capacity to increase the recombinant product.

As these experiments were taking place, resveratrol was included in a patent in order to be used as an additive for recombinant protein production in CHO cells. This study found resveratrol able to cause up to a 1.44-fold increase in production when added at 1mM concentration with no negative effects (Tian 2016). Our study showed that resveratrol, in concentrations as low as 50 µM, caused a considerable delay of the cell curve when added at the beginning of the culture. It also caused a drastic drop in viability and a decay in the final

titre in low concentrations. Concentrations above 100 µM caused complete repression of the cell growth and IgG production with a complete loss of cell viability (Appendix 2). These differences in the effects of resveratrol are difficult to reconcile. Other studies performed with CHO cells (Basso *et al.*, 2013; Mallebrera *et al.*, 2015) and different mammalian host systems (Lu, Ou and Lu, 2013; Quoc Trung *et al.*, 2013), identified a much lower tolerance of the compounds than what claimed by Tian and colleagues. This indicates that probably the results claimed in this patent are an exception to the rule and that most likely, the range of sensitivity of most mammalian cells, and more specifically CHO cells, is lower than what was claimed.

Regardless of the differences in the results in the use of resveratrol to improve recombinant protein production in CHO cells, it seems that this chemical can be used in different cell lines and for the production of different recombinant proteins with successful outcomes, although the specific feeding regime may need to be adjusted for each specific case.

7.2.2 What would be a plausible cellular mechanism to explain the improvement in recombinant IgG production by resveratrol?

Cell cycle results showed that there was a drop in viability at the end of the cell growth adaptation phase. This was then followed by the accumulation peak of cells passing through S phase. This phenomenon could be associated to the capacity of resveratrol to interfere with DNA duplication, repair and segregation (Basso et al., 2013; Traversi et al., 2016), thus accumulating cells in the S phase through direct (N'soukpoé-Kossi et al., 2015) and indirect (Leone et al., 2010) mechanisms late in the culture (Subramanian, Soundar and Mangoli, 2016). Previous studies report that DNA damage occurs at high concentrations with a

subsequent possibility of apoptotic events (Basso et al., 2013; Uchiumi et al., 2016). However, not all studies reported the same results (Sainz et al., 2003). One of the mechanisms of resveratrol's toxicity on CHO cell dividing cultures, could be its interaction with topoisomerases during the S phase (Leone et al., 2012; Basso et al., 2013). Recent enzymatic studies identified the capacity of resveratrol to inhibit topoisomerase II by preventing the attachment of ATP to the protein complex in human models (Lee, Wendorff and Berger, 2017).

The toxic behaviour of resveratrol seen along the different chapters of this project seems to be linked to the capacity of cell cultures to grow. This relates to resveratrol's capacity to interference with DNA replication, repair and segregation. This hypothesis also correlates with cancer studies where resveratrol was identified to have anti-tumour effects due to its capacity to selectively cause higher toxic effects in highly dividing tissues (Zhou et al., 2011; Trung et al., 2015).

The connection between the arrest at S phase and the growth inhibition should not be assumed. There is a strong correlation between the peak of cells in S phase, the drop in viability and the start of the exponential phase (section 4.2.2). However, growth arrest previous to the exponential phases is difficult to be explained by S phase interference with replication as cells in the cell cycle phase do not increase consistently during this period. This means that another mechanism could be at play, an idea that was also speculated in previous studies (Della Ragione et al., 1998). Furthermore, resveratrol has been found to stop cell cycle in other phases (Rubiolo et al., 2012; Gokbulut et al., 2013) or to stop it in a non-specific way (Pozo-Guisado et al., 2002).

It is likely that the results observed by resveratrol are due to complex effects. Due to its bioactive characteristics, it is likely that resveratrol is causing a pleiotropic effect on CHO cells by interfering with signaling and metabolic pathways in different ways (Hahnvajanawong et al., 2011; Rubiolo et al., 2012; Bosutti and Degens, 2015).

7.2.3 How do catechins help the production of recombinant IgG in CHO cell cultures?

Present results from experimentation with catechins showed that these chemicals were able to increase q_p within different setups (section 3.3.1.2) and enhance recombinant production (section 5.2.2). It was also apparent that the chemicals with a galloyl group (ECG, EGCG, GCG) had a more severe effect over the different parameters studied in comparison to those without this group (catechin and epicatechin). Out of these compounds studied, only catechin and EGCG had a previous tracking record as chemical additives in recombinant protein production.

Catechin was studied recently and was patented to improve recombinant protein production. When using catechin at high concentrations (1 mM), titre was improved by 17% in 20 L reactors. The reason behind these was the elongation of the culture time due to catechin decreasing ammonia and lactate levels (Tian, 2016). In general, our results seem to correlate with the data by Tian et al, although we achieved higher increases of the final titre by the addition of lower concentrations. Scale down studies in this area tend to show big improvements in recombinant protein production, but when scaled-up, the gain observed is often reduced. On the other hand, viable cell growth was clearly inhibited in our study at low concentrations. The addition of high concentrations of catechin did not seem to cause any inhibition in the Tian et al study. This could be the result of the use of different cell lines

(aCD137 vs DG44) or different growth conditions. The resilience of cells to suffer toxic effects seems to be consistent when comparing our research and respective patent for resveratrol and catechin (Tian, 2016).

The catechin family seems to be capable of improving recombinant protein production in CHO cells. Both previous studies and the results of this study, indicate that catechins can be used successfully in different cell lines and for the production of different recombinant proteins. Furthermore, the effect seems to be transferable among all the chemicals studied, although each of them has different optimization conditions.

7.2.4 What is a plausible cellular mechanism to explain the fact that catechins improve recombinant IgG production?

Catechins caused an inhibitory effect on cell cultures in a concentration-dependent manner. The degree of cell arrest seems to be linked to the structure. Catechin was the less effective in reducing cell growth, while EGCG and ECG and GCG had very similar trends. EC was found between both extremes. The structure of the compounds seems to be key in the different effects over cell growth inhibition, as the chemicals with the galloyl group (EGCG, GCG and ECG) had a more severe effect. Viability had a direct relation to growth inhibition. EGCG and GCG caused considerable effects while catechin and epicatechin were less impactful. The addition of any of the catechins at the end of exponential did not cause an effect on viability (section 5.2.2).

All catechins affected cell cycle in similar ways with an increase of G_2/M and S phases while and a decrease of the G_1/G_0 phase (section 5.2.2). EGCG is the most studied compound of the

catechin family. Previous studies indicate that this compound is able to inhibit cell cycle in the S phase (Shabana *et al.*, 2014; Shen *et al.*, 2014). Huang et al looked into the effect of catechin in murine microglial cells. Catechin caused cell cycle arrest in S phase (Q. Huang *et al.*, 2005). Comparative studies of the effect of different catechin compounds on the cell cycle were consistent in identifying different behaviours depending on the presence of the galloyl group (Tan *et al.*, 2000). A further comparative study of compounds with galloyl groups indicated that ECG, gallocatechin (GC) and EGCG cause very similar responses on the cell cycle arrest. All the chemicals inhibit cell growth in a concentration-dependent manner and cause inhibition of Nf-κB, an increase in S phase and a decrease in G_1/G_0 (Kürbitz *et al.*, 2011).

The mechanism by which catechins are acting on the cell cycle could include their inhibitory effect on the topoisomerase enzymes. EGCG was found to inhibit topoisomerase I and II (Bandele 2008) by sequestrating the enzyme in a complex that seems to be mediated by hydrogen peroxide (Lopez-Lazaro 2011). This inhibition of topoisomerases leads to a G_2/M and S phase arrest (Cliby 2002). A comparative enzymatic study describes the inhibition capacity according to catechin structure, with EGCG being the most effective in inhibiting topoisomerases followed by ECG; EC had a very low inhibitory capacity (Suzuki 2001). This trend of enzyme inhibition correlates with the studies of cell growth arrest presented here (section 4.2.3.1).

Regardless of the proven capacity of these compounds to interfere with topoisomerases, these chemicals also tend to affect the regulation of many different cell cycle proteins such as p21, p27 and Nf-κB (Shabana *et al.*, 2014; Shen *et al.*, 2014). It is likely that the effect of

catechins over cell cycle arrest occurs at many levels; there might be pleiotropic mechanisms linked to the high bioactive capability of the compound (Ye *et al.*, 2017)

7.2.5 How can the catechin feeding regime help the quality of the product of recombinant IgG production?

Catechin was able to cause a relative reduction of the acidic species in the purified IgG product and an increase in the amount of protein with main charge. Epigallocatechin-gallate was found to have very similar effects (Hossler *et al.*, 2015). The study also showed that the mechanism by which epigallocatechin gallate reduces the acidic species was transferable to other proteins, cell line expression level or scale up conditions. The addition of epigallocatechin gallate caused a decrease of the acidic species during the first stages of the culture, but after 48 hours, the relative increase of the acidic species was the same as observed using control (Hossler *et al.*, 2015).

The charge heterogeneity shift caused by catechin could be used for adjusting the biosimilar charge variant profile of antibodies. The deacidification profile seen could also have a positive impact on the shelf-life and stability of the product, as acidification of the product is often the result of aging and depredatory pathways (Gandhi *et al.*, 2012; Leblanc *et al.*, 2017).

7.2.6 How do these newly defined molecules fit the current state of the art for chemical addition on recombinant CHO cell culture feeding strategies?

Previous studies have used mild hypothermia, hyperosmotic pressure and the addition of small molecules with no direct nutritional value to improve q_p or reduce recombinant protein production problems such as aggregation (Johari *et al.*, 2015b).

Temperature shift is the most common strategy used in mammalian cell cultures. Mild hypothermia has been used to slow cellular growth while allowing protein synthesis to continue, improving the q_p values and reducing aggregation (Chen, Wu and Liu, 2004; Trummer *et al.*, 2006; Kou *et al.*, 2011; Gomez *et al.*, 2012; Johari *et al.*, 2015a). Osmolyte chemicals such as glycine betaine have also been used. This chemical achieves slower cellular growth and in some circumstances, it can improve the q_p value (Ryu *et al.*, 2000; Tae Kyung *et al.*, 2000; Kim and Lee, 2002).

Other low-molecular weight additives have also been used. Butyric acid, valeric acid, valproic acid, 4-phenylbutyric acid and zinc have been added to recombinant CHO cell culture media (Yam *et al.*, 2007; Jiang and Sharfstein, 2008; Yang, Lu and Nguyen, 2014; Coronel *et al.*, 2016; Avello *et al.*, 2017; Paul *et al.*, 2018; Prabhu, Gadre and Gadgil, 2018). Valeric acid (pentanoic acid) produced higher product titres and increased q_p for an unnamed recombinant protein in CHO cells (Liu, Chu and Hwang, 2001; Coronel *et al.*, 2016). Valproic acid (2-propylpentanoic acid) addition to cell culture media has also been reported to improve antibody expression (Yang, Lu and Nguyen, 2014; Paul *et al.*, 2018). 4-phenylbutyrate has also been used to minimize aggregation in proteins expressed in CHO cells (Yam *et al.*, 2007). The number of chemical additives developed, and the understanding of their mechanism is limited.

The capacity of these chemicals to shift cell growth into productivity is not exclusive, as other strategies involving low temperature and osmolytes (eg. glycine betaine) have already been developed. However, the mechanism by which they induce cell arrest and protein improvement is not the same as the ones previously described. Catechins and resveratrol compounds caused a significant decrease in the relative quantity of cells in the G_1/G_0 phase. This is contrasting the common trend of chemical cell cycle arrest strategies which focus on specific cell cycle arrest in G_1/G_0 and on increasing cell size (Hendrick *et al.*, 1999; Carvalhal, Marcelino and Carrondo, 2003; Bi, Shuttleworth and Al-Rubeai, 2004; Dutton, Scharer and Moo-Young, 2006). Furthermore, not all cell lines are susceptible to these strategies, as the added chemicals are often very specific in the way they interact with the production process and cannot always be used across different cell lines or recombinant molecules reliably.

Conclusively, the chemicals studied in the present study could be used as an alternative or combining tools to improve recombinant protein production in CHO cell lines.

7.2.7 What future work needs to be done to further assess these chemicals and make them reliable for industry purposes?

The initial screening process was very efficient in identifying chemicals able to shift cell growth into specific protein production. This was done conservatively, to ensure reliable candidates for future steps of the project. As a result, other candidates cannot be discarded as non suitable. The change of parametres, such as using different concentrations, altering the shaking conditions and adding times could make a drastic difference as illustrated in the present report. A better screening system would have involved different cell lines, each one with a well-defined bottleneck for the production of biologics.

While a lot of work has been done on catechins and resveratrol during the present project, further studies are needed in order to have a better understanding of the mechanisms of the chemicals on the cell and their feasibility as additives in industry.

In the present report, it was presumed that a main mechanism of action of resveratrol and catechins could be the inhibition capacity on the topoisomerases as well as their effect on the regulation of gene expression. A study of chemical localization inside the cell as well as the study of the gene expression through q-PCR could give more information about the effect over different metabolic pathways.

In order to assess if the results displayed here are adaptable to an industry set-up, issues like the size of the reactor need to be considered. Scale down studies in this area tend to show big improvements in recombinant protein production, but when scaled-up, the gain observed is often reduced. Industry reactors can reach volumes of up to 2000 L. Shear stress, pH and dissociation of relevant gases such as CO_2 or O_2 are some of the principal variables that could affect the cell population conditions, the results of adding these chemicals to the media and the quality of the product when changing the cell culture size (Brunner *et al.*, 2017).

Finally, a further study of the glycosylation pattern of the recombinant IgG is essential. This is a very important parameter that can determine the quality of the product. On the same line, a study of the shelf-life of the product when formulated, could also bring interesting information about the long-term effects of the chemicals.

Overall, these future experiments could help understand the adaptability of the chemicals to industry standards. This would also empower the capacity to use them in an engineering

context. Lastly, the study of other chemical candidates such as tocopherol or luteolin which showed positive results during the screening stage could be of interest.

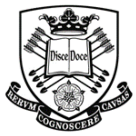
Disce Doce
Rerum Cognoscere Causas

References

References

Abcam (2012) 'Propidium iodide staining of cells to assess DNA cell cycle Flow', *Abcam*, pp. 1–3.

Acosta-martin, A. E. *et al.* (2016) 'Detection of busulfan adducts on proteins', *Rapid communications in mass spectrometry*, 30, pp. 2517–2528. doi: 10.1002/rcm.7730.

Ahn, Y.-H. *et al.* (1999) 'Effect of glycine betaine as osmoprotectant on the production of erythropoietin by cho cells in hyperosmotic serum free media culture', *Animal Cell Technology*, 10(3), pp. 247–250.

Alessandri, L. *et al.* (2012) 'Increased serum clearance of oligomannose species present on a human IgG1 molecule Leslie', *mAbs*, 4(4), pp. 509–520. doi: 10.4161/mabs.20450.

Allen, M. J. *et al.* (2008) 'Identification of novel small molecule enhancers of protein production by cultured mammalian cells', *Biotechnology and Bioengineering*, 100(6), pp. 1193–1204. doi: 10.1002/bit.21839.

De Almeida, S. F. *et al.* (2007) 'Chemical chaperones reduce endoplasmic reticulum stress and prevent mutant HFE aggregate formation', *Journal of Biological Chemistry*, 282(38), pp. 27905–27912. doi: 10.1074/jbc.M702672200.

Almo, S. C. and Love, J. D. (2014) 'Better and faster: Improvements and optimization for mammalian recombinant protein production', *Current Opinion in Structural Biology*. Elsevier Ltd, 26(1), pp. 39–43. doi: 10.1016/j.sbi.2014.03.006.

Altman, D. G. and Bland, J. M. (2005) 'Standard deviations and standard errors.', *Methods in medical research*, 331, p. 903.

Andrasi, M., Gyemant, G. and Gaspar, A. (2014) 'Analysis of Rituximab, A Therapeutic Monoclonal Antibody by Capillary Zone Electrophoresis', *Journal of chromatography separation techniques*, 6, pp. 1–8. doi: 10.4172/2157-7064.1000259.

Anfinsen, C. B. (1973) 'Principles that Govern the Folding of Protein Chains', *Science*, 181(4096), pp. 223–230. doi: 10.1126/science.181.4096.223.

Antunes, L. M. G. *et al.* (2005) 'Effects of H2O2, Fe2+and Fe3+on curcumin-induced chromosomal aberrations in CHO cells', *Genetics and Molecular Biology*, 28(1), pp. 161–164. doi: 10.1590/S1415-47572005000100028.

Armagan, A. *et al.* (2008) 'Caffeic acid phenethyl ester modulates methotrexate-induced oxidative stress in testes of rat', *Human and Experimental Toxicology*, 27(7), pp. 547–552. doi: 10.1177/0960327108092293.

Auger, C. *et al.* (2005) 'Dietary wine phenolics catechin, quercetin, and resveratrol efficiently protect hypercholesterolemic hamsters against aortic fatty streak accumulation', *Journal of Agricultural and Food Chemistry*, 53(6), pp. 2015–2021. doi: 10.1021/jf048177q.

Avello, V. *et al.* (2017) 'Impact of sodium butyrate and mild hypothermia on metabolic and physiological behaviour of CHO TF 70R cells', *Electronic Journal of Biotechnology*. Elsevier España, S.L.U., 27, pp. 55–62. doi: 10.1016/j.ejbt.2017.03.008.

Baek, E. *et al.* (2016) 'Chemical inhibition of autophagy: Examining its potential to increase the specific productivity of recombinant CHO cell lines', *Biotechnology and Bioengineering*, 113(9), pp. 1953–1961. doi: 10.1002/bit.25962.

Baeshen, M. N. *et al.* (2015) 'Production of Biopharmaceuticals in E. coli: Current scenario and future perspectives.', *Journal of microbiology and biotechnology*, 25(7), pp. 953–962. doi: 10.4014/jmb.1405.05052.

Basso, E. *et al.* (2013) 'Effects of resveratrol on topoisomerase II-?? activity: Induction of micronuclei and inhibition of chromosome segregation in CHO-K1 cells', *Mutagenesis*, 28(3), pp. 243–248. doi: 10.1093/mutage/ges067.

Bastianetto, S. *et al.* (2006) 'Neuroprotective effects of green and black teas and their catechin gallate esters against β-amyloid-induced toxicity', *European Journal of Neuroscience*, 23(1), pp. 55–64. doi:

10.1111/j.1460-9568.2005.04532.x.

Beck, A. *et al.* (2013) 'Characterization of therapeutic antibodies and related products', *Analytical Chemistry*, Jan.

Bertolotti, a *et al.* (2000) 'Dynamic interaction of BiP and ER stress transducers in the unfolded-protein response.', *Nature cell biology*, 2(6), pp. 326–332. doi: 10.1038/35014014.

Bi, J. X., Shuttleworth, J. and Al-Rubeai, M. (2004) 'Uncoupling of Cell Growth and Proliferation Results in Enhancement of Productivity in p21CIP1-Arrested CHO Cells', *Biotechnology and Bioengineering*, 85(7), pp. 741–749. doi: 10.1002/bit.20025.

Bieschke, J. *et al.* (2010) 'EGCG remodels mature alpha-synuclein and amyloid-beta fibrils and reduces cellular toxicity.', *Proceedings of the National Academy of Sciences of the United States of America*, 107(17), pp. 7710–7715. doi: 10.1073/pnas.0910723107.

Bleiholder, C. *et al.* (2013) 'Ion mobility spectrometry reveals the mechanism of amyloid formation of Aβ(25-35) and its modulation by inhibitors at the molecular level: Epigallocatechin gallate and scyllo-inositol', *Journal of the American Chemical Society*, 135(45), pp. 16926–16937. doi: 10.1021/ja406197f.

Borana, M. S. *et al.* (2014) 'Curcumin and kaempferol prevent lysozyme fibril formation by modulating aggregation kinetic parameters', *Biochimica et Biophysica Acta - Proteins and Proteomics*. Elsevier B.V., 1844(3), pp. 670–680. doi: 10.1016/j.bbapap.2014.01.009.

Bosutti, A. and Degens, H. (2015) 'The impact of resveratrol and hydrogen peroxide on muscle cell plasticity shows a dose-dependent interaction.', *Scientific reports*, 5, p. 8093. doi: 10.1038/srep08093.

Braakman, I. and Bulleid, N. J. (2011) 'Protein Folding and Modification in the Mammalian Endoplasmic Reticulum', *Annual Review of Biochemistry*, 80(1), pp. 71–99. doi: 10.1146/annurev-biochem-062209-093836.

van den Bremer, E. T. J. Van Den *et al.* (2015) 'Human IgG is produced in a pro-form that requires

clipping of C-terminal lysines for maximal complement activation', *mAbs*, 7(4), pp. 672–680.

Brunner, M. *et al.* (2017) 'Investigation of the interactions of critical scale-up parameters (pH, pO2and pCO2) on CHO batch performance and critical quality attributes', *Bioprocess and Biosystems Engineering*. Springer Berlin Heidelberg, 40(2), pp. 251–263. doi: 10.1007/s00449-016-1693-7.

Buchberger, A., Bukau, B. and Sommer, T. (2010) 'Protein quality control in the cytosol and the endoplasmic reticulum: brothers in arms.', *Molecular cell*. Elsevier Inc., 40(2), pp. 238–52. doi: 10.1016/j.molcel.2010.10.001.

Buren, N. V. A. N. *et al.* (2009) 'Elucidation of Two Major Aggregation Pathways in an IgG2 Antibody', *Journal of Pharmaceutical Sciences*, 98(9), pp. 3013–3030. doi: 10.1002/jps.

Byoun, S. and Park, H. (2006) 'Short-term Hypothermic Preservation of CHO Cells Using Serum-Free Media', *Korean Society for Biotechnology and Bioengineering*, 21(4), pp. 306–311.

Carvalhal, A. V., Marcelino, I. and Carrondo, M. J. T. (2003) 'Metabolic changes during cell growth inhibition by p27 overexpression', *Applied Microbiology and Biotechnology*, 63(2), pp. 164–173. doi: 10.1007/s00253-003-1385-5.

Carver, J. H., Carrano, A. V and Macgregor, J. T. (1983) 'galangin on Chinese hamster ovary cells in vitro', *Mutation research*, 113, pp. 45–60.

Chelius, D., Rehder, D. S. and Bondarenko, P. V (2005) 'Identification and Characterization of Deamidation Sites in the Conserved Regions of Human Immunoglobulin Gamma Antibodies', *Analytical Chemistry*, 77(18), pp. 6004–6011.

Chen, Z., Wu, B. and Liu, H. (2004) 'Temperature shift as a process optimization step for the production of pro-urokinase by a reCHO cell line in high-density perfusion culture', *Journal of Bioscience and Bioengineering*, 97(4), pp. 239–243.

Cho, J. a. *et al.* (2014) '4-Phenylbutyrate Attenuates the ER Stress Response and Cyclic AMP Accumulation in DYT1 Dystonia Cell Models', *PLoS ONE*, 9(11), p. e110086. doi:

10.1371/journal.pone.0110086.

Choi, A. Y. *et al.* (2011) 'Luteolin induces apoptosis through endoplasmic reticulum stress and mitochondrial dysfunction in Neuro-2a mouse neuroblastoma cells', *European Journal of Pharmacology*. Elsevier B.V., 668(1–2), pp. 115–126. doi: 10.1016/j.ejphar.2011.06.047.

Chollet, M. E. *et al.* (2015) 'The chemical chaperone sodium 4-phenylbutyrate improves the secretion of the protein CA267T mutant in CHO-K1 cells trough the GRASP55 pathway.', *Cell & bioscience*. BioMed Central, 5, p. 57. doi: 10.1186/s13578-015-0048-4.

Chung, S. *et al.* (2019) 'An in vitro FcRn- dependent transcytosis assay as a screening tool for predictive assessment of nonspecific clearance of antibody therapeutics in humans', *mAbs*. Taylor & Francis, 11(5), pp. 942–955. doi: 10.1080/19420862.2019.1605270.

Churches, Q. I. *et al.* (2014) 'Naturally occurring polyphenolic inhibitors of amyloid beta aggregation', *Bioorganic & Medicinal Chemistry Letters*. Elsevier Ltd, 24(14), pp. 3108–3112. doi: 10.1016/j.bmcl.2014.05.008.

Conte, A., Pellegrini, S. and Tagliazucchi, D. (2003) 'Synergistic protection of PC12 cells from β-amyloid toxicity by resveratrol and catechin', *Brain Research Bulletin*, 62(1), pp. 29–38. doi: 10.1016/j.brainresbull.2003.08.001.

Coronel, J. *et al.* (2016) 'Valeric acid supplementation combined to mild hypothermia increases productivity in CHO cell cultivations', *Biochemical Engineering Journal*. Elsevier B.V., 114, pp. 101–109. doi: 10.1016/j.bej.2016.06.031.

DeZengotita, V. M. *et al.* (2002) 'Selected amino acids protect hybridoma and CHO cells from elevated carbon dioxide and osmolality', *Biotechnology and Bioengineering*, 78(7), pp. 741–752. doi: 10.1002/bit.10255.

Dick, L. W. J. *et al.* (2007) 'Determination of the Origin of the N-Terminal Pyro-Glutamate Variation in Monoclonal Antibodies Using Model Peptides', *Biotechnology and Bioengineering*, 97(3), pp. 544–553. doi: 10.1002/bit.

Dick, L. W. J. *et al.* (2008) 'C-Terminal Lysine Variants in Fully Human Monoclonal Antibodies : Investigation of Test Methods and Possible Causes', *Biotechnology and Bioengineering*, 100(6), pp. 1132–1143. doi: 10.1002/bit.21855.

Dobson, C. M. (2003) 'Protein Folding and Misfolding', *Nature*, 426, pp. 884–890. doi: 10.1007/978-3-642-22230-6.

Du, Z. *et al.* (2015) 'Use of a small molecule cell cycle inhibitor to control cell growth and improve specific productivity and product quality of recombinant proteins in CHO cell cultures', *Biotechnology and Bioengineering*, 112(1), pp. 141–155. doi: 10.1002/bit.25332.

Dutton, R. L., Scharer, J. and Moo-Young, M. (2006) 'Cell cycle phase dependent productivity of a recombinant Chinese hamster ovary cell line', *Cytotechnology*, 52(1), pp. 55–69. doi: 10.1007/s10616-006-9041-4.

Ehrnhoefer, D. E. *et al.* (2008) 'EGCG redirects amyloidogenic polypeptides into unstructured, off-pathway oligomers.', *Nature structural & molecular biology*, 15(6), pp. 558–566. doi: 10.1038/nsmb.1437.

Eisele, Y. S. *et al.* (2015) 'Targeting protein aggregation for the treatment of degenerative diseases', *Nature Reviews Drug Discovery*. Nature Publishing Group, pp. 759–780. doi: 10.1038/nrd4593.

El-Khattouti, A. *et al.* (2015) 'CD133+melanoma subpopulation acquired resistance to caffeic acid phenethyl ester-induced apoptosis is attributed to the elevated expression of ABCB5: Significance for melanoma treatment', *Cancer Letters*. Elsevier Ireland Ltd, 357(1), pp. 83–104. doi: 10.1016/j.canlet.2014.10.043.

Eletto, D. *et al.* (2014) 'Redox controls UPR to control redox.', *Journal of cell science*, 127, pp. 3649–3658. doi: 10.1242/jcs.153643.

Endo, H. *et al.* (2014) 'Structure activity relationship study of curcumin analogues toward the amyloid-beta aggregation inhibitor', *Bioorganic & Medicinal Chemistry Letters*. Elsevier Ltd, 24(24), pp. 5621–5626. doi: 10.1016/j.bmcl.2014.10.076.

Esser, P and Weitzmann, L. (2011) 'Evaporation From Cell Culture Plates', *Thermo Scientific Bolletin*, (2).

Fabris, S. *et al.* (2008) 'Antioxidant properties of resveratrol and piceid on lipid peroxidation in micelles and monolamellar liposomes', *Biophysical Chemistry*, 135(1–3), pp. 76–83. doi: 10.1016/j.bpc.2008.03.005.

Fazzio, A., Marilley, D. and Azzi, A. (1997) 'The effect of alfa-Tocopherol and beta-tocopherol on proliferation, protein kinase C activity and gene expression in different cell lines.', *Biochemistry and molecular biology international*, 41(1), pp. 93–101.

Fekete, S. *et al.* (2013) 'Analytical strategies for the characterization of therapeutic monoclonal antibodies', *TrAC - Trends in Analytical Chemistry*. Elsevier Ltd, 42, pp. 74–83. doi: 10.1016/j.trac.2012.09.012.

Ferreira, N., Saraiva, M. J. and Almeida, M. R. (2012) 'Epigallocatechin-3-gallate as a potential therapeutic drug for TTR-related amyloidosis: "In vivo" evidence from FAP mice models', *PLoS ONE*, 7(1), pp. 5–14. doi: 10.1371/journal.pone.0029933.

Fliedl, L., Grillari, J. and Grillari-Voglauer, R. (2014) 'Human cell lines for the production of recombinant proteins: on the horizon', *New Biotechnology*. Elsevier B.V., 32(6), pp. 673–679. doi: 10.1016/j.nbt.2014.11.005.

Flintoff, W. F., Davidson, S. V and Siminovitch, L. (1976) 'Isolation and partial characterization of three methotrexate-resistant phenotypes from Chinese hamster ovary cells.', *Somatic cell genetics*, 2, pp. 245–261.

Flores-Ortiz, L. F. *et al.* (2014) 'Physicochemical properties of Rituximab', *Journal of Liquid Chromatography and Related Technologies*, 37(10), pp. 1438–1452. doi: 10.1080/10826076.2013.794738.

Fomina-Yadlin, D. *et al.* (2015) 'Transcriptome analysis of a CHO cell line expressing a recombinant therapeutic protein treated with inducers of protein expression', *Journal of Biotechnology*. Elsevier

B.V., 212, pp. 106–115. doi: 10.1016/j.jbiotec.2015.08.025.

Food and Drug Administration (2015) 'Novel New Drugs 2014'.

Le Fourn, V. *et al.* (2014) 'CHO cell engineering to prevent polypeptide aggregation and improve therapeutic protein secretion', *Metabolic Engineering*, 21, pp. 91–102. doi: 10.1016/j.ymben.2012.12.003.

Freund, N. W. and Croughan, M. S. (2018) 'A simple method to reduce both lactic acid and ammonium production in industrial animal cell culture', *International Journal of Molecular Sciences*, 19(2). doi: 10.3390/ijms19020385.

Fried, J., Perez, A. G. and Clarkson, B. D. (1976) 'Flow Cytofluorometric Analysis of Cell Cycle Distributions Using Propidium Iodide', *The Journal of Cell Biology*, 71(1), pp. 172–181.

Gandhi, S. *et al.* (2012) 'Elucidation of Degradants in Acidic Peak of Cation Exchange Chromatography in an IgG1 Monoclonal Antibody Formed on Long-Term Storage in a Liquid Formulation', *Pharmacological Research*, 29, pp. 209–224. doi: 10.1007/s11095-011-0536-0.

Garnier, a *et al.* (1994) 'Scale-up of the adenovirus expression system for the production of recombinant protein in human 293S cells.', *Cytotechnology*, 15(1–3), pp. 145–155. doi: doi: 10.1007/bf00762389.

Gemelli, T. F. *et al.* (2015) 'Evaluation of Safety of Arrabidaea chica Verlot (Bignoniaceae), a Plant with Healing Properties', *Journal of Toxicology and Environmental Health - Part A: Current Issues*. Taylor & Francis, 78(18), pp. 1170–1180. doi: 10.1080/15287394.2015.1072070.

Ginsberg, J. (2008) 'Development of Deep-tank Fermentation', *Pfizer Inc.*

Goetze, A. M. *et al.* (2011) 'High-mannose glycans on the Fc region of therapeutic IgG antibodies increase serum clearance in humans', *Glycobiology*, 21(7), pp. 949–959. doi: 10.1093/glycob/cwr027.

Gokbulut, A. A. *et al.* (2013) 'Resveratrol and quercetin-induced apoptosis of human 232B4 chronic

lymphocytic leukemia cells by activation of caspase-3 and cell cycle arrest.', *Hematology*, 18(3), pp. 144–150. doi: 10.1179/1607845412Y.0000000042.

Gomez, N. *et al.* (2012) 'Culture temperature modulates aggregation of recombinant antibody in cho cells', *Biotechnology and Bioengineering*, 109(1), pp. 125–136. doi: 10.1002/bit.23288.

Gonçalves, a. M. *et al.* (2013) 'Pichia pastoris: A recombinant microfactory for antibodies and human membrane proteins', *Journal of Microbiology and Biotechnology*, 23(5), pp. 587–601. doi: 10.4014/jmb.1210.10063.

Gramer, M. J. *et al.* (1995) 'Removal of Sialic Acid from a Glycoprotein in CHO Cell Culture Supernatant by Action of an Extracellular CHO Cell Sialidase', *Biotechnology*, 13(July), pp. 692–698.

Gramer, M. J. and Goochee, C. F. (1993) 'Glycosidase Activities in Chinese Hamster Ovary Cell Lysate and Cell Culture Supernatant', *Biotechnology Progress*, 9, pp. 366–373.

Gusnard, D. and Kirschner, R. H. (1977) 'Cell and organelle shrinkage during preparation for scanning electron microscopy: effects of fixation, dehydration and critical point drying', *Journal of Microscopy*, 110(1), pp. 51–57. doi: 10.1111/j.1365-2818.1977.tb00012.x.

Hadavand, N., Valadkhani, M. and Zarbakhsh, A. (2011) 'Biologicals Current regulatory and scienti fi c considerations for approving biosimilars in Iran', *Biologicals*. Elsevier Ltd, 39(5), pp. 325–327. doi: 10.1016/j.biologicals.2011.06.019.

Hahnvajanawong, C. *et al.* (2011) 'Inhibition of cell cycle progression and apoptotic activity of resveratrol in human intrahepatic cholangiocarcinoma cell lines', *Asian Biomedicine*, 5(6), pp. 775–785. doi: 10.5372/1905-7415.0506.116.

Hartl, F. U., Bracher, A. and Hayer-Hartl, M. (2011) 'Molecular chaperones in protein folding and proteostasis.', *Nature*, 475(7356), pp. 324–332. doi: 10.1038/nature10317.

Hartl, F. U. and Hayer-Hartl, M. (2009) 'Converging concepts of protein folding in vitro and in vivo', *Nature structural & Molecular Biology*, 16(6), pp. 574–581. doi: 10.1038/nsmb.1591.

Hayashi, T. and Su, T.-P. (2007) 'Sigma-1 Receptor Chaperones at the ER- Mitochondrion Interface Regulate Ca2+ Signaling and Cell Survival', *Cell*, 131(3), pp. 596–610. doi: 10.1016/j.cell.2007.08.036.

Hendrick, V. *et al.* (1999) 'MODULATION OF CELL CYCLE FOR OPTIMAL RECOMBINANT PROTEINPRODUCTION', *Animal Cell Technology: Products from Cells, Cells as Products*, pp. 179–181.

Ho, S. C. L. *et al.* (2013) 'Control of IgG LC: HC ratio in stably transfected CHO cells and study of the impact on expression, aggregation, glycosylation and conformational stability', *Journal of Biotechnology*. Elsevier B.V., 165(3–4), pp. 157–166. doi: 10.1016/j.jbiotec.2013.03.019.

Hobro, A. J. and Smith, N. I. (2017) 'An evaluation of fixation methods: Spatial and compositional cellular changes observed by Raman imaging', *Vibrational Spectroscopy*. Elsevier B.V., 91, pp. 31–45. doi: 10.1016/j.vibspec.2016.10.012.

Hosoi, T. *et al.* (2014) 'Caffeine attenuated ER stress-induced leptin resistance in neurons.', *Neuroscience letters*. Elsevier Ireland Ltd, 569, pp. 23–6. doi: 10.1016/j.neulet.2014.03.053.

Hossler, P. *et al.* (2015) 'Cell culture media supplementation of bioflavonoids for the targeted reduction of acidic species charge variants on recombinant therapeutic proteins', *Biotechnology Progress*, 31(4), pp. 1039–1052. doi: 10.1002/btpr.2095.

Hsiao, G. *et al.* (2007) 'Characterization of a novel and potent collagen antagonist, caffeic acid phenethyl ester, in human platelets: In vitro and in vivo studies', *Cardiovascular Research*, 75(4), pp. 782–792. doi: 10.1016/j.cardiores.2007.05.005.

Huang, L. *et al.* (2005) 'In Vivo Deamidation Characterization of Monoclonal Antibody by LC / MS / MS', *Analytical Chemistry*, 77(5), pp. 1432–1439. doi: 10.1021/ac0494174.

Huang, Q. *et al.* (2005) '(+)-Catechin, an ingredient of green tea, protects murine microglia from oxidative stress-induced DNA damage and cell cycle arrest.', *Journal of Pharmacological Sciences*, 98(1), pp. 16–24. doi: 10.1254/jphs.FPJ04053X.

Huh, J. H. *et al.* (2013) 'Pharmaceutical Biotechnology The Identification of Free Cysteine Residues

Within Antibodies and a Potential Role for Free Cysteine Residues in Covalent', *Journal of Pharmaceutical Sciences*. Elsevier Masson SAS, 102(6), pp. 1701–1711. doi: 10.1002/jps.23505.

Hussain, H., Maldonado-Agurto, R. and Dickson, A. J. (2014) 'The endoplasmic reticulum and unfolded protein response in the control of mammalian recombinant protein production', *Biotechnology Letters*, 36(8), pp. 1581–1593. doi: 10.1007/s10529-014-1537-y.

Hwang, S. J. *et al.* (2011) 'Effect of chemical chaperone addition on production and aggregation of recombinant flag-tagged COMP-angiopoietin 1 in chinese hamster ovary cells', *Biotechnology Progress*, 27(2), pp. 587–591. doi: 10.1002/btpr.579.

IFPMA, I. F. of P. M. A. (2012) 'The Pharmaceutical Industry and Global Health : Facts and Figures 2012'.

IFPMA, I. F. of P. M. A. (2014) 'The Pharmaceutical Industry and Global Health : Facts and Figures 2014'.

Jaramillo-García, V. *et al.* (2018) 'Chemical characterization and cytotoxic, genotoxic, and mutagenic properties of Baccharis trinervis (Lam, Persoon) from Colombia and Brazil', *Journal of Ethnopharmacology*. Elsevier Ireland Ltd, 213(July 2017), pp. 210–220. doi: 10.1016/j.jep.2017.10.027.

Jayapal, K. *et al.* (2007) 'Recombinant protein therapeutics from CHO cells-20 years and counting', *Chemical Engineering Progress*, 103(10), pp. 40–47. Available at: http://www.aiche.org/sites/default/files/docs/pages/CHO.pdf.

De Jesus, M. and Wurm, F. M. (2011) 'Manufacturing recombinant proteins in kg-ton quantities using animal cells in bioreactors', *European Journal of Pharmaceutics and Biopharmaceutics*. Elsevier B.V., 78(2), pp. 184–188. doi: 10.1016/j.ejpb.2011.01.005.

Jiang, Z. and Sharfstein, S. T. (2008) 'Sodium butyrate stimulates monoclonal antibody over-expression in CHO cells by improving gene accessibility', *Biotechnology and Bioengineering*, 100(1), pp. 189–194. doi: 10.1002/bit.21726.

Jin, U. H. *et al.* (2008) 'Caffeic acid phenethyl ester induces mitochondria-mediated apoptosis in

human myeloid leukemia U937 cells', *Molecular and Cellular Biochemistry*, 310(1–2), pp. 43–48. doi: 10.1007/s11010-007-9663-7.

Johari, Y. B. *et al.* (2015a) 'Integrated cell and process engineering for improved transient production of a "difficult-to-express" fusion protein by CHO cells', *Biotechnology and Bioengineering*, 112(12), pp. 2527–2542. doi: 10.1002/bit.25687.

Johari, Y. B. *et al.* (2015b) 'Integrated cell and process engineering for improved transient production of a "difficult-to-express" fusion protein by CHO cells', *Biotechnology and Bioengineering*, 112(12), pp. 2527–2542. doi: 10.1002/bit.25687.

Jones, D. *et al.* (2003) 'High-level expression of recombinant IgG in the human cell line per.c6.', *Biotechnol Prog*, 19(1), pp. 163–168. doi: 10.1021/bp025574h.

Jovanovic, S. V *et al.* (1994) 'Flavonoids as Antioxidants', *Journal of the American Chemical Society*, 116(11), pp. 4846–4851. doi: 10.1021/ja00090a032.

Kaas, C. *et al.* (2015) 'Sequencing the CHO DXB11 genome reveals regional variations in genomic stability and haploidy', *BMC Genomics*, 16(1), p. 160. doi: 10.1186/s12864-015-1391-x.

Kaisermayer, C. *et al.* (2016) 'Biphasic cultivation strategy to avoid Epo-Fc aggregation and optimize protein expression', *Journal of Biotechnology*. Elsevier B.V., 227, pp. 3–9. doi: 10.1016/j.jbiotec.2016.03.054.

Kanda, Y. *et al.* (2006) 'Comparison of biological activity among nonfucosylated therapeutic IgG1 antibodies with three different N -linked Fc oligosaccharides : the high-mannose , hybrid , and complex types', *Glycobiology*, 17(1), pp. 104–118.

Kavakli, H. S. *et al.* (2010) 'Caffeic acid phenethyl ester decreases oxidative stress index in blunt spinal cord injury in rats', *Hong Kong Journal of Emergency Medicine*, 17(3), pp. 250–255. doi: 10.1177/102490791001700308.

Kim, J. K. *et al.* (2010) 'Protective Effects of Kaempferol (3,4',5,7-tetrahydroxyflavone) against Amyloid

Beta Peptide (Aβ)-Induced Neurotoxicity in ICR Mice', *Bioscience, Biotechnology, and Biochemistry*, 74(2), pp. 397–401. doi: 10.1271/bbb.90585.

Kim, J. Y., Kim, Y. G. and Lee, G. M. (2012) 'CHO cells in biotechnology for production of recombinant proteins: Current state and further potential', *Applied Microbiology and Biotechnology*, 93(3), pp. 917–930. doi: 10.1007/s00253-011-3758-5.

Kim, N. S. and Lee, G. M. (2002) 'Response of recombinant Chinese hamster ovary cells to hyperosmotic pressure: Effect of Bcl-2 overexpression', *Journal of Biotechnology*, 95(3), pp. 237–248. doi: 10.1016/S0168-1656(02)00011-1.

Kishishita, S. *et al.* (2015) 'Optimization of chemically defined feed media for monoclonal antibody production in Chinese hamster ovary cells', *Journal of Bioscience and Bioengineering*. Elsevier Ltd, 120(1), pp. 78–84. doi: 10.1016/j.jbiosc.2014.11.022.

Kmetič, I. *et al.* (2009) 'Lindane-induced cytotoxicity and the role of vitamin e in Chinese hamster ovary (CHO-K1) cells', *Toxicology Mechanisms and Methods*, 19(8), pp. 518–523. doi: 10.1080/15376510903280107.

Kou, T. C. *et al.* (2011) 'Detailed understanding of enhanced specific productivity in Chinese hamster ovary cells at low culture temperature', *Journal of Bioscience and Bioengineering*. The Society for Biotechnology, Japan, 111(3), pp. 365–369. doi: 10.1016/j.jbiosc.2010.11.016.

Krishan, A. (1975) 'RAPID FLOW CYTOFLUOROMETRIC MAMMALIAN ANALYSIS OF IODIDE STAINING', *The Journal of Cell Biology*, 66, pp. 188–193.

Krishnan, R., Rendeiro, D. and San-Dadi, S. (2010) 'WO 2010/036767 Al'.

Kubota, K. *et al.* (2006) 'Suppressive effects of 4-phenylbutyrate on the aggregation of Pael receptors and endoplasmic reticulum stress', *Journal of Neurochemistry*, 97(5), pp. 1259–1268. doi: 10.1111/j.1471-4159.2006.03782.x.

Kumar, N. *et al.* (2014) 'Synthesis, structural elucidation, and in vitro antiproliferative activities of

mixed-ligand titanium complexes', *Medicinal Chemistry Research*, 23(8), pp. 3897–3906. doi: 10.1007/s00044-014-0963-7.

Kumar, N., Gammell, P. and Clynes, M. (2007) 'Proliferation control strategies to improve productivity and survival during CHO based production culture: A summary of recent methods employed and the effects of proliferation control in product secreting CHO cell lines', *Cytotechnology*, 53(1–3), pp. 33–46. doi: 10.1007/s10616-007-9047-6.

Kürbitz, C. *et al.* (2011) 'Epicatechin gallate and catechin gallate are superior to epigallocatechin gallate in growth suppression and anti-inflammatory activities in pancreatic tumor cells', *Cancer Science*, 102(4), pp. 728–734. doi: 10.1111/j.1349-7006.2011.01870.x.

Kuryatov, A., Mukherjee, J. and Lindstrom, J. (2013) 'Chemical Chaperones Exceed the Chaperone Effects of RIC-3 in Promoting Assembly of Functional ??7 AChRs', *PLoS ONE*, 8(4), pp. 1–11. doi: 10.1371/journal.pone.0062246.

Lacy, E. R., Baker, M. and Brigham-burke, M. (2008) 'Free sulfhydryl measurement as an indicator of antibody stability', *Analytical Chemistry*, 382, pp. 66–68. doi: 10.1016/j.ab.2008.07.016.

Ladiwala, A. R. a *et al.* (2010) 'Resveratrol selectively remodels soluble oligomers and fibrils of amyloid A?? into off-pathway conformers', *Journal of Biological Chemistry*, 285(31), pp. 24228–24237. doi: 10.1074/jbc.M110.133108.

Lao, M. S. and Toth, D. (1997) 'Effects of ammonium and lactate on growth and metabolism of a recombinant Chinese hamster ovary cell culture', *Biotechnology Progress*, 13(5), pp. 688–691. doi: 10.1021/bp9602360.

Leblanc, Y. *et al.* (2017) 'Charge variants characterization of a monoclonal antibody by ion exchange chromatography coupled on-line to native mass spectrometry : Case study after a long-term storage at + 5 ◦C', *Journal of Chromatography B*. Elsevier B.V., 1048, pp. 130–139. doi: 10.1016/j.jchromb.2017.02.017.

Lee, C. L. *et al.* (2010) 'Ixorapeptide i and ixorapeptide II, bioactive peptides isolated from Ixora

coccinea', *Bioorganic and Medicinal Chemistry Letters*. Elsevier Ltd, 20(24), pp. 7354–7357. doi: 10.1016/j.bmcl.2010.10.058.

Lee Ching, H. *et al.* (1996) 'Mutual interactions among ingredients of betel quid in inducing genotoxicity on Chinese hamster ovary cells', *Mutation Research - Genetic Toxicology*, 367(2), pp. 99–104. doi: 10.1016/0165-1218(95)00081-X.

Lee, J. H., Wendorff, T. J. and Berger, J. M. (2017) 'Resveratrol: A novel type of topoisomerase II inhibitor', *The Journal of Biological Chemistry*. Applied Microbiology and Biotechnology, 292(51), pp. 21011–21022. doi: 10.1021/cb500798y.

Lee, Y. J., Kim, S. J. and Heo, T. H. (2011) 'Protective effect of catechin in type I Gaucher disease cells by reducing endoplasmic reticulum stress', *Biochemical and Biophysical Research Communications*. Elsevier Inc., 413(2), pp. 254–258. doi: 10.1016/j.bbrc.2011.08.080.

Lehmann, A. R. and Kirk-Bell, S. (1972) '{Post-Replication} Repair of {DNA} in {Ultraviolet-Irradiated} Mammalian Cells', *European Journal of Biochemistry*, 31(3), pp. 438–445. doi: 10.1111/j.1432-1033.1972.tb02550.x.

Lenin, R. *et al.* (2012) 'Amelioration of glucolipotoxicity-induced endoplasmic reticulum stress by a chemical chaperone in human THP-1 monocytes', *Experimental Diabetes Research*, 2012(c). doi: 10.1155/2012/356487.

Leone, S. *et al.* (2010) 'Resveratrol induces DNA double-strand breaks through human topoisomerase II interaction', *Cancer Letters*. Elsevier Ireland Ltd, 295(2), pp. 167–172. doi: 10.1016/j.canlet.2010.02.022.

Leone, S. *et al.* (2012) 'Resveratrol acts as a topoisomerase II poison in human glioma cells', *International Journal of Cancer*, 131(3). doi: 10.1002/ijc.27358.

Lewis, N. E. *et al.* (2013) 'Genomic landscapes of Chinese hamster ovary cell lines as revealed by the Cricetulus griseus draft genome.', *Nature biotechnology*. Nature Publishing Group, 31(8), pp. 759–65. doi: 10.1038/nbt.2624.

Li, Y.-C. *et al.* (2008) 'Protective Effects of Antioxidants on Micronuclei Induced by Irradiated 9-Fluorenone/N,N-Dimethyl-p-toluidine in CHO Cells', *Journal of Biomedical Materials Research*, 84B(1), pp. 58–63. doi: 10.1002/jbmb.

Liu, C., Chu, I. and Hwang, S. (2001) 'Pentanoic acid, a novel protein synthesis stimulant for Chinese Hamster Ovary (CHO) cells.', *Journal of bioscience and bioengineering*, 91(1), pp. 71–5. doi: http://dx.doi.org/10.1016/S1389-1723(01)80114-6.

Liu, H. *et al.* (2008) 'Heterogeneity of monoclonal antibodies', *Journal of Pharmaceutical Sciences*. Elsevier Masson SAS, 97(7), pp. 2426–2447. doi: 10.1002/jps.21180.

Liu, H. *et al.* (2016) 'Impact of Cell Culture on Recombinant Monoclonal Antibody Product Heterogeneity', *Biotechnology Progress*, 32(5), pp. 1103–1013. doi: 10.1002/btpr.2327.

Liu, H. F. *et al.* (2010) 'Recovery and purification process development for monoclonal antibody production', *mAbs*, 2(5), pp. 480–499. doi: 10.4161/mabs.2.5.12645.

Liu, Y. *et al.* (2001) 'A domain-sw apped RNase A dimer w ith implications for amyloid formation', *Nature*, 8(3), pp. 211–214.

Lloyd, D. R. *et al.* (1999) 'The role of the cell cycle in determining gene expression and productivity in CHO cells.', *Cytotechnology*, 30(1–3), pp. 49–57. doi: 10.1023/A:1008093404237.

Lloyd, D. R. *et al.* (2000) 'Relationship between cell size, cell cycle and specific recombinant protein productivity.', *Cytotechnology*, 34(1–2), pp. 59–70. doi: 10.1023/A:1008103730027.

Long, L. H. *et al.* (2007) 'Different cytotoxic and clastogenic effects of epigallocatechin gallate in various cell-culture media due to variable rates of its oxidation in the culture medium', *Mutation Research - Genetic Toxicology and Environmental Mutagenesis*, 634(1–2), pp. 177–183. doi: 10.1016/j.mrgentox.2007.07.009.

Lu, L. Y., Ou, N. and Lu, Q. Bin (2013) 'Antioxidant Induces DNA damage, cell death and mutagenicity in human lung and skin normal cells', *Scientific Reports*, 3, pp. 1–11. doi: 10.1038/srep03169.

Lyubarskaya, Y. *et al.* (2006) 'Analysis of recombinant monoclonal antibody isoforms by electrospray ionization mass spectrometry as a strategy for streamlining characterization of recombinant monoclonal antibody charge heterogeneity', *Analytical Biochemistry*, 348(1), pp. 24–39. doi: 10.1016/j.ab.2005.10.003.

Ma, W., Goldberg, E. and Goldberg, J. (2017) 'ER retention is imposed by COPII protein sorting and attenuated by 4-phenylbutyrate', *eLife*, 6, pp. 1–22. doi: 10.7554/eLife.26624.

Maeda, E. *et al.* (2012) 'Analysis of Nonhuman N -Glycans as the Minor Constituents in Recombinant Monoclonal Antibody Pharmaceuticals', *Analytical Chemistry*, 84, p. 2373−2379.

Mallebrera, B. *et al.* (2015) 'Cytoprotective effect of resveratrol diastereomers in CHO-K1 cells exposed to beauvericin', *Food and Chemical Toxicology*. Elsevier Ltd, 80, pp. 319–327. doi: 10.1016/j.fct.2015.03.028.

Marambaud, P., Zhao, H. and Davies, P. (2005) 'Resveratrol promotes clearance of Alzheimer's disease amyloid-?? peptides', *Journal of Biological Chemistry*, 280(45), pp. 37377–37382. doi: 10.1074/jbc.M508246200.

Mendoza-Espinosa, P. *et al.* (2009) 'Disorder-to-order conformational transitions in protein structure and its relationship to disease', *Molecular and Cellular Biochemistry*, 330(1–2), pp. 105–120. doi: 10.1007/s11010-009-0105-6.

Mo, J. *et al.* (2016) 'Understanding the Impact of Methionine Oxidation on the Biological Functions of IgG1 Antibodies Using Hydrogen/Deuterium Exchange Mass Spectrometry', *Analytical Chemistry*, 88(19), pp. 9495–9502. doi: 10.1021/acs.analchem.6b01958.

Molecular Probes, I. (1999) 'Propidium iodide nucleic acid stain', *Molecular Probes*, pp. 1–3. doi: 10.1101/pdb.caut676.

Mortazavi, M. *et al.* (2018) 'Coordinate effects of betaine in reducing intra and extracellular erythropoietin aggregation', *Research Journal of Biotechnology*, 13, pp. 79–84.

Murugesan, M. and Manju, V. (2013) 'Luteolin promotes mitochondrial protection during acute and chronic periods of isoproterenol induced myocardial infarction in rats', *Egyptian Heart Journal*. The Egyptian Heart Journal, 65(4), pp. 319–327. doi: 10.1016/j.ehj.2013.02.005.

N'soukpoé-Kossi, C. N. *et al.* (2015) 'Structural modeling for DNA binding to antioxidants resveratrol, genistein and curcumin.', *Journal of Photochemistry and Photobiology B: Biology*, 151, pp. 69–75. doi: 10.1016/j.jphotobiol.2015.07.007.

Van Ness, K. P. *et al.* (2005) 'US 6872549 B2'. doi: 10.1038/incomms1464.

Nisha, V. M. *et al.* (2014) 'Apigenin and Quercetin Ameliorate Mitochondrial Alterations by Tunicamycin-Induced ER Stress in 3T3-L1 Adipocytes', *Applied Biochemistry and Biotechnology*, 174(4), pp. 1365–1375. doi: 10.1007/s12010-014-1129-2.

Noh, S. M., Shin, S. and Lee, G. M. (2018) 'Comprehensive characterization of glutamine synthetase-mediated selection for the establishment of recombinant CHO cells producing monoclonal antibodies', *Scientific Reports*. Springer US, 8(1), pp. 1–11. doi: 10.1038/s41598-018-23720-9.

Ombelli, M. *et al.* (2011) 'Competitive protein adsorption on polysaccharide and hyaluronate modified surfaces.', *Biofouling*, 27(5), pp. 505–518. doi: 10.1080/08927014.2011.585711.

Ono, K. *et al.* (2004) 'Curcumin Has Potent Anti-Amyloidogenic Effects for Alzheimer's ??-Amyloid Fibrils In Vitro', *Journal of Neuroscience Research*, 75(6), pp. 742–750. doi: 10.1002/jnr.20025.

Onuchic, J. N. and Wolynes, P. G. (2004) 'Theory of protein folding', *Current Opinion in Structural Biology*, 14(1), pp. 70–75. doi: 10.1016/j.sbi.2004.01.009.

Ozdal, T., Capanoglu, E. and Altay, F. (2013) 'A review on protein-phenolic interactions and associated changes', *Food Research International*. Elsevier Ltd, 51(2), pp. 954–970. doi: 10.1016/j.foodres.2013.02.009.

Ozturk, G. *et al.* (2012) 'The anticancer mechanism of caffeic acid phenethyl ester (CAPE): review of melanomas, lung', *European Review for Medical and Pharmacological Sciences*, 16, pp. 2064–2068.

doi: 10.1016/j.egypro.2017.09.655.

Pace, A. L. *et al.* (2013) 'Asparagine Deamidation Dependence on Buffer Type , pH , and Temperature', *Journal of Pharmaceutical Sciences*. Elsevier Masson SAS, 102(6), pp. 1712–1723. doi: 10.1002/jps.23529.

Painter, R. B. (1980) 'Effect of caffeine on DNA synthesis in irradiated and unirradiated mammalian cells', *Journal of Molecular Biology*, 143(3), pp. 289–301. doi: 10.1016/0022-2836(80)90191-6.

Pany, S., You, Y. and Das, J. (2016) 'Curcumin Inhibits Protein Kinase Cα Activity by Binding to Its C1 Domain', *Biochemistry*, 55(45), pp. 6327–6336. doi: 10.1021/acs.biochem.6b00932.

Park, J. H. *et al.* (2016) 'Valeric acid induces cell cycle arrest at G1 phase in CHO cell cultures and improves recombinant antibody productivity', *Biotechnology Journal*, 11(4), pp. 487–496. doi: 10.1002/biot.201500327.

Park, S. H. *et al.* (2013) 'Induction of endoplasmic reticulum stress-mediated apoptosis and non-canonical autophagy by luteolin in NCI-H460 lung carcinoma cells', *Food and Chemical Toxicology*. Elsevier Ltd, 56, pp. 100–109. doi: 10.1016/j.fct.2013.02.022.

Paul, A. J. *et al.* (2018) 'Identification of process conditions influencing protein aggregation in Chinese hamster ovary cell culture', *Biotechnology and Bioengineering*, 115(5), pp. 1173–1185. doi: 10.1002/bit.26534.

Percell Biologyca AB (2000) 'Growth of Recombinant and Non- recombinant CHO-cells', *Application Notes*, 113.

Pereira, A. *et al.* (2018) '13 C Flux Analysis Reveals that Rebalancing Medium Amino Acid Composition can Reduce Ammonia Production while Preserving Central Carbon Metabolism of CHO Cell Cultures', *Biotechnology Journal*, 13, p. 1700518. doi: 10.1002/biot.201700518.

Pereira, S., Kildegaard, H. F. and Andersen, M. R. (2018) 'Impact of CHO Metabolism on Cell Growth and Protein Production: An Overview of Toxic and Inhibiting Metabolites and Nutrients',

Biotechnology Journal, 13(3), pp. 1–13. doi: 10.1002/biot.201700499.

Perkins, M. *et al.* (2000) 'Determination of the Origin of Charge Heterogeneity in a Murine Monoclonal Antibody', *Pharmacological Research*, 17(9), pp. 1110–1117.

Pietta, P. G. (2000) 'Flavonoids as antioxidants', *Journal of Natural Products*, 63(7), pp. 1035–1042. doi: 10.1021/np9904509.

Pilbrough, W., Munro, T. P. and Gray, P. (2009) 'Intraclonal protein expression heterogeneity in recombinant CHO cells', *PLoS ONE*, 4(12). doi: 10.1371/journal.pone.0008432.

Ponniah, G. *et al.* (2017) 'Characterization of charge variants of a monoclonal antibody using weak anion exchange chromatography at subunit levels', *Analytical Biochemistry*. Elsevier Inc, 520, pp. 49–57. doi: 10.1016/j.ab.2016.12.017.

Pozarowski, P. and Darzynkiewicz, Z. (2004) 'Analysis of cell cycle by flow cytometry.', *Methods Mol Biol*, 281, pp. 301–311. doi: 10.1385/1-59259-811-0:301.

Pozo-Guisado, E. *et al.* (2002) 'The antiproliferative activity of resveratrol results in apoptosis in MCF-7 but not in MDA-MB-231 human breast cancer cells: Cell-specific alteration of the cell cycle', *Biochemical Pharmacology*, 64(9), pp. 1375–1386. doi: 10.1016/S0006-2952(02)01296-0.

Prabhu, A., Gadre, R. and Gadgil, M. (2018) 'Zinc supplementation decreases galactosylation of recombinant IgG in CHO cells', *Applied Microbiology and Biotechnology*. Applied Microbiology and Biotechnology, 102(14), pp. 5989–5999. doi: 10.1007/s00253-018-9064-8.

Prasad, S., Khadatare, P. B. and Roy, I. (2011) 'Effect of Chemical Chaperones in Improving the Solubility of Recombinant Proteins in Escherichia coli', *Applied and Environmental Microbiology*, 77(13), pp. 4603–4609. doi: 10.1128/AEM.05259-11.

Puck, T. T., Cieciura, S. J. and Robinson, A. (1958) *Long-Term Cultivation of Euploid Cells From Human and Animal Subjects*, *Genetics of somatic mammalian cells*.

Quoc Trung, L. *et al.* (2013) 'Resveratrol Induces Cell Cycle Arrest and Apoptosis in Malignant NK Cells via JAK2/STAT3 Pathway Inhibition', *PLoS ONE*, 8(1). doi: 10.1371/journal.pone.0055183.

Della Ragione, F. *et al.* (1998) 'Resveratrol arrests the cell division cycle at S/G2 phase transition.', *Biochemical and biophysical research communications*, 250(1), pp. 53–58. doi: 10.1006/bbrc.1998.9263.

Reinhart, D. *et al.* (2014) 'In search of expression bottlenecks in recombinant CHO cell lines - A case study', *Applied Microbiology and Biotechnology*, 98(13), pp. 5959–5965. doi: 10.1007/s00253-014-5584-z.

Ren, D. *et al.* (2009) 'An improved trypsin digestion method minimizes digestion-induced modifications on proteins', *Analytical Biochemistry*. Elsevier Inc., 392(1), pp. 12–21. doi: 10.1016/j.ab.2009.05.018.

Renard, J. M. *et al.* (1988) 'Evidence that monoclonal antibody production kinetics is related to the integral of the viable cells curve in batch systems', *Biotechnology Letters*, 10(2), pp. 91–96.

Robb, E. L. and Stuart, J. A. (2014) 'The stilbenes resveratrol, pterostilbene and piceid affect growth and stress resistance in mammalian cells via a mechanism requiring estrogen receptor beta and the induction of Mn-superoxide dismutase', *Phytochemistry*. Elsevier Ltd, 98, pp. 164–173. doi: 10.1016/j.phytochem.2013.11.019.

Robben, J. H. *et al.* (2006) 'Rescue of Vasopressin V2 Receptor Mutants by Chemical Chaperones: Specificity and Mechanism', *Molecular biology of the cell*, 17(January), pp. 379–386. doi: 10.1091/mbc.E05.

Roth, A., Schaffner, W. and Hertel, C. (1999) 'Phytoestrogen kaempferol (3,4',5,7-tetrahydroxyflavone) protects PC12 and T47D cells from ??-amyloid-induced toxicity', *Journal of Neuroscience Research*, 57(3), pp. 399–404. doi: 10.1002/(SICI)1097-4547(19990801)57:3<399::AID-JNR12>3.0.CO;2-W.

Roth, S. D. *et al.* (2012) 'Chemical Chaperones Improve Protein Secretion and Rescue Mutant Factor

VIII in Mice with Hemophilia A', *PLoS ONE*, 7(9). doi: 10.1371/journal.pone.0044505.

Rubiolo, J. A. *et al.* (2012) 'Resveratrol Inhibits Proliferation of Primary Rat Hepatocytes in G0/G1 by Inhibiting DNA Synthesis', *Folia Biologica*, 58(4), pp. 166–172.

Ryu, J. S. *et al.* (2000) 'Osmoprotective effect of glycine betaine on foreign protein production in hyperosmotic recombinant Chinese hamster ovary cell cultures differs among cell lines', *Biotechnology and Bioengineering*, 70(2), pp. 167–175. doi: 10.1002/1097-0290(20001020)70:2<167::AID-BIT6>3.0.CO;2-P.

Sainz, R. M. *et al.* (2003) 'Antioxidant activity of melatonin in Chinese hamster ovarian cells: Changes in cellular proliferation and differentiation', *Biochemical and Biophysical Research Communications*, 302(3), pp. 625–634. doi: 10.1016/S0006-291X(03)00230-4.

Sakakibara, D. *et al.* (2009) 'Protein structure determination in living cells by in-cell NMR spectroscopy', *Nature*, 458(7234), pp. 102–105. doi: 10.1038/nature07814.

Sambrook, J. F. (1990) 'The involvement of calcium in transport of secretory proteins from the endoplasmic reticulum', *Cell*, 61(2), pp. 197–199. doi: 10.1016/0092-8674(90)90798-J.

Saphire, E. O. *et al.* (2002) 'Contrasting IgG Structures Reveal Extreme Asymmetry and Flexibility', *Journal of Molecular Biology*, 319, pp. 9–18. doi: 10.1016/S0022-2836(02)00244-9.

Sato, N. *et al.* (2004) 'Fluctuation of chromatin unfolding associated with variation in the level of gene expression', *PLoS ONE*, 4(7), pp. 619–630. doi: 10.1371/journal.pone.0008432.

Schlatter, S. *et al.* (2005) 'On the optimal ratio of heavy to light chain genes for efficient recombinant antibody production by CHO cells.', *Biotechnology progress*, 21(1), pp. 122–33. doi: 10.1021/bp049780w.

Schuler, M. *et al.* (2010) 'Evaluation of phenolphthalein, diazepam and quinacrine dihydrochloride in the in vitro mammalian cell micronucleus test in Chinese hamster ovary (CHO) and TK6 cells', *Mutation Research - Genetic Toxicology and Environmental Mutagenesis*. Elsevier B.V., 702(2), pp. 219–229. doi:

10.1016/j.mrgentox.2010.04.004.

Shabana, S. M. *et al.* (2014) 'Anti-Proliferative and Pro-Apoptotic Effects of (-)-Epigallocatechin-3-Gallate Encapsulated in Chitosan Nanoparticles on Human Prostate Carcinoma Cells', *Journal of Pharmaceutics & Pharmacology*, 2(1), pp. 1–8. doi: 10.13188/2327-204X.1000007.

Sheikholeslami, Z., Jolicoeur, M. and Henry, O. (2013) 'The impact of the timing of induction on the metabolism and productivity of CHO cells in culture', *Biochemical Engineering Journal*. Elsevier B.V., 79, pp. 162–171. doi: 10.1016/j.bej.2013.07.015.

Shen, F. J. *et al.* (1996) 'The Application of tert-Butylhydroperoxide Oxidation to Study Sites of Potential Methionine Oxidation in a Recombinant Antibody', *Analytical Chemistry Dept. Genentech, Inc*, pp. 275–284.

Shen, X. *et al.* (2014) 'Epigallocatechin-3-gallate inhibits cell growth, induces apoptosis and causes S phase arrest in hepatocellular carcinoma by suppressing the AKT pathway', *International Journal of Oncology*, 44(3), pp. 791–796. doi: 10.3892/ijo.2014.2251.

Soloneski, S., Reigosa, M. A. and Larramendy, M. L. (2003) 'Vitamin E prevents ethylene bis(dithiocarbamate) pesticide zineb-induced sister chromatid exchange in Chinese hamster ovary cells', *Mutagenesis*, 18(6), pp. 505–510. doi: 10.1093/mutage/geg026.

Song, Y. S. *et al.* (2002) 'Caffeic acid phenethyl ester inhibits nitric oxide synthase gene expression and enzyme activity', *Cancer Letters*, 175(1), pp. 53–61. doi: 10.1016/S0304-3835(01)00787-X.

Storniolo, C. E. *et al.* (2014) 'Classification of Chemical Chaperones Based on Their Effect on Protein Folding Landscapes', *Journal of Biological Chemistry*. Elsevier Inc., 6(1), pp. 1–12. doi: 10.1371/journal.pone.0054505.

Su, D. *et al.* (2013) 'Comparision of Piceid and Resveratrol in Antioxidation and Antiproliferation Activities In Vitro', *PLoS ONE*, 8(1). doi: 10.1371/journal.pone.0054505.

Subramanian, M., Soundar, S. and Mangoli, S. (2016) 'DNA damage is a late event in resveratrol-

mediated inhibition of *Escherichia coli*', *Free Radical Research*, 50(7), pp. 708–719. doi: 10.3109/10715762.2016.1169404.

Sunley, K. and Butler, M. (2010) 'Strategies for the enhancement of recombinant protein production from mammalian cells by growth arrest', *Biotechnology Advances*. Elsevier Inc., 28(3), pp. 385–394. doi: 10.1016/j.biotechadv.2010.02.003.

Tae Kyung, K. *et al.* (2000) 'Osmoprotective effect of glycine betaine on thrombopoietin production in hyperosmotic Chinese hamster ovary cell culture: Clonal variations', *Biotechnology Progress*, 16(5), pp. 775–781. doi: 10.1021/bp000106y.

Tai, M. *et al.* (2015) 'Protective effects of luteolin against acetaminophen-induced acute liver failure in mouse', *International Immunopharmacology*. Elsevier B.V., 27(1), pp. 164–170. doi: 10.1016/j.intimp.2015.05.009.

Tan, X. *et al.* (2000) 'Differences of four catechins in cell cycle arrest and induction of apoptosis in LoVo cells', *Cancer Letters*, 158(1), pp. 1–6. doi: 10.1016/S0304-3835(00)00445-6.

Tang, L. *et al.* (2013) 'Conformational characterization of the charge variants of a human IgG1 monoclonal antibody using H/D exchange mass spectrometry', *mAbs*, 5(1), pp. 114–125. doi: 10.4161/mabs.22695.

Tatsumi, K. and Strauss, B. S. (1979) 'Accumulation of DNA growing points in caffeine-treated human lymphoblastoid cells', *Journal of Molecular Biology*, 135(2), pp. 435–449. doi: 10.1016/0022-2836(79)90445-5.

Thompson, L. H. and Baker, R. M. (1973) 'Isolation of Mutants of Cultured Mammalian Cells', *Methods in Cell Biology*, 6, pp. 209–281.

Thorpe, A. S. *et al.* (2009) 'Root exudate is allelopathic in invaded community but not in native community: Field evidence for the novel weapons hypothesis', *Journal of Ecology*, 97(4), pp. 641–645. doi: 10.1111/j.1365-2745.2009.01520.x.

Tian, J. (2016) 'WO 2016/130734 Al'.

Torkashvand, F. and Vaziri, B. (2017) 'Main Quality Attributes of Monoclonal Antibodies and Effect of Cell Culture Components', *Iranian biomedical journal*, 21(3), pp. 131–141. doi: 10.18869/acadpub.ibj.21.3.131.

Traganos, F., Kaminska-Eddy, B. and Darzynkiewicz, Z. (1991) 'Caffeine reverses the cytotoxic and cell kinetic effects of Novantrone (mitoxantrone)', *Cell Proliferation*, 24(3), pp. 305–319. doi: 10.1111/j.1365-2184.1991.tb01159.x.

Traversi, G. *et al.* (2016) 'Resveratrol and its methoxy-derivatives as modulators of DNA damage induced by ionising radiation', *Mutagenesis*, 31(4), pp. 433–441. doi: 10.1093/mutage/gew002.

Trummer, E. *et al.* (2006) 'Process Parameter Shifting: Part I. Effect of DOT, pH, and Temperature on the Performance of Epo-Fc Expressing CHO Cells Cultivated in Controlled Batch Bioreactors', *Bioresource and Bioengineering*, 94(6), pp. 1033–1044. doi: 10.1002/bit.

Trung, L. Q. *et al.* (2015) 'Resveratrol selectively induces apoptosis in malignant cells with the JAK2V617F mutation by inhibiting the JAK2 pathway', *Molecular Nutrition and Food Research*, 59(11), pp. 2143–2154. doi: 10.1002/mnfr.201500166.

Tsao, Y. S. *et al.* (2005) 'Monitoring Chinese hamster ovary cell culture by the analysis of glucose and lactate metabolism', *Journal of Biotechnology*, 118, pp. 316–327. doi: 10.1016/j.jbiotec.2005.05.016.

Uchiumi, F. *et al.* (2016) 'The effect of trans-resveratrol on the expression of the human DNA-repair associated genes', *Integrative Molecular Medicine*, 3(5), pp. 783–792. doi: 10.15761/IMM.1000246.

Urlaub, G. *et al.* (1983) 'Deletion of the Diploid Dihydrofolate reductase Locus from Cultured MAmmalian Cells', *Cell*, 33, pp. 405–412.

Urlaub, G. and Chasin, L. a (1980) 'Isolation of Chinese hamster cell mutants deficient in dihydrofolate reductase activity.', *Proceedings of the National Academy of Sciences of the United States of America*, 77(7), pp. 4216–4220. doi: VL - 77.

Vergara, M. *et al.* (2014) 'Differential effect of culture temperature and specific growth rate on CHO cell behavior in chemostat culture', *PLoS ONE*, 9(4), pp. 1–6. doi: 10.1371/journal.pone.0093865.

Vlasak, J. *et al.* (2009) 'Identification and characterization of asparagine deamidation in the light chain CDR1 of a humanized IgG1 antibody', *Analytical Biochemistry*. Elsevier Inc., 392(2), pp. 145–154. doi: 10.1016/j.ab.2009.05.043.

Walsh, G. (2010) 'Biopharmaceutical benchmarks 2010', *Nature*, 28(9), pp. 917–924.

Walsh, G. (2014) 'Biopharmaceutical benchmarks 2014', *Nature*, 32(10), pp. 992–1000. doi: http://dx.doi.org/10.1038/nbt.3040.

Walsh, G. and Jefferis, R. (2006) 'Post-translational modifications in the context of therapeutic proteins', *Nature Biotechnology*, 24(10), pp. 1241–1252. doi: 10.1038/nbt1252.

Wang, K. *et al.* (2016) 'Effects of Chinese Propolis in Protecting Bovine Mammary Epithelial Cells against Mastitis Pathogens-Induced Cell Damage', *Mediators of Inflammation*. Hindawi Publishing Corporation, 2016. doi: 10.1155/2016/8028291.

Wang, Q., Groenendyk, J. and Michalak, M. (2015) 'Glycoprotein Quality Control and Endoplasmic Reticulum Stress', *Molecules*, 20(8), pp. 13689–13704. doi: 10.3390/molecules200813689.

Wei, Z. *et al.* (2007) 'Identification of a Single Tryptophan Residue as Critical for Binding Activity in a Humanized Monoclonal Antibody against Respiratory Syncytial Virus', *Analytical Chemistry*, 79(7), pp. 2797–2805.

Wiebe, M. E. *et al.* (1989) 'A multifaced approach to assure that recombinant T-Pa is free of adventittious virus', *Developments in Biological Standardization*, pp. 147–148.

Wright, H. T. and Urry, D. W. (2008) 'Nonenzymatic Deamidation of Asparaginyl and Glutaminyl Residues in Protein', *Critical Reviews in Biotechnology and Molecular Biology*, 26(1), pp. 1–52. doi: 10.3109/10409239109081719.

Wu, J. *et al.* (2015) 'Quercetin, luteolin and epigallocatechin gallate alleviate TXNIP and NLRP3-mediated inflammation and apoptosis with regulation of AMPK in endothelial cells', *European Journal of Pharmacology*, 745, pp. 59–68. doi: 10.1016/j.ejphar.2014.09.046.

Wurm, F. (2013) 'CHO Quasispecies—Implications for Manufacturing Processes', *Processes*, 1(3), pp. 296–311. doi: 10.3390/pr1030296.

Wurm, F. M. (2004) 'Production of recombinant protein therapeutics in cultivated mammalian cells.', *Nature biotechnology*, 22(11), pp. 1393–1398. doi: 10.1038/nbt1026.

Wurm, F. M. and Hacker, D. (2011) 'First CHO genome', *Nature Biotechnology*. Nature Publishing Group, 29(8), pp. 718–720. doi: 10.1038/nbt.1943.

Xu, X. *et al.* (2011) 'The genomic sequence of the Chinese hamster ovary (CHO)-K1 cell line', *Nature Biotechnology*. Nature Publishing Group, 29(8), pp. 735–741. doi: 10.1038/nbt.1932.

Xue, Y., Dong, J. and Liang, J. (2016) 'Chinese hamster ovary-sphingomyelin synthase2 biospecific extraction and liquid chromatography with tandem mass spectrometry analysis for the prediction of bioactive components of Rhizoma Polygoni Cuspidati', *Journal of Separation Science*, 39(6), pp. 1067–1072. doi: 10.1002/jssc.201501075.

Yam, G. H. F. *et al.* (2007) 'Sodium 4-phenylbutyrate acts as a chemical chaperone on misfolded myocilin to rescue cells from endoplasmic reticulum stress and apoptosis', *Investigative Ophthalmology and Visual Science*, 48(4), pp. 1683–1690. doi: 10.1167/iovs.06-0943.

Yan, D., Geusz, M. E. and Jamasbi, R. J. (2012) 'Properties of Lewis Lung Carcinoma Cells Surviving Curcumin Toxicity', *Journal of Cancer*, 3, pp. 32–41. doi: 10.7150/jca.3659.

Yang, W. C., Lu, J. and Nguyen, N. B. (2014) 'Addition of Valproic Acid to CHO Cell Fed-Batch Cultures Improves Monoclonal Antibody Titers', *Molecular Biotechnology*, 56, pp. 421–428. doi: 10.1007/s12033-013-9725-x.

Ye, F. *et al.* (2017) 'Epigallocatechin gallate has pleiotropic effects on transmembrane signaling by

altering the embedding of transmembrane domains', *Journal of Biological Chemistry*, 292(24), pp. 9858–9864. doi: 10.1074/jbc.C117.787309.

Yeh, H. W. *et al.* (2009) 'Comparative cytotoxicity of five current dentin bonding agents: Role of cell cycle deregulation', *Acta Biomaterialia*. Acta Materialia Inc., 5(9), pp. 3404–3410. doi: 10.1016/j.actbio.2009.05.036.

Yoon, S. K. and Ahn, Y. (2007) 'Effect of Glycine Betaine on Follicle-Stimulating Hormone Production by Chinese Hamster Ovary Cells at Low Culture Temperature', *Korean Society for Biotechnology and Bioengineering Journal*, 22(2), pp. 109–113.

Zhang, J. *et al.* (2010) 'Discovery and synthesis of novel luteolin derivatives as DAT agonists', *Bioorganic and Medicinal Chemistry*. Elsevier Ltd, 18(22), pp. 7842–7848. doi: 10.1016/j.bmc.2010.09.049.

Zhang, J. J. *et al.* (2010) 'Discovery and synthesis of novel luteolin derivatives as DAT agonists Jiange', *Bioorganic & Medicinal Chemistry*. Elsevier Ltd, 18, pp. 7842–7848. doi: 10.1016/j.fct.2013.02.022.

Zhang, W. and Czupryn, M. J. (2002) 'Free Sulfhydryl in Recombinant Monoclonal Antibodies', *Biotechnology Progress*, 18, pp. 509–513.

Zhang, Y. *et al.* (2013) 'Transport by OATP1B1 and OATP1B3 enhances the cytotoxicity of epigallocatechin 3-O-gallate and several quercetin derivatives', *Journal of Natural Products*, 76(3), pp. 368–373. doi: 10.1021/np3007292.

Zhao, G. *et al.* (2010) 'Neurochemistry International Functional activation of monoamine transporters by luteolin and apigenin isolated from the fruit of Perilla frutescens (L .) Britt', 56, pp. 168–176. doi: 10.1016/j.neuint.2009.09.015.

Zhou, J.-H. *et al.* (2011) 'Resveratrol induces apoptosis in pancreatic cancer cells.', *Chinese medical journal*, 124(11), pp. 1695–9. doi: 10.3760/cma.j.issn.0366-6999.2011.11.017.

Zhu, H. (2012) 'Cell Cycle Analysis Using Propidium Iodide Staining with GFP Detection', *bio-protocol*,

2(7), pp. 1–3.

Zhu, J. (2012) 'Mammalian cell protein expression for biopharmaceutical production', *Biotechnology Advances*. Elsevier Inc., 30(5), pp. 1158–1170. doi: 10.1016/j.biotechadv.2011.08.022.

Appendices

Appendices

9.1 Appendix 1: Calculation of LC_{50} and GI_{50}

Luis Toronjo Urquiza

23/12/2018

```
########################
# Calculation of LC50 #
########################

calcula.lc <- function(status, conc, lc=0.5, alfa=0.05, func='probit', arr
ed=2)
{
  #Testing if status is a matrix with 2 columns
  if(!is.matrix(status))
    stop('The status matrix must be a matrix with 2 columns')
  else{
    if(dim(status)[2]!=2)stop('The status matrix must have 2 column')
  }
  #A function to invert the linear function from a model object, eg. x=(y-
a)/b
  invlin<-function(x,y){
    return((y-x$coef[1])/x$coef[2])
  }
  #The model itself with the matrix as the outcome and the concentration v
ector as the independent
  modelo<-glm(status~conc, family = binomial(func))
  #Getting the significance for the model
  signif<-as.numeric(anova(modelo, test='Chisq')[2,c(1,4:5)])
  #Getting the point estimate from the model for the desired LC(default=50
%-0.5)
  fit<-as.numeric(invlin(modelo, family(modelo)$linkfun(lc)))
  #Getting the standard error of the estimate, in the link function scale
  erro<-predict(modelo, se.fit=T, type='response', newdata=data.frame(conc
=fit))$se.fit
  #Calculating the lower and upper CI based on the error and the chosen al
pha (defaults to 95%CI)
  lwr<-invlin(modelo, family(modelo)$linkfun(lc+qnorm(alfa/2)*erro))
  upr<-invlin(modelo, family(modelo)$linkfun(lc-qnorm(alfa/2)*erro))
  #Packaging everything in an object to be returned
  lc_resp<-round(data.frame(lc,fit,lwr,upr), arred)
  #For the Anova, special rounding is required
  lc_resp<-cbind(lc_resp, df=round(signif[1]), chisq=round(signif[2],2), p
val=signif[3])
  #Returning the object
```

```
  return(lc_resp)
}


LC50<-read.csv('LC50.csv',na.strings=c("","  ","NA"))


Treatment<-c(unique(as.character(LC50$Treatment)))

LCAll1<-matrix(NA,nrow=length(Treatment),ncol =8 )

colnames(LCAll1)<- c('Treatment','Measurement', '[LC50]','Lower','Upper','
df','ChiSq','p-val')

for (dx in 1:length(Treatment)){

  Treat<-Treatment[dx]

  LC50loop<-subset(LC50[,c(2:length(LC50))],LC50$Treatment==Treatment[[dx]
])

  LC50loop<-LC50loop[1:24,]

  if (nrow(subset(LC50loop, is.na(LC50loop$live.cells)))<length(LC50loop$l
ive.cells)){

    LC50loop<-as.matrix(LC50loop)

    rslt<-calcula.lc(LC50loop[,c("live.cells","dead.cells")],LC50loop[,c("
Concentration")])


    LCAll1[dx,2]<-rslt[1,1]
    LCAll1[dx,3]<-rslt[1,2]
    LCAll1[dx,4]<-rslt[1,3]
    LCAll1[dx,5]<-rslt[1,4]
    LCAll1[dx,6]<-rslt[1,5]
    LCAll1[dx,7]<-rslt[1,6]
    LCAll1[dx,8]<-rslt[1,7]
  }
  LCAll1[dx,1]<-Treatment[dx]
}



LCAll2<-matrix(NA,nrow=length(Treatment),ncol =8 )

colnames(LCAll2)<- c('Treatment','Measurement', '[LC50]','Lower','Upper','
df','ChiSq','p-val')

for (dx in 1:length(Treatment)){
```

```
  Treat<-Treatment[dx]

  LC50loop<-subset(LC50[,c(2:length(LC50))],LC50$Treatment==Treatment[[dx]
])

  LC50loop<-LC50loop[25:length(LC50loop[,1]),]


  if (nrow(subset(LC50loop, is.na(LC50loop$live.cells)))<length(LC50loop$l
ive.cells)){

    LC50loop<-as.matrix(LC50loop)

    rslt<-calcula.lc(LC50loop[,c("live.cells","dead.cells")],LC50loop[,c("
Concentration")])


    LCAll2[dx,2]<-rslt[1,1]
    LCAll2[dx,3]<-rslt[1,2]
    LCAll2[dx,4]<-rslt[1,3]
    LCAll2[dx,5]<-rslt[1,4]
    LCAll2[dx,6]<-rslt[1,5]
    LCAll2[dx,7]<-rslt[1,6]
    LCAll2[dx,8]<-rslt[1,7]
  }
  LCAll2[dx,1]<-Treatment[dx]
}

LCAll<-matrix(NA,nrow=length(Treatment),ncol =8 )

colnames(LCAll)<- c('Treatment','Measurement', '[LC50]','Lower','Upper','d
f','ChiSq','p-val')

for (dx in 1:length(Treatment)){

  Treat<-Treatment[dx]

  LC50loop<-(subset(LC50[,c(2:length(LC50))],LC50$Treatment==Treatment[[dx
]]))


  if (nrow(subset(LC50loop, is.na(LC50loop$live.cells)))<length(LC50loop$l
ive.cells)){

    LC50loop<-as.matrix(LC50loop)

    rslt<-calcula.lc(LC50loop[,c("live.cells","dead.cells")],LC50loop[,c("
Concentration")])

    LCAll[dx,2]<-rslt[1,1]
    LCAll[dx,3]<-rslt[1,2]
    LCAll[dx,4]<-rslt[1,3]
```

```
    LCAll[dx,5]<-rslt[1,4]
    LCAll[dx,6]<-rslt[1,5]
    LCAll[dx,7]<-rslt[1,6]
    LCAll[dx,8]<-rslt[1,7]
  }
  LCAll[dx,1]<-Treatment[dx]
}


write.csv(LCAll,file='LC50Results.csv')


################################################################################
################################################################################

################################################################################
################################################################################



########################
# Calculation of GI50 #
########################

calcula.lc <- function(status, conc, lc=0.5, alfa=0.05, func='probit', arr
ed=2)
{
  #Testing if status is a matrix with 2 columns
  if(!is.matrix(status))
    stop('The status matrix must be a matrix with 2 columns')
  else{
    if(dim(status)[2]!=2)stop('The status matrix must have 2 column')
  }
  #A function to invert the linear function from a model object, eg. x=(y-
a)/b
  invlin<-function(x,y){
    return((y-x$coef[1])/x$coef[2])
  }
  #The model itself with the matrix as the outcome and the concentration v
ector as the independent
  modelo<-glm(status~conc, family = binomial(func))
  #Getting the significance for the model
  signif<-as.numeric(anova(modelo, test='Chisq')[2,c(1,4:5)])
  #Getting the point estimate from the model for the desired LC(default=50
%-0.5)
  fit<-as.numeric(invlin(modelo, family(modelo)$linkfun(lc)))
  #Getting the standard error of the estimate, in the link function scale
  erro<-predict(modelo, se.fit=T, type='response', newdata=data.frame(conc
=fit))$se.fit
  #Calculating the lower and upper CI based on the error and the chosen al
pha (defaults to 95%CI)
  lwr<-invlin(modelo, family(modelo)$linkfun(lc+qnorm(alfa/2)*erro))
  upr<-invlin(modelo, family(modelo)$linkfun(lc-qnorm(alfa/2)*erro))
```

```
  #Packaging everything in an object to be returned
  lc_resp<-round(data.frame(lc,fit,lwr,upr), arred)
  #For the Anova, special rounding is required
  lc_resp<-cbind(lc_resp, df=round(signif[1]), chisq=round(signif[2],2), p
val=signif[3])
  #Returning the object
  return(lc_resp)
}

GI50<-read.csv('GI50.csv',na.strings=c("","  ","NA"))

GI50$Rlt.Growth<-round(GI50$Rlt.Growth)

GI50$Rlt.Inhibit<-round(GI50$Rlt.Inhibit)

Treatment<-c(unique(as.character(GI50$Treatment)))

GIAll1<-matrix(NA,nrow=length(Treatment),ncol =8 )

colnames(GIAll1)<- c('Treatment','Measurement', '[GI50]','Lower','Upper','
df','ChiSq','p-val')

for (dx in 1:length(Treatment)){

  Treat<-Treatment[dx]

  GI50loop<-subset(GI50[,c(2:length(GI50))],GI50$Treatment==Treatment[[dx]
])

  GI50loop<-GI50loop[1:24,]

  if (nrow(subset(GI50loop, is.na(GI50loop$Rlt.Growth)))<length(GI50loop$R
lt.Growth)){

    GI50loop<-as.matrix(GI50loop)

    rslt<-calcula.lc(GI50loop[,c("Rlt.Growth","Rlt.Inhibit")],GI50loop[,c(
"Concentration")])


    GIAll1[dx,2]<-rslt[1,1]
    GIAll1[dx,3]<-rslt[1,2]
    GIAll1[dx,4]<-rslt[1,3]
    GIAll1[dx,5]<-rslt[1,4]
    GIAll1[dx,6]<-rslt[1,5]
    GIAll1[dx,7]<-rslt[1,6]
    GIAll1[dx,8]<-rslt[1,7]
  }
  GIAll1[dx,1]<-Treatment[dx]
}
```

```
GIAll2<-matrix(NA,nrow=length(Treatment),ncol =8 )

colnames(GIAll2)<- c('Treatment','Measurement', '[GI50]','Lower','Upper','
df','ChiSq','p-val')

for (dx in 1:length(Treatment)){

  Treat<-Treatment[dx]

  GI50loop<-subset(GI50[,c(2:length(GI50))],GI50$Treatment==Treatment[[dx]
])

  GI50loop<-GI50loop[25:length(GI50loop[,1]),]


  if (nrow(subset(GI50loop, is.na(GI50loop$Rlt.Growth)))<length(GI50loop$R
lt.Growth)){

    GI50loop<-as.matrix(GI50loop)

    rslt<-calcula.lc(GI50loop[,c("Rlt.Growth","Rlt.Inhibit")],GI50loop[,c(
"Concentration")])


    GIAll2[dx,2]<-rslt[1,1]
    GIAll2[dx,3]<-rslt[1,2]
    GIAll2[dx,4]<-rslt[1,3]
    GIAll2[dx,5]<-rslt[1,4]
    GIAll2[dx,6]<-rslt[1,5]
    GIAll2[dx,7]<-rslt[1,6]
    GIAll2[dx,8]<-rslt[1,7]
  }
  GIAll2[dx,1]<-Treatment[dx]
}

GIAll<-matrix(NA,nrow=length(Treatment),ncol =8 )

colnames(GIAll)<- c('Treatment','Measurement', '[GI50]','Lower','Upper','d
f','ChiSq','p-val')

for (dx in 1:length(Treatment)){

  Treat<-Treatment[dx]

  GI50loop<-(subset(GI50[,c(2:length(GI50))],GI50$Treatment==Treatment[[dx
]]))


  if (nrow(subset(GI50loop, is.na(GI50loop$Rlt.Growth)))<length(GI50loop$R
lt.Growth)){
```

```
    GI50loop<-as.matrix(GI50loop)

    rslt<-calcula.lc(GI50loop[,c("Rlt.Growth","Rlt.Inhibit")],GI50loop[,c(
"Concentration")])

    GIAll[dx,2]<-rslt[1,1]
    GIAll[dx,3]<-rslt[1,2]
    GIAll[dx,4]<-rslt[1,3]
    GIAll[dx,5]<-rslt[1,4]
    GIAll[dx,6]<-rslt[1,5]
    GIAll[dx,7]<-rslt[1,6]
    GIAll[dx,8]<-rslt[1,7]
  }
  GIAll[dx,1]<-Treatment[dx]
}


write.csv(GIAll,file='GI50Results.csv')
```

9.2 Appendix 1: Cell growth curves for IgG characterization experiments

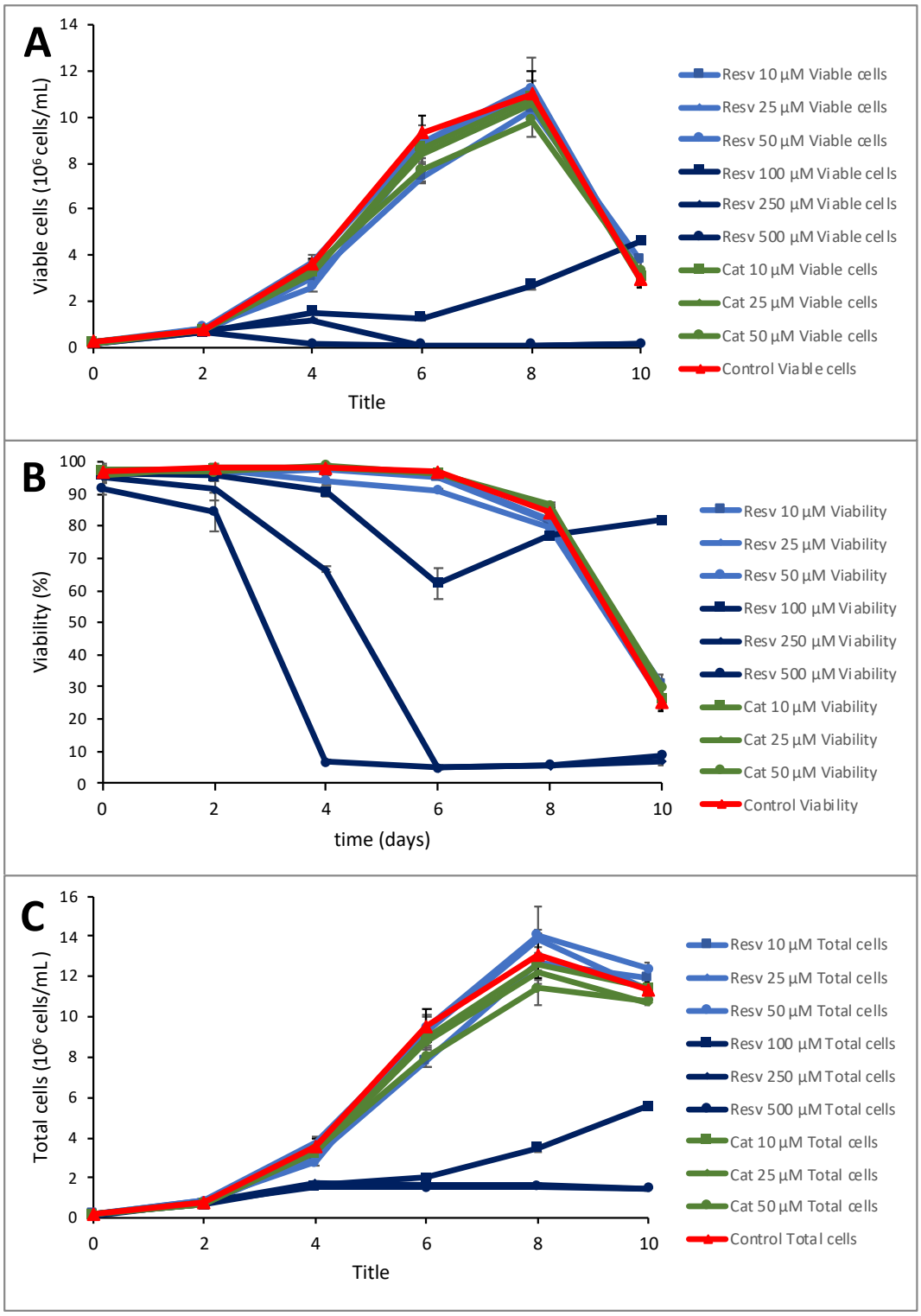

Effect of catechin (Cat) (green) and resveratrol (Resv)(blue) treatments in viable cell density (A), viability (B) and total cell density (C) when added at days 3 for different concentrations. Cells were incubated in 125mL Erlenmeyer flasks with initial 33 mL volume for 10 days under shaking conditions. The error bars represent the standard deviation of triplicates and the experiment was carried twice independently.

9.3 Appendix 3: SDS-PAGE of purified IgG

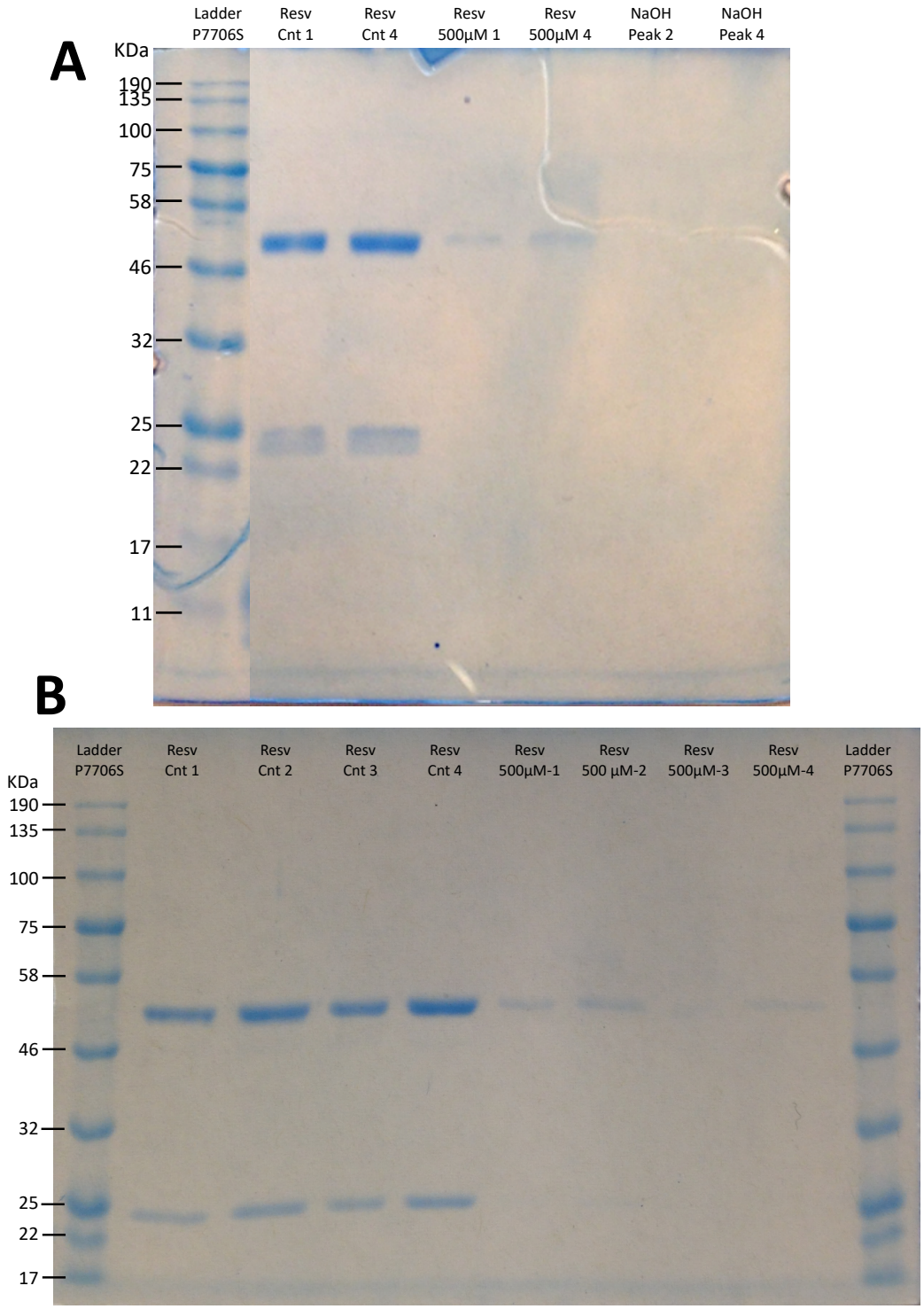

SDS-PAGE gels of initial and final sample purified for each batch. Preliminary (A) and final gel (B) done with control (Cnt), resveratrol (Resv) at 500 µM treatment and final wash (NaOH peak) samples from purified IgG recombinant proteins produced in CHO cell line.

9.4 Appendix 2: Alignment of CEX spectra and quantification of basic and acidic species

Luis Toronjo Urquiza

23/12/2018

```
#######################################################
# alignment of cation exchange chromatograms and  #
# quantification of acidic and basic species for  #
#                    Resveratrol                  #
#######################################################

library(sp)
library(raster)
library(ncdf4)
#library(NoiseFiltersR)
library(readxl)

#First we collect the files from chromeleon and extract the data from them
and save then in csv files to be later processed

#insert a table with the number of files from chromeleon that need to be a
nalysed(.CDF)
# and the corresponding names of the sample types (Control Resv Cat etc)
flnams<-read_excel('filenames.xlsx',col_names=F) #we want this file to be
excel because that way it can be differentiated
# the created files are .csv and the software for alignment mistaken it fo
r reading file
colnames(flnams)<-c('file','name')

#pre-determine parameters of time of measurement
mintime<-NULL
maxtime<-NULL
maxreading<-NULL


#create a loop that will go through the filenames extracting the files one
by one
for (xxd in 1:length(flnams$file)){

  #select the file we want to work on
  tempfl<-as.character(flnams$file[[xxd]])

  #opens the file
  test<-nc_open(tempfl)

  #this command shows all the variables in the spectrum file
```

```
  #attributes(test$var)

  ### get the desired variables out of the file ###

  # outputs the intensity of the signal (y-axis) dependent variable
  intensity<-ncvar_get(test,'ordinate_values')

  ##outputs the length (time) of the chromatogram
  #actual_run_time_length<-ncvar_get(test,'actual_run_time_length')

  #length of time between data points (in seconds)
  timeinterval<-ncvar_get(test,'actual_sampling_interval')

  #creates a vector that matches the time of acquisition of the intensity
values
  time<-seq_along(intensity)*timeinterval

  #creates the table joining both time and intensity variables
  chrom<-as.data.frame(cbind(time,intensity))

  #we need to select the right range of the spectra to study (from minute
2.5 to 17.75 MINUTES is the entire time of chromatography)
  #this time was selected based on a high intensity chromatogram obtained
from high concentrated Fujifilm IgG samples.
  chrom<-chrom[17000:156000,]


  #create a csv document in the directory to later analyse
  write.table(chrom,paste(as.character(flnams$name[[xxd]]), ".csv", sep =
""),sep=' ', row.names=FALSE,col.names=FALSE)

  #this actualizes the extreme values for time and intensity, if a value i
s more extreme it refreshes it
  mintime<-min(c(mintime,min(chrom$time)))
  maxtime<-max(c(maxtime,max(chrom$time)))
  maxreading<-max(c(maxreading,max(chrom$intensity)))


}




### COMPILE ALL SPECTRA ###

library(ChemoSpec) #used for the alignment and correction for the spectra
#library(R.utils)
library(baseline)


#creates a file that combines all the spectra csv files together, make sur
```

```
e is empty of other csv files as the program will pick them
#all the same and will cause errors
ssp <- files2SpectraObject(
  gr.crit = c('Control','Resv010','Resv025','Resv050','Resv100'),
  freq.unit = "time(seconds)",
  int.unit = "mAU(280nm)",
  descrip = "Control",
  #,out.file = "mydata"
  debug=T
)

#command that shows the general info of the spectra
sumSpectra(ssp)

# command that works for ploting the graphs
plotSpectra(ssp,
            which = c(4,8,12,16,20),
            yrange = c(0, (maxreading+(maxreading/10)*4)),
            offset = maxreading/10,
            lab.pos = mintime*1.5,
            xlim = c(mintime, maxtime)
)




### ALIGN SPECTRA ###

#library('BiocManager') #pakcages for alignment
#library('MassSpecWavelet')
#library('impute')
#library(speaq)
# Does alignment, but since the main point of alignment is the maximum pea
k this method is not efficient
#ssp2<-clupaSpectra(ssp, bT=0.005)


library(Rfast)
# find the max values for all the chromatograms and output the time
allmax<-rowMaxs(ssp$data)


unmatch<-(-allmax+max(allmax))


ssp2<-ssp

# extend the matrix
ssp2$data<-matrix(data=NA,nrow =20,ncol = (length(ssp$data[1,])+ (max(allm
ax)-min(allmax))))
```

```
#reinsert the values to the matrix
for (xxf in 1:length(ssp2$data[,1])){
  ssp2$data[xxf,]<-c(seq(0,0,length.out=unmatch[xxf]),ssp$data[xxf,], seq(
0,0,length.out=(max(allmax)-min(allmax)-unmatch[xxf])))
}

#extend the x axis time
ssp2$freq<-seq(from=ssp$freq[1],by=(ssp$freq[2]-ssp$freq[1]),length.out=le
ngth(ssp2$data[1,]))


# command that works for ploting the graphs for alingment
plotSpectra(ssp2,
            which = c(4,8,12,16,20),
            yrange = c(0, (max(ssp2$data[1,])+(max(ssp2$data[1,]/10)*6))),
            offset = max(ssp2$data[1,]/8),
            lab.pos = min(ssp2$freq)*1.5,
            xlim = c(min(ssp2$freq), max(ssp2$freq))
)



### CUT THE EXCESS ###

#cut the excess of chromatogram. This will leave the same distance to the
maximum peak for all samples
#ensures that if there are any differences in acidic or basic species, the
se are not due to a shift in the retention
#time of the main peak.

#it was decided to cut between 250 and 1400 seconds
#first extract the position of the time values for the ssp2
lowcrop<-which(round(ssp2$freq,digits = 2)==250.00)
highcrop<-which(round(ssp2$freq,digits = 2)==1400.00)

#cut the sides of the time series
ssp2$freq<-ssp2$freq[lowcrop:highcrop]
#cut the sides of the data series
ssp2$data<-ssp2$data[,lowcrop:highcrop]


# command that works for plotting the graphs for alignment
plotSpectra(ssp2,
            which = c(4,8,12,16,20),
            yrange = c(0, (max(ssp2$data[1,])+(max(ssp2$data[1,]/10)*6))),
            offset = max(ssp2$data[1,]/8),
            lab.pos = min(ssp2$freq)*1.5,
            xlim = c(min(ssp2$freq), max(ssp2$freq))
)
```

```
### CREATE BASELINE ###
# creates a baseline for all chromatograms and corrects by it
ssp2<-baselineSpectra(ssp2,
                      int = FALSE,
                      method = "modpolyfit",
                      deg=1, #the higher the degree the further from the d
esired baseline. Linear is the best adjustment for the data in this case
                      retC = TRUE)


### CORRECT NEGATIVE VALUES ###

# we shift all values up to make the minimum value of each spectra 0, this
will help when normalizing all the values
# as negative values subtract the positive ones and the final area of the
curve
# adjusting for baseline could give different cumulative areas other than
one.
for (dxx in 1:length(ssp2$data[,1])){
  ssp2$data[dxx,]<-ssp2$data[dxx,]+abs(min(ssp2$data[dxx,]))
}

# command that works for plotting the graphs for alignment
plotSpectra(ssp2,
            which = c(4,8,12,16,20),
            yrange = c(0, (max(ssp2$data[1,])+(max(ssp2$data[1,]/10)*6))),
            offset = max(ssp2$data[1,]/8),
            lab.pos = min(ssp2$freq)*1.5,
            xlim = c(min(ssp2$freq), max(ssp2$freq))
)


### NORMALIZE ###
#normalization of the data to a total area under the curve of 1
ssp2<-normSpectra(ssp2, method = "TotInt", RangeExpress = NULL)

plotSpectra(ssp2,
            which = c(4,8,12,16,20),
            yrange = c(0, (max(ssp2$data[1,])+(max(ssp2$data[1,]/10)*6))),
            offset = max(ssp2$data[1,]/8),
            lab.pos = min(ssp2$freq)*1.5,
            xlim = c(min(ssp2$freq), max(ssp2$freq))
)



#export the data for  the different spectra but does it in a trasposed for
m
# this leaves rows for time points and columns for spectra
#outputs it as  a data frame and joins the time period

ftr<-NULL
```

```
ftr<-matrix(NA, nrow =length(ssp2$freq), ncol = 2)

ftr[,1]<-ssp2$freq
ftr[,2]<-ssp2$data[1,]
ftr<-as.data.frame(ftr)



# next we need to make the graph smooth so that it is easier to find local
minima and maxima
loessMod10 <- loess(V2~V1, data=ftr, span=0.05)



#this is the formula that fill detect local minima and maxima
findpeaks2 <- function(vec,bw=1,x.coo=c(1:length(vec)))
{
  pos.x.max <- NULL
  pos.y.max <- NULL
  pos.x.min <- NULL
  pos.y.min <- NULL
  for(i in 1:(length(vec)-1))   {       if((i+1+bw)>length(vec)){
    sup.stop <- length(vec)}else{sup.stop <- i+1+bw
    }
    if((i-bw)<1){inf.stop <- 1}else{inf.stop <- i-bw}
    subset.sup <- vec[(i+1):sup.stop]
    subset.inf <- vec[inf.stop:(i-1)]

    is.max   <- sum(subset.inf > vec[i]) == 0
    is.nomin <- sum(subset.sup > vec[i]) == 0

    no.max   <- sum(subset.inf > vec[i]) == length(subset.inf)
    no.nomin <- sum(subset.sup > vec[i]) == length(subset.sup)

    if(is.max & is.nomin){
      pos.x.max <- c(pos.x.max,x.coo[i])
      pos.y.max <- c(pos.y.max,vec[i])
    }
    if(no.max & no.nomin){
      pos.x.min <- c(pos.x.min,x.coo[i])
      pos.y.min <- c(pos.y.min,vec[i])
    }
  }
  return(list(pos.x.max,pos.y.max,pos.x.min,pos.y.min))
}


#run the code to find local minima and maxima and save it as lists
minmax<-findpeaks2(loessMod10$fitted)

# format it into a data frame with two columns (time, intensity)
```

```
tblt<-as.data.frame(rbind(t(rbind(minmax[[1]],minmax[[2]])),t(rbind(minmax
[[3]],minmax[[4]]))))

#organize the maxima and minima chronologically in the data frame
library(dplyr)
tblt<-arrange(tblt,tblt$V1)


#find highest max in the table and output the row position
highestpeak<-which.max(tblt[,2])


# Identify the local minima of the graph before and after the mean peak
lowbond<-tblt$V1[highestpeak-1]
highbond<-tblt$V1[highestpeak+1]


#find the relative areas of the three regions for all the samples

# calculate complete area under the curve, this is important as the proces
s does not lead to equal values
totalarea<-rowSums(ssp2$data)

acid<-rowSums(ssp2$data[,0:lowbond])/totalarea

meanpeak<-rowSums(ssp2$data[,lowbond:highbond])/totalarea

base<-rowSums(ssp2$data[,highbond:length(ssp2$data[1,])])/totalarea



names<-ssp2$names

grps<-ssp2$alt.sym

finaldata<-cbind(names,grps,acid,meanpeak,base)

write.table(finaldata,'finaldata resv.csv', sep=',', row.names=FALSE)


##############################################################################
##############################################################################
```

9.5 Appendix 3: Sequence coverage of LC and HC

Luis Toronjo Urquiza

23/12/2018

```
  ################################################################
  #Code to process de sequence coverage of the Mass Spec results#
  ################################################################

library(readxl) # to read and import excel files
library(magicfor)  # to extract data from for loop
library(seqinr) # to import sequences from fasta files
library(tibble) # to add columns to data frames
library(plyr) #to help binding tables of different sizes
################################################################################
###

  #Imports the fasta file to r with the sequence to analyze
  fasta<-read.fasta(file = 'AntiCD20.fasta.txt', seqtype = 'AA')

  #conver each chain into a vector with the aas
  HC<-unlist(fasta[1])
  LC<-unlist(fasta[2])

  seqchoice<-'HC'

  if (seqchoice=='LC') {

    aachain<-LC # Decide what chain will be assest

    Sequence<-read.csv('Seq.csv') #Select the file name for the analysis

    Sequence<-Sequence[,c(1:9)]

    colnames(Sequence)<-c('Chem','Conc','Length','Chain','StartPos','EndPo
s','Sample','Intensity','Treatment')

    Subsequence<-subset(Sequence, Chain=='Anti_CD20_LC')
  }

  if (seqchoice=='HC') {

    aachain<-HC # Decide what chain will be assess

    Sequence<-read.csv('Seq.csv') #Select the file name for the analysis

    Sequence<-Sequence[,c(1:9)]
```

```
    colnames(Sequence)<-c('Chem','Conc','Length','Chain','StartPos','EndPo
s','Sample','Intensity','Treatment')

    Subsequence<-subset(Sequence, Chain=='Anti-CD20_HC')
  }

  SumTable<-matrix(NA,nrow =length(unique(Subsequence$Treatment)) ,ncol =
length(aachain))

  tretm<-matrix(NA,ncol=1,nrow = length(unique(Subsequence$Treatment)))

  tretm<-as.data.frame(tretm)

  for (pdx in 1:length(unique(Subsequence$Treatment))){

    treatments<-unique(Subsequence$Treatment)

    tretm[pdx,1]<-as.character(treatments[pdx])

    Subsequence2<-subset(Subsequence,Treatment==as.character(treatments[pd
x]))

    Table<-matrix(NA,nrow =length(Subsequence2$Intensity) ,ncol = length(a
achain))

    Table<-as.data.frame(Table)

    for (dz in 1:length(Subsequence2$Intensity)) {

      Table[dz,seq(by=1, from=Subsequence2$StartPos[dz],to=Subsequence2$En
dPos[dz])]<-Subsequence2$Intensity[dz]

    }

    SumTable[pdx,]<-colSums(Table, na.rm = T)

  }

colnames(SumTable)<-paste(c(1:length(aachain)),aachain)

rownames(SumTable)<-unique(Subsequence$Treatment)

SumTable<-t(SumTable)



#create pallate of colours for the heat map
library('circlize')
color.palette  <- c("red",'white', (colorRampPalette(c("aliceblue","steelb
lue"))(n=100000)))
```

```
#create rowlabels
Rowss<-matrix(' ',ncol=1,nrow=(length(SumTable[,1])))

Rowss<-as.data.frame(Rowss,stringsAsFactors = FALSE)

RowsNum<-seq(by=10, from = 10, to = (floor(length(SumTable[,1])/10)*10) )

RowsNum<-as.data.frame(RowsNum,stringsAsFactors = FALSE)

for (ptx in 1:length(RowsNum[,1])){

  Rowss[RowsNum[ptx,1],1]<-RowsNum[ptx,1]

}
SumTable2<-SumTable

rownames(SumTable2)<-Rowss[,1]

SumTable2<-SumTable2[,c(1,2,3,4,6,7,8,5)]

library('ComplexHeatmap')
Heatmap(SumTable2,
        name = 'Intensity',
        cluster_rows = F,
        cluster_columns = F,
        row_names_side = 'left',
        column_names_side = 'bottom',
        column_title = 'Treatment',
        column_title_side = 'bottom',
        row_names_gp = gpar(cex=0.8),
        column_names_gp = gpar(cex=1),
        row_title = 'peptide sequence',
        col = color.palette
        )
```

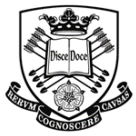
Disce Doce
Rerum Cognoscere Causas

9.6 Appendix 4: Identification of mass shift differences between sample treatments

Luis Toronjo Urquiza

23/12/2018

```
#########################################################
# Comparison of mass shift differences across         #
# sample treatments for Light chain mass spect data   #
#########################################################


###################################
# COMPARISON OF LIGHT CHAIN DATA #
###################################


## Supplementary material for the book chapter:
## "Detection of unknown chemical adduct modifications on proteins: from w
et to dry laboratory"
## Paola Antinori, Theo Michelot, Pierre Lescuyer, Markus Muller and Adeli
na E. Acosta-Martin
## in Mass Spectrometry of Proteins: Methods and Protocols - Quantitative
Proteomics and associated Bioinformatics
##
## This script has been modified, adapted and improved for MaxQuant-type d
ata,from:
## Acosta-Martin AE, Antinori P, Uppugunduri CR, Daali Y, Ansari M, Scherl
A, M?ller M, Lescuyer P. (2016)
## Detection of busulfan adducts on proteins. Rapid Commun Mass Spectrom 3
0: 2517-2528

##This code was redesigned to check mass difference shifts differences bet
ween two samples, in a one to one
##comparison and identify outliers for both samples compared

##  system.Exporting:

   #1) a final pdf file with all the plots comparing the the samples one t
o one and a label that is considered
   #   an outlier base on the z-threshold desired by the user.

   #2)a final pdf file with histograms relating to each of the peaks that
were considered outliers before.

   #3)a final csv table of the possible peaks in each histogram (as there
is maybe more than one in each histogram)
   #  showing the specific mass shift, and to which sample apartains with
respect to which compared partner.

##This program is currently designed to run a maximum of 28 comparisons, b
```

```
ut if the user need to add more
 #increase the vector 'nonzeroZ' to de desired number.


##############################################
##Libraries needed during for the analysis##
##############################################
library(ggplot2)
library(FSA)
library(data.table)
library(quantmod)
library(ggrepel)


set.seed(123) # for reproducibility of bootstrap


##############################
## Parameters of the study ##
##############################

by<-0.05            # General bin: Da distance in which the entire range o
f massshifts will split to be compared

range<-c(-750,750) # Part of the spectrum of Da mass shifts that will be s
tudy

zthresh<-3.5         # The minimum z-score value of each 'by' bin to be co
nsidered an outlier for further analysis

brks<-50           # Approximated number of bins for each histogram(how ma
ny times the by bin is broken into)

mbpk<-0.01        # Minimum distance in Da to consider different local max
imum peaks
                   # of mass shift difference for a histogram

pksmin<-3          # Threshold to consider a peak a possible maximum (elim
inates noise in the histograms)
                   # This is for frequency so the use integrers is ideal.
The value given is consider as well.


##################
## Files Outcome##
##################

Plotname<-'ZscoreplotLC.pdf'  #Name of the pdf file compilating all the pl
ot Z-score comparisons

Histname<-'HistLC.pdf'        #Name of the pdf file compilating all the hi
stograms
```

```
FullTablname<-'PeaksLC.csv'   #Name of the csv file compilating all the re
levant peaks

Comparison<-'CompareLC.pdf'   #Name of the pdf file compilating groups in
scatter plot

############################
## Load and prepare data ##
############################

# all files to compare one to one.
 #Naming the samples
 allCond1 <- c("Rsv10LC","Rsv25LC","Rsv50LC",
               "Rsv100LC","Rsv10LC","Rsv10LC",
               "Rsv10LC","Rsv25LC","Rsv25LC",
               "Rsv50LC","Cat10LC","Cat25LC",
               "Cat50LC","Cat10LC","Cat10LC",
               "Cat25LC","Rsv10LC","Rsv10LC",
               "Rsv10LC","Rsv25LC","Rsv25LC",
               "Rsv25LC","Rsv50LC","Rsv50LC",
               "Rsv50LC","Rsv100LC","Rsv100LC",
               "Rsv100LC")

 #Referencing the files
 allFile1Prot <- c("allPeptides_Rsv10.txt","allPeptides_Rsv25.txt","allPep
tides_Rsv50.txt",
                   "allPeptides_Rsv100.txt","allPeptides_Rsv10.txt","allPep
tides_Rsv10.txt",
                   "allPeptides_Rsv10.txt","allPeptides_Rsv25.txt","allPept
ides_Rsv25.txt",
                   "allPeptides_Rsv50.txt","allPeptides_Cat10.txt","allPept
ides_Cat25.txt",
                   "allPeptides_Cat50.txt","allPeptides_Cat10.txt","allPept
ides_Cat10.txt",
                   "allPeptides_Cat25.txt","allPeptides_Rsv10.txt","allPept
ides_Rsv10.txt",
                   "allPeptides_Rsv10.txt","allPeptides_Rsv25.txt","allPept
ides_Rsv25.txt",
                   "allPeptides_Rsv25.txt","allPeptides_Rsv50.txt","allPept
ides_Rsv50.txt",
                   "allPeptides_Rsv50.txt","allPeptides_Rsv100.txt","allPep
tides_Rsv100.txt",
                   "allPeptides_Rsv100.txt")

 #Naming the samples
 allCond2 <- c("Control","Control","Control",
               "Control","Rsv25LC","Rsv50LC",
               "Rsv100LC","Rsv50LC","Rsv100LC",
               "Rsv100LC","Control","Control",
               "Control","Cat25LC","Cat50LC",
               "Cat50LC","Cat10LC","Cat25LC",
               "Cat50LC","Cat10LC","Cat25LC",
```

```
              "Cat50LC","Cat10LC","Cat25LC",
              "Cat50LC","Cat10LC","Cat25LC",
              "Cat50LC")

 #Referencing the files
 allFile2Prot <- c("allPeptides_Control.txt","allPeptides_Control.txt","al
lPeptides_Control.txt",
                   "allPeptides_Control.txt","allPeptides_Rsv25.txt","allPe
ptides_Rsv50.txt",
                   "allPeptides_Rsv100.txt","allPeptides_Rsv50.txt","allPep
tides_Rsv100.txt",
                   "allPeptides_Rsv100.txt","allPeptides_Control.txt","allP
eptides_Control.txt",
                   "allPeptides_Control.txt","allPeptides_Cat25.txt","allPe
ptides_Cat50.txt",
                   "allPeptides_Cat50.txt","allPeptides_Cat10.txt","allPept
ides_Cat25.txt",
                   "allPeptides_Cat50.txt","allPeptides_Cat10.txt","allPept
ides_Cat25.txt",
                   "allPeptides_Cat50.txt","allPeptides_Cat10.txt","allPept
ides_Cat25.txt",
                   "allPeptides_Cat50.txt","allPeptides_Cat10.txt","allPept
ides_Cat25.txt",
                   "allPeptides_Cat50.txt")



#########################################################
##Actual coding no more variables need to be added##
#########################################################

# number of comparisons
nbComp <- length(allCond1)

allZscore <- list()
allData1 <- list()
allData2 <- list()

# define bins for general mass shifts comparisons
by <-by
range <-range
breaks <- seq(range[1]-by/2,range[2]+by/2,by=by)
mids <- seq(range[1],range[2],by=by)

for(i in 1:nbComp) {
    # iterate over conditions and files
    cond1 <- allCond1[i]
    file1Prot <- allFile1Prot[i]

    cond2 <- allCond2[i]
    file2Prot <- allFile2Prot[i]

    cat("Comparison",i,'in',nbComp,cond1,"vs.",cond2,"...\n")
```

```
    # load files
    cat("Reading files... ")
    allData1Prot <- read.csv(file1Prot,header=TRUE,sep="\t")

    allData2Prot <- read.csv(file2Prot,header=TRUE,sep="\t")

    cat("Done.\n")



    # Keep columns: ########################################################
###################
    #  - Raw.file
    #  - DP.Mass.Difference
    #  - DP.PEP
    #  - DP.Proteins
    data1Prot <- allData1Prot[,c(1,34,37,45)]
    data2Prot <- allData2Prot[,c(1,34,37,45)]

    # Select Light Chain IgG only ("Anti_CD20_LC") ########################
###################
    data1Prot <- subset(data1Prot, DP.Proteins=="Anti_CD20_LC")
    data2Prot <- subset(data2Prot, DP.Proteins=="Anti_CD20_LC")


    # # if only one protein (also, comment out all HSA-related lines above
)#################
    data1 <- data1Prot
    data2 <- data2Prot

    # remove DP PEP > 0.01  ################################################
###################
    data1 <- subset(data1, DP.PEP<0.01)
    data2 <- subset(data2, DP.PEP<0.01)

    # remove empty rows ("NA") #############################################
###################
    data1 <- subset(data1, !is.na(DP.Mass.Difference))
    data2 <- subset(data2, !is.na(DP.Mass.Difference))

    # remove out-of-bound mass differences #################################
###################
    data1 <- subset(data1, DP.Mass.Difference>range[1] & DP.Mass.Differenc
e<range[2])
    data2 <- subset(data2, DP.Mass.Difference>range[1] & DP.Mass.Differenc
e<range[2])

    # lists of raw files ###################################################
###################
    listfiles1 <- unique(data1$Raw.file)
    listfiles2 <- unique(data2$Raw.file)
```

```
    ############################
    ## Calculate the Z scores ##
    ############################
    # resample nbRep times over the "raw file" column
    nbRep <- 100
    h1mat <- matrix(NA,nrow=nbRep,ncol=length(breaks)-1)
    h2mat <- matrix(NA,nrow=nbRep,ncol=length(breaks)-1)
    pb <- txtProgressBar(min = 1, max = nbRep, style = 3)
    for(rep in 1:nbRep) {
        dmass1 <- NULL
        dmass2 <- NULL

        # sample over runs (indicated by "raw file" column)
        samp1 <- sample(listfiles1,replace=TRUE)
        for(file in samp1)
            dmass1 <- c(dmass1,data1$DP.Mass.Difference[which(data1$Raw.fi
le==file)])
        samp2 <- sample(listfiles2,replace=TRUE)
        for(file in samp2)
            dmass2 <- c(dmass2,data2$DP.Mass.Difference[which(data2$Raw.fi
le==file)])

        h1mat[rep,] <- hist(dmass1,breaks=breaks,plot=FALSE)$counts
        h2mat[rep,] <- hist(dmass2,breaks=breaks,plot=FALSE)$counts

        setTxtProgressBar(pb, rep)
    }
    cat("\n\n")

    # MSH(condition 1) - MSH(condition 2)
    dh <- hist(data1$DP.Mass.Difference,breaks=breaks,plot=FALSE)$counts -
        hist(data2$DP.Mass.Difference,breaks=breaks,plot=FALSE)$counts

    # variances on counts for each condition
    var1 <- apply(h1mat,2,var)
    var2 <- apply(h2mat,2,var)

    # Z-scores
    Zscore <- rep(0,length(dh))
    ind <- which(var1+var2>0) # var1+var2=0 -> Zscore=0
    Zscore[ind] <- dh[ind]/(sqrt(var1[ind]+var2[ind]))

    allZscore[[i]] <- Zscore
    allData1[[i]] <- data1
    allData2[[i]] <- data2
}

# non-zero Z scores
                          #for (i in 1:nbComp) {
                          #  nonzeroZ <- c(allZscore[[(i)]])
                          #}
```

```
# non-zero Z scores
nonzeroZ <- c(allZscore[[1]],allZscore[[2]],allZscore[[3]],allZscore[[4]],
allZscore[[5]],
              allZscore[[6]],allZscore[[7]],allZscore[[8]],allZscore[[9]],
allZscore[[10]],
              allZscore[[11]],allZscore[[12]],allZscore[[13]],allZscore[[1
4]],allZscore[[15]],
              allZscore[[16]],allZscore[[17]],allZscore[[18]],allZscore[[1
9]],allZscore[[20]],
              allZscore[[21]],allZscore[[22]],allZscore[[23]],allZscore[[2
4]],allZscore[[25]],
              allZscore[[26]],allZscore[[27]],allZscore[[28]])


#              allZscore[[29]],allZscore[[30]],
#              allZscore[[31]],allZscore[[32]],allZscore[[33]],allZscore[[
34]],allZscore[[35]],
#              allZscore[[36]],allZscore[[37]],allZscore[[38]],allZscore[[
39]],allZscore[[40]],
#              allZscore[[41]],allZscore[[42]],allZscore[[43]],allZscore[[
44]],allZscore[[45]],
#              allZscore[[46]],allZscore[[47]],allZscore[[48]],allZscore[[
49]],allZscore[[50]],
#              allZscore[[51]],allZscore[[52]],allZscore[[53]],allZscore[[
54]],allZscore[[55]],
#              allZscore[[56]],allZscore[[57]],allZscore[[58]],allZscore[[
59]],allZscore[[60]],
#              allZscore[[61]],allZscore[[62]],allZscore[[63]],allZscore[[
64]],allZscore[[65]],
#              allZscore[[66]],allZscore[[67]],allZscore[[68]],allZscore[[
69]],allZscore[[70]],
#              allZscore[[71]],allZscore[[72]],allZscore[[73]],allZscore[[
74]],allZscore[[75]],
#              allZscore[[76]],allZscore[[77]],allZscore[[78]],allZscore[[
79]],allZscore[[80]],
#              allZscore[[81]],allZscore[[82]],allZscore[[83]],allZscore[[
84]],allZscore[[85]],
#              allZscore[[86]],allZscore[[87]],allZscore[[88]],allZscore[[
89]],allZscore[[90]],
#              allZscore[[91]],allZscore[[92]],allZscore[[93]],allZscore[[
94]],allZscore[[95]],
#              allZscore[[96]],allZscore[[97]],allZscore[[98]],allZscore[[
99]],allZscore[[100]])

#Reduces the vector to only comparisons which give
nonzeroZ <- nonzeroZ[nonzeroZ!=0]

# significance threshold

thresh <-zthresh

# y-axis range
```

```
   #general range for all z-score plots
ylim <- 1.1*c(min(nonzeroZ),max(nonzeroZ))

   #Specific range for individual z-score plots
#ylim <-1.1*c(min(allZscore[[i]]),max(allZscore[[i]]))

##############################################################################
###################
## Plot Z-scores ##
###################
##############################################################################
pdf(Plotname) #To safe the plots in a pdf file at the working directory

par(mfrow=c(1,1))
for(i in 1:nbComp) {
  # plot Z-scores against mass shift
  plot(mids,allZscore[[i]],type="h",lwd=2,ylim=ylim,xlab="Mass Shift (Da)"
, ylab="Z score",
       main=paste(allCond1[i],"vs.",allCond2[i]))
  abline(h=0,lwd=2)

  # plot significance threshold
  abline(h=c(-thresh,thresh),lty=2,col="darkgrey")

  # label significant peaks
  offset <- max(nonzeroZ)/20;
  idxp1 <- which(allZscore[[i]]>thresh)
  idxp2 <- which(allZscore[[i]]< (-thresh))

  if(length(idxp1)>0) {
    for(idp1 in idxp1) {
      mass1 <- allData1[[i]]$DP.Mass.Difference
      label1 <- median(mass1[abs(mass1-mids[idp1])<by])
      text(x=mids[idp1],y=allZscore[[i]][idp1]+offset,labels=round(label1,
3))
    }
  }

  if(length(idxp2)>0) {
    for(idp2 in idxp2) {
      mass2 <- allData2[[i]]$DP.Mass.Difference
      label2 <- median(mass2[abs(mass2-mids[idp2])<by])
      text(x=mids[idp2],y=allZscore[[i]][idp2]-offset,labels=round(label2,
3))
    }
  }
}
par(mfrow=c(1,1))

dev.off()

##############################################################################
#####################################################
```

```
## Plot histogram of mass shifts around each peak ##
#####################################################
#########################################################################

pdf(Histname) #To safe the plots in a pdf pdf file at the working director
y

idntpk<-NULL #vector to compile all the relevant mass shift peaks

for(i in 1:nbComp) {
  # label significant peaks
  idxh1 <- which(allZscore[[i]]>thresh)
  idxh2 <- which(allZscore[[i]]< (-thresh))


  ####################################################
  ## creates the histograms of (+) z-scores peaks ##
  ####################################################

  idntpk1<-NULL
  if(length(idxh1)>0) {

    for(idh1 in idxh1) {
      massA <- allData1[[i]]$DP.Mass.Difference
      mass1<-massA[abs(massA-mids[idh1])<by]
      res1<-hist(mass1,breaks=brks,xlab="Mass Shift (Da)",
                 main=paste(allCond1[i],"vs.",allCond2[i],", mass shift ="
,round(median(mass1[abs(mass1-mids[idh1])<by]),3)))
      abline(v=median(mass1[abs(mass1-mids[idh1])<by]),col=2)

      ##extracting information from the histgram##
      midshist1<-res1$mids
      countshist1<-res1$counts
      relpos1<-seq(1,length(midshist1),1)
      tabl1=data.frame(relpos=relpos1, sample=allCond1[i],compare=allCond2
[i],Zscore=(allZscore[[i]])[idh1],massf=midshist1,counts=countshist1)

      ##Normalizing distance between relevant peaks##

      by<-by                          #Initial bin to compare among samples
      brkbin<-length(countshist1)  #Actual break of the by bin (not always
equal to the breaks asked for)
      mbpk1<-mbpk                      # Distance in Da to consider diferent
maximum peaks
                                      #Find decimal places of the mbpk
      dcpl<-if ((mbpk1 %% 1) != 0) {
        nchar(strsplit(sub('0+$', '', as.character(mbpk1)), ".", fixed=TRU
E)[[1]][[2]])
      } else {
        return(0)
      }
      distance<-by/brkbin          #distance of each bar in the histgram i
n Da
```

```
                                    #Vector of Da distances with equal numb
er of decimal places to the mbpk
      m<-signif(seq(1,1000,1)*distance,digits=dcpl)
      pksdis1<-which.max(m>=mbpk1)    #Looks for the lower number of bins
that will satisfy the mbpk


      ##Find reliable maximum peaks in Histgrams##
      pks1<-NULL
      pksmin1<-pksmin #minimum threshold to consider a maximum peak
      shape1 <- diff(sign(diff(countshist1, na.pad = FALSE)))
      pks1 <-unlist(sapply(which(shape1 < 0), FUN = function(pksi1){
        pksz1 <- pksi1 - pksdis1 + 1
        pksz1 <- ifelse(pksz1 > 0, pksz1, 1)
        pksw1 <- pksi1 + pksdis1 + 1
        pksw1 <- ifelse(pksw1 < length(countshist1), pksw1, length(countsh
ist1))
        if(countshist1[pksi1+1]>=pksmin1) {
          if(all(countshist1[c(pksz1 : pksi1, (pksi1 + 2) : pksw1)] <= cou
ntshist1[pksi1 + 1])){
              return(pksi1 + 1)}
            else {return(NULL)}} else {return(NULL)}
      }))

      ##When there are relevant peaks adds them to the vector##
      if(length(pks1)) {
        tmp1    <- setDT(tabl1, key = 'relpos')[J(pks1)]
        idntpk1 <- rbind(idntpk1, tmp1)
      }
    }
  }

  ######################################################
  ## creates the histograms of (-) z-scores peaks ##
  ######################################################
   idntpk2<-NULL
  if(length(idxh2)>0) {
    for(idh2 in idxh2) {
      massB <- allData2[[i]]$DP.Mass.Difference
      mass2<-massB[abs(massB-mids[idh2])<by]
      res2<-hist(mass2,breaks=brks,xlab="Mass Shift (Da)",
                 main=paste(allCond2[i],"vs.",allCond1[i],", mass shift ="
,round(median(mass2[abs(mass2-mids[idh2])<by]),3)))
      abline(v=median(mass2[abs(mass2-mids[idh2])<by]),col=2)

      ##extracting information from the histgram############################


      midshist2<-res2$mids
      countshist2<-res2$counts
      relpos2<-seq(1,length(midshist2),1)
      tabl2=data.frame(relpos=relpos2,sample=allCond2[i],compare=allCond1[
i],counts=countshist2,Zscore=(allZscore[[i]])[idh2],massf=midshist2)
```

```
      ##Normalizing distance between relevant peaks#######################



      by<-by                          #Initial bin to compare among samples
      brkbin<-length(countshist2)  #Actual break of the by bin (not always
equal to the breaks asked for)
      mbpk2<-mbpk                     # Distance in Da to consider diferent m
aximum peaks
                                      #Find decimal places of the mbpk
      dcpl<-if ((mbpk2 %% 1) != 0) {
        nchar(strsplit(sub('0+$', '', as.character(mbpk2)), ".", fixed=TRU
E)[[1]][[2]])
      } else {
        return(0)
      }
      distance<-by/brkbin             #distance of each bar in the histgram i
n Da
                                      #Vector of Da distances with equal numb
er of decimal places to the mbpk
      m<-signif(seq(1,1000,1)*distance,digits=dcpl)
      pksdis2<-which.max(m>=mbpk2)    #Looks for the lower number of bins
that will satisfy the mbpk

      ##Find peaks in Histgrams###############################################


      pks2<-NULL
      pksmin2<-pksmin #minimum threshold to consider a maximum peak
      shape2 <- diff(sign(diff(countshist2, na.pad = FALSE)))
      pks2 <-unlist(sapply(which(shape2 < 0), FUN = function(pksi2){
        pksz2 <- pksi2 - pksdis2 + 1
        pksz2 <- ifelse(pksz2 > 0, pksz2, 1)
        pksw2 <- pksi2 + pksdis2 + 1
        pksw2 <- ifelse(pksw2 < length(countshist2), pksw2, length(countsh
ist2))
        if(countshist2[pksi2+1]>=pksmin2) {
          if(all(countshist2[c(pksz2 : pksi2, (pksi2 + 2) : pksw2)] <= cou
ntshist2[pksi2 + 1])){
            return(pksi2 + 1)}
          else {return(NULL)}} else {return(NULL)}
        }))


      ##When there are relevant peaks adds them to the vector##
      if(length(pks2)) {
        tmp2    <- setDT(tabl2, key = 'relpos')[J(pks2)]
        idntpk2 <- rbind(idntpk2, tmp2)
      }
    }
  }
```

```
  ##When there are relevant peaks adds them to the final vector##
  if(length(idntpk1)) {
    idntpk <- rbind(idntpk,idntpk1)}
  if(length(idntpk2)){
    idntpk <- rbind(idntpk,idntpk2)
  }
}

dev.off()

##Remove duplicatres
idntpk<-unique(idntpk)

##Remove relative position column
idntpk$relpos <- NULL

#Rearrange columns in the desired order
idntpk[,c(idntpk$sample,idntpk$compare,idntpk$Sam,idntpk$Com,idntpk$massf,
idntpk$Zscore,idntpk$counts)];

##Export the complete table with all information from relevant peaks to an
cvs (Excel) file
write.csv(idntpk,FullTablname)



##Creating columns to greate groups Resveratrol,Catechin and Control
idntpk$Sam <- substr(idntpk$sample, 0, 3)

idntpk$Com<- substr(idntpk$compare, 0, 3)


## round frequency of the histgram and mass shift
idntpk$massf<-round(idntpk$massf, digits=2)
idntpk$Zscore<-round(idntpk$Zscore, digits=2)



pdf(Comparison)


#Create subset of datatables for later analysis and export as a csv file

#Frist comparison group

Comp1<-subset(idntpk,Sam=='Rsv' & Com=='Rsv')

Zscr<-tapply(Comp1$Zscore,Comp1$massf, FUN=mean)

Frq<-tapply(Comp1$counts,Comp1$massf, FUN=sum)

Comp1=rbind(Zscr,Frq)
```

```
Comp1<-t(Comp1)

masshift<-rownames(Comp1)


Comp1<- cbind(masshift, data.frame(Comp1, row.names=NULL))

Comp1$masshift<- as.numeric(as.character(Comp1$masshift))

Comp1<-Comp1[order(Comp1$masshift),]

Comp1=data.frame(masshift=Comp1$masshift,AvgZscore=Comp1$Zscr,TotFrequency
=Comp1$Frq)

if (length(Comp1)){write.csv(Comp1,'Comp1')}
if (length(Comp1)){
ggplot(Comp1, aes(x=masshift, y=AvgZscore, size=TotFrequency))+
  geom_point(colour= "blue4", alpha= 0.5)+scale_size(range = c(1,15))+
  theme_bw()+
  xlab("Mass Shift (Da)")+ ylab("Average Z-score")+
  geom_abline(intercept = 0, slope = 0)+
  geom_abline(intercept = 0, slope = 90)+
  geom_label_repel(label=Comp1$masshift, size=2.5, label.padding = 0.15)+
  scale_x_continuous(limits = 1.2*c(min(Comp1$masshift),max(Comp1$masshift
)))+
  scale_y_continuous(limits = 1.2*c(min(Comp1$AvgZscore),max(Comp1$AvgZsco
re)))+
  annotate("text", x=c(min(Comp1$masshift-5)), y=c(0), label=c("Peak\n Los
s"))+
  annotate("text", x=c(1.2*max(Comp1$masshift-5)), y=c(0), label=c("Peak\n
Gain"))+
  annotate("text", y=c(1.2*max(Comp1$AvgZscore)), x=c(37), label=c("Condit
ion 1"))+
  annotate("text", y=c(1.2*min(Comp1$AvgZscore)), x=c(37), label=c("Condit
ion 2"))+
  ggtitle('Rsv vs Rsv LC')+labs(size='Frequency')
}



#Second comparison group

Comp2<-subset(idntpk,Sam=='Cat' & Com=='Cat')

Zscr<-tapply(Comp2$Zscore,Comp2$massf, FUN=mean)

Frq<-tapply(Comp2$counts,Comp2$massf, FUN=sum)

Comp2=rbind(Zscr,Frq)

Comp2<-t(Comp2)
```

```
masshift<-rownames(Comp2)


Comp2<- cbind(masshift, data.frame(Comp2, row.names=NULL))

Comp2$masshift<- as.numeric(as.character(Comp2$masshift))

Comp2<-Comp2[order(Comp2$masshift),]

Comp2=data.frame(masshift=Comp2$masshift,AvgZscore=Comp2$Zscr,TotFrequency
=Comp2$Frq)

if (length(Comp2)){write.csv(Comp2,'Comp2')}

if (length(Comp2)){
ggplot(Comp2, aes(x=masshift, y=AvgZscore, size=TotFrequency))+
  geom_point(colour= "blue4", alpha= 0.5)+scale_size(range = c(1,15))+
  theme_bw()+
  xlab("Mass Shift (Da)")+ ylab("Average Z-score")+
  geom_abline(intercept = 0, slope = 0)+
  geom_abline(intercept = 0, slope = 90)+
  geom_label_repel(label=Comp2$masshift, size=2.5, label.padding = 0.15)+
  #scale_x_continuous(limits = 1.2*c(min(Comp2$masshift),max(Comp2$masshif
t)))+
  #scale_y_continuous(limits = 1.2*c(min(Comp2$AvgZscore),max(Comp2$AvgZsc
ore)))+
  #annotate("text", x=c(min(Comp2$masshift-5)), y=c(0), label=c("Peak\n Lo
ss"))+
  #annotate("text", x=c(1.2*max(Comp2$masshift-5)), y=c(0), label=c("Peak\
n Gain"))+
  #annotate("text", y=c(1.2*max(Comp2$AvgZscore)), x=c(37), label=c("Condi
tion 1"))+
  #annotate("text", y=c(1.2*min(Comp2$AvgZscore)), x=c(37), label=c("Condi
tion 2"))+
  ggtitle('Cat vs Cat LC')+labs(size='Frequency')
}


#Third comparison group

RsvvsCon1<-subset(idntpk,Sam=='Rsv' & Com=='Con')
RsvvsCon2<-subset(idntpk,Com=='Rsv' & Sam=='Con')
Comp3<-rbind(RsvvsCon1,RsvvsCon2)

Zscr<-tapply(Comp3$Zscore,Comp3$massf, FUN=mean)

Frq<-tapply(Comp3$counts,Comp3$massf, FUN=sum)

Comp3=rbind(Zscr,Frq)

Comp3<-t(Comp3)
```

```
masshift<-rownames(Comp3)


Comp3<- cbind(masshift, data.frame(Comp3, row.names=NULL))

Comp3$masshift<- as.numeric(as.character(Comp3$masshift))

Comp3<-Comp3[order(Comp3$masshift),]

Comp3=data.frame(masshift=Comp3$masshift,AvgZscore=Comp3$Zscr,TotFrequency
=Comp3$Frq)

if (length(Comp3)){write.csv(Comp3,'Comp3')}

if (length(Comp3)){
  ggplot(Comp3, aes(x=masshift, y=AvgZscore, size=TotFrequency))+
    geom_point(colour= "blue4", alpha= 0.5)+scale_size(range = c(1,15))+
    theme_bw()+
    xlab("Mass Shift (Da)")+ ylab("Average Z-score")+
    geom_abline(intercept = 0, slope = 0)+
    geom_abline(intercept = 0, slope = 90)+
    geom_label_repel(label=Comp3$masshift, size=2.5, label.padding = 0.15)
+
    #scale_x_continuous(limits = 1.2*c(min(Comp3$masshift),max(Comp3$massh
ift)))+
    #scale_y_continuous(limits = 1.2*c(min(Comp3$AvgZscore),max(Comp3$AvgZ
score)))+
    #annotate("text", x=c(min(Comp3$masshift-5)), y=c(0), label=c("Peak\n
Loss"))+
    #annotate("text", x=c(1.2*max(Comp3$masshift-5)), y=c(0), label=c("Pea
k\n Gain"))+
    #annotate("text", y=c(1.2*max(Comp3$AvgZscore)), x=c(37), label=c("Con
dition 1"))+
    #annotate("text", y=c(1.2*min(Comp3$AvgZscore)), x=c(37), label=c("Con
dition 2"))+
    ggtitle('Rsv vs Con LC')+labs(size='Frequency')
}


#Forth comparison

CatvsCon1<-subset(idntpk,Sam=='Cat' & Com=='Con')
CatvsCon2<-subset(idntpk,Com=='Cat' & Sam=='Con')
Comp4<-rbind(CatvsCon1,CatvsCon2)


Zscr<-tapply(Comp4$Zscore,Comp4$massf, FUN=mean)

Frq<-tapply(Comp4$counts,Comp4$massf, FUN=sum)

Comp4=rbind(Zscr,Frq)
```

```
Comp4<-t(Comp4)

masshift<-rownames(Comp4)


Comp4<- cbind(masshift, data.frame(Comp4, row.names=NULL))

Comp4$masshift<- as.numeric(as.character(Comp4$masshift))

Comp4<-Comp4[order(Comp4$masshift),]

Comp4=data.frame(masshift=Comp4$masshift,AvgZscore=Comp4$Zscr,TotFrequency
=Comp4$Frq)

if (length(Comp4)){write.csv(Comp4,'Comp4')}

if (length(Comp4)){
  ggplot(Comp4, aes(x=Comp4$masshift, y=Comp4$AvgZscore, size=Comp4$TotFre
quency))+
    geom_point(colour= "blue4", alpha= 0.5)+scale_size(range = c(1,15))+
    theme_bw()+
    xlab("Mass Shift (Da)")+ ylab("Average Z-score")+
    geom_abline(intercept = 0, slope = 0)+
    geom_abline(intercept = 0, slope = 90)+
    geom_label_repel(label=Comp4$masshift, size=2.5, label.padding = 0.15)
+
    #scale_x_continuous(limits = 1.2*c(min(Comp4$masshift),max(Comp4$massh
ift)))+
    #scale_y_continuous(limits = 1.2*c(min(Comp4$AvgZscore),max(Comp4$AvgZ
score)))+
    #annotate("text", x=c(min(Comp4$masshift-5)), y=c(0), label=c("Peak\n
Loss"))+
    #annotate("text", x=c(1.2*max(Comp4$masshift-5)), y=c(0), label=c("Pea
k\n Gain"))+
    #annotate("text", y=c(1.2*max(Comp4$AvgZscore)), x=c(37), label=c("Con
dition 1"))+
    #annotate("text", y=c(1.2*min(Comp4$AvgZscore)), x=c(37), label=c("Con
dition 2"))+
    ggtitle('Cat vs Con LC')+labs(size='Frequency')
}


#Fith Comparison

RsvvsCat1<-subset(idntpk,Sam=='Rsv' & Com=='Cat')
RsvvsCat2<-subset(idntpk,Com=='Rsv' & Sam=='Cat')
Comp5<-rbind(RsvvsCat1,RsvvsCat2)


Zscr<-tapply(Comp5$Zscore,Comp5$massf, FUN=mean)
```

```
Frq<-tapply(Comp5$counts,Comp5$massf, FUN=sum)

Comp5=rbind(Zscr,Frq)

Comp5<-t(Comp5)

masshift<-rownames(Comp5)


Comp5<- cbind(masshift, data.frame(Comp5, row.names=NULL))

Comp5$masshift<- as.numeric(as.character(Comp5$masshift))

Comp5<-Comp5[order(Comp5$masshift),]

Comp5=data.frame(masshift=Comp5$masshift,AvgZscore=Comp5$Zscr,TotFrequency
=Comp5$Frq)

if (length(Comp5)){write.csv(Comp5,'Comp5')}

if (length(Comp5)){
  ggplot(Comp5, aes(x=Comp5$masshift, y=Comp5$AvgZscore, size=Comp5$TotFre
quency))+
    geom_point(colour= "blue4", alpha= 0.5)+scale_size(range = c(1,15))+
    theme_bw()+
    xlab("Mass Shift (Da)")+ ylab("Average Z-score")+
    geom_abline(intercept = 0, slope = 0)+
    geom_abline(intercept = 0, slope = 90)+
    geom_label_repel(label=Comp5$masshift, size=2.5, label.padding = 0.15)
+
    #scale_x_continuous(limits = 1.2*c(min(Comp5$masshift),max(Comp5$massh
ift)))+
    #scale_y_continuous(limits = 1.2*c(min(Comp5$AvgZscore),max(Comp5$AvgZ
score)))+
    #annotate("text", x=c(min(Comp5$masshift-5)), y=c(0), label=c("Peak\n
Loss"))+
    #annotate("text", x=c(1.2*max(Comp5$masshift-5)), y=c(0), label=c("Pea
k\n Gain"))+
    #annotate("text", y=c(1.2*max(Comp5$AvgZscore)), x=c(37), label=c("Con
dition 1"))+
    #annotate("text", y=c(1.2*min(Comp5$AvgZscore)), x=c(37), label=c("Con
dition 2"))+
    ggtitle('Rsv vs Cat LC')+labs(size='Frequency')
}

dev.off()
```

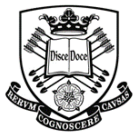

9.7 Appendix 5: Z-plots from mass shift comparison

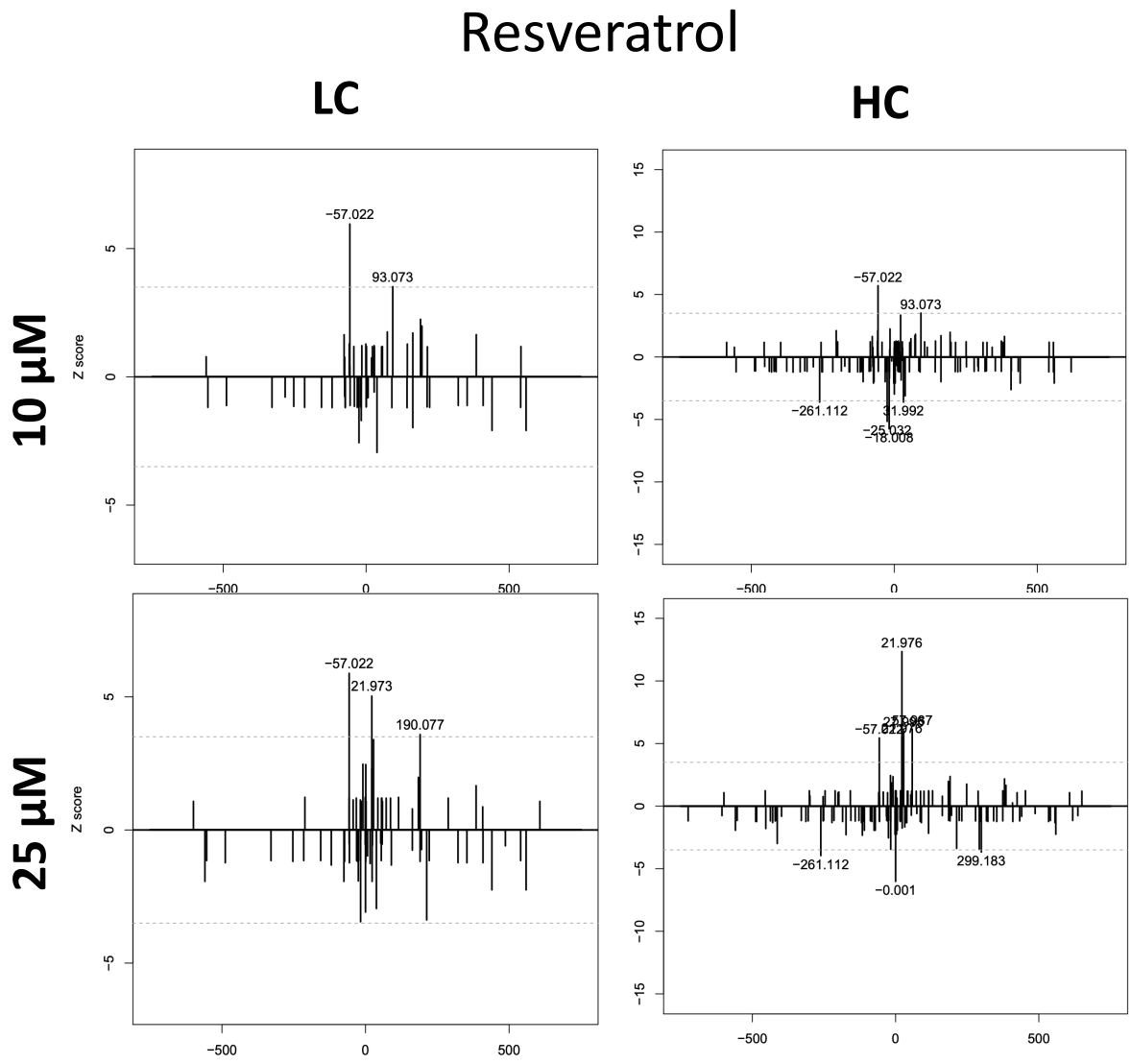

Resveratrol

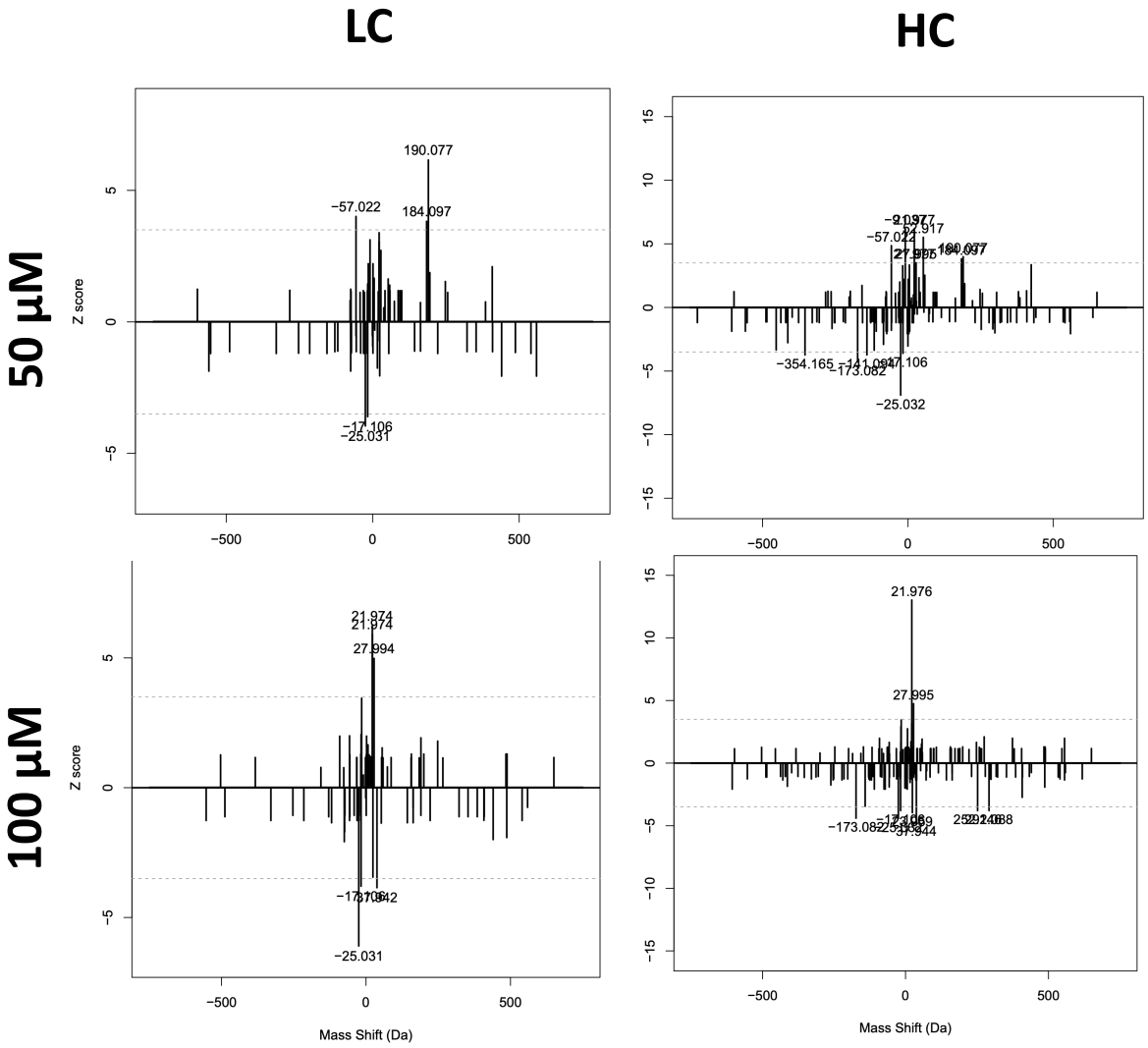

Catechin

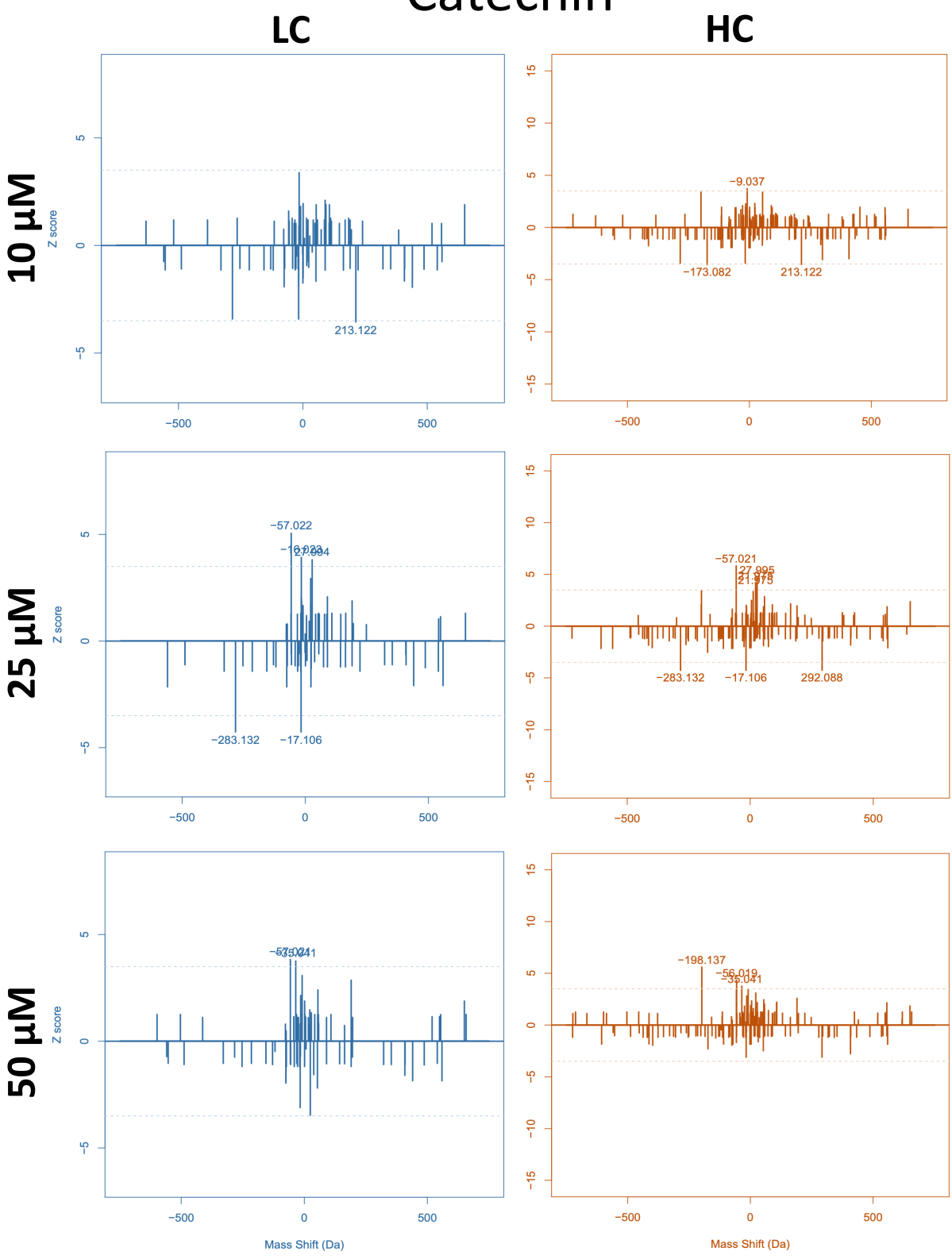
LC
HC
10 µM
25 µM
50 µM
Z score
213.122
−9.037
−173.082
213.122
−57.022
−283.132
−17.106
−57.021
−283.132
−17.106
292.088
−198.137
−56.019
−35.041
Mass Shift (Da)
Mass Shift (Da)


Disce Doce
Verum Gnosce Res Cavas

9.8 Appendix 6: Mass spectrometry modifications results analysis

Luis Toronjo Urquiza

23/12/2018

```
        ######################################################
        # Search and Export consistent modifications from  #
        # specific search mass spectrometry data           #
        ######################################################

library(readxl) #for the use of read_excel
library(bazar) # for the use of is.empty


#Parameter that defines the minimum number of samples that can be missing
to consider it for further study
 # or it will be ignored and counted as NA
#Example: if i put 1 only measurements of a modification of a specific tre
atment that appear in 3 out of the 4
#replicates will be considered, the rest will not be consider consistent a
nd will not be counted
xdd<-1
#Set working directory before using this code(desktop)

# First import the file with the file names
filename<-read_excel('Names.xlsx',col_names=F)

#command to save all the plots created by the code
pdf("MSplotsAllFinal.pdf")

#create a matrix previous to import all the data so that the information c
an be collected
allresult<-matrix(NA,nrow=8,ncol = 1)

colnames(filename)<-'names'

#creates a for loop that goes through the file names import them

# format the data and add it the already created file
for (d in 1:length(filename$names)){
#Import Csv file
MyData<-NULL
Modif<-NULL
#imports the file of the working directory, specify that has headers and t
hat is comma separated
 MyData<-read.csv(as.character(filename[d,1]),header = T, sep = ',')
#Name the modification the code is corrently extrancting for future refere
nces
 Modif<-sub("-.*", "", as.character(filename[d,1]))
```

```
#select Columns of interest (information, intensity and ration mod/base)
MyData<- MyData[ ,c(2,4,6,8,146,424,425,428,429,156:219)]

#Select Rows asociated with Anti_CD20_LC/HC
MyData<-subset(MyData, Protein=='Anti_CD20_LC' | Protein=='Anti-CD20_HC')

#Select only the files that have some modifications, of the rows are 2,whi
ch is the original dimension,
# no modifications were found and further analysis is not need meaning. It
will jump to the next file
if (nrow(MyData)>2){
#Change values that are 0 to Na
MyData[MyData==0]<-NA

#create a column variable where the modification is stated for each row, a
s the data will be merge
# and it might be difficult to identify to what modification the signal co
rresponds
MyData$Modification<-(Modif)

#creates variable name were the peptide chain, the position and the modifi
cation is determine
MyData$ModID<-paste(MyData$Protein,formatC(as.character(MyData$Positions.w
ithin.proteins), width=3, flag="0"),Modif, sep="-")

#create a matrix to insert all the data for the z value for loop
results<-NULL
results<-matrix(NA, nrow =16, ncol = 1)

#create a iteration loop in order to obtain all the means and SD of each s
ample for each modification.=
for (z in 1:nrow(MyData)){

  rowresult<-NULL
  rowresult<-matrix(, nrow =16, ncol = 2)
  x<-NULL
 for (x in 1:16){
   mean<-NULL
   stnd<-NULL
   NAnum<-NULL

   mean<-rowMeans(MyData[z,(x*4+6):(x*4+9)], na.rm = T)
   stnd<-sd(MyData[z,(x*4+6):(x*4+9)], na.rm = T)
   NAnum<-rowSums(is.na(MyData[z,(x*4+6):(x*4+9)]))


   rowresult[x,1]<-mean
   rowresult[x,2]<-stnd

   #if more than half the values are missing we want to omit this value
```

```
   if(NAnum>xdd){rowresult[x, ]<-NA}
 }
  results<-cbind(results,rowresult)
}

#eliminate the first empty column
results<-results[,c(2:ncol(results))]

#Change name of rows
rownm<-NULL
rownm<-colnames(MyData)
rownm<-rownm[c(10,14,18,22,26,30,34,38,42,46,50,54,58,62,66,70)]
rownames(results)<-rownm

#Change name of columns
colnm<-NULL
p<-NULL
for (p in 1:nrow(MyData)){
  p1<-NULL
  p2<-NULL
  p1<-paste(MyData$ModID[p],'Avrg',sep = ' ')
  p2<-paste(MyData$ModID[p],'StDv',sep = ' ')

  colnm<-c(colnm,p1,p2)
}

colnames(results)<-colnm
results<-as.data.frame.matrix(results)

results2<-results[1:8,]

#select only ratio values and order them
ratioresults<-NULL
ratioresults<-results[9:16,]
#this exposes the modifications that occurs 100% of the times and instead
of ratio puts the intensity of the signal
ratioresults[is.na(ratioresults)]<-results2[is.na(ratioresults)]

#lowers all the numbers to 20 if they are above, vales above 20 2000% of t
he times are modified. also helps to graph it
ratioresults[ratioresults>20]<-20

#previous step we made all the standard devations 20 as well, we get them
back to zero
for (lx in 1:(length(ratioresults)/2)){
  lxcol<-lx*2
  temprat<-NULL
  temprat<-ratioresults[,lxcol]
  temprat[temprat==20]<-0
  ratioresults[,lxcol]<-temprat

}
```

```
ratioresults<-ratioresults[c(4,1,2,3,6,7,8,5),]
ratioresults<-as.data.frame.matrix(ratioresults)

library(ggplot2)
n<-NULL
 for (n in 1:nrow(MyData) ) {
 grtbl<-NULL
 grtbl<-ratioresults[,c((n*2)-1,(n*2))]
 rownames(grtbl)<-c(' Ctrl','Cat10','Cat25','Cat50', 'Rsv010','Rsv025','Rs
v050','Rsv100')
 grtbl<-cbind(rownames(grtbl), data.frame(grtbl))
 colnames(grtbl)<-c('Treatment','Mean','SD')

  grtbl[is.na(grtbl)]<-0
#if the data in the tabe is all 0 then we dont need to graph it
 if(max(grtbl[,2:3])>0){
 #graph

   g<-ggplot(grtbl, aes(x=Treatment, y= Mean, fill=Treatment))+
     geom_col(color=c('#990000',"#006633", "#006633", "#006633",'#000033',
'#000033','#000033','#000033'),
              fill=c('#990000',"#00CC33", "#009900", "#006633",'#0099FF','
#0000FF','#000066','#000033'))+
     geom_errorbar(aes(ymin =Mean - SD, ymax =Mean + SD), width=0.4, colou
r="black", alpha=0.9, size=1.3)+
     labs(title = MyData$ModID[n], y= "Ratio (Mod/Base)", x = "Treatment")
+
     theme(panel.background = element_rect(fill = "white", colour = "grey5
0"))+
     theme(axis.text = element_text(size = 12,face = 'bold'))+
     theme( axis.line = element_line(colour = "black",size = 0.75, linetyp
e = "solid"))+
     theme(axis.title.x = element_text(size=14,face = 'bold',colour = 'bla
ck'))+
     theme(axis.title.y = element_text(size=14,face = 'bold',colour = 'bla
ck'))+
     theme(title = element_text(size=16,face = 'bold'))
  print(g)
  }
 }
allresult<-cbind(allresult,ratioresults)
}
}
#comand to stop the addtion of plots to the pdf file and export the file
dev.off()

write.csv(allresult,'allresult.csv')
```